Association of Type 1 Inositol 1,4,5-Trisphosphate Receptor (IP_3R1) with Protein Kinase A and A-Kinase Anchoring Protein 9 (AKAP9) in platelets

Arti N Trivedi

PhD Medical Sciences

The University of Hull and The University of York
Hull York Medical School

February 2017

ABSTRACT

Cyclic adenosine monophsphoate (cAMP) signalling is thought to regulate inositol-1,4,5 trisphosphate (IP_3)-mediated calcium (Ca^{2+}) mobilisation in platelets through protein kinase A (PKA)-mediated phosphorylation, leading to inhibition of inositol-1,4,5 trisphosphate receptors (IP_3Rs). A-kinase Anchoring Proteins (AKAPs) are known to be involved in spatial and temporal regulation of PKA-mediated phosphorylation; however the precise molecular mechanisms regulating the PKA-mediated inhibition of IP_3Rs remain to be fully understood.

To further understand this, the presence and functional importance of a novel PKA/IP_3R/AKAP signalling complex in platelets was studied. Protein complexes identified using co-immunoprecipitation and analysed using immunoblotting, while Ca^{2+} measurements were made using spectrofluorometry. We show that platelet stimulation with thrombin evoked a sharp increase in intracellular Ca^{2+} levels, which was blocked by IP_3R1 antagonist, 2-Aminoethoxydiphenyl borate (2-APB). This suggested Ca^{2+} mobilisation through IP_3Rs. Furthermore, activation of cAMP signalling by prostacyclin (PGI_2)-treatment restricted Ca^{2+} mobilisation in response to thrombin treatment, suggesting that an involvement of cAMP pathway in regulation of IP_3R channel activity. Furthermore, the presence of all three isoforms of IP_3R in platelets was confirmed by immunoblotting. PGI_2-induced phosphorylation of IP_3R1 on Serine1756 (Ser1756) was blocked by pharmacological inhibitors of PKA, and mimicked by direct activators of PKA and adenylyl cyclase. Immunoprecipitates of IP_3R1 also showed an associated PKA activity, owing to the co-immunoprecipitation of PKA with IP_3R1. The functional importance of this association was explored using a cell-permeable peptide PKA-AKAP disruptor peptide; St-Ht31. St-Ht31 inhibited PGI_2-induced phosphorylation of IP_3R1 and blunted the ability of PGI_2 to inhibit the Ca^{2+} mobilisation. This suggests a role of AKAPs in regulation of Ca^{2+} mobilisation. Numerous AKAPs have been putatively identified in platelets through transcriptomics and proteomics studies. Here, we show the presence of AKAP9 in platelets. Moreover, using co-immunoprecipitation, the association of AKAP9 with PKA/IP_3R1 was also suggested. These data suggest the presence of a novel PKA/IP_3R1/AKAP9 signalling complex in platelets that may modulate intracellular Ca^{2+} mobilisation.

PAPERS

Trivedi A.N., Mahaut-Smith, M, Naseem K, (In preparation) Association of Type 1 Inositol 1,4,5-Trisphosphate Receptor type 1 (IP_3R1) with Protein Kinase A and A-Kinase Anchoring Protein 9 (AKAP9) in platelets

ORAL PRESENTATIONS

Trivedi, A.N. (2015), *Association of Type 1 Inositol 1,4,5-Trisphosphate Receptor (IP_3R1) with Protein Kinase A (PKA) and A-kinase Anchoring Protein 9 (AKAP9) in platelets*, Cell Biology of Megakaryocytes & Platelets (GRS) - From Cells to Clinics: Megakaryocytes and Platelets in Health and Disease, (19 April 2015) Tuscany, Italy

POSTER PRESENTATIONS

Trivedi, A.N. (2015), *Association of Type 1 Inositol 1,4,5-Trisphosphate Receptor (IP_3R1) with Protein Kinase A (PKA) and A-kinase Anchoring Protein 9 (AKAP9) in platelets*, Cell Biology of Megakaryocytes & Platelets (GRC) - Bridging the Divide Between Megakaryocytes and Platelets, (19-24 April 2015) Tuscany, Italy

CONTENTS

LIST OF FIGURES

Chapter V: Examination of the Potential Association of AKAP9 with IP_3R1-PKA complex

Chapter VI: General Discussion

LIST OF TABLES

ABBREVIATIONS

Abbreviation	Full form
$\alpha_2\beta_1$	Integrin alpha 2 beta 1
$\alpha_{IIb}\beta_3$	Integrin alpha 2b beta 3
ABP	Actin Binding Protein
AC	Adenylyl cyclase
ACD	Acid citrate dextrose
ADP	Adenosine 5'-diphosphate
AKAP(s)	A kinase anchoring protein(s)
AMP	Adenosine 5'-monophosphate
APS	Ammonium Persulphate
ATP	Adenosine 5'-triphosphate
BSA	Bovine serum albumin
Ca^{2+}	Calcium ion
cAMP	Cyclic adenosine 5'-monophosphate
CBD	cAMP binding domain
cGMP	Cyclic guanosine 5’-monophosphate
COX-1	Cycloxygenase-1
CRACM	Calcium Release Activated Calcium Modulator
c-subunit	PKA Catalytic subunit
C-terminal	Carboxyl-terminal
D’/D domain	Docking / Dimersation domain
DAG	Diacylglycerol
DMSO	Dimethyl sulphoxide
DTS	Dense tubular system
ECL	Enhanced chemiluminescence
ECM	Extracellular matrix
EDRF	Endothelial-derived relaxing factor
EDTA	Ethylenediaminetetraacetic acid
EGTA	Ethyleneglycoltetraacetic acid
Epac	Exchange Proteins Activated by cAMP
Fsk	Forskolin
GP	Glycoprotein
GPCR	G-protein coupled receptor
GTP	Guanosine-5'-triphosphate
H^+	Hydrogen ion
H89	Protein kinase A inhibitor

HEPES	4-(2-hydroxyethyl)-1-piperazineethanesulfonic acid
HRP	Horseradish peroxidise
IB	Immunoblot
IgG	Immunoglobulin G
IP_3	Inositol tris-phosphate
IP_3R (I, II and III)	Inositol 1,4,5 trisphosphate receptor (I, II and III)
Ip	Prostacyclin receptor
IP	Immunoprecipitation
K_d	Dissociation constant
KT5720	Cell-permeable inhibitor of PKA
MLCK	Myosin Light Chain Kinase
m/z ratio	Mass-to-charge ratio
N-terminal	Amino-terminal
NO	Nitric Oxide
NOS	Nitric Oxide Synthase
OCS	Open Cannicular System
PAGE	Polyacrylamide Gel Electrophoresis
PAR (1 and 4)	Protease activated receptor (1 and 4)
PBS	Phosphate- buffered saline
PDE	Phosphodiesterase
PGE_2	Prostaglandin E_2
PGI_2	Prostaglandin I_2, also called prostacylin
PI 3-kinase	Phosphatidylinositol 3-kinase
PIP_2	Phosphatidylinositol 4, 5-bisphosphate
PKA	Protein kinase A
PKA I	Protein kinase A type I
PKA II	Protein kinase A type II
PKC	Protein kinase C
PKG	Protein kinase G
PLA_2	Phospholipase A_2
PLCβ	Phospholipase C beta
pPKAs	Phospho-PKA substrate antibody
PRP	Platelet rich plasma
PVDF	Polyvinylidene Difluoride
R	Background-corrected 340/380nm ratios
R_{min}	Minimum 340/380 ratio
R_{max}	Maximal 340/380 ratio
R-subunit	PKA regulatory subunit
RI-subunit	PKA regulatory subunit type I
RII-subunit	PKA regulatory subunit type II

RIAD	RI anchoring disruptor
SD	Standard deviation
SEM	Standard error of mean
SDS	Sodium dodecyl sulphate
SDS-PAGE	Sodium dodecyl sulphate polyacrylamide gel electrophoresis
sGC	Soluble guanylyl cyclase
SOCE	Store Operated Calcium Entry
STIM	Stromal Interaction Molecule
TBS-T	Tris buffered saline – tween
TEMED	Tetramethylethylenediamine
TRPC	Transient Receptor Potential Channel
TxA_2	Thromboxane A_2
TxS	Thromboxane Synthase
VASP	Vasodilator-stimulated phosphoprotein
vWf	von Willebrand factor
WCL	Whole cell lysate

Amino acid Abbreviations

A	Ala	Alanine
C	Cys	Cystine
D	Asp	Aspartic Acid
E	Glu	Glutamic Acid
F	Phe	Phenylalanine
G	Gly	Glycine
H	His	Histidine
I	Ile	Isoleucine
K	Lys	Lysine
L	Leu	Leucine
M	Met	Methionine
N	Asn	Asparagine
P	Pro	Proline
Q	Gln	Glutamine
R	Arg	Arginine
S	Ser	Serine
T	Thr	Threonine
V	Val	Valine
W	Trp	Tryptophan
Y	Tyr	Tyrosine

ACKNOWLEDGEMENTS

I would like to thank Prof. Khalid Naseem for giving me the opportunity to work on this project and for providing excellent supervision throughout. I would also like to thank my co-supervisor, Dr. Simon Calaminus for his technical inputs. I acknowledge our collaborator, Prof. Martyn Mahaut-Smith and his team at the University of Leicester for allowing me to work in their laboratory. The work described in this thesis would not have been possible without the technical support and guidance provided by Prof. Mahaut-Smith and is team. I also take the opportunity to acknowledge Prof. Carmen Dessauer for providing us with the AKAP9 antibody.

I would also like to thank the post-doctoral researchers in Naseem lab, Dr. Simbarashe Magwenzi, Dr. Ahmed Aburima, Dr. Zaher Raslan, Dr. Katie Wraith, Dr. Benjamin Spurgeon and Dr. Sreemoti Banerjee for their support and guidance. On a similar note, I would like to thank my fellow PhD students, Casey Woodward, Robert Law and Kochar Walladbegi for always being available for a “quick catch-up over hot choc.” My friend and fellow PhD student, Pooja Joshi also deserves a special mention for helping me look at the bright side of the challenges of lab work. I extend many thanks to the blood donors without whom this work would not have been possible. In the same vain, I thank my examiners for taking the time to read and analyse my work and for engaging in stimulating discussions.

I would also like to thank my family and husband for supporting me in every way possible. Lastly but most importantly, I would like to thank God, the Almighty for guiding me through the good and the not-so-good times.

AUTHOR'S DECLARATION

I confirm that this work is original and that if any passage(s) or diagram(s) have been copied from academic papers, books, the Internet or any other sources these are clearly identified by the use of quotation marks and the reference(s) is fully cited. I certify that, other than where indicated, this is my own work and does not breach the regulations of HYMS, the University of Hull or the University of York regarding plagiarism or academic conduct in examinations. I have read the HYMS Code of Practice on Academic Misconduct, and state that this piece of work is my own and does not contain any unacknowledged work from any other sources. I confirm that any patient information obtained to produce this piece of work has been appropriately anonymised.

CHAPTER I - INTRODUCTION

1.1. Introduction

Platelets are anucleate cells present at concentrations of 1.5-4 x 10^8 cells/mL and have a lifespan of 7-10 days in circulation. Upon vascular injury platelets become activated and form a primary haemostatic plug to prevent excessive blood loss, although they also participate in inflammatory and wound healing responses (George 2000). However in disease states, platelets undergo inappropriate activation causing pathological thrombosis, thus obstructing the blood flow through the circulatory system as evident in stroke, angina or myocardial infarction (Gawaz 2004). This can lead to further complications such as anoxia, infarction and cell death. Aberrant platelet activation is also linked to diseases such as diabetes and atherosclerosis (Gawaz 2004; Koyama & Nishizawa 2005).

A balance between thrombogenic and anti-thrombogenic factors is required to enable normal platelet function. Nitric oxide (NO) and prostaglandin I_2 (PGI_2 or prostacyclin), released from the endothelium, play a crucial role in maintaining the platelets in quiescent state by inhibiting multiple aspects of platelet function and controlling platelet recruitment at the site of injury (Schwarz et al. 2001; Rivera et al. 2009). These endothelial-derived inhibitors regulate platelet function through the activation of cyclic nucleotide signalling pathways, which are the most potent endogenous mechanism of inhibiting platelet activation. A key target for cyclic nucleotide signalling and particularly cAMP/PKA pathway is the control of intracellular calcium (Ca^{2+}) concentrations (Smolenski 2012). The mobilisation of intracellular Ca^{2+} upon platelet activation is facilitated by phospholipase-mediated release of inositol-1,4,5 trisphosphate (IP_3). This lipid messenger then binds to inositol-1,4,5 trisphosphate receptors (IP_3Rs), which are also substrates for cyclic nucleotide signalling, to cause the release of Ca^{2+} from intracellular stores (Ferris et al. 1989)

This chapter will review literature forming the basis of current understanding of cAMP/PKA signalling, with IP_3R being the substrate of interest.

1.2. Platelet Ultrastructure

1.2.1. Platelet organelles

Although lacking a nucleus, platelets possess all the other cell organelles (*Figure 1.1*). Platelet mitochondria recognised by internal cristae, are a source of energy during platelet lifespan. Peroxisomes and lysosomes contain variety of catalases and degradative enzymes respectively and function in decomposition of pinocytosed/phogacytosied material. Platelets also possess two types of specialised granules, α-granules and dense granules. α-granules contain a range of proteins such as von Willebrand factor (vWf), fibrinogen, thrombomodulin, platelet factor 4 and clotting factors (such as Factor(F) V and FXIIIa). Clotting factors enable the activation and function of the coagulation cascade on release in response to platelet activation. Dense granules are about five times less abundant than α-granules and contain low molecular weight compounds such as adenosine tri-phosphate (ATP), adenosine di-phosphate (ADP), serotonin and Ca^{2+}. Release of dense granule contents is vital for platelet shape change during platelet activation (Frojmovic & Milton 1982).

1.2.2. Platelet membrane and cytoskeleton

Platelet plasma membrane is made up of asymmetrically distributed phospholipid bilayer, within which embedded glycoprotein (GP) receptors and other membrane proteins, that are essential for platelet activation and sub-endothelial adhesion (Shattil et al. 1998). The external leaflet of resting platelet membrane consists of mainly neutral phospholipids such as phosphotidylcholine, phosphatidylethanolamine and a small amount of sphingomyelin and sugar-linked spignolipids. The cytoplasmic leaflet however contains negatively charged phosphatidylserine and phosphatidylinositol, and neutral phosphotidylcholine and phosphatidylethanolamine (Daleke 2003; Smith 2009). The platelet cytoskeleton, primarily composed of microtubules and actin lies beneath the phospholipid bilayer and is responsible for the discoid shape of unstimulated platelets (Hartwig & Italiano 2003; Hartwig & Italiano). Molecular rearrangement of microtubules and actin is required for morphological changes upon cell activation. The platelet membrane contains a variety of

platelet agonists and adhesion receptors that mediate platelet response to agonists and causes adhesion to extracellular ligands respectively.

Figure 1.1

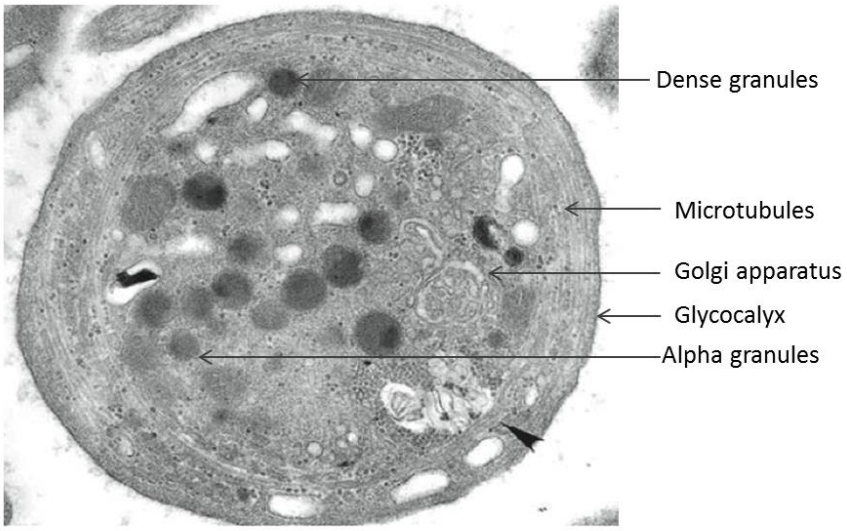

Figure 1.1 **– Equatorial cross-section showing main features of platelet ultrastructure**

The equatorial cross-section of a discoid platelet shows the main features of platelet ultrastructure. The figure shows circumferential coil of microtubules that are responsible for platelet shape change and platelet granules (α- and dense granules) that act as stores for various agonists. Golgi apparatus is also seen here, which acts as the lipid transport system across the cell (George 2000).

1.3. Platelet Activatory Signalling

A prime function of platelets is to arrest the blood flow and form a haemostatic thrombus at the site of injury. This process is initiated by a coordinated interplay between platelet membrane receptors and platelet proteins leading to adhesion of circulating blood platelets to the site of injury, followed by the formation of a haemostatic plug. This process is greatly assisted by the shear forces in the vasculature. However, in pathological state, the platelet plug formation can lead to conditions such as myocardial infarction and arterial thrombosis (Rivera et al. 2009; Woulfe et al. 2004).

1.3.1 Thrombus formation

Thrombus formation can be divided into three main stages – initiation, extension and stabilisation as detailed below. However, these stages do not occur consecutively and are to some degree integrated, with individual platelets undergoing multiple processes simultaneously (*Figure 1.2*).

1.3.1.1. Initiation

Vascular injury leads to the exposure of the extracellular matrix proteins such as vWf, collagen, fibronectin, thrombospondin-1, and laminin, which trap and activate platelets. Under high shear conditions such as those in microvasculature and stenoic arteries, vWf interacts with the exposed collagen fibres of the sub-endothelium. Here, the vWf undergoes a conformational change and is immobilised on the collagen fibres (Siedlecki et al. 1996). This initiates the binding of platelets via its receptor GPIb-IX-V, which comprises of a complex of subunits GPIbα, GPIbβ, GPV and GPIX (Modderman et al. 1992). However, this association is transient due to the high association/dissociation rate between GPIb-IX-V and vWf. The association between vWf-GPIba causes the platelets to 'roll' along the exposed sub-endothelial matrix (Savage et al. 1996). However, under low shear rates such as those in larger arteries and veins, vWf engages with integrin αIIbβ3 to form stable bonds. The tethered platelets are sufficiently slowed down to enable the engagement by platelet-

specific immunoglobulin receptor GPVI. Subsequently, these are fully activated by the binding of collagen to GPVI. Downstream signalling events induced by GPVI then drive a number of events required for platelet-mediated haemostasis including shape change, secretion, Ca^{2+} mobilisation, all of which result in platelet activation. As a result, another collagen receptor, integrin $\alpha_2\beta_1$, undergoes a conformational change and becomes activated. Activated integrin $\alpha_2\beta_1$ is responsible for platelet-ECM contact leading to platelet adhesion, whereas the activation of platelet integrins $\alpha_{IIb}\beta_3$ mediates platelet-platelet contact respectively. Consequently, a platelet monolayer is formed at the site of injury (Rivera et al. 2009; Shattil et al. 1998) (*Figure 1.2*).

1.3.1.2. Extension

Post the formation of platelet monolayer, more platelets are recruited via the process of secondary platelet activation. This facilitates platelet plug formation and this requires a number of platelet-derived secondary agonists. Activated platelets undergo degranulation to release ADP from dense granules. ADP can cause co-activation of two purinergic receptors on the platelet surface, P_2Y_1 and P_2Y_{12} (Jin & Kunapuli 1998). While P_2Y_1 is coupled to $G_{\alpha q}$ and stimulates Phospholipase C-β (PLCβ) leading to IP_3 production and intracellular Ca^{2+} mobilisation, P_2Y_{12} is coupled to $G_{\alpha i}$, and is involved in the inhibition of adenylyl cyclase (AC), thereby regulating cAMP levels in platelets (Jin et al. 1998; Daniel et al. 1998). Another key platelet agonist, thrombin is formed as a result of interaction between tissue factor from the sub-endothelium and the plasma coagulation factors from the coagulation cascade on the surface of an activated platelet (Heemskerk et al, 2002). Exposure of phosphotidylserine on the platelet membrane is initiated by the elevation of Ca^{2+} (Sims et al, 1989) and supports the formation of prothrombinase complex (Pei et al, 1993). Binding of thrombin to G-protein Coupled Receptors (GPCRs) protease-activated receptor-1 (PAR1) and protease-activated receptor-4 (PAR4) causes platelet shape change and activation (Rivera et al. 2009; Offermanns et al. 1994). Elevated levels of intracellular Ca^{2+} in activated platelets induce activation of cytosolic phospholipase A_2, which initiates the release of arachidonic acid from phosphatidylcholine, a plasma membrane lipid. Further COX-mediated hydrolysis of arachidonic acid causes the production of thromboxane A_2 (TxA_2), another platelet

agonist which binds to the thromboxane receptor (Irvine 1982; Needleman et al. 1976). ADP, thrombin and TxA_2 bind to GPCRs on the platelet surface, activate PLCβ and therefore drive Ca^{2+} mobilisation (Rivera et al. 2009). This then drives further platelet activation ultimately leading to exposure and activation of integrins such as $\alpha_{IIb}\beta_3$ by 'inside-out signalling' (Shattil et al. 1998; Stalker et al. 2012; Stalker et al. 2014).

1.3.1.3. Stabilisation

Stabilisation phase ensures the stability of thrombus. Activated integrins, especially integrin $\alpha_{IIb}\beta_3$ mediates platelet-platelet contact by enabling the formation of stable bridges between the platelets (Shattil et al. 1998; Stalker et al. 2012; Stalker et al. 2014). Integrin $\alpha_{IIb}\beta_3$ can bind to several ligands such as vWF, fibronectin and thrombospondin-1, however, $\alpha_{IIb}\beta_3$-fibrinogen binding functions as a bridge between adjacent activated platelets enabling paracrine signalling between activated platelets in the developing thrombus (Savage et al. 1992). Integrins bound to their respective ligands can further activate and recruit more platelets by the process of 'outside-in signalling' (Shattil et al. 1998; Stalker et al. 2012; Stalker et al. 2014). Furthermore, junctional adhesion molecules that support platelet-platelet and platelet-leukocyte signalling interactions also contribute to the stabilisation of the thrombus (Brass et al. 2008). Finally, the formation of a fibrin mesh on activation of coagulation cascade stabilises the thrombus (Rivera et al. 2009; Stalker et al. 2012).

Figure 1.2

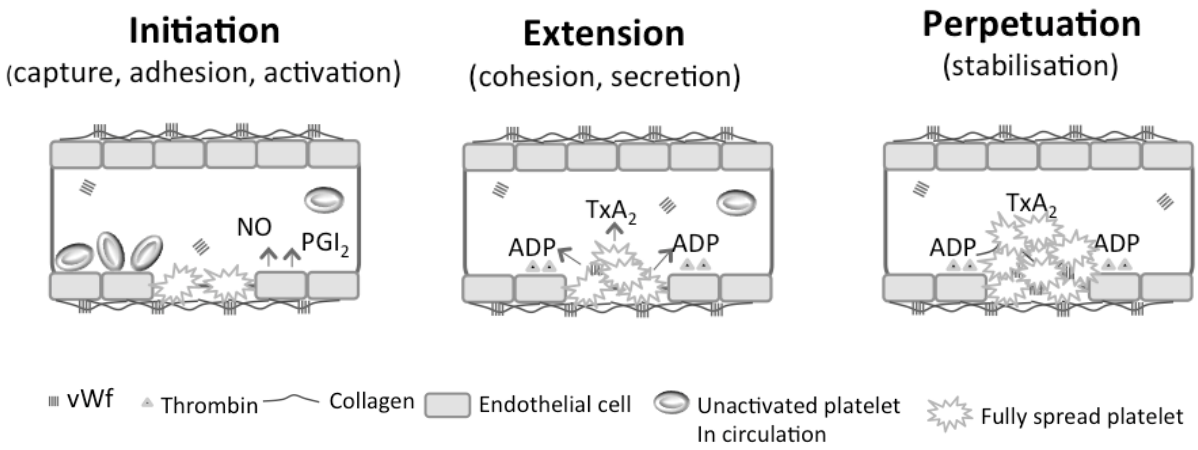

***Figure 1.2* – Stages in thrombus formation**.

In the absence of vascular injury, endothelial thromboregulatory mechanisms ensure that platelets are remain in a quiescent state. The initiation stage involves the capturing of the platelets by vWf and collagen to form a monolayer. In the extension stage, further platelet activation is caused by the release of other platelet agonists and more platelets are recruited to the growing thrombus. The stabilisation phase ensures that close contacts between platelets and the fibrin meshwork to ensure clot stabilisation. Figure redrawn from (Lawrence F. Brass, 2006).

1.3.2 Calcium signalling in platelets

Calcium ions are important second messengers that regulate numerous cell functions such as muscle contraction, apoptosis, (Parekh & Putney 2005), fertilisation (Saunders et al. 2002), megakaryocyte cytoskeletal rearrangement and cell adhesion (Di Buduo et al. 2014) and platelet activation (Hathaway & Adelstein 1979; Shattil & Brass 1987). Under resting conditions, platelets have basal Ca^{2+} levels of 50-100nM (Cancela et al. 2002) however elevation of intracellular Ca^{2+} can occur either as a consequence of introduction of extracellular Ca^{2+} through the plasma membrane or the release from compartmentalised Ca^{2+} stores (such as Dense Tubular System (DTS)).

Activation of GPVI stimulates tyrosine kinase signalling pathway, and involves subsequent activation of phospholipase C isoforms and hydrolysis of phosphoinositide-4,5-bisphosphate (PIP_2) to IP_3 and 1,2-diacyl-glycerol (DAG). (Blake et al, 1994). IP_3 diffuses through the cytoplasm to bind IP_3R. This causes the receptor activation (see §1.5) and subsequent release of Ca^{2+} from DTS (Bird et al. 2004). Although there are various organelles that function as Ca^{2+} stores, the DTS is the largest source of intracellular Ca^{2+} in platelets. For this reason, IP_3Rs, the primary Ca^{2+} release channels are also highly concentrated on DTS. Elevation in intracellular Ca^{2+} leads to platelet shape change (Hathaway & Adelstein 1979), degranulation and aggregation (Shattil & Brass 1987). DAG on the other hand, activates Non-store operated Ca^{2+} entry channels in the plasma membrane (described in §1.3.2.2). While the release of intracellular Ca^{2+} is required for platelet activation it must be kept within defined limits. To achieve this, sarcoplasmic/endoplasmic Ca^{2+}-ATPases (SERCAs) pumps act to move Ca^{2+} back into intracellular stores. SERCAs pump two molecules of Ca^{2+} for every ATP molecule hydrolysed, and is counter-transported by hydrogen ions (H^+) in exchange of Ca^{2+} (Yu et al. 1993).

1.3.2.1 Store Operated Ca^{2+} entry

Whilst there is a significant understanding of the mechanism of Ca^{2+} release from intracellular platelet stores, the process of entry of extracellular Ca^{2+} remains to be fully understood. In platelets and other non-excitable cells, IP_3-mediated elevation in intracellular

Ca^{2+} also causes the entry of extracellular Ca^{2+} by a mechanism known as Store-Operated Ca^{2+} entry (SOCE) (Putney 2007). Ca^{2+} sensor molecule called *Stromal Interaction Molecule 1* (STIM1) is known to initiate SOC channel opening in response to elevation of intracellular Ca^{2+} (Liou et al. 2005; Zhang et al. 2005). Mice bearing mutations in STIM1 displayed elevated basal Ca^{2+} levels and premature platelet activation as a result of perpetually open SOC channels (Grosse et al. 2007). Furthermore, platelets from STIM1 knock-out mice displayed severely compromised functional response to stimulatory agonists, and unaltered $\alpha_{IIb}\beta_3$ activation (Varga-Szabo et al., 2008). In addition to STIM1, *calcium-release activated calcium modulator* (CRACM or Orai1), is crucial for regulation of SOCE in platelets. Orai1 multimerises and interacts with STIM1, whereas the extracellular residues form a part of the ion-selective pore (Vig et al. 2006). Orai1 is widely expressed in platelets. Similar to STIM1 knockout in the platelets, knockout of Orai1 abolishes SOCE and reduces intracellular Ca^{2+} elevation evoked by ADP, thrombin and CRP (Braun et al., 2009). However, unlike STIM1, Orai1 is not required for maintenance of Ca^{2+} in stores. Additionally, in these mice, thrombus formation is also compromised under flow (Braun et al. 2009; Authi 2009). These findings establish STIM1 and Orai1 to be key players in regulation of SOCE in platelets, with STIM1 being the sensor that detects mobilisation of Ca^{2+} from intracellular stores and regulates Orai1. Overall, these reports stress the importance of SOCE in maintenance of platelet function.

Transient Receptor Potential channels (TRPC) are candidate store operated Ca^{2+} (SOC) channels in platelets. Electrophysiological studies which have shown diminished SOCE on pharmacological inhibition of TRPC (Carter et al. 2006; Authi., 2007). Over 20 TRP genes have been reported in mammals. The TRP proteins can be further divided into three main groups – TRPM, TRPV and TRPC (Clapham et al. 2001). Of these groups, the TRPC proteins are predominant in platelets, with TRPC1-4 and TRPC6 reported in platelets and megakaryocytes (Berg et al. 1997; den Dekker et al. 2001; Rosado & Sage 2000). TRPC1 is localised to lipid rafts in the platelet plasma membrane (Brownlow & Sage 2005), however conflicting reports suggest it being present in miniscule amounts on platelet internal membranes (Hassock et al. 2016; Varga-Szabo, Authi, et al. 2008). Although there have been suggestions of coupling between IP_3R and TRPCs, the precise regulation of SOCE remains to be fully understood (Rosado & Sage 2000).

Figure 1.3

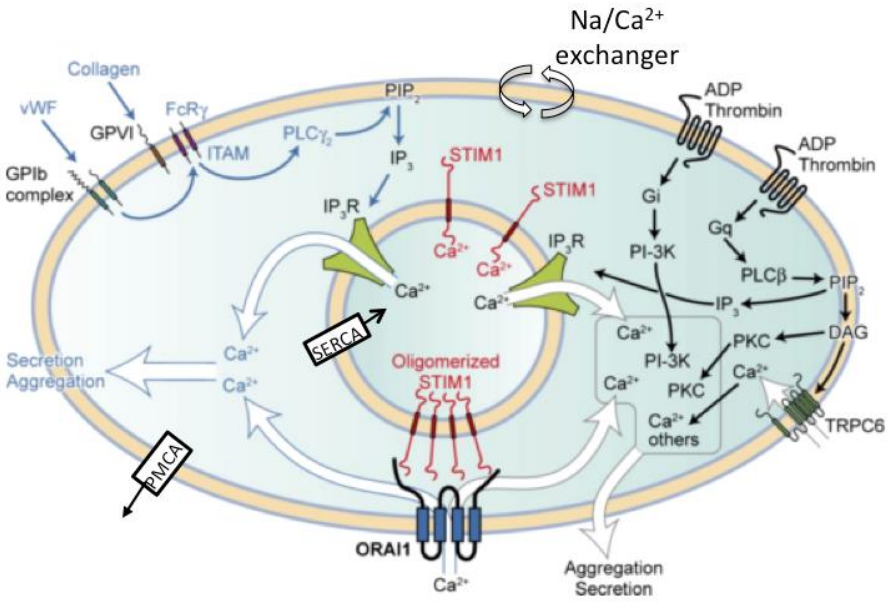

***Figure 1.3* – Calcium signalling pathways in platelets**

Ca^{2+} signalling lies at the core of platelet activation, therefore understanding these mechanisms is essential. As shown in the figure, all agonists that activate PLC contribute to the production of IP_3. The subsequent elevation of cytosolic Ca^{2+} is a consequence of release through IP_3R. The further triggers the entry of Ca^{2+} from extracellular stores known as the store operated Ca^{2+} entry (SOCE). STIM1, is the Ca^{2+} sensor molecule that primarily regulates SOCE by regulation of *Orai1* channels. Furthermore, TRPC6 regulated by DAG is the primary mediator of non-SOCE. Apart from these, PCMA (Receptor-mediated Ca^{2+} entry) occurs directly through P2X receptor which is activated by the binding of ATP. It has been suggested that P2X receptor plays an important role in amplification of low concentration agonist-mediated responses. Figure adapted from Authi (2009)

1.3.2.2. Non-store operated Ca^{2+} entry

A group of selective cation channels, called the TRPC channels, are responsible for the non-store operated Ca^{2+} entry (non-SOCE) in platelets. Their mechanism of activation is poorly understood, however some reports suggest TRPC6, found in platelets undergoes activation in response to DAG, a product of PLCβ-mediated hydrolysis of PIP_2 (Berridge et al. 2003b; Hassock 2002). TRPC6 is also a substrate for PKA, however Ca^{2+} response is independent of the phosphorylation status of the protein (Hassock 2002). These findings suggest TRPC6 to be the primary mediator of non-SOCE in platelets (Varga-Szabo et al. 2009; Hassock 2002). However, contrasting reports suggest the involvement of TRPC6 with both non-SOCE and SOCE (Jardín et al. 2008). The precise mechanisms of non-SOCE remain elusive and require further research in this area.

1.3.2.3. Receptor Operated Ca^{2+} entry

In platelets, direct receptor operated Ca^{2+} entry occurs through the P2X receptor (MacKenzie et al. 1996) which is activated by the binding of ATP. It has been suggested that P2X receptor plays an important role in amplification of low concentration agonist-mediated responses. Platelets from P2X transgenic mice display compromised aggregation and degranulation in response to low dose of collagen, whereas normal responses were observed at higher agonist concentrations. Furthermore, platelets from P2X knockout mice display weak thrombus forming capacity (Hechler et al. 2003; Fung et al. 2012).

To summarise, platelet activatory pathways cause an elevation in intracellular Ca^{2+}. This occurs either by mobilisation of Ca^{2+} from the stores (such as DTS) or initiating the influx of Ca^{2+} from outside medium. However, the crux of Ca^{2+} signalling pathways lies in the activation of PLC, leading to the formation of IP_3 and DAG. Both IP_3 and DAG contribute to further signalling pathways as described in §1.3. Ca^{2+} signalling as it lies at the core of platelet activation, therefore understanding these mechanisms is essential. Additionally, this would aid a better understanding of platelet inhibitory mechanisms that primarily focus regulating the levels of intracellular Ca^{2+}.

1.4. Platelet regulation by endothelium

The endothelium can limit the thrombus size and growth by a group of responses termed as endothelial thromboregulation. Control of platelet function by NO, PGI_2 and CD39 is crucial in early stages of thromboregulatory mechanisms (Marcus & Safier 1993; Clemetson 1999).

1.4.1. Platelet regulation by NO

NO is produced by intact endothelial cells and biosynthesised by family of enzymes called nitric oxide synthase (NOS) (Furchgott & Zawadzki 1980). NOS enzymes oxidise L-arginine, their initial substrate to produce L-citrulline and NO (Radomski et al. 1990). NOS exists in three differentially expressed isoforms including neuronal NOS (NOS I), inducible NOS (NOS II) and endothelial NOS (NOS III) (Hanafy et al., 2001). Most of the NO produced in the endothelial cells diffuses into the vascular system, although small amounts of NO are described in platelets (Mehta et al. 1995). Platelet NOS III is reported to be Ca^{2+}-dependant, and its activity can potentiate in response to ADP and arachidonic acid (Radomski et al. 1990).

NO can diffuse through the membrane to bind to its intracellular receptor soluble guanylyl cyclase (sGC) (Bellamy & Garthwaite, 2002) to cause a conformational change, which increases its catalytic activity. This initiates the hydrolysis of guanosine 5'-triphosphate (GTP) to cyclic guanosine 5'-monophosphate (cGMP) causing an increase in platelet cGMP levels (*Figure 1.6*). cGMP, a second messenger acts via effectors such as phosphodiesterases (PDE) and ion-gated channels, however Protein Kinase G (PKG) is its main effector (Naseem & Roberts, 2011). PKG, a member of AGC kinase family, is composed of three functional domains – the N-terminal domain, a regulatory domain and the catalytic domain. The regulatory domain comprises of two cGMP-binding sites; occupation of both of which induces a conformational change and subsequent activation of the enzyme (Hofmann, 2005). There are two isoforms of PKG – PKGI and PKGII, however PKGI is more abundant in platelets. The PKG isoforms differ in their N-terminal domain, rendering them differential substrate specificity (Hofmann, 2005). Activated PKG is capable of phosphorylating serine/threonine residues of several substrates and consequently causing platelet inhibition

(Bult et al. 1988). PKG-deficient mice are shown to exhibit increased prothrombotic phenotype (Massberg et al., 1999). Platelet-specific sGC-knock-out mice also display a compromised platelet aggregation (Zhang et al. 2011). However, it is important to appreciate that in platelets, NO-induced cAMP signalling is also being complemented by PGI_2-induced cAMP signalling (as described in §1.4.2), therefore forming the core of the platelet inhibitory mechanisms.

1.4.2. Platelet regulation by PGI_2

PGI_2 is a potent vasodilator and physiological platelet inhibitor, with a half-life of 3 minutes under physiological conditions (Vane & Botting 1995). In platelets, Ca^{2+} dependent cytosolic PLA_2 hydrolyses the membrane phospholipids at *Sn-2* position forming Arachidonic Acid and lyso-lipids (Irvine 1982). The arachidonic acid can be oxidised by platelet cyclooxygenase 1 (COX1) to prostaglandin G_2 (PGG_2). PGG_2 can be further reduced to unstable prostaglandin endoperoxide H_2 (PGH_2) via the hydroperoxide activity of the same enzyme. PGH_2 can be converted to prostaglandin E_2, prostaglandin D_2, prostaglandin $F_{2\alpha}$, PGI_2, and TxA_2 by a variety of synthases. Platelets lack prostacyclin synthase (PGIS), but do contain thromboxane synthase (TxS) which converts PGH_2 to TxA_2 (Needleman et al. 1976). Endothelial cells are rich in PGIS enzyme, which converts PGH_2 to PGI_2 (*Figure 1.3*), which is later released in the blood stream (Vane & Botting 1995). PGI_2 can then bind to its receptor, which causes activation of AC and activates cAMP signalling pathway as described in detailed in §1.5.

PGI_2 is the most potent physiological platelet inhibitor (Weksler et al. 1977; Moncada et al. 1976; Moncada, 1982) and vasodilator (Parente & Perretti 2003). Reduced levels of PGI_2 are associated with cardiovascular conditions such as myocardial infarction (Stein et al.; Akopov et al. 1993), stroke and atherosclerosis (Narumiya et al. 1999; Gawaz 2004). PGI_2 production is shown to be upregulated in atherosclerotic mice and during platelet aggregation (FitzGerald et al. 1984). Knocking-out the *PGIS* gene, that encodes the PGI_2 receptor, causes the mice to become hypertensive and susceptible to vascular disorders (Yokoyama et al. 2002). Furthermore, a reduction in PGI_2 production is also implicated in the pathogenesis of pulmonary hypertension (Rubin 1995). Similarly, vascular disease patients also display a

decreased sensitivity to PGI_2 (Sinzinger et al. 1981; Fitscha et al. 1985). It has been suggested that the effects are seen as a result of loss of regulatory mechanisms of PGI_2 (Yang et al. 2002; Murata et al. 1997).

1.4.2.1. PGI_2 receptor

The PGI_2 receptor (Ip) belongs to the prostanoid family of GPCRs and is present on the plasma membrane of platelets and smooth muscle cells (Narumiya et al. 1999). The Ip receptor undergoes several post-translational modifications such as phosphorylation (Smyth et al. 1998; Smyth et al. 1996), glycosylation (Zhang et al. 2001) and isoprenyl modification (Hayes et al. 1999). While the receptor glycosylation is reported to be associated with ligand binding and down-stream signalling (Zhang et al. 2001), Protein Kinase C-mediated phosphorylation at ser328 causes receptor desensitisation (Smyth et al. 1998; Smyth et al. 1996). The C-terminal of the Ip receptor undergoes isoprenyl modification, which enables coupling to AC (Smyth & FitzGerald 2002) and inhibits Ca^{2+} mobilisation (Hayes et al. 1999), therefore aiding cAMP accumulation.

The Ip receptor consists of seven transmembrane domains with a short extended N-terminal and a long C-terminal region, which houses the PGI_2-binding pocket. Domains VI and VII specifically recognise the side chains of PGI_2, whereas transmembrane domains I and II recognise the cyclopentane ring of the prostanoids. Apart from PGI_2, the Ip receptor also recognises PGE_2 and β-adrenergic agents and binds with PGI_2 analogues such as iloprost and cicaprost with the same affinity as PGI_2 (Smyth & FitzGerald 2002; Narumiya et al. 1999). Platelets from mice deficient in Ip receptor display increased thrombotic potential perhaps caused by the loss of platelet regulatory machinery (Yang et al. 2002). Patients lacking Ip receptor also display increased susceptibility to angiogenesis and diminished PGI_2-induced platelet inhibition (Kahn et al. 1996), therefore stressing the importance of Ip receptor and PGI_2 as a regulator of platelet activation.

Figure 1.4

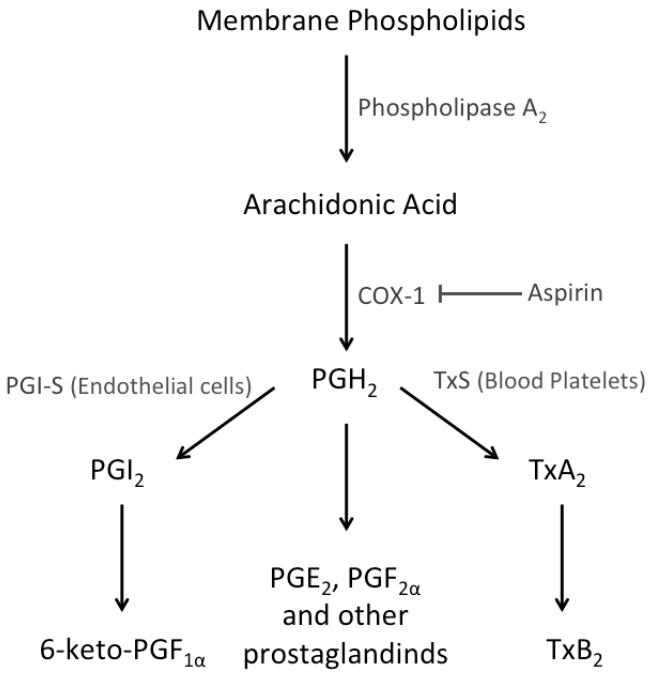

***Figure 1.4* – Cascade showing Arachidonic Acid metabolism along the COX pathway**

PLA_2-mediated hydrolysis of membrane phospholipids causes the production of Arachiodnic Acid, which is metabolised by Cycloxygenase -1 (COX1) to produce Prostaglandin H_2. In blood platelets, thromboxane synthase (TxS) converts PGH_2 to TxA_2, and subsequently to TxB_2 (the stable isoform of TxA_2). PGH_2 is converted to PGI_2 in endothelial cells in the presence of Prostacyclin synthase enzyme.

1.5. cAMP/PKA signalling pathway

The binding of PGI_2 to the platelet Ip receptor causes the activation of the stimulatory $G_{\alpha s}$ subunit of the receptor. Activated $G_{\alpha s}$ binds to AC which hydrolyses the ATP to form cAMP (Hurley 1999). Nine differentially expressed isoforms of AC have been described, however only – AC3, AC6 and AC7 have been reported to be present in platelets, with AC5/6 being the most abundant in platelets (Rowley et al. 2011; Burkhart et al. 2014). All AC isoforms share structural homology and are composed of two clusters of six transmembrane domains each (TM_1 and TM_2) and cytoplasmic domains (C_1 and C_2) each (Krupinski et al. 1989; Hanoune & Defer 2001). The transmembrane domains are restricting AC to membranes, whereas the interaction between C_1 and C_2 forms the catalytic core (*Figure 1.5*) (Artymiuk et al. 1997; Hurley 1999).

ACs have three nucleotide binding sites and Mg^{2+} binding site; occupation of all the binding sites causes the hydrolysis of ATP to cAMP. The precise mechanism of conversion of ATP to cAMP remains to be fully understood, however the interaction of Lys-923 and Asp-1000 with the purine ring of the ATP molecule renders AC specificity to ATP (Liu et al. 1997) (*Figure 1.5*). cAMP subsequently binds to the cAMP-binding regions of PKA and activates it causing consequent transfer of gamma-phosphate, which causes the phosphorylation of numerous substrates in platelets (*Figure 1.5*). cAMP-mediaited substrate phosphorylation is thought to be the mechanism by which platelet function is regulated.

Forskolin, a plant-derived compound is also an activator of GPCR-coupled ACs. Forskolin causes several hydrophobic and hydrogen bonding interactions between the C_1 and C_2 domains of the catalytic core, thereby activating AC (Artymiuk et al. 1997; Hurley 1999). The Forskolin-binding residues are conserved across all the AC isoforms except AC9, which renders it insensitive to Forskolin (Hurley 1999).

Figure 1.5

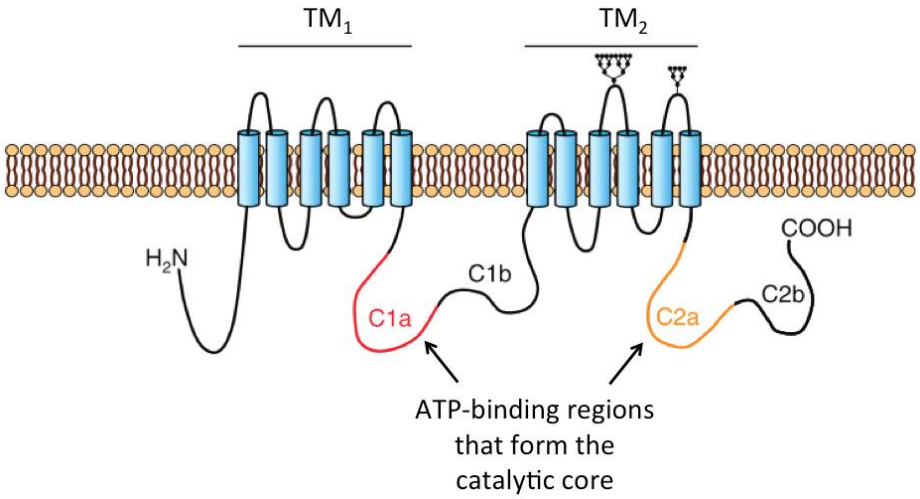

***Figure 1.5* – General structure of adenylyl cyclase**

The illustration shows the general structure of adenylyl cyclase, composed of two clusters (TM_1 and TM_2) of 6 transmembrane domains each (shown in blue) and two cytoplasmic domains (C_1 and C_2). The cytoplasmic domains form the catalytic core, where the ATP binds to C1a (shown in red) and C2b (shown in orange), before being converted to cAMP. Illustration adapted from (Willoughby & Cooper 2007).

1.5.1 Termination of cyclic nucleotide signalling by phosphodiesterase (PDEs)

PDEs are a family of enzymes that regulate cAMP signalling by hydrolysing the 5' phosphodiester bonds on cyclic nucleotides converting them to inactive 5'-nucleotide metabolites (Omori and Kotera, 2007). There are 11 types of PDEs reported (Bender & Beavo 2006), but platelets are known to express only PDE2, PDE3 and PDE5 (Haslam et al. 1999; Omori & Kotera 2007). The enzymatic activity and subcellular localisation of PDEs is regulated by the N-terminal domain, whereas the C-terminal domains render specificity towards cyclic nucleotides (Omori & Kotera 2007).

Platelets express cGMP-stimulated PDE2, which can hydrolyse both cAMP and cGMP with equal affinity. PDE3A is inhibited by cGMP and has a 10-fold higher preference towards hydrolysis of cAMP over cGMP. PDE5 activity is exclusive to cGMP (*Figure 1.6*) (Haslam et al. 1999). The precise contribution of each PDE isoform in regulating platelet function remains unclear. However PDE3A, the most abundant of the three PDE isoforms found in platelets (Shakur et al. 2001), has been suggested to be a major player in platelet regulation (Manns et al. 2002). Studies in platelets first suggested that cGMP acts as a competitive inhibitor of PDE3, thereby increasing the levels of cAMP and mediating platelet inhibition (Maurice & Haslam 1990). This could perhaps be an evolutionary mechanism to control the levels of cGMP so as to allow for cAMP binding to PDE3 (Maurice & Haslam 1990). Inhibiting PDE3 using pharmacological inhibitors has been shown to inhibit platelet aggregation and Ca^{2+} mobilisation (Manns et al. 2002). Furthermore, inhibition of PDE3A is also associated with increased PKA activity and Vasodilator-stimulated phosphoprotein (VASP) phosphorylation at ser157 (Manns et al. 2002).

Although PDE3 is the primary regulator of PKA signalling pathway, cross-talk between cGMP and cAMP is not uncommon. For example, PDE2 is activated in response to high levels of cGMP, and hydrolyses cAMP (Dickinson et al. 1997; Dunkern & Hatzelmann 2005). However, PDE2 inhibitors alone have a little effect on platelet function (Manns et al. 2002). Contrarily, treatment with PDE3 inhibitors effectively compromise platelet aggregation (Shakur et al. 2001). PDE5 activation is thought to potentiate the effects of NO therefore blunting platelet aggregation and secretion response (Ito et al. 1996; Dunkern & Hatzelmann 2005).

Figure 1.6

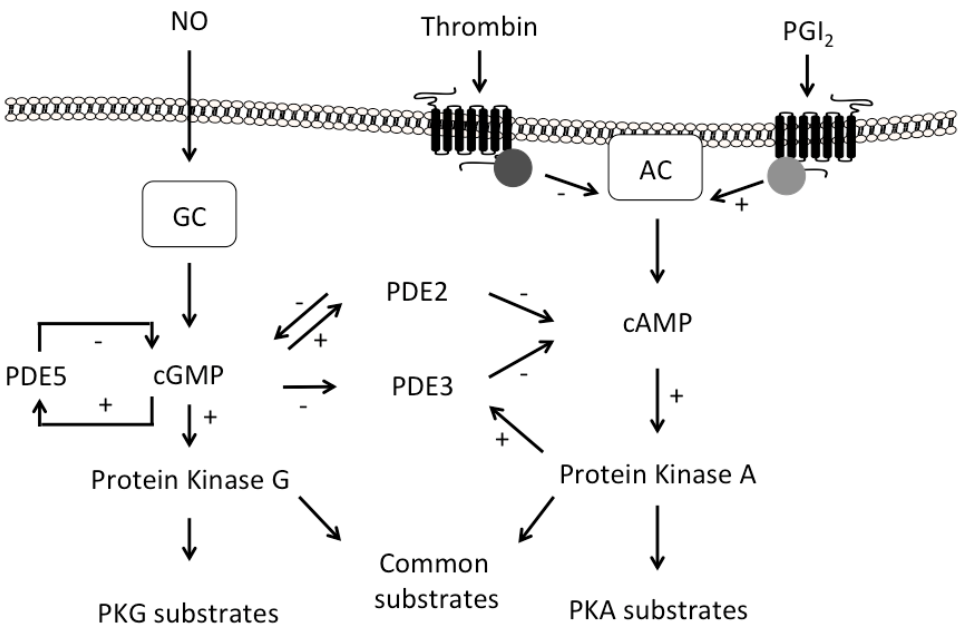

***Figure 1.6* – Cyclic nucleotide signalling pathway**

A schematic showing the pathways showing cGMP and cAMP pathways. Figure adapted from (Schwarz et al. 2001).

1.5.2. Protein Kinase A

In the absence of cAMP, PKA is a heterotetramer composed of a dimer of regulatory subunits (R-subunits) held together by two catalytic subunits (c-subunits). Four molecules of cAMP bind cooperatively at the cAMP-binding sites on the regulatory subunits, which unleashes the active catalytic subunits which phosphorylate the ser and thr residues of substrates (*Figure 1.7*) (Skalhegg & Tasken 2000). There are two isoforms of the R-subunits, RI and RII, which give rise to two types of PKA termed PKA-I and PKA-II depending on which R-subunits are present (Corbin et al. 1975; Potter et al. 1979). PKA-I is more sensitive to cAMP and mostly cytosolic whereas PKA-II is associated with membrane/organelles and is less sensitive to cAMP (Skalhegg & Tasken 2000). Furthermore, multiple differentially expressed isoforms of PKA subunits have been identified - RIα, RIβ, RIIα, RIIβ, Cα, Cβ and Cγ. These subunits can form homo- or heterodimers, therefore giving rise to different isoforms of PKA. However, the platelets are most abundant in RIβ and RIIβ (Rowley et al. 2011; Beck et al. 2012). The extent to which different PKA isoforms contribute to platelet regulation is still unknown.

Although there are various isoforms of the R-subunits, they share the same general structure. The C-terminal region of R-subunits has a dimerization domain responsible for enabling interaction with the c-subunits, whereas the N-terminal houses the docking/dimerization (D/D') domain, a PKA inhibitor site and two cAMP binding sites (CBD) called site A and B respectively (Heller et al. 2004). Each CBD has a phosphate binding cassette, where the ribose phosphate of cAMP molecule anchors (Taylor et al. 2008). The D/D' domain is connected to the CBD-A via a linker sequence containing putative autophosphorylation site in RII-subunit (Martin et al. 2007) and a pseudo-phosphorylation site for RI-subunit (Kim et al. 2007). The D/D' domain and cAMP binding regions are conserved across isoforms (Canaves & Taylor 2002) but the linker sequence is highly variable (*Figure 1.7*) (Vigil et al. 2006).

PKA c-subunit structure comprises of N-terminal lobe, a short linker sequence and a large helical C-terminal lobe. The N-terminal of catalytic subunit is involved in Mg-ATP binding, whereas the C-terminal brings about the catalytic reaction and houses the substrate binding sequence. The C-terminal tail forms a part of the active site and is highly conserved,

whereas the N-terminal tail is responsible for membrane interactions and is therefore controls the localisation of PKA. The N-terminal and C-terminal tails are also responsible for orientating the catalytic core in the optimal position for catalysis (*Figure 1.7*) (Taylor et al. 2008). In the unactivated form of PKA, only CBD-B is exposed, binding of cAMP to which then causes a conformational change that exposes CBD-A. Binding of cAMP to this site causes a conformational change exposing the site A, where the cAMP binds in a positively cooperative manner and causes PKA activation (Kim et al. 2007; Potter et al. 1979; Skalhegg & Tasken 2000). On PKA activation, the c-subunits can become activated and phosphorylate the substrates containing the consensus motif (Arg-Arg-X-Ser/Thr, Arg-Lys-X-Ser/Thr, Lys-Arg-X-Ser/Thr or Lys-Lys-X-Ser/Thr) (Taylor et al. 2008). There is an incomplete understanding of the re-association of the R-subunits and c-subunits post PKA activation, however certain reports suggest dephosphorylation of RII can cause regeneration of PKA holoenzyme (Oliveria et al. 2007).

Several pharmacological compounds are available that exploit the structural hallmarks of PKA and compromise its ability to function. Compounds KT5720, synthesised from fungus *Nocardiopsis* sp and H89, isoquinoline derivative acts as a competitive antagonists for the ATP-binding site on the PKA catalytic subunit (Kase et al. 1987; Chijiwa et al. 1990). Blockage of the ATP-binding site on the catalytic subunit prevents it from phosphorylating the relevant ser/thr residues, therefore inhibiting its function. PKA can also be inhibited by using compounds such as *Rp*-adenosine-3',5'-cyclic monophosphorothioate (*Rp*-cAMPS) that compete for the cAMP-binding site on the regulatory subunit of PKA, therefore preventing enzyme activation (de Wit et al. 1984). These pharmacological compounds can be essential tools to dissect and study PKA signalling pathway.

Figure 1.7

a

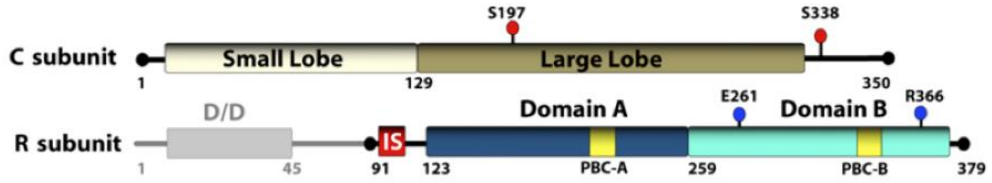

b

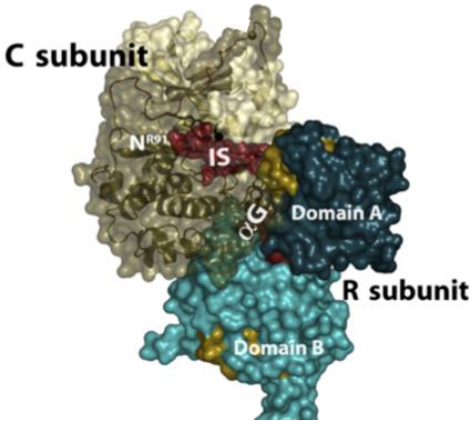

c

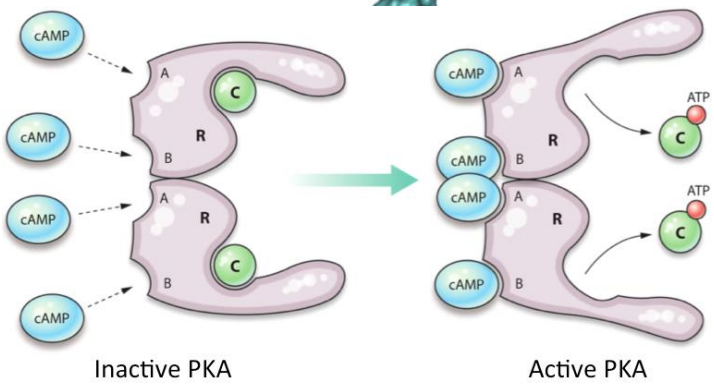

***Figure 1.7* – Overview of structure of Protein Kinase A holoenzyme**

The illustration shows the structure of PKA holoenzyme, whereby the catalytic subunit (shown in pale dirty green) is bound to regulatory subunit (shown in teal). The PBC domains are shown in yellow and the inhibitor sequence is shown in dark red. The structure of regulatory and catalytic subunits in (a) and the structure of the holoenzyme is shown in (b). Figure adapted from (Kim et al. 2007). (c) Cartoon showing the PKA holoenzyme in its inactive and active state. Binding of cAMP molecules shown in blue to regulatory subunits (shown in lilac) unleashes catalytic subunits (shown in green), which can phosphorylate the PKA substrates. Figure adapted from (Murray 2008).

1.5.2.1. Protein Kinase A substrates in platelets

Phosphorylation is a key regulatory mechanism in cells. Enhanced phosphorylation seen in genetic conditions (Cohen 2001) and cancers (Radivojac et al. 2008) highlights the importance of reversible phosphorylation in cells. In other cell types, the downstream effects of cAMP are mediated by exchange proteins activated by cAMP (Epac)(de Rooij et al. 1998), cyclic nucleotide-gated ion channels (Nakamura & Gold 1987) and PKA (Hayes & Mayer 1981). In contrast, platelet cAMP signalling is thought to be exclusively mediated through PKA, due to the miniscule levels of cAMP activated Epac and the absence of cyclic nucleotide gated ions channels (Schmidt, et al, 2013; Schwarz et al. 2001). To date it is thought that PKA-mediated substrate phosphorylation functions as an inhibitory mechanism in platelets. Phosphorylation of PKA substrates (as listed in *Table 1.1*) inhibits platelet activation by compromising Ca^{2+} elevation or cytoskeletal rearrangement and granule secretion (Schwarz et al. 2001).

As described in §1.3, integrin αIIbβ3 plays a vital role in platelet activation. In the process, several cytoskeletal proteins participate in signalling pathways leading to actin polymerisation and cytoskeletal rearrangement. For example, VASP a well-established membrane-bound PKA substrate, is involved with regulation of actin polymerisation in cells (Harbeck et al. 2000). PKA-phosphorylation of VASP at ser157 suppresses VASP binding to F-actin and actin polymerisation. Furthermore, VASP phosphorylation at ser157 correlates with down-regulation of fibrinogen receptor (αIIbβ3) (Horstrup et al. 1994). Furthermore, platelets from VASP knockout mice show impaired aggregation response (Aszódi et al. 1999), suggesting the importance of VASP in platelet regulation.

In addition to VASP, there are other PKA substrate proteins involved in regulation of platelet cytoskeletal rearrangement. One such protein is Caldesmon, which binds actin and aids its translocation (Hettasch & Sellers 1991; Hemric et al. 1994). PKA-mediated phosphorylation of Caldesmon helps stabilise platelet cytoskeleton and control platelet activation (Hettasch & Sellers 1991). Another cytoskeletal protein, Actin-binding protein (ABP) is involved in stabilisation of actin filaments during platelet activation. It is also a reported PKA substrate (Chen & Strachers 1989). PKA-mediated phosphorylation of ABP is reported to stabilise the protein and protect from further ADP-induced fibrinogen binding (Chen & Stracher 1989;

Bennett et al. 1999). In addition to these, other platelet cytoskeletal proteins such as Myosin light chain kinase (MLCK) (Nishikawa et al. 1984) and RhoA (Aburima et al. 2013) are also substrate for PKA (*Table 1.1*). PGE_1-mediated activation of cAMP-signalling pathway caused a time and concentration-dependant phosphorylation of RhoA at ser188 (Aburima et al. 2013). The importance of RhoA as a physiological substrate is highlighted by reports suggesting altered shape change, diminished response to $G_{\alpha q}$ agonists and compromised clot retraction response in megakaryocyte-specific RhoA knockout mice (Pleines et al. 2012). Similarly, knocking out MLCK gene results in impaired cytoskeletal reorganisation in response to fibrinogen-binding (Tournoij et al. 2010).

In addition to cytoskeletal proteins, an intracellular Ca^{2+} channel protein, IP_3R is also reported to be a substrate for PKA (Ferris et al. 1991). On agonist-stimulated platelet activation, IP_3 is generated, which binds to IP_3R and activates it. This causes the channel to open leading to elevation in intracellular Ca^{2+}. However, PKA-mediated phosphorylation is reported to interfere with this, therefore supporting platelet inhibitory pathways (Cavallini et al. 1996). PKA-mediated phosphorylation is the focus of the work described here and is discussed in more detail in Section §1.6, Chapter V.

Table 1.1

Protein	M.W. (kDa)	Proposed role of substrate phosphorylation	Reference
ABP	240	Stabilisation of platelet cytoskeleton	(Chen & Strachers 1989)
Caldesmon	82	Stabilisation of platelet cytoskeleton	(Hettasch & Sellers 1991)
$G\alpha_{13}$	44	Inhibits TxA_2 induced aggregation	(Manganello et al. 1999)
GP1bβ	24	Inhibition of collagen-induced actin polymerisation and platelet-vWf binding	(Fox & Berndt 1989)
Hsp27	27	Reduced actin polymerisation	(Butt et al. 2001)
IP_3R	313	Inhibition of $[Ca^{2+}]_i$ release via IP_3R	(Cavallini et al. 1996)
MLCK	105	Unknown	(Nishikawa et al. 1984)
PDE3A	110	Degradation of cAMP	(Macphee et al. 1988)
Rap1b	22	Unknown	(Altschuler & Lapetina 1993; Lapetina et al. 1989)
Rho A	22	Regulation of actin dynamics	(Aburima et al. 2013)
TP	50	Inhibition of TxA_2 associated G protein activation	(Reid & Kinsella 2003)
VASP	46/50	Regulation of actin dynamics	(Horstrup et al. 1994)

***Table 1.1* – Summary of PKA substrates in platelets**

The table lists the PKA substrates identified till date, with the proposed role of phosphorylation. The substrate(s) are group based on the proposed mechanism of platelet inhibition. The substrate(s) highlighted in pale red inhibit platelets by compromising of Ca^{2+} elevation, those highlighted in grey regulate cytoskeletal rearrangement. The substrates shown in blue limit the activity of GPCRs and TxA_2 receptor. Table adapted from (Schwarz et al. 2001; Smolenski 2012).

1.6. Inositol 1,4,5 tris-phosphate receptor (IP_3R)

While a number of PKA substrates have been identified in platelets, their precise role in platelet function is unclear. IP_3R1 is reported to be a substrate for PKA (Ferris et al. 1991). Since cAMP signalling is a potent regulator of intracellular Ca^{2+} concentrations (Ferris et al. 1989; Ferris et al. 1991), it is important to understand how this occurs. The IP_3 system (described in §1.3.2.) is critical to Ca^{2+} mobilisation and therefore understanding its regulation by cAMP signalling is important to how platelet function is modulated.

IP_3R was first purified from brain tissue. Its reconstitution in lipid vesicles led to its characterisation as an IP_3-binding Ca^{2+} release channel (Patterson et al. 2004). In mammals, three types of IP_3Rs – IP_3R1, IP_3R2 and IP_3R3 encoded by *ITPR1*, *ITPR2* and *ITPR3* genes respectively have been reported (Nakagawa et al. 1991). All the three subtypes are structurally homologous. Despite this, the receptors are differentially expressed, with IP_3R1 being the most highly expressed of the three isoforms in platelets (El-Daher et al., 2000) and the focus of this work. The three subtypes of IP_3Rs have subtle functional differences, and exhibit differential levels of PKA-mediated phosphorylation (Wojcikiewicz & Luo, 1998). Transfection studies reveal that IP_3Rs also differ in their affinity towards the ligand, IP_3. It has been shown that IP_3R2 and IP_3R3 having the highest and lowest affinity respectively towards IP_3, irrespective of this IP_3-binding to the receptor causes the channel to open and cause release of intracellular Ca^{2+} (Newton et al. 1994).

Apart from these three IP_3R subtypes, *ITPR1* undergoes alternative splicing therefore generating IP_3R1 SII+ and SII- splice variants (*Figure 1.8*). SII+ is the longer isoform and is predominantly found in brain, whereas SII- variant is localised in neuronal tissues (Danoff et al. 1991). No difference in the Ca^{2+} or IP_3-regulation between the splice variants is observed (Tu et al. 2002; Boehning et al. 2001), although these undergo differential PKA-mediated phosphorylation (Danoff et al. 1991). Genetic ablation studies suggest functional redundancy between IP_3R isoforms. Deletion of IP_3R1 can be embryonic lethal in mice but IP_3R2 and IP_3R3 knockout mice are viable (Patterson et al., 2004). However, B-lymphocytes deficient in IP_3R1 and IP_3R2 were able to generate Ca^{2+} signals suggesting that these were functioning only on IP_3R3. Conversely, Ca^{2+} signals remained unaltered in B-lymphocytes lacking only IP_3R3 (Sugawara et al. 1997). The physiological significance of the presence of

multiple subtypes and splice variants of IP_3R can be explained by the findings that suggest differential expression of these receptors at different time points during cellular development in mammals (Vermassen et al. 2004; Foskett et al. 2007), however the precise receptor expression patterns during platelet development remain to be studied.

1.6.1 Structure of IP_3R

Functional IP_3Rs are formed of four subunits; with each subunit comprising 2700 residues (Taylor et al. 1999; Foskett et al. 2007). The primary structure of the IP_3Rs comprise of N-terminal ligand binding domains, C-terminal channel domain and the modulatory domain. The C-terminal channel region houses six membrane-spanning helices with the C-terminal projecting towards the cytoplasm (Jiang et al. 2002; Nakade et al. 1991). The receptor selectivity filter is comprised of Gly-Val-Gly-Asp residues of which Asp2550 is vital for Ca^{2+} selectivity (Boehning et al. 2001). First 788 amino acids of the N-terminal bind to IP_3, although mutational analysis shows multiple ligand-binding sites on the N-terminal region. The charged IP_3 molecule interacts with positively charged amino acids; this makes the tertiary structure of the receptor to be crucial in defining the ligand-binding pocket (Yoshikawa et al. 1996; Yoshikawa et al. 1999). The N-terminal of the channel directly binds to the C-terminus of the adjacent subunit of the tetramer (Boehning & Joseph 2000). However, its functional consequence remains to be understood. The modulatory domain of the receptor lies between N- and C-terminal regions and is the least conserved of the regions across IP_3R subtypes (Patterson et al., 2004). The channel pore is relatively separated from the N-terminal, which means that IP_3-binding induces a significant conformational alteration to stimulate Ca^{2+} channel activity (*Figure 1.8*) (Mignery & Südhof 1990).

1.6.2. Regulation of IP_3R

IP_3 is the primary ligand for IP_3Rs and its binding to the receptor causes a conformational change that opens the channel pore and enables mobilisation of intracellular Ca^{2+}. However, it is unclear if the occupation of all four IP_3-binding sites is essential for IP_3R activation (Taylor & Tovey 2010). Cooperative binding of IP_3 and lag in receptor activation post-binding of the first IP_3 molecule is perhaps an evolutionary mechanism to protect against spontaneous receptor activity (Marchant & Taylor 1997; Dufour et al. 1997). However, mutational analysis reveals that occupancy of fewer than four IP_3-binding sites is required for receptor activation (Boehning & Joseph 2000; Marchant & Taylor 1997).

In addition to IP_3, several small molecules can also regulate the channel activity. Cytosolic Ca^{2+} regulates IP_3R activity (Suematsu et al. 1984; Jean & Klee 1986) in a biphasic manner. Lower concentrations of Ca^{2+} potentiate the effects of IP_3, whereas at higher concentrations of cytosolic Ca^{2+} are inhibitory to IP_3-mediated Ca^{2+} mobilisation (Hirata et al. 1984; Iino 1990). In the presence of IP_3, the Ca^{2+}-binding site is activatory, however it switches to being inhibitory in the absence of IP_3 (Mak et al. 2003). Platelet-specific studies relating to this have yet to be performed, however it is speculated that this co-regulation of IP_3R by Ca^{2+} and IP_3 prevents spontaneous receptor activity (Marchant & Taylor 1997). Calmodulin, a ubiquitously expressed accessory protein, is a prime candidate for the Ca^{2+}-sensor protein that regulates all three isoforms of IP_3R in mammalian cells. It is speculated that one lobe of the bi-lobular protein binds to Ca^{2+} and interacts with the Ca^{2+}-sensitive suppressor domain on the receptor (Kang et al. 2011; Taylor & Laude, 2002). However, mutational studies preventing Ca^{2+}-calmodulin binding have failed to show significant effect on IP_3R function, indicating that the precise mechanism of IP_3R regulation by calmodulin remains to be understood (Zhang & Joseph 2001).

IP_3R in the mammalian cells also has two binding sites for ATP, and is regulated in a biphasic manner in response to ATP-binding (Maeda et al. 1991; Furuichi et al. 1989). The stimulatory effects of ATP are a consequence of it binding to adenine nucleotide-binding regions, whereas the inhibitory effects occur at higher ATP concentrations. Due to charged

Figure 1.8

a

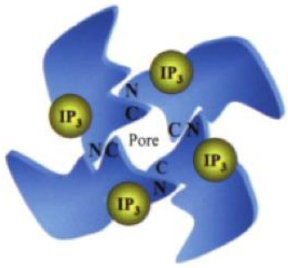

b

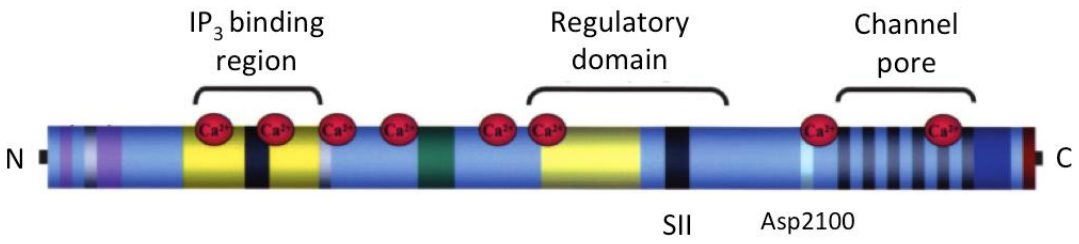

***Figure 1.8* – Overview of structure of IP_3R**

(a) Illustration shows the tetrameric structure of IP_3R, modelled from cryo-electronmicroscopy data and biochemical data. The N- and C- terminals are annotated on the model and IP_3-binding regions are shown in yellow. (b) The biochemical structure of IP_3R, with the regulatory and channel domain labelled on the illustration. The IP_3-binding and Ca^{2+}-binding regions on the IP_3R are shown in yellow and red respectively. Calmodulin-binding region is shown in lilac. The SII+ splice variant contains the SII region shown on the illustration, however this region is missing in SII- splice variant of IP_3R1. Illustration adapted from (Patterson et al. 2004)

nature of ATP, it competes for the IP_3-binding site of IP_3R, therefore inhibiting the receptor (Willcocks et al. 1987; Nunn & Taylor 1990).

1.6.2.1 Phosphorylation of the IP_3R by PKA

IP_3R is a substrate for PKA (Ferris et al. 1991; El-daher et al. 2000), Protein Kinase G (Komalavilas and Lincoln, 1994) and tyrosine kinases (Harnick et al., 1995) in multiple cells types. However the current work is primarily focused on PKA-mediated phosphorylation of IP_3R1.

PKA phosphorylates two serine sites (Ser1589 and Ser1756), on the receptor (Ferris et al., 1991), both of which are located in the regulatory domain. Alternative splicing of the sequence between these two phosphorylation sites results in two splice variants of IP_3R1, which are termed SII(+) and SII(-) (Danoff et al., 1991). In many cells, PKA-mediated phosphorylation activates the receptor by altering its sensitivity to IP_3. Both ser1589 and ser1756 are important for the activation of SII(-) variant whereas SII(+) variant is sensitised to PKA on phosphorylation of ser1756 (Wagner et al., 2003).

There are contrasting reports in literature about the functional consequence of PKA-mediated phosphorylation, depending upon if the IP_3R was from intact cells or was purified from cells. For example, PKA-mediated phosphorylation of IP_3R is reported to potentiate Ca^{2+} mobilisation in intact liver cells (Hajnóczky et al. 1993), whereas PKA-mediated phosphorylation of IP_3R1 is reported to be inhibitory in purified hepatocytes (Volpe et al. 1990) and purified brain cells (Supattapone et al. 1988). Contrastingly in platelets, Quintion et al suggest PKA-mediated phosphorylation to be activatory in IP_3R1 from purified platelet membranes (Quinton & Dean 1992) whereas Cavallini et al have shown it to be inhibitory in intact platelets (Cavallini et al. 1996). The precise reasons for such discrepancies remain unknown yet. PKA-mediated IP_3R phosphorylation is however is reported to decrease the receptor affinity to IP_3 and inhibit calcium mobilisation in platelets (Cavallini et al. 1996; Quinton & Dean 1992). The precise understandings of the mechanisms that drive cAMP-mediated phosphorylation are yet unclear, however links between Ca^{2+} responses during

megakaryocytopoiesis and PKA pathway have been highlighted, therefore suggesting the importance of cross talk between Ca^{2+} and PKA signalling pathway.

The inhibitory effects of PGI_2 towards Ca^{2+} mobilisation have been shown to develop during later stages of megakaryocytopoiesis. This is also accompanied by increase in the expression of PKA-c subunit (den Dekker et al, 2002a). Iloprost has been shown to induce Ca^{2+} elevation in megakaryocytes. Furthermore, Forskolin has been shown to cause a similar response independent of IP_3R and PKA by inducing Rap1 activation (den Dekker et al, 2002b).

1.7. Compartmentalisation of cAMP signalling

cAMP signalling is localised to specific cellular compartments by a group of functionally linked proteins called the A-kinase anchoring proteins (AKAPs). AKAPs provide spatial and temporal regulation of cAMP signalling by localising PKA isoforms to specific signalling sub-domains. Since the first identification of AKAPs, over 50 different isoforms have been identified (Taskén & Aandahl 2004). Although AKAP isoforms are not identical in structure, certain structural features are conserved across the family. The highly conserved 14-18 amino acid amphiphatic helix binds to PKA R-subunit (*Figure 1.9*) and localises it in the proximity of PKA substrate. The helical alignment is crucial for PKA-binding and is formed as a result of orientation of all the charged residues along one face of the helix and the hydrophobic residues towards the other (Carr et al. 1991). The amphiphatic helix of AKAP binds residues 1-23 of the N-terminal of the D/D' domain of RII-subunit and residues 12-61 of RI-subunit (Pidoux & Tasken 2010). The precise mechanism that determines the affinity of the AKAPs to the type of PKA R-subunit remains to be understood. However, phosphorylation of PKA RIIα-subunit at Ser99 is reported to increase the affinity of PKA to AKAPs (Margarucci et al. 2011). This is in agreement with other studies that suggest that increased anchoring of PKA-RII subunit to AKAP9 (Aye et al, 2009) could result in increased phosphorylation of its targets.

Nevertheless, dual-specific AKAPs that have equal affinity for both RI subunit dimerisation domain and the D/D' domain are also reported (Banky et al. 1998). Another feature conserved across AKAP family of proteins is the presence of the tethering domain, which exploits lipid-protein interactions to localise the AKAP at specified sub-cellular domains (Carnegie & Scott 2003). For example, AKAP 15/18 undergoes myristoylation and palmitoylation in the tethering domain such that it is localised in the proximity of L-type Ca^{2+} channel (Fraser et al. 1998). Tethering domains allow targeting of several AKAPs to one subcellular region. For example, *D*AKAP1, *D*AKAP2, PAP7 and Rab32 are tethered to PKA in mitochondria (Taskén & Aandahl 2004). This suggests that there may perhaps be yet unknown mechanisms targeting the localisation of AKAPs to specific subcellular domains.

Figure 1.9

a

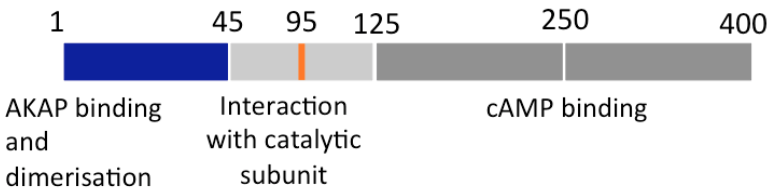

b

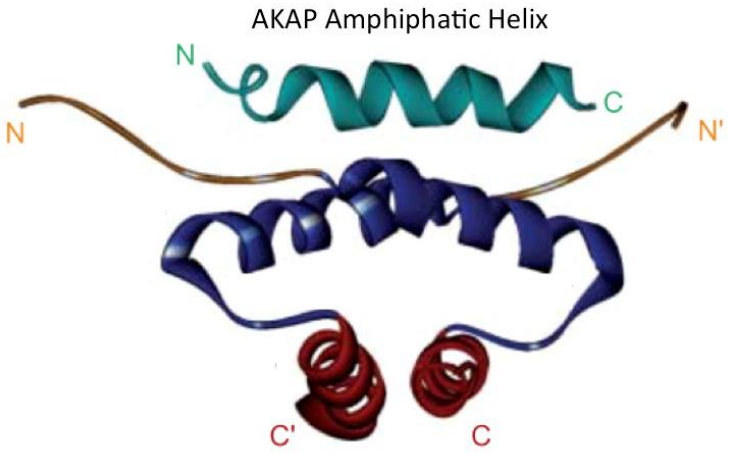

***Figure 1.9* – Overview of AKAP binding to PKA regulatory subunit**

(a) Illustration shows the RII structure of RII. The AKAP binds to the D/D' domain shown in blue, and the RII autophosphorylation site is shown in orange. Structure redrawn from (Colledge et al. 1999). (b) Illustration shows the ribbon structure of PKA regulatory subunit, with the C-terminal dimerization domain shown in dark red. The upper two helices shown in blue maintain contact with the AKAP amphiphatic helix shown in teal. Adapted from (Pidoux & Tasken 2010).

In addition to mutational analysis and transfection studies, the AKAP-PKA disruptor peptides have been used to gain a better understanding of the functional importance of AKAPs. These AKAP-PKA disruptor peptides mimic the amphiphatic helix of the AKAPs and compete for the PKA-binding site. Ht31 was the first disruptor peptide identified. Computer-aided analysis shows the presence of an 18 amino acid long Ht31-amphiphatic helix, which aids its interaction with PKA R-subunits (Carr et al. 1991; Carr et al. 1992). Ht31 disrupts the anchoring of AKAPs to both PKA RI-subunit and RII-subunit (Herberg et al. 2000). Specific AKAP-RI subunit and AKAP-RII subunit interactions can be delineated by peptides such as R-I Anchoring Disruptor (RIAD) peptide (Carlson et al. 2006) and SuperAKAP (Gold et al. 2006).

AKAPs provide spatial regulation of signalling pathways by integrating with various multi-protein signalling complexes. Multiple AKAPs have been reported in platelets with each AKAP potentially responsible for regulating a particular signalling node (Rowley et al. 2011; Beck et al. 2012). Moesin, an AKAP identified in platelets is shown to target PKA-I to lipid rafts, where it can phosphorylate GPIbβ. PKA-mediated phosphorylation of GPIbβ is thought to interfere with thrombus formation and restrict binding of vWf to the receptor (Raslan et al. 2015a). Of the 15 AKAPs that are known to be present in platelets, the functional role of all has not yet been verified. For this reason, we rely on the studies performed in other cell types to educate us on the potential role of AKAPs in platelets. For example, membrane-associated AKAP79 associates with glutamate receptors and facilitates PKA-mediated phosphorylation of Ser845 which regulates synaptic plasticity in brain cells (Taskén & Aandahl 2004). Transfection studies in HEK239 cells suggest that cytoskeletal associated AKAP-KL interacts with actin cytoskeleton and regulates cell polarity and transepithelial signalling processes (Dong et al. 1998). Mutations in *D*AKAP2 and AKAP-*Lbc* are reported to increase the susceptibility to breast cancer (Wirtenberger et al. 2007). This suggests that AKAPs have a wide range of regulatory roles, and genetic mutations in AKAP genes are associated with disease conditions.

1.7.1. AKAP9

AKAP9, encoded by the *AKAP9* gene located on 7q21 exists as multiple splice variants. AKAP9 splice variants exhibit cell- and tissue-specific patterns. AKAP9 is reported to be primarily present in brain, liver and cardiac cells (Pidoux & Tasken 2010). Proteomics studies have shown AKAP9 to be present in platelets (Margarucci et al. 2011). The smallest splice variant of AKAP9 known as Yotiao was first identified to be associated with NMDA receptor (Lin et al. 1998). Two other AKAP9 splice variants - AKAP350 (Schmidt et al., 1999) and AKAP450 (Witczak et al., 1999) have also been identified. Yotiao is reported to be localised to the plasma membrane whereas the other two isoforms are localised in centrosome and golgi apparatus (Westphal et al. 1999; Schmidt et al. 1999; Lin et al. 1998; Witczak 1999). Yotiao has an open reading frame of 5.1kb, which encodes a leucine-rich 1642 amino acid protein, with GC-rich N-terminus. The C-terminus of the protein houses an in-frame stop codon, followed by untranslated 3' region and a poly-A tail (Lin et al. 1998). Not much is known about the structures of various splice variants of AKAPs, however about 50% of the coding sequences of Yotiao are found in AKAP350 (Schmidt et al. 1999). Irrespective of this, AKAP9 (and its splice variants) are shown to form multi-protein complexes.

AKAP350 is reported to associate with centrosomes and is suggested to regulate cell cycle (Schmidt et al. 1999), whereas Yotiao forms a scaffold protein that is of NMDA-PP1-PKA signalling complex. NMDA receptor is a substrate for PKA (Murphy et al. 2014; Skeberdis et al. 2006). Yotiao is shown to simultaneously interact with the C-terminal tail of NR1 subunit of NMDA receptor (Lin et al. 1998), and PKA RII-subunits along with type 1 phosphatase PP1. Data from electrophysiological experiments suggests that PP1, when active binds to Yotaio, which in turn limits the NMDA activity until activated PKA phosphorylates NMDA and enhances channel modulation (Westphal et al. 1999). In cardiac cells, Yotaio directs PKA, PDE and PDE4 towards the α-subunit of KCNQ1, a potassium channel. Here, Yotiao coordinates PKA-mediated phosphorylation of KCNQ1 at Ser27 and PP1-mediated dephosphorylation of this site, which in turn regulates cardiac repolarisation (Kurokawa et al. 2004). Mutations in Yotiao or KCNQ which disrupt the complex formation are associated with long Q-T syndrome, a type of inheritable arrhythmias (Chen & Kass 2006). Yotaio is also concentrated in the brain cells and is known to regulate brain activity by directly complexing with the N-terminus of AC2. Yotiao is also known associate with AC1,3 and 9, of which AC2

and 3 are inhibited by Yotaio (Piggott et al. 2008). Critically in the context of this work, Yotiao has also been reported to coordinate the association between PP1, PKA and IP_3R1 in brain. Moreover, the interaction between IP_3R1 and AKAP9 is mediated via Leucine/Isoleucine zipper motifs, whereas PP1 interacts with the C-terminal of the IP_3R1 (Tu et al. 2004). Alternatively, the association of AKAP450 with IP_3R1 and PKA RII has also been reported in golgi apparatus of cerebellar granule cells (Collado-Hilly & Coquil 2009). These data reiterate the role of AKAPs in spatial regulation of cell signalling.

1.8. Aims and Objectives

1.8.1 Hypothesis

Circulating platelets scan the vascular endothelium for damage and adhere to sites of injury where the extracellular matrix proteins, collagen and vWF, has become exposed. Endothelial cells release PGI_2 into the blood stream to counterbalance unwanted platelet activation. PGI_2 stimulates cAMP-dependent signalling cascade and activates PKA. Downstream of this, PKA can phosphorylate number of platelet proteins that are important to platelet function (*Table 1.1*). PKA-mediated phosphorylation of these and other proteins is thought to be the basis of inhibition of platelets in response to cAMP elevating agents.

A key target for cyclic nucleotide signalling and particularly cAMP/PKA pathway is the control of intracellular Ca^{2+} concentrations. The mobilisation of intracellular Ca^{2+} upon platelet activation is mediated by phospholipase-mediated release of IP_3, which in turn binds to IP_3Rs, which are also substrates for PKA (Ferris et al. 1991; Haug et al. 1999). PKA-induced phosphorylation of IP_3R1 has been reported to inhibit Ca^{2+} mobilisation and therefore cause platelet inhibition (Cavallini et al. 1996). Although widely reported, a full characterisation of PKA-mediated IP_3R1 phosphorylation remains to be performed in platelets. Furthermore, the association of IP_3R1/PKA with scaffolding proteins that provide the spatial control of PKA-mediated IP_3R phosphorylation also remains unexplored in platelets. The work described here examines the mechanism of PKA-mediated IP_3R1 phosphorylation. We hypothesise PKA to be in a complex with IP_3R1, with AKAP9 being the scaffolding protein that ensures spatial regulation of PKA-mediated IP_3R phosphorylation.

1.8.2. Aims and Objectives

The aim of this work was to characterise the PKA-cAMP signalling pathway with respect to IP_3R1 in platelets and understand the functional effects of IP_3R1 phosphorylation in platelets.

This was achieved by addressing the following objectives -

1. Validate the presence of PKA in platelets and the activity of PKA signalling pathway
2. Validate the presence of IP_3R1 in platelets and characterise PKA-mediated IP_3R1 phosphorylation
3. Identify the presence of multi-protein signalling complex between IP_3R1-PKA-AKAP9
4. Understand the functional consequence of disruption of IP_3R1-PKA-AKAP9 using AKAP-disruptor peptide, St-Ht31

CHAPTER II - MATERIALS AND METHODS

2.1. Antibodies

Table 2.1

Antibody target	Details	Supplier	Experiment conditions
β - tubulin	Mouse	Millipore	IB:1/1000
AKAP9	Rabbit	Santa Cruz	IB:1/1000
AKAP9	Rabbit	Custom-made	IB: 1/2000
HRP-linked anti-Goat			IB: 1/10000
HRP-linked anti-Mouse		Amersham	IB: 1/10000
HRP-linked anti-Rabbit		Amersham	IB: 1/10000
IP_3R1	Rabbit	Santa Cruz	IB: 1/1000; IP: 2µg
IP_3R2	Goat	Santa Cruz	IB: 1/1000; IP: 2µg
IP_3R3	Goat	Santa Cruz	IB:1/1000
Normal Rabbit IgG	Rabbit	Millipore	IP: 2µg
Normal Mouse IgG	Mouse	Millipore	IP: 2µg
Phospho-$IP_3R1^{ser1756}$	Rabbit	Cell Signalling	IB:1/1000
PKA c	Mouse	BD Transduction	IB:1/1000
PKA – RI	Mouse	BD Transduction	IB:1/1000
PKA – RI	Rabbit	Cell Signalling	IB: 1/1000; IP: 2µg
PKA - RIIβ	Mouse	BD Transduction	IB:1/1000
Phospho-PKA substrate (RRXS*/T*)	Rabbit	Cell Signalling	IB:1/1000
Phospho-$VASP^{ser157}$	Rabbit	Cell Signalling	IB:1/1000

***Table 2.1* – Antibodies and Suppliers**

All the antibodies used in the work detailed in this thesis are detailed along with the suppliers and the conditions of use

2.2. Chemicals and reagents

The chemicals, reagents and instruments are listed in Appendix I

2.3. Methodologies used in the preparation of human blood platelets

Whole blood obtained from healthy, adult volunteers, in accordance with the ethical permission granted by the ethics committee of the Hull York Medical School (UK). Exclusion criteria were smoking, chronic illness, and taking Non-Steroidal Anti-inflammatory medication within 14 days prior to bleeding. In all cases, informed consent was obtained in accordance with the Declaration of Helsinki.

Blood was collected by venepuncture of the ante-cubital fossa vein, using 21G butterfly needle (*Abbot Laboratories, USA*). The first 3ml of blood was discarded to exclude platelets activated during the venepuncture. Subsequently, blood was drawn in 20mL syringes containing pre-warmed anticoagulant acid-citrate dextrose (ACD) (ACD; 29.9mM sodium citrate, 113.8mM, glucose, 72.6mM NaCl and 2.9mM citric acid, pH 6.5) in the ratio of 5:1 (v/v) (Riba et al., 2008). The blood was gently transferred to 50ml falcon tubes and mixed gently.

2.3.1. Platelet Isolation by lowering the pH

Platelets were isolated by lowering the pH, using method adapted from Mustard and colleagues (Mustard et al., 1989). Whole blood was centrifuged (*Universal 320, Hettich*) at 200g for 20 minutes at 20°C to obtain platelet rich plasma (PRP). After carefully removing the PRP using a pasture pipette, such that the buffy coat remained undisturbed, the PRP was treated with 0.3M citric acid (pH = 6.5) (1:50 v/v) and subsequently pelleted by centrifugation at 800g for 12 minutes. The supernatant was discarded and the platelet pellet was re-suspended in wash buffer (0.036M citric acid, 10mM ethylenediaminetetraacetic acid, (EDTA), 0.005M KCl, 0.09M NaCl; pH 6.5) and centrifuged again at 800g for 10 minutes at 20°C to remove any residual plasma. The final pellet was re-suspended in modified Tyrode's buffer (137mM NaCl, 2.7mM KCl, 1mM $MgCl_2$, 5.6mM Glucose, 3.3mM NaH_2PO_4, 20mM 4-(2-hydroxyethyl)-1-piperazineethanesulfonic acid (HEPES); pH 7.4). The platelet count was adjusted as per the requirement of the experiment.

2.3.2. Quantification of platelet numbers

Platelet numbers were quantified using the Beckman Z1 Coulter® particle counter (*High Wycombe, UK*). The Coulter counter works on the principle that when a particle passes through an aperture, concurrent with an electric current, the change in electrical impedance is proportional to the volume of particle passing through the aperture (Briggs et al., 2007).

Washed platelets were diluted in Coulter® Isoton® II diluent (1:20,000) and processed by the Coulter counter using a probe aperture of 50µm.

2.4. Measurement of aggregation in suspended platelets.

Light transmission aggregometry is based on the principle that platelet aggregation in response to agonists would increase the light scattering through the platelet suspension, which is detected by a photocell (Born, 1962). It is assumed using small volumes of platelet suspension with stirring, forms a homogenous suspension that is optically refractive. However, post agonist stimulated activation, the platelets undergo shape change and aggregate into clumps which allow more light to pass through (Born et al., 1978). Platelet aggregation, which is dependent on the extent of platelet activation, is proportional to the extent of light transmission.

Aggregation was monitored using a Chrono-log dual-channel light aggregometer. Washed platelets (2.5×10^8 platelets/mL) were incubated at 37°C with stirring (1000rpm) for 1 minute prior to stimulation with the required agonist to ensure uniform distribution of platelets in the suspension. Non-stimulated platelet suspension represents 0% aggregation. The aggregometer was calibrated against modified Tyrode's buffer, which represents maximal light transmission. The aggregation was recorded for 4 minutes at 37°C with stirring (1000rpm) for each sample and expressed as a percentage increase in light transmission through agonist-stimulated platelet suspension compared to that through non-treated platelet suspension. Percentage aggregation was calculated as [(Distance from base-line to maximal aggregation achieved / Distance from baseline to theoretical 100% aggregation) x 100). Aggregation was performed in the absence of added Ca^{2+}.

Figure 2.1

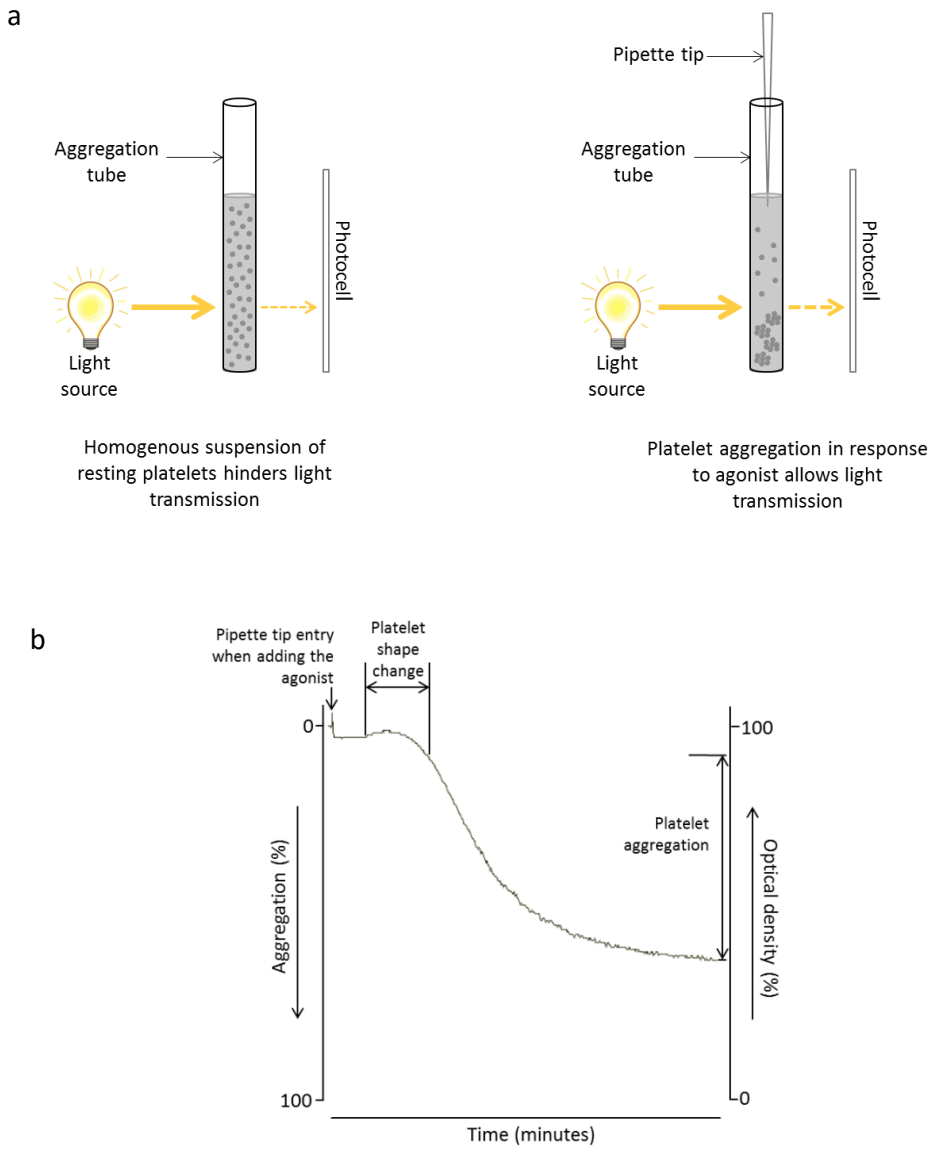

***Figure 2.1* – Measurement of aggregation in suspended platelets using light transmission aggregometry.**

(a) Illustration shows the principle of platelet aggregation in a light transmission aggregometer. Platelet response to agonist stimulation allows the light to refract through, which is detected by the photocell and quantified using the Aggrolink computer software. *(b)* Illustration shows a representative aggregation trace, showing the changes in light transmission with respect to time.

2.5. Methodologies for assessment of platelet signalling

Platelet were analysed by solubilising their cellular membranes using Laemelli buffer (50mM Tris base, 4% w/v SDS, 20% v/v Glycerol, trace bromophenol blue, 5% v/v 2-mercaptoethanol, pH 6.8), followed by separation of proteins using gel electrophoresis and identification using Immunoblotting.

2.5.1. Preparation of platelet samples

The sample preparation methodology for SDS-PAGE was based on the method described by Laemmli (Laemmli, 1970). All the samples were prepared at 37°C with stirring (800rpm) as per the requirement of the treatment. The platelets were lysed by the addition of 2x Laemmli buffer. 2-mercaptoethanol, a reducing agent aided reduction of the proteins to their primary structure. The samples were boiled for 5 minutes before analysing them by SDS-PAGE or stored at 20°C.

2.5.1.1. Quantification of platelet protein concentration

Protein concentration in lysates solubilised in IP lysis buffer (150mM NaCl, 10mM Tris base, 1mM EGTA, 1mM EDTA, 1% Igepal (v/v), pH 7.4), was quantified using the Bio-Rad *DC* Protein Assay kit (Bio Rad, UK) according to manufacturer's protocol, based on the Lowry assay (Lowry et al., 1951). This colorimetric assay measures the intensity of blue colour, which develops as a result of reaction between protein and copper tartrate in alkaline medium and subsequent reduction (removal of 3 oxygen atoms) by Folin reagent. The intensity of the blue colour measured at a wavelength of 750nm is directly proportional to protein concentration in the sample. The standard curve was plotted using BSA solutions of definite concentration. The samples and standards were diluted 1:1 in the assay buffer and subsequently assayed in triplicate. The light absorption at a wavelength of 750nm was measured using a multiplate reader (*Tecan infinite M200, Männedorf, Switzerland*).

2.5.2. Sodium dodecyl sulphate-polyacrylamide gel electrophoresis (SDS-PAGE)

Gel electrophoresis was performed to resolve proteins based on their electrophoretic mobility through a porous gel matrix when electric current is applied. In polyacrylamide gel electrophoresis (PAGE), the gels are mainly composed of linear polymers of acrylamide cross linked by N, N'-methylene bisacrylamide. The polymerisation of acrylamide is initiated by N, N, N', N'-tetramethylethylenediamine (TEMED). TEMED catalyses the production of SO_4^- free radicals from ammonium persulphate (APS), which in turn accelerates the polymerisation process. The effective pore size of the polyacrylamide gel is inversely proportional to the concentration of acrylamide in the gel mixture. SDS, an anionic reagent, imparts an overall negative charge to the protein by binding to amino acids and denatures complex protein structures rendering them in a rod-shaped conformation. In addition to SDS, the presence of reducing agents such as 2-mercaptoethanol enables disruption of di-sulphide bridges linking adjacent cysteine residues. SDS binds to denatured proteins in a mass-to-charge (*m/z*) ratio (1.4g of SDS/1g protein), therefore allowing protein separation based on disparity in protein migration.

2.5.2.1. Methodology for SDS-PAGE

SDS-PAGE was run using the Tris-glycine system under reducing conditions in accordance with the method of Laemmli (Laemmli, 1970). Polyacrylamide gel (1.5mM) comprising of 4% stacking gel (pH 6.8) and 10-18% acrylamide resolving gels (pH 8.8) or precast Mini-PROTEAN® TGX™ gels (*Bio-Rad, CA*) comprising of 4-20% gradient acrylamide were used for gel electrophoresis. Each gel contained 10 wells for protein loading. The biotinylated marker and the pre-stained marker were also run along with the sample.

Densitometry on western blots was performed using ImageJ software and the data were expressed as Mean±SEM.

2.5.3. Immunoblotting

Immunoblotting is used to detect the protein of interest from a protein homogenate (Towbin et al., 1979), by transferring the proteins from a gel to adhesive matrix such as nitrocellulose or polyvinylidene difluoride (PVDF) under electric current. Proteins bind to PVDF membranes through hydrophobic interactions. Post transfer, the membranes can be probed with specific primary antibodies against the target proteins. Subsequently, the membrane is incubated with a secondary antibody, commonly conjugated to horseradish peroxidase (HRP). Proteins can be visualised by exposing the photographic film by enhanced chemiluminescence (ECL). Luminescence is caused by the oxidation of luminol by hydrogen peroxide, which is catalysed by HRP and prolonged by an "enhancer" such as p-coumaric acid (Thorpe et al., 1985).

2.5.3.1 Methodology for Immunoblotting

Proteins separated by SDS-PAGE were transferred to 0.2µm PVDF supplied in the Trans Blot® Turbo™ Transfer pack (*Bio-Rad, CA*), using the Trans Blot® Turbo™ blotting system (*Bio-Rad, CA*). Unless specified otherwise, the membranes were blocked in either BSA/TBS-T (10%, w/v) or semi-skimmed milk/TBS-T (5%, w/v) for 45 minutes with agitation at room temperature to prevent non-specific antibody binding and subsequently probed with primary antibody of interest, overnight at 4°C. The membranes were washed twice with TBS-T for 15 minutes each and subsequently probed with HRP-conjugated secondary antibody (1:10000) and anti-biotin (1:2000) for 1 hour. The membranes were washed with TBS-T (5 washes, 15 minute each, unless specified otherwise). Membranes were incubated with ECL solutions (ECL1, 90%v/v dH_2O, 10% v/v 10% Trizma base, 0.065% H_2O_2; ECL2, 88.6% v/v dH_2O, 10% v/v 10% Trizma base, 0.996% v/v Luminol, 0.465% v/v Coumaric Acid) for 90 seconds and used to expose Amersham Hyperfilm ECL (GE healthcare) for times ranging upto 5 minutes. The photographic films were developed using Carestream® Kodak® autoradiography GBX developer/replenisher (*St. Louis, MO*) and Carestream® Kodak® autoradiography GBX fixer/replenisher (*St. Louis, MO*).

Figure 2.2

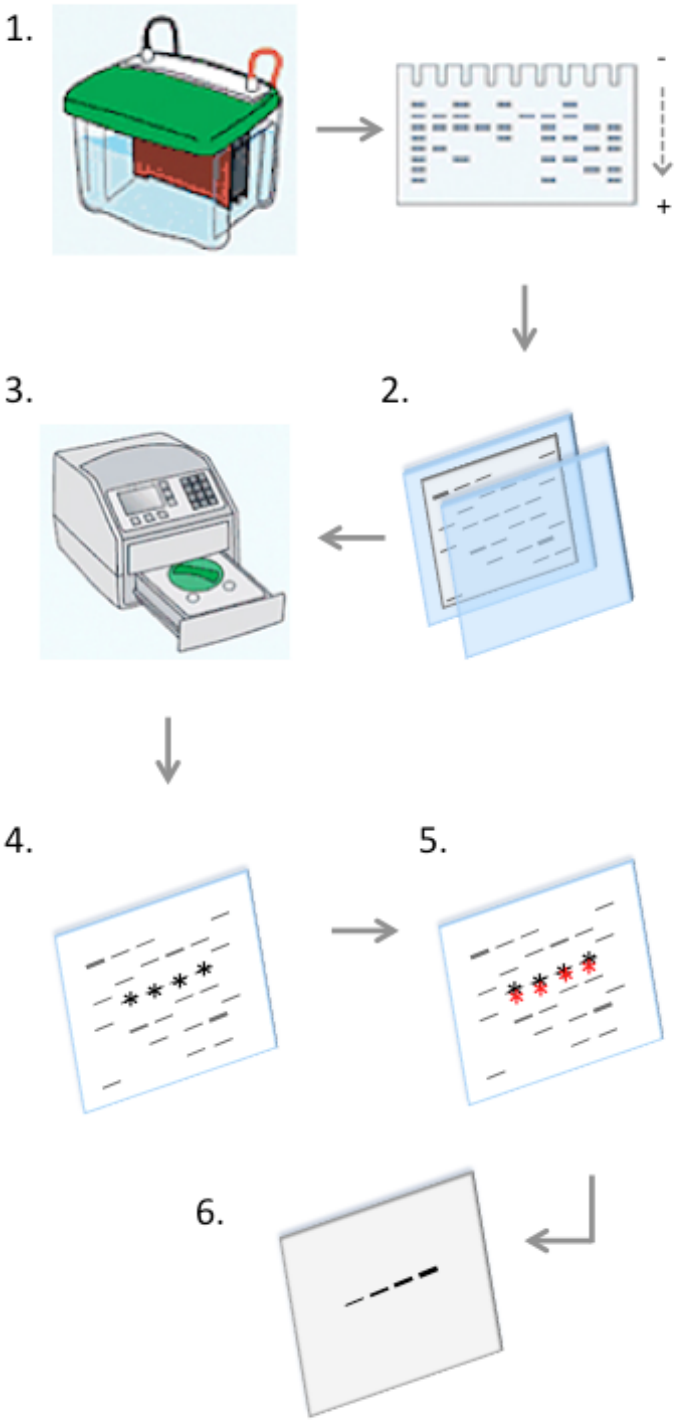

1. Samples loaded on the gel and gel electrophoresis performed under constant voltage for a specified time interval to resolve proteins.
2. Post protein resolution, the proteins transferred to the PVDF membrane using semi-dry transfer. Polyacrylamide gel was placed on blotting paper-PVDF stack such that the proteins were facing down on PVDF.
3. The transfer sandwich was placed in the A Trans-Blot® Turbo™ tray and subjected to a current of 1.3A and a varying voltage not exceeding 25 volts for 10 minutes.
4. Membranes blocked for 45 minutes in either 10% BSA or 5% Milk to reduce non-specific Ab binding. Membranes subsequently incubated overnight with 1° Ab (*) at 4°C.
5. Membranes incubated with 2° Ab (*), which binds to the 1° Ab.
6. Proteins visualised by exposing the photographic film by ECL.

Figure 2.2 **– The principle of SDS-PAGE and Immunoblotting**

2.5.4. Immunoprecipitation

Immunoprecipitation was employed to isolate a specific protein from a mixture of proteins in a cell lysate. An antibody raised against a specific epitope of the protein is allowed to bind Protein A- or G-immobilised sepharose beads. Protein A and G, isolated from the cell wall of Staphylococcus aureus, possess binding capabilities to the constant region of most antibodies. This allows the study of single purified proteins and/or protein complexes or to concentrate proteins that would otherwise be scant to be detected by western blotting.

2.5.4.1. Methodology for Immunoprecipitation

Samples were prepared as described in §2.5.1, with the exception that the reactions were terminated by the addition of IP lysis buffer in the presence of protease (1:100) and phosphatase (1:200) inhibitor cocktails (*Sigma Aldrich, St. Louis, MO*). The samples were incubated with agitation, at 4°C for 30 minutes before being centrifuged (10,000rpm) to isolate cell debris. IgePal, a non-ionic detergent used in the IP lysis buffer solubilised the cellular proteins without disrupting the protein complexes.

A 50% (w/v) suspension of either Protein A or Protein G sepharose beads was prepared in 0.1% TBS-T (slurry). Cell lysates (500µg of protein) were pre-cleared by incubating with slurry (25µl) at 4°C with agitation, to reduce non-specific binding of proteins to sepharose beads. The beads and insoluble cell debris were pelleted by centrifugation at 10,000rpm for 1 minute using MiniSpin® plus centrifuge (*Eppendorf; Hamburg, Germany*). The supernatant was used to perform the immunoprecipitation.

The pre-cleared lysates were incubated overnight, at 4°C with agitation, with the antibody of interest to allow the protein-Ab binding. The lysate-Ab samples were subsequently incubated with slurry (25µL per sample) for 1 hour at 4°C with agitation. The samples were centrifuged for 1 minute at 10,000rpm; the resultant supernatant was discarded. The pellet was sequentially washed once with IP lysis buffer and twice with 0.1% TBS-T to remove any residual proteins. The beads were boiled with Laemmeli buffer for 5 minutes to liberate the antibody and precipitated protein from the beads. The beads isolated by centrifugation at

Figure 2.3

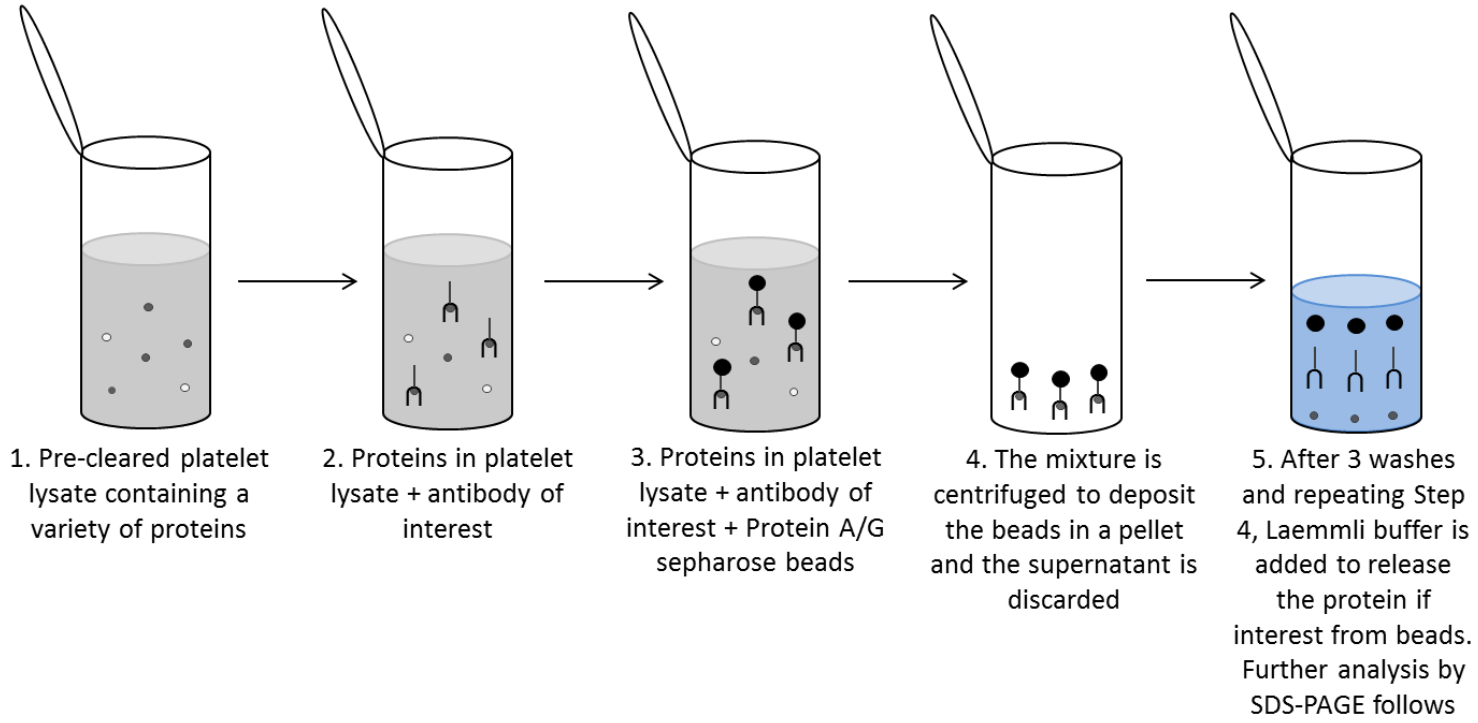

Figure 2.3 **– The Principle of Immunoprecipitation.**

10,000g for 1 minute in MiniSpin® plus centrifuge (*Eppendorf; Hamburg, Germany*). The liberated protein was resolved by SDS-PAGE (§2.5.2) and further analysed by immunoblotting (§2.5.3).

2.5.5. cAMP Pull-down assay

cAMP and PKA are heavily involved in regulation of platelet homeostasis. While immunoprecipitation enables isolation of proteins from cell lysate, enrichment of proteins specifically involved in cAMP-PKA signalling was important to better understand the signalling cascade. cAMP binds exclusively to PKA in platelets; agarose beads with cAMP immobilised on them were used to enrich proteins that directly bound to cAMP (i.e. PKA) or indirectly bound to PKA. This technique was adapted from Scholten *et al* (Scholten et al. 2006). This technique was primarily used to study single purified protein and/or protein complexes along with immunoprecipitation (§2.5.4).

2.5.5.1. Methodology for cAMP Pull-down assay

Samples were prepared as described in §2.5.1, with the exception that the reactions were terminated by the addition of IP lysis buffer in the presence of protease (1:100) and phosphatase (1:200) inhibitor cocktails (*Sigma Aldrich, St. Louis, MO*). Cell lysates (500µg of protein) were pre-cleared to reduce non-specific protein binding, by incubating with slurry 25µl of slurry of Et-OH-NH agarose beads (*BioLog, Germany*) (50%v/w in 0.1% TBS-T) for 1 hour at 4°C with agitation. The beads and insoluble cell debris were pelleted by centrifugation at 10,000g for 1 minute in the MiniSpin® plus centrifuge while the supernatant containing the proteins and complexes was collected.

The collected supernatant was enriched for cAMP-binding proteins by overnight incubation, at 4°C with agitation, with 8-AHA-cAMP beads slurry (30µl per sample). The samples were centrifuged for 1 minute at 10,000rpm and the bead-protein complex was pelleted. The resultant supernatant was discarded. The pellet was washed sequentially once with IP lysis buffer and twice with TBS-T (0.1%) to remove any residual unbound proteins. The beads

were boiled with Laemmeli buffer for 5 minutes to liberate the precipitated protein from the beads. The beads isolated by centrifugation at 10,000rpm for 1 minute MiniSpin® plus centrifuge (*Eppendorf; Hamburg, Germany*), and the supernatant, containing liberated proteins was resolved by SDS-PAGE (§2.5.2) and further analysed by immunoblotting (§2.5.3).

2.6. PepTag® Assay for Non-Radioactive Detection of PKA activity (Kemptide assay)

Protein complexes were isolated and studied using protein enrichment techniques, however the kinase activity associated with these complexes was studied using PepTag® Assay. Historically, this was achieved using protocols that involved the transfer of radioactive gamma phosphate onto the substrate of interest. While this was effective, due to technical restrictions an alternative non-radioactive PepTag® Assay was employed for the detection of PKA activity associated with the precipitated protein of interest.

The assay uses a brightly coloured, fluorescent peptide as a substrate (L-R-R-A-S-L-G) (Kemptide) to the kinase of interest. PKA-mediated phosphorylation of the kemptide substrate alters its net charge and the subsequent migration on the agarose gel. The phosphorylated substrates gain a net negative charge and migrate towards the positive electrode, whereas the non-phosphorylated substrates gain an overall positive charge and migrate towards the negative electrode.

2.6.1. Methodology for Kemptide assay

Proteins were immunoprecipitated as described in §2.5.4, with the exception that proteins were not eluted using Laemelli buffer. Instead, the beads complex was washed in PKA extraction buffer (350mM K_3PO_4, pH = 6.8, 0.1mM DTT), followed by the addition of 1:1(v/v) PKA extraction buffer: PKA activation solution (5µM cAMP in dH_2O) to activate PKA. The beads were incubated with agitation at room temperature for 1 hour. Post incubation period, the tubes were removed from the rotator and incubated at 30^oC for 1 minute.

Reaction tubes were prepared as shown in *Table 2.2* and incubated at room temperature for 30 minutes at room temperature.

Table 2.2

Reagent	Sample	Positive control	Negative control	Notes
PepTag® PKA reaction 5x Buffer (100mM Tris-HCl (pH 7.4) 50mM $MgCl_2$, 5mM ATP)	5µl	5µl	5µl	At 4°C
PepTag® A1 Peptide (L-R-R-A-S-L-G; 0.4µg/µl)	5µl	5µl	5µl	At 4°C
PKA activator solution		5µl	5µl	At 4°C
cAMP-dependent PKA c		5µl		At 4°C
PKA activator + Sample	15µl			RT
Deionised water		5µl	10µl	RT
Total volume	25µl	25µl	25µl	

***Table 2.2* – Preparation of sample tubes for Kemptide Assay**

The reactions were terminated by boiling the samples at 95°C for 10 minutes and resolved on 0.8% agarose gel at 100V for 20 minutes. The gels were photographed using the Syngene transilluminator (*Syngene; Cambridge, UK*)

To quantify phosphorylation, the excised and melted phosphorylation bands were treated with glacial acetic acid and gel solubilisation solution to prevent agarose from solidifying. The mixture was transferred to 96-well plate and the absorbance was read at a wavelength of 570nm using TeCan plate reader (*TeCan, Männedorf, Switzerland*).

2.7. Measurement of intracellular Ca^{2+} concentrations in platelets

Agonist-induced intracellular Ca^{2+} release is an absolute requirement for platelet activation. For this reason, attempts have been made to measure intracellular Ca^{2+} using various fluorescent indicators, for over 80 years. In the past Ca^{2+} research was primarily limited by the restricted portfolio of the non-ratiometric Ca^{2+} indicator dyes that were available, however, now highly sensitive ratiometric dyes are available. In the present study intracellular Ca^{2+} was measured in platelets loaded with a cell-permeable ratiometric Ca^{2+} indicator, Fura-2-acetoxymethyl ester (Fura-2-AM). The compound being hydrophobic, can permeate the cell-membrane. Once internalised, the intracellular esterases hydrolyse the acetomethyl group while the Fura-2 remains contained inside the cell. Ultra-violet (UV) light was passed through Fura-2-loaded platelet suspensions. Upon Ca^{2+}-binding, Fura-2 has an excitation ratio 340/380nm, which can be detected as analogue signals. These were digitalised and recorded by specialist software.

2.7.1. Methodology for the measurement of intracellular Ca^{2+} in platelets

To measure intracellular Ca^{2+} in platelet suspensions, PRP was loaded with Fura-2-AM (2µM) at 37°C for 45 minutes in dark. Henceforth, the platelet suspensions were kept in dark to avoid photo-bleaching of the indicator. PRP was subsequently centrifuged at 350g for 20 minutes. The resulting pellet containing Fura-2 loaded platelets was collected and re-suspended in nominally Ca^{2+}-free saline (1:1v/v PRP/Ca^{2+}-free saline).

Washed platelet suspensions (1ml) were transferred to 4.5ml UV grade plastic cuvettes, which were pre-warmed at 37°C for 3 minutes with constant stirring (1000rpm). The Fura- 2 was excited by a 75W xenon arc lamp filtered by three pairs of band-pass filters centred at 340 and 380nm (10nm bandwidth) in a filter wheel which spun at 45Hz. Emission was filtered between 490-600nm and measured by a photomultiplier tube (PMT). Data was collected using 4-point averaging, giving a final data acquisition rate of 11.25Hz. The analogue signals were then converted to digital signals and recorded using Carin proprietary software (*Carin Research, Kent*).

Ca^{2+} levels were estimated from the ratio of the 340 and 380nm excited signals, the method of Grynkiewicz et al was utilised (Grynkiewicz et al., 1985).

The maximal and minimal fluorescence ratio was measured for each experiment, allowing the Spectrophotometer to be calibrated accordingly. The maximum fluorescence ratio was measured by lysing the cells with digitonin (50µM), which released the Fura-2 into the saline containing $CaCl_2$ (2mM). The minimum fluorescence ratio was measured by chelating Ca^{2+} ions with EGTA (10mM) and TRIS base (10mM) to ensure that the pH remained alkaline for optimum EGTA-mediated Ca^{2+} buffering. The background fluorescence was measured by quenching the dye with $MnCl_2$ (10mM). Background corrected values were used to calculate R_{min} (minimum 340/380 ratio) and R_{max} (maximal 340/380 ratio) and the proportionality constant (ratio of the 380 signal at minimal vs maximal Ca^2). In calculating these, R_{min} and R_{max} were multiplied by a viscosity correction factor of 0.85 (Poenie, 1990). Background-corrected 340/380nm ratios (R) were then converted to $[Ca^{2+}]_i$ using equation shown below, where the dissociation constant for Fura-2 (K_d) = 224 nM (Grynkiewicz et al. 1985).

$$[Ca^{2-}]_i = Kd\ x\ \frac{F_{380\,max}}{F_{380\,min}}\ x\ \frac{(R - R\,min)}{(R\,max - R)}$$

2.8. Statistical Analysis

Data are expressed as Mean ± SEM. Quantification of western blots using densitometry was performed using ImageJ software. Percentage aggregation response was calculated as follows

$$\text{Percentage aggregation} = \frac{\text{Distance from baseline to maximal aggregation achieved}}{\text{Distance from baseline to theoritical maximal aggregation achieved}}\ x\ 100$$

Statistical comparisons of data were carried out using Student's t-test and one-way ANOVA. Student's t-test was used to analyze the statistical difference between two groups whereas ANOVA was used to compare three or more independent groups. Statistical tests were performed between preparations using Microsoft Excel 2007 and GraphPad Prism 6. Statistical significance was considered for values of $p<0.05$.

CHAPTER III: CHARACTERISATION OF PKA-MEDIATED SUBSTRATE PHOSPHORYLATION

3.1. Introduction

Platelet activation is a tightly regulated by a number of interconnected biochemical mechanisms. A balance between thrombogenic and anti-thrombogenic factors is required to enable normal platelet function. NO and PGI_2 released from the endothelium, play a crucial role in maintaining the platelets in quiescent state by inhibiting multiple aspects of platelet function and controlling platelet recruitment at the site of injury (Schwarz et al., 2001, Rivera et al., 2009). These endothelial-derived inhibitors regulate platelet function through cyclic nucleotide activated signalling pathways, which represent the most potent endogenous mechanism of inhibiting platelet activation. Though there are two main players in cyclic nucleotide signalling - cAMP and cGMP, this thesis is primarily focused on cAMP-PKA signalling pathway.

The binding of PGI_2 to the platelet IP receptor causes the activation of the stimulatory $G_{\alpha s}$ subunit of the receptor. Activated $G_{\alpha s}$ binds to transmembrane AC which hydrolyses the ATP to form cAMP (Smolenski, 2012). cAMP can bind to the cAMP-binding regions of PKA leading to enzyme activation and consequent phosphorylation at ser/thr residues of substrates (Schwarz et al., 2001). Phosphorylation of substrates regulates calcium mobilisation, integrin activation and reorganisation of actin cytoskeleton (Aburima et al., 2013), therefore inducing platelet inhibition.

Using physiological (PGI_2) and non-physiological compounds (forskolin, 8-CPT, KT5720), the effect of PKA-mediated substrate phosphorylation on platelet signalling was studied. Similarly, the presence of PKA, the primary effector of cAMP was also established.

3.1.1. Hypothesis

This chapter tests the hypothesis that PGI_2 induces PKA activation and subsequent substrate phosphorylation.

3.1.2. Aims and Objectives

This chapter aimed to establish the presence of various protein components involved cAMP-PKA signalling in platelets. Furthermore, physiological and synthetic compounds were used to characterise the cAMP signalling pathway. The objectives of this chapter were -

1. Investigate the effect of PGI_2 on platelet aggregation and Ca^{2+} release
2. Characterise PKA-mediated substrate phosphorylation
3. Establish the presence of PKA subunits in platelets

3.2. Effect of PGI_2 on thrombin-induced platelet aggregation

In the first instance, the inhibitory effect of PGI_2 on thrombin-stimulated G-protein mediated platelet aggregation was tested. Washed platelets were pre-incubated with increasing concentration of PGI_2 (0.1nM - 100nM) for 1 minute at 37^{o}C, followed by treatment with thrombin (0.1U/ml). The aggregation response was measured for 3 minutes. Percentage aggregation response was calculated as described in §2.8.

A concentration-dependent inhibition of platelet aggregation was observed on PGI_2 treatment as illustrated by the representative traces (*Figure 3.1a*). Thrombin triggered 72±3.06% aggregation response, whereas pre-treatment with a 10nM PGI_2 gave only 12±4.33% aggregation response. At 100nM of PGI_2 a complete inhibition of aggregation was observed as shown by the quantification data (*Figure 3.1b*). To conclude, at near physiological concentrations, PGI_2 compromised platelet aggregation. These data are in line with previous findings that direct towards an inhibitory nature of PGI_2 in platelet aggregation. Furthermore, the ability of PGI_2 to compromise G-protein-mediated platelet aggregation shows that PGI_2 targets platelet function common to different agonists.

Figure 3.1

a

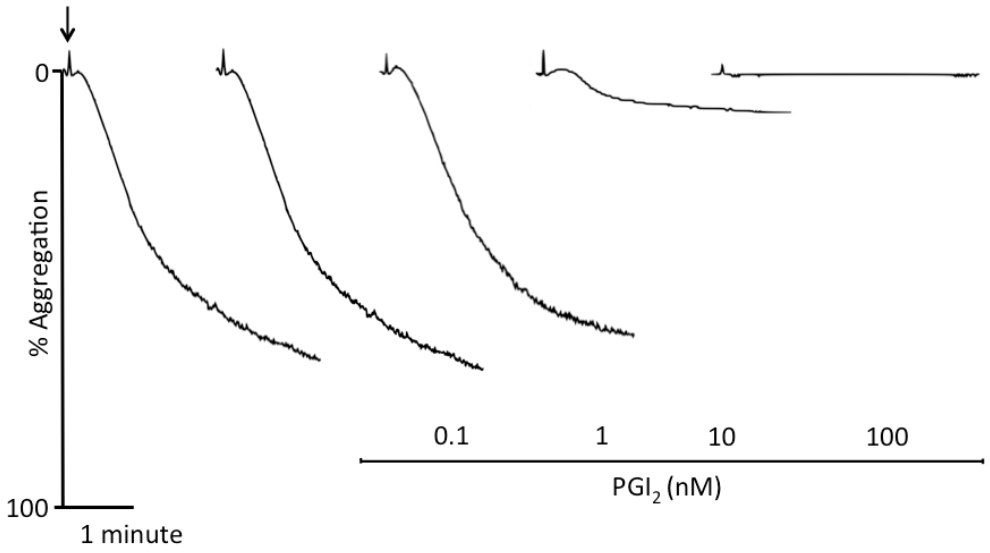

b

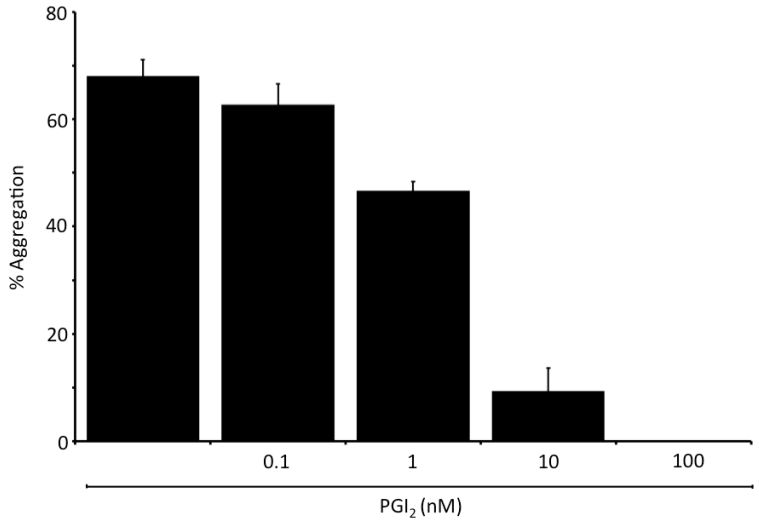

***Figure 3.1* – The influence of the thrombin-induced platelet aggregation response to increasing concentration of PGI_2.**

(a) Washed platelets ($2.5x10^8$cells/ml) were pre-treated with increasing concentration of PGI_2 (0.1-100nM) for 1 minute at 37°C, followed by treatment with thrombin (0.1U/ml). Aggregation was monitored for 3 minutes under constant stirring (1000rpm) at 37°C using Chrono-log dual channel aggregometer. The traces were generated by aggro-link computer software (n=3). Representative trace shown. The arrow shows the point of addition of thrombin. The trace shows a concentration dependant inhibition of platelet aggregation on PGI_2 treatment as supported by **(b)** Quantification of aggregation data, presented as Mean ± SEM (n=3).

3.3. The effect of PGI_2 on protein phosphorylation in platelets

Phosphorylation, a key regulatory mechanism, alters platelet function by affecting platelet signalling pathways. Therefore, the effect of PGI_2-induced and PKA-mediated phosphorylation of various PKA substrates was considered in a concentration-dependent manner using increasing concentration (0.1-100nM) of PGI_2. Similarly, the temporal effects of phosphorylation were studied by treating the platelets with a constant concentration of PGI_2 for increasing time intervals (0-60 minutes).

3.3.1. Substrate phosphorylation in response to increasing concentration of PGI_2

Substrate phosphorylation was studied in platelets treated with increasing concentration of PGI_2 (0.1 - 100nM) for 1 minute at 37^{o}C. The lysates were resolved by SDS-PAGE followed by immunoblotting with anti-phospho-PKA substrate antibody (RRXS*/T*) (pPKAs), an antibody that recognises PKA consensus phosphorylation sequence (-Arg-Arg-X-Ser/Thr-X). These experiments also examined the phosphorylation of VASP at ser157 ($pVASP^{Ser157}$), a well-established PKA substrate, which was used as a positive control for PKA phosphorylation. Furthermore, discrepancies in protein loading were accounted for by using β-tubulin as the protein loading control.

Washed platelets were treated with increasing concentration of PGI_2 (0.1 - 100nM). The phosphorylation status of all PKA substrates was explored using pPKA substrate antibody. Proteins corresponding to apparent molecular weight of 20, 42 and 52kDa were phosphorylated under untreated conditions, as shown by the appearance of corresponding protein bands. A proportional increase in band intensity of these was observed on treatment with increasing concentration of PGI_2 (0.1 – 100nM) (*Figure 3.2a*). In addition to these, proteins corresponding to the apparent molecular weight of 30, 40 and 70kDa were not phosphorylated under untreated conditions but were phosphorylated in a concentration-dependent manner in response to PGI_2-treatment. The results suggest that PKA phosphorylates multiple substrates; albeit each substrate possesses a unique phosphorylation profile as shown by varying intensity of phosphorylation bands at a specific time interval.

Figure 3.2

a

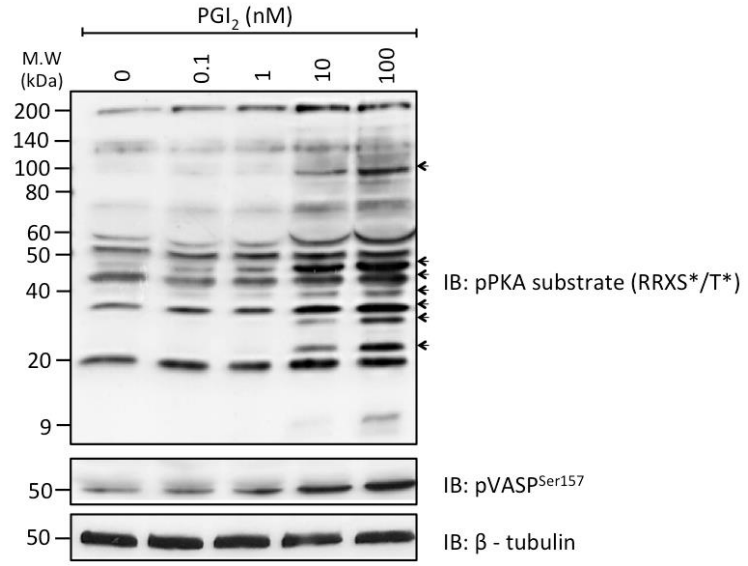

b

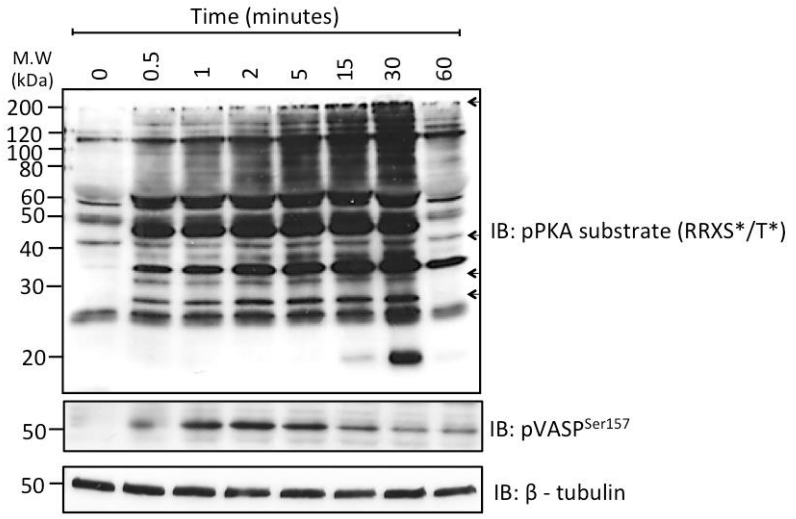

***Figure 3.2* – PGI_2 induces PKA substrate phosphorylation in a concentration and time-dependant manner as examined by immunoblotting**

(a) Washed platelets ($5x10^8$ cells/ml) were treated with increasing concentration of PGI_2 (0.1 - 100nM) for 1 minute at 37^oC, with constant stirring for the first 15 seconds. At the end of 1 minute, the signalling was terminated by lysing the platelets with 2x Laemmli buffer (1:1v/v). 30µg of protein was loaded on 10-18% gradient gel and resolved as described previously. Immunoblotted was performed using anti-phospho-PKA substrate antibody (1:1000) and anti-$pVASP^{Ser157}$ antibody. Anti-β-tubulin (1:1000) was used as a loading control (n=3). A concentration-dependant increase in PGI_2-induced phosphorylation of substrate was seen, as indicated by arrows **(b)** Similarly, washed platelets were treated with a constant dose of PGI_2 (100nM) for increasing time period (0.5 - 60 minutes), and handled as previously detailed, displayed a temporal regulation of phosphorylation, as indicated by arrows. (n=3).

The phosphorylation pattern of VASP at ser157, a well-established PKA substrate was also studied. An increase in the intensity of band corresponding to $pVASP^{Ser157}$ (50kDa) correlates to the increasing concentration of PGI_2; therefore suggesting that VASP undergoes phosphorylation at ser157 in a concentration-dependent manner (*Figure 3.2a*).

3.3.2. Temporal pattern of substrate phosphorylation in response to PGI_2 treatment

To assess the temporal patterns of PGI_2-induced substrate phosphorylation, washed platelets were treated with a constant concentration of PGI_2 (100nM) for varying time intervals (0.5 to 60 minutes). Proteins corresponding to apparent molecular weight of 42, 52 and 60kDa were phosphorylated under untreated conditions, as shown by the appearance of corresponding protein bands. The intensity of these bands increased on treatment with PGI_2 (at 0.5 minutes onwards), and was maintained until 30 minutes, after which the band intensity was blunted to untreated levels. This means that the substrates corresponding to the molecular weights of 42, 52 and 60kDa underwent a rapid phosphorylation at 0.5 minutes, which was sustained until 30 minutes, before being blunted to untreated levels at 60 minutes (*Figure 3.2b*). Protein band corresponding to the apparent molecular weight of 120kDa showed basal phosphorylation, which increased in a time-dependent manner. However, protein bands corresponding to the molecular weight of 32 and 50kDa showed an increase in band-intensity corresponding rapid phosphorylation from 0.5 minutes, which peaked around 2-5 minutes. The protein phosphorylation gradually diminished from there on, however failed to reach band intensities corresponding to untreated levels. Likewise, the band corresponding to pVASP (50kDa) underwent rapid PGI_2-induced phosphorylation at 0.5 minutes, which peaked at 2 minutes and was maintained until 5 minutes, after which the band intensity gradually diminished (*Figure 3.2b*).

Overall, the results indicate that there are multiple PKA substrates that undergo PGI_2-induced phosphorylation. The temporal regulation of each protein is distinctive though, i.e. the phosphorylation peaks at different time-points and is maintained for varying time intervals.

3.3.3. Protein Kinase A mediates Protein Phosphorylation.

Having established concentration- and temporal effects of PGI_2-induced substrate phosphorylation, it was essential to by-pass the Ip receptor to investigate downstream effects of PKA activation. To achieve this, Forskolin, an activator of AC (Seamon et al., 1981) and 8-CPT-6-Phe-cAMP, a synthetic cAMP analogue were used.

Washed platelets were incubated with forskolin (5µM) and 8-CPT-6-Phe-cAMP (10µM) respectively, for 5 minutes at 37^{o}C, with constant stirring for the first 15 seconds, to enable uniform distribution of forskolin and 8-CPT-6-Phe-cAMP throughout the washed platelet suspension. Forskolin would cause a direct activation of AC and therefore stimulate cAMP-signalling pathway, without the involvement of Ip receptor. 8-CPT-6-Phe-cAMP, is a synthetic non-hydrolysable analogue of cAMP, which means it triggers the activation of cAMP signalling pathway downstream of PKA. Washed platelets treated with PGI_2 (100nM) for 1 minute at 37^{o}C were used as a positive control. At the end of incubation period, the samples were lysed with Laemelli buffer and handled as described in §2.5.1-2.5.3. PKA substrate phosphorylation was studied by probing with anti-pPKAs and anti-pVASP^{Ser157} antibodies. Forskolin and 8-CPT-6-Phe-cAMP, both caused substrate phosphorylation downstream of PKA, as indicated by the appearance of phosphorylation bands. Proteins corresponding to apparent molecular weights of 30, 50 and 120 kDa were not phosphorylated under untreated conditions, however, underwent phosphorylation on treatment; albeit to varying degree. The band intensity for these phosphorylation bands was the most potent when treated with PGI_2 and Forskolin. 8-CPT-6-Phe-cAMP also brought about phosphorylation of these proteins, however was slightly weaker (*Figure 3.3a*). The difference in the intensity of the phosphorylation could be explained by the difference in the mechanism of PKA activation between the two compounds (§3.5).

PKA signalling mechanism was further dissected using inhibitors to block key proteins of the pathway (*Figure 3.3b*). An Ip receptor antagonist, RO1138452 (1µM) was used to inhibit Ip receptor. PKA inhibitors (Rp-8-CPT-6-Phe-cAMPS and KT5720) possessed limited specificity when used independently, hence they were used in combination (Murray, 2008). Rp-8-CPT-6-Phe-cAMPS competes for the cAMP binding site on PKA R-subunit,

Figure 3.3

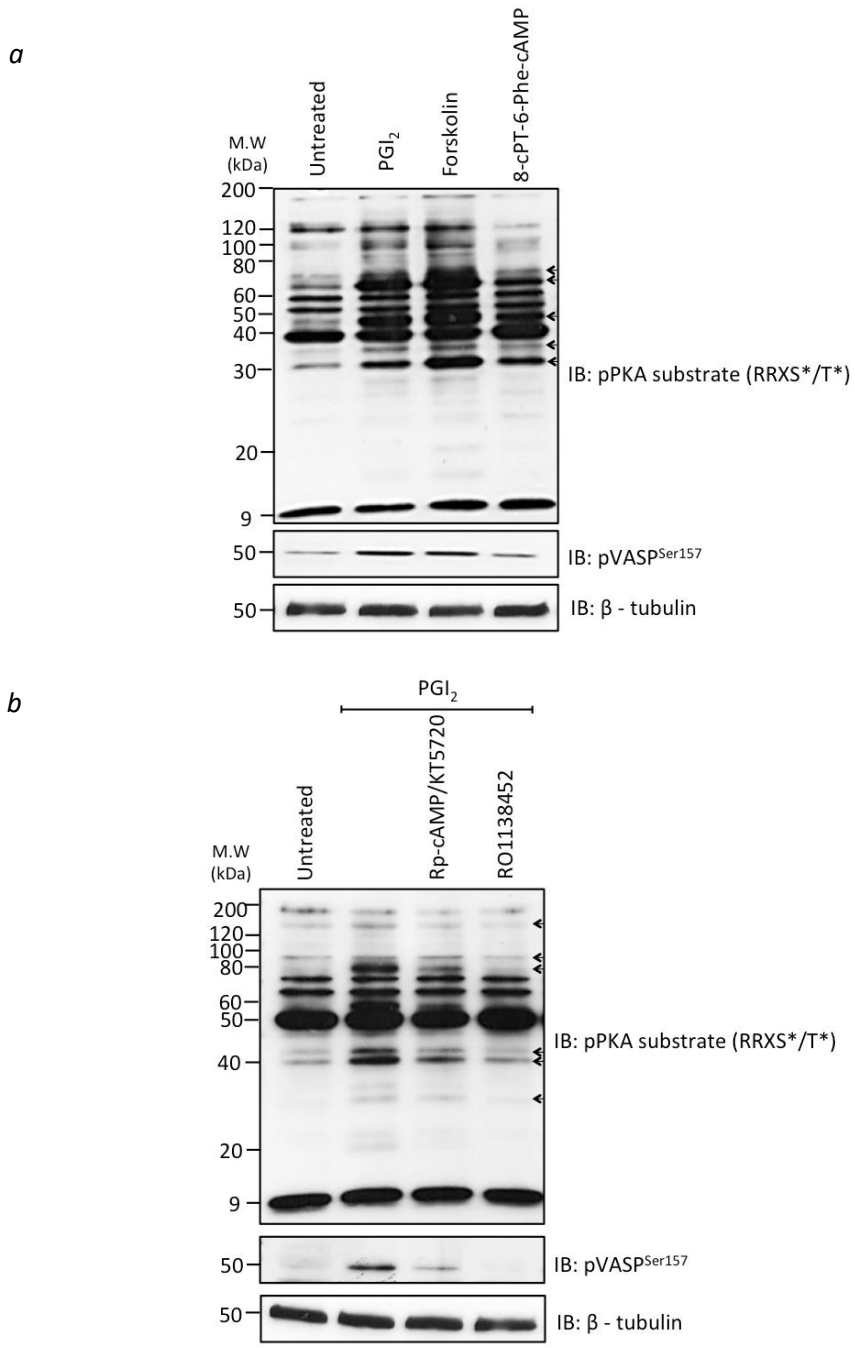

***Figure 3.3* – Confirmation of PKA-mediated substrate protein phosphorylation by immunoblotting using PGI_2 independent activatory of cAMP signalling.**

(a) Washed platelets ($5x10^8$ cells/ml) were treated with Forskolin (5µM) and 8-CPT-6-Phe-cAMP (50µM) for 5 minutes at 37°C, with constant stirring for the first 15 seconds. Platelets were handled as described previously. Immunoblotting was performed using anti-phospho-PKA substrate antibody (1:1000) and anti-$pVASP^{Ser157}$ antibody. Anti-β-tubulin (1:1000) was used as a loading control (n=3). **(b)** Similarly, washed platelets were treated with RO1138452 and Rp-8-CPT-6-Phe-cAMPS/KT5720 for 20 minutes at 37°C, prior to treatment with PGI_2 (100nM) for 1 minute. The samples were processed as described previously (n=3).Presence of substrate phosphorylation bands on treatment Forskolin and 8-CPT-6-Phe-cAMP (as in (a)) and blunting of phosphorylation response in (b) both indicate substrate phosphorylation is caused downstream of PKA

whereas KT5720 is a competitive inhibitor for the ATP-binding site on the PKA c-subunit (Murray, 2008).

In both the cases, the platelets were pre-incubated with the respective compounds for 20 minutes at 37^{o}C prior to treatment with PGI_2 (100nM) for 1 minute. A positive control, of platelets treated with PGI_2 was also analysed alongside the samples treated with the antagonists. Protein bands corresponding to the molecular weight of 40, 55 and 80 kDa showed no basal phosphorylation, but on treatment with PGI_2, a phosphorylation band appeared, suggesting that PGI_2 induces the phosphorylation of these substrates. However, treatment with RO1138452 and the PKA inhibitors blunted the phosphorylation response of these proteins. VASP also mirrored the phosphorylation response of these proteins. This primarily indicates that these proteins are PKA substrates and that the phosphorylation response occurs downstream of PKA (*Figure 3.3b*).

To summarise, here we show that pharmacological activators of PKA (forskolin and 8-cPT-6-Phe-cAMP) cause phosphorylation of PKA substrates. PKA-mediated phosphorylation is blunted on treatment with PKA inhibitors (Rp-cAMP/KT5720) and Ip receptor antagonist (RO1138452). This suggests that substrate phosphorylation occurs downstream of PKA.

3.4 Validating the presence of PKA in platelets

Having established that PGI_2 most likely signals through PKA, we wished to establish which elements of the PKA heterodimer were present in platelets. This was an important element of the study, since we will go on to establish how these subunits interact with specific PKA substrates.

3.4.1. Characterisation of the PKA subunits present in platelets.

The presence of PKA, which is composed of two R-subunits and a pair of c-subunits is well established in platelets (Kaulen and Gross, 1974, Booyse et al., 1976, Margarucci et al., 2011), however, to validate these findings using western blotting, increasing concentration of protein was resolved using SDS-PAGE followed by immunoblotting using antibodies specific to PKA RI-, RII- and PKA c-subunits respectively. The increase in band intensity corresponding to the protein concentration implies the presence of all PKA subunits in platelets (Aburima et al., 2013) (*Figure 3.4a*) as supported by findings from the transcriptomics study (Margarucci et al., 2011).

Furthermore, PKA subunits were immunoprecipitated from the platelet lysates using the corresponding antibodies. The presence of a protein band in the platelet lysate lane and immunoprecipitation lane but the absence of the corresponding band in the IgG lane (*Figure 3.4b*) indicates successful precipitation of PKA RI-subunit in platelets. Similar approach was adopted to validate the presence of PKA RII-subunit (*Figure 3.4c*) and the c-subunit (*Figure 3.4d*). *Figure 3.4* confirms the presence of PKA in platelets. It was vital to be able to isolate the PKA subunits using immunoprecipitation, as this approach is later applied to study the interaction of PKA subunits with PKA substrates.

To summarise, here we show that PKA RI-, RII- and the c-subunits are present in platelets as can be detected by western blotting and immunoprecipitation.

Figure 3.4

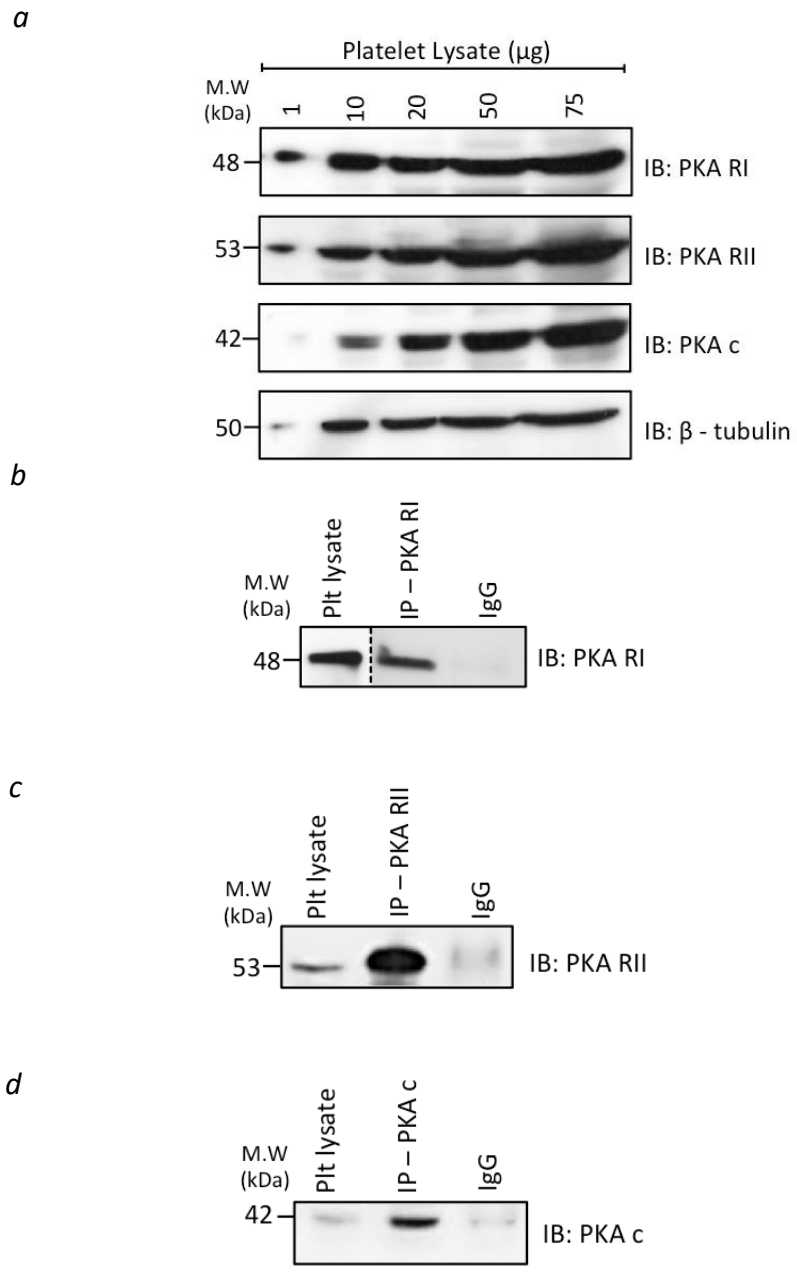

***Figure 3.4* – Identification of the presence of PKA in platelets using immunoblotting.**

(a) Washed platelets ($5x10^8$ cells/ml), lysed with with 2x Laemmli buffer (1:1v/v) were resolved on 10-18% gradient gel by SDS-PAGE for 90 minutes at 120V. Proteins were transferred onto a PVDF membrane using the turbo blot system. Membranes were blocked with 10% BSA and immunoblotted using anti-PKA RI, Anti-PKA RII and anti-PKA c antibodies (1:1000). The increase in band intensity corresponding to the protein concentration implies the presence of all PKA subunits in platelets. Anti - β-tubulin (1:1000) was used as a loading control (n=3). **(b)** PKA RI (2µg), **(c)** PKA RII (2µg) and **(d)** PKA c (2µg) were precipitated from untreated platelet lysates as previously described. The presence of a protein band in the platelet lysate lane and immunoprecipitation lane but not in the IgG lane indicates successful precipitation of PKA RI-subunit, RII-subunit and c-subunit in platelets. This suggests the presence of PKA subunits in platelets.

3.4.2. Presence of PKA as a complex between R- and c-subunits

PKA, in its inactive state is reported to be a heterotetramer composed of two R-subunits and two c-subunits (Taylor, 1989). To validate the existence of these protein-protein interactions in platelets, co-immunoprecipitation approach was adopted, whereby the PKA c-subunit antibody was precipitated by covalently coupling to amine-reactive resin and probing for interacting proteins (PKA RI- and RII-subunit). Post-elution, the lysate was resolved by SDS-PAGE and immunoblotted using antibodies raised against individual PKA regulatory subunits. The appearance of bands corresponding to the reported molecular weight of c-subunit in the platelet lysate lane (Aburima et al., 2013) and the immunoprecipitate lane but not in the IgG control lane (*Figure 3.5*) indicates the success of the precipitation protocol.

Furthermore, on probing with PKA RII-subunit antibody, the bands corresponding to the reported molecular weight of RII-subunit appeared in the platelet lysate and the immunoprecipitate lane but not in the IgG control lane. This suggests an interaction between c- and RII-subunits. Using a similar approach, an interaction between c- and RI-subunits was also detected, however the protein band corresponding to the apparent molecular weight of RI-subunit was very weak. This could perhaps suggest a weak interaction between the two proteins (*Figure 3.5*). Due to the limitation of the experimental technique, the strength of the interaction between R-subunits and c-subunits could not be quantified. Alternatively, the possibility that RI-subunit is less abundant than RII-subunit cannot be ignored.

Here, using co-immunoprecipitation, we show the presence of PKA as a complex between R- and c-subunits.

Figure 3.5

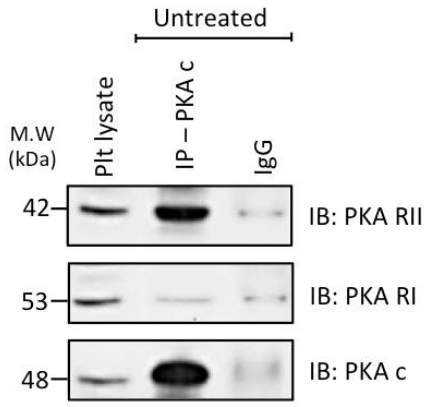

***Figure 3.5* – Identification of the presence of PKA subunits and their presence as a heteromeric protein complex in platelets.**

Protein-Protein interactions were studied by precipitating the antigen (bait protein) and probing for any interacting proteins. Anti-PKA c antibody (2µg) was coupled covalently to amine-reactive resin. Post-elution, the lysate was resolved on 10-18% gel at 120V for 90 minutes. The proteins were transferred to PVDF membrane using the Turbo-Blot transfer system (Bio- Rad) and immunoblotted for anti-PKA RI and anti-PKA RII. The presence of bands corresponding to the reported molecular weight of PKA RI- and RII-subunit in the platelet lysate and the immunoprecipitate lane but not in the IgG control lane suggests an association between the PKA R-subunits and PKA c-subunit (n=2).

3.4.4. Associated PKA catalytic activity with the R-subunits

PKA causes phosphorylation by transferring the terminal phosphate of the ATP to the hydroxyl group of the protein. Having established the presence of PKA heterotetramer in platelets, it was essential to assess the associated PKA activity. To achieve this, non-radioactive PepTag PKA assay was used to measure associated PKA catalytic activity from PKA RI and RII immunoprecipitates (§2.5.4 and §2.6). Alongside the samples, a positive control (of recombinant PKA catalytic subunit; 2μg/ml) and a negative control (no PKA/ sample added) were resolved.

Upon phosphorylation by PKA, the PKA substrate peptide tag (Leu-Arg-Arg-Ala-Ser-Leu-Gly) acquires an overall negative charge and migrates towards the positive electrode on agarose gel electrophoresis, therefore providing a visual representation of PKA activity, as shown by the positive control. Similarly, in the absence of PKA or when the PKA is unable to phosphorylate the substrate, the overall charge is positive, and therefore the net migration is towards the negative electrode (*Figure 3.6a*).

PKA RII-subunit displays a significantly higher associated PKA activity compared to the IgG control ($p=0.0024$). RI-subunit also shows associated PKA activity, however the difference compared to IgG is not significant ($p=0.3379$) (*Figure 3.6b*). Post PKA activation for the PepTag Assay, the immunoprecipitated protein was eluted from the solid support using 2x Laemmeli buffer and resolved to assess the success of immunoprecipitation. The presence of a band corresponding to the supposed molecular weight of the protein in the immunoprecipitate lane but its absence in the IgG lane confirms the success of the protein immunoprecipitation (*Figure 3.6c*). The data suggests that PKA R-subunits display an associated catalytic activity.

Figure 3.6

a

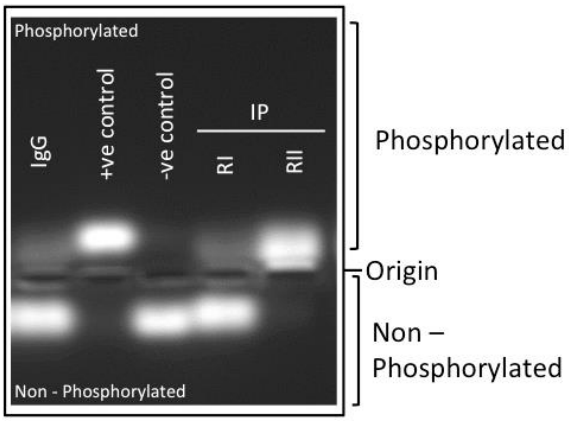

b

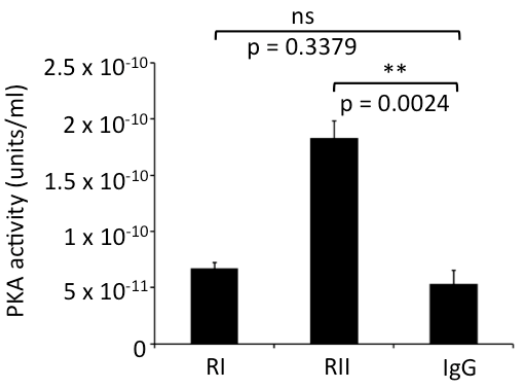

c

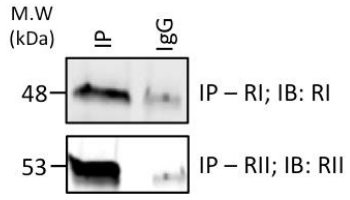

***Figure 3.6* – Immunoprecipiated PKA regulatory subunits have and associated PKA catalytic activity.**

(a) PKA RI- and RII-subunits were immunoprecipitated as described previously, except that the associated PKA c was released and activated. The net PKA activity was assayed using a highly specific coloured PKA substrate peptide tag and resolved on 0.4% Agarose gel. **(b)** The coloured bands were melted and quantified using TeCan Spectrophotometer. PKA RII-subunit displayed a significantly higher associated PKA activity compared to the IgG control (p=0.0024). **(c)** The success of the immunoprecipitation protocol was assessed by eluting the remaining protein from the beads followed by Immunoblotting for the same. The presence of a band corresponding to the supposed molecular weight of the protein in the immunoprecipitate lane but its absence in the IgG lane confirms the success of the protein immunoprecipitation (n=3)

3.5. Discussion

Reversible protein phosphorylation is a critical mechanism for cellular regulation. The physiological significance of protein phosphorylation is highlighted by research showing enhanced protein phosphorylation in several genetic diseases (Cohen, 2001), cancers (Radivojac et al., 2008) and age-related diseases (Mattson et al., 2004). Reversible phosphorylation as a post-translational modification first came under the scientific spotlight with the identification of PKA (Smith et al., 1972). In other cell types, the downstream effects of cAMP signalling are mediated by Epac (de Rooij et al., 1998), cyclic nucleotide-gated ion channels (Nakamura & Gold, 1987) and PKA (Hayes & Mayer, 1981). However in platelets, cAMP signalling is exclusive to PKA activation (Schwarz et al., 2001).

Using aggregation, we show the effect of PGI_2 on platelet function (*Figure 3.1*). A concentration-dependent inhibition of thrombin-induced aggregation in the presence of PGI_2 is observed. Elevation in cAMP is reported to compromise platelet granule secretion, which is vital for platelet aggregation (Aburima et al., 2013). PKA is shown to down-regulate Protein Kinase C (PKC) activity, a Ca^{2+}-dependent protein by compromising the availability of Ca^{2+}. As a result, phosphorylation of PKC substrates, important in platelet granule release is restrained. For example, PKC-mediated phosphorylation of MARCKS can cause rearrangement of actin cytoskeleton and consequently dense granule secretion. PKA-mediated inhibition of PKC prevents this process and therefore cause platelet inhibition (Elzagallaai et al., 2000; Hartwig et al., 1992). A second major site of action for PKA is the suppression of the mobilisation of intracellular Ca^{2+} in cells. Since an increase in the intracellular Ca^{2+} is critical for supporting platelet aggregation mechanism which target this can modulate aggregation. The precise mechanisms that allow cAMP signalling to target Ca^{2+} are yet unclear, however speculations suggest the inhibition of Ca^{2+}-dependant enzymes (Geiger et al., 1994) and the phosphorylation of IP_3R (Cavallini et al., 1996; El-daher et al., 2000) could contribute towards platelet inhibition.

In the light of these findings, the concentration and temporal nature of PGI_2-induced and PKA-mediated phosphorylation of a variety of PKA substrates was also studied using western blotting (*Figure 3.2*). A phospho-PKA substrate (pPKAs) specific antibody, which detects the phosphorylated ser/thr residues with arg at -3 position, was used to detect the

potential PKA substrates. In addition to this, pVASP^{Ser157} antibody was used as a positive control since VASP is a known target for PKA in platelets (Holt et al.,1998). The results show that activation cAMP signalling and PKA leads to phosphorylation of multiple substrates in concentration and time-dependant manner. For each protein, the phosphorylation is induced at specific concentration and time, and is prolonged for a specific time interval. This is in parallel with previous reports that suggest unique protein-specific phosphorylation patterns could be a consequence of compartmentalisation of specific cAMP micro-domains, that regulate specific signalling complexes (Zaccolo & Pozzan, 2002). Also, termination of cAMP signalling conferred by PDEs, could also contribute to time-dependant blunting of phosphorylation response (Pidoux & Tasken, 2010). To further dissect PKA-mediated phosphorylation, pharmacological and localised activation of PKA was accomplished using forskolin and 8-cPT-6-Phe-cAMP respectively (*Figure 3.3a*). Forskolin fits in the substrate-binding cleft between the catalytic subunit pair of AC. This causes conformational reorganisation of the enzyme and activates it (Tesmer et al., 1997). 8-cPT-6-Phe-cAMP, a membrane permeable synthetic analogue of cAMP was used as a direct activator of PKA (Sandberg et al., 1991; Schwede et al., 2000), however some non-specific effects on PKG in platelets have also been reported (Christensen, 2003). Nevertheless, both forskolin and 8-cPT-6-Phe-cAMP caused phosphorylation of PKA substrates including VASP. A closer look at the results shows that forskolin and PGI_2 caused a more potent phosphorylation compared to 8-cPT-6-Phe-cAMP (as indicated by the appearance of more/intense bands) (*Figure 3.3a*). However, it is vital to recognise that while 8-cPT-6-Phe-cAMP causes a widespread elevation of cAMP and therefore PKA activation, forskolin is a pharmacological activator of AC, which subsequently causes localised activation of PKA. This could result in differing levels of PKA activation and a consequent change in the pattern of substrate phosphorylation. Also, the platelets may display a varying sensitivity to both these compounds, therefore resulting in differing phosphorylation band intensities. Furthermore, the difference in the optimal incubation time between the two compounds could also explain this difference. However, in combination the data suggested that localised and pharmacological elevation in cAMP levels in platelets successfully caused PKA-mediated substrate phosphorylation.

To further strengthen the findings, Ip receptor and PKA were blocked pharmacologically (*Figure 3.3b*). RO1138452, an Ip receptor antagonist, competitively occupies to the agonist-

binding site on the Ip receptor, therefore interfering with PGI_2-induced receptor activation (Bley et al., 2006; Jones et al., 2006). To address PKA directly we used a combination of inhibitors that targeted different parts of the PKA holoenzyme. PKA, in its inactive state is composed of a pair of c-subunits bound to two R-subunits (Corbin et al,; 1973; Potter et al., 1979). KT5720 competes for the ATP–binding site on the PKA c-subunit. This interferes with the ability of the c-subunit to transfer the gamma phosphate onto its substrate and cause phosphorylation (Kase et al., 1987; Murray, 2008). Rp-cAMP, competes with cAMP for the cAMP-binding site on the R-subunits. This restricts the conformational change associated with PKA activation and subsequent unleashing of c-subunits (de Wit et al., 1984; Murray, 2008). We show here that pharmacological interference with the cAMP signalling pathway compromises the PKA-mediated phosphorylation of substrates (*Figure 3.3b*). However, it is interesting to note that the extent of effect is specific to each substrate. Again, this could due to the differing affinities of PKA-mediated phosphorylation towards each substrate. This means that the concentration of cAMP pathway antagonists used may perhaps not be sufficient to completely ablate PKA activity and therefore the downstream phosphorylation events. Furthermore, the varying sensitivity of platelets to pharmacological compounds could also result in compromising phosphorylation to varying degrees.

There are significant structural differences between R- and c-subunits of PKA, but both of these are conserved across the animal kingdom (Kim et al., 2007). However, multiple isoforms of both the R- and c-subunits have been reported. Cloning of cDNAs have identified two isoforms each of RI-subunit (RIα and RIβ) (Clegg et al., 1988; Lee et al., 1983; Mårten et al., 1987) and RII-subunit (RIIα and RIIβ) (Scott et al., 1987). The existence of these R-subunit isoforms gives rise to PKA type I and type II, both of which exhibit differential localisation (Corbin et al., 1975). Potential PKA isoforms have been reported to be present in platelets, and we confirmed the presence of PKA RI-, RII- and c-subunits using western blotting and immunoprecipitation (*Figure 3.4)*. This was essential as we later endeavour to establish the interaction dynamics between PKA and its substrates. Owing to the lack of isoform-specific antibodies for PKA, we were unable to establish the abundance of each PKA subunit in platelets. Nevertheless, RIβ and RIIβ have been reported to be the most abundant isoforms in platelets (Rowley et al., 2011; Schwarz et al., 2001). Furthermore, using co-immunoprecipitation, we show that in its inactive state PKA exists as a complex between

the regulatory and catalytic subunits (*Figure 3.5*), as is supported by previous research (Corbin et al., 1973; Potter et al., 1979). The results show the co-immunoprecipitation band for RII-subunit to be more robust as compared to that for RI-subunit. However, this may not perhaps be representative of the potential abundance of RI-subunit and RII-subunit. It is possible that the difference in band intensities for RI- and RII-subunits could perhaps be as a consequence of differing affinities of the antibodies in question towards the respective proteins. Also, due to the limitation of the experimental approach used, the strength of this interaction could not be established. However previous research suggests that perhaps owing to structural differences between RI- and RII-subunits, PKA c-subunit has a greater affinity towards RII-subunit (i.e. the formation of PKA II holoenzyme is preferred), whereas RI-subunits are more likely to exist as a free dimer (Otten & McKnight, 1989). Alternatively, the discrepancies in the efficiency of the antibodies to precipitate the relevant protein could also result in variations in band sizes.

Having established the existence of the PKA holoenzyme as a complex between R-subunits and c-subunits, it was essential to explore the potential of unactivated PKA to phosphorylate protein substrates. To achieve this, PKA-c subunit associated with PKA RI- and RII-subunits was first extracted using immunoprecipitation. Next non-radioactive PKA assay was employed, whereby a brightly coloured PKA-substrate is used as a marker of PKA activity. On PKA-mediated phosphorylation of the substrate, the overall charge is altered to negative and therefore altering its net migration on agarose gel towards positive electrode. A key structural feature of each R-subunit is the presence of two cAMP-binding sites. On binding of four cAMP molecules, the holoenzyme undergoes a conformational change and releases the catalytically active PKA-c dimer from the cAMP-bound R-subunits (Kopperud et al., 2002), which can phosphorylate protein substrates. Here we show that RII-subunit immunoprecipitate displays a stronger kinase activity compared to RI-subunit immunoprecipiate (*Figure 3.6*). Since kinase activity is primarily a consequence of PKA catalytic activity, the results suggest that PKA c-subunit displays preferential association towards RII- over RI-subunit. These findings are in line with the suggestion of evolutionary preference towards the formation of PKA RII holoenzyme (Otten & McKnight, 1989). However, it is important to consider that the assay is greatly affected by the efficiency of the antibodies used for isolating RI- and RII-subunits by immunoprecipitation. For this reason, it

would be naïve to conclude anything about the preferential existence of each type of PKA holoenzyme. Nevertheless, the assay shows the PKA is active in platelets. PKA-mediated phosphorylation of platelet proteins results in inhibition of actin reorganisation is one of the mechanisms by which PKA inhibits platelet activation.

Platelet activation and aggregation primarily occurs as a consequence of inside-out signalling. This involves conformational alteration of glycoprotein IIb/IIIa to enable binding soluble fibrinogen (Bennett et al., 1999; Calderwood, et al., 2000). This process is also complemented by platelet cytoskeletal rearrangement and actin reorganisation to drive the key morphological changes. PGI_2, the physiological activator of PKA, mediates platelet inhibitory effects by binding to the Ip receptor, and activating AC (Armstrong, 1996). PGI_2-induced activation of AC causes the hydrolysis of ATP to form cAMP, which subsequently binds and activates PKA. Activated PKA can inhibit platelet activation by compromising key events in platelet activatory pathways such as intracellular Ca^{2+} elevation, platelet granule secretion and cytoskeletal rearrangement. Some reports suggest β_3-endonexin, a crucial fibrinogen-binding protein undergoes PKA-mediated phosphorylation (Kashiwagi et al., 1997; Shattil et al., 1995), however the precise mechanisms regulation of integrin activation remain unclear. Another key PKA substrate is the cytoskeleton-associated protein VASP, which is localised in dynamic membrane regions and stress fibres (Reinhard et al., 2001). Phosphorylation of VASP is reported to correspond to downregulation of actin polymerisation (Harbeck et al., 2000) and inhibition of fibrinogen receptor (Horstrup et al., 1994).

To summarise, this chapter demonstrates the presence of PKA signalling machinery in platelets. Also, the role of PGI_2 in platelet inhibition was also established. Having characterised the PKA-mediated phosphorylation in this chapter, the following chapter will focus on the effect of PGI_2 on Ca^{2+} mobilisation in platelets.

CHAPTER IV: CHARACTERISATION OF PKA-MEDIATED IP_3R PHOSPHORYLATION

4.1. Introduction

Regulation of intracellular Ca^{2+} is a key event in platelet haemostasis. The mobilisation of intracellular Ca^{2+} upon agonist-induced platelet activation is mediated by phospholipase-mediated release of IP_3 (Ferris, et al., 1989). This lipid messenger binds to IP_3Rs, tetrameric Ca^{2+} channels, causing a structural rearrangement leading to the mobilisation of Ca^{2+} stores (Ferris et al., 1989). There are three isoforms of IP_3R – IP_3R1, IP_3R2 and IP_3R3, each encoded by different genes – *ITPR1*, *ITPR2* and *ITPR3* respectively. Each of the three subtypes are differentially located (Joseph, 1996); albeit all reported to be present in platelets with IP_3R1 being predominant (El-daher et al., 2000). IP_3R is reported to be phosphorylated by Protein Kinase C (Ferris et al., 1991), Protein Kinase G (Komalavilas & Lincoln, 1996) and PKA (Ferris et al., 1991). The specific sites of phosphorylation are yet to be determined. However, with regards to the work described in this thesis, PKA-mediated phosphorylation and consequent regulation of IP_3R resulting in phosphorylation and consequent inhibition of the receptor has been particularly appealing (Cavallini et al., 1996; Supattapone et al., 1988). IP_3R1 has been reported to undergo PKA-mediated phosphorylation at ser1756 and ser1589, both of which are located in the regulatory region of the receptor (Ferris, et al., 1991). However a platelet-specific characterisation of the sites remains to be performed in platelets.

Intracellular signalling is thought to be controlled through compartmentalisation. Protein components of a signalling cascade are proposed to be organised in a macromolecular complex with each other, therefore providing specificity for cell signalling (Zaccolo & Pozzan, 2003). Previous studies have shown an association between PKA and IP_3R1 in rat brain (Collado-Hilly & Coquil, 2009; Tu et al., 2004) and rat adrenal cells (Hur et al., 2005), however this remains to be studied in human platelets. In this chapter, we explore and characterise the phosphorylation profile of IP_3R1 using physiological agents (such as PGI_2) and non-physiological compounds (such as Forskolin, 8-cPT-6-Phe-cAMP, Rp-8-CPT-6-Phe-cAMPS and KT5720). Furthermore, the effect of this phenomenon on mobilisation of intracellular Ca^{2+} was also studied. Subsequently, the technique of co-immunoprecipitation was applied to study the association between IP_3R1 and PKA in platelets.

4.1.1. Hypothesis

This chapter tests the hypothesis that IP_3R1 is a substrate for PKA and examines the possible consequences of PGI_2 treatment on Ca^{2+} release. The possible association between IP_3R1 and PKA in platelets was also explored.

4.1.2. Aims and Objectives

This chapter aims to establish the presence of IP_3R1 in platelets and characterise its phosphorylation patterns. The objectives of this chapter were to -

1. Confirm the presence of IP_3R1 in human platelets
2. Characterise the PKA-mediated phosphorylation of IP_3R1
3. Identify IP_3R1-PKA complex in platelets

4.2. Intracellular Ca^{2+} mobilisation in platelets

4.2.1 Intracellular Ca^{2+} mobilisation in response to Thrombin

Platelet activation in response to stimulatory agonists (such as thrombin) is associated with the increase in intracellular Ca^{2+} (Authi, et al., 1993). Thrombin has been shown to induce platelet aggregation in a concentration-dependent manner. Here, we aim to test this in principle and study the effect of thrombin treatment on Ca^{2+} mobilisation. To achieve this, intracellular Ca^{2+} levels were measured in Fura-2-AM labelled platelets suspended in nominally Ca^{2+}-free saline, that were treated with an increasing concentration of thrombin (0.001U/ml to 1 U/ml) for 1 minute at 37^{o}C. The Ca^{2+} levels were monitored for 3 minutes post stimulation. Elevation in Ca^{2+} correlated with increasing concentration of thrombin (*Figure 4.1b*); however the time taken for Ca^{2+} mobilisation showed an inverse relationship with thrombin concentration (*Figure 4.1c*). For example, at the highest concentration of thrombin used (1U/ml), it took 5.07 seconds to reach a maximal Ca^{2+} of 300.31nM. On the other hand, at the lowest thrombin concentration (0.001U/ml), the maximal Ca^{2+} concentration of 72.08nM was reached in 158.01 seconds (*Figure 4.1*). As can be seen, 0.001 U/ml and 0.01U/ml of thrombin does not induce a measurable increase over basal, hence these concentrations were not considered appropriate for the use in subsequent experiments. 1U/ml could be intoxicating to platelets. From our results and others in the lab, 0.1U/ml was considered an optimal concentration to use for these experiments (*Figure 4.1*).

To summarise, the results suggest that stimulation of platelets with thrombin causes an elevation in Ca^{2+}. The Ca^{2+} levels do not return to basal levels within the 3 minutes post treatment. The concentration of thrombin used caused a proportional elevation in Ca^{2+}, whereas an inverse relationship with time taken to achieve those Ca^{2+} levels was observed.

Figure 4.1

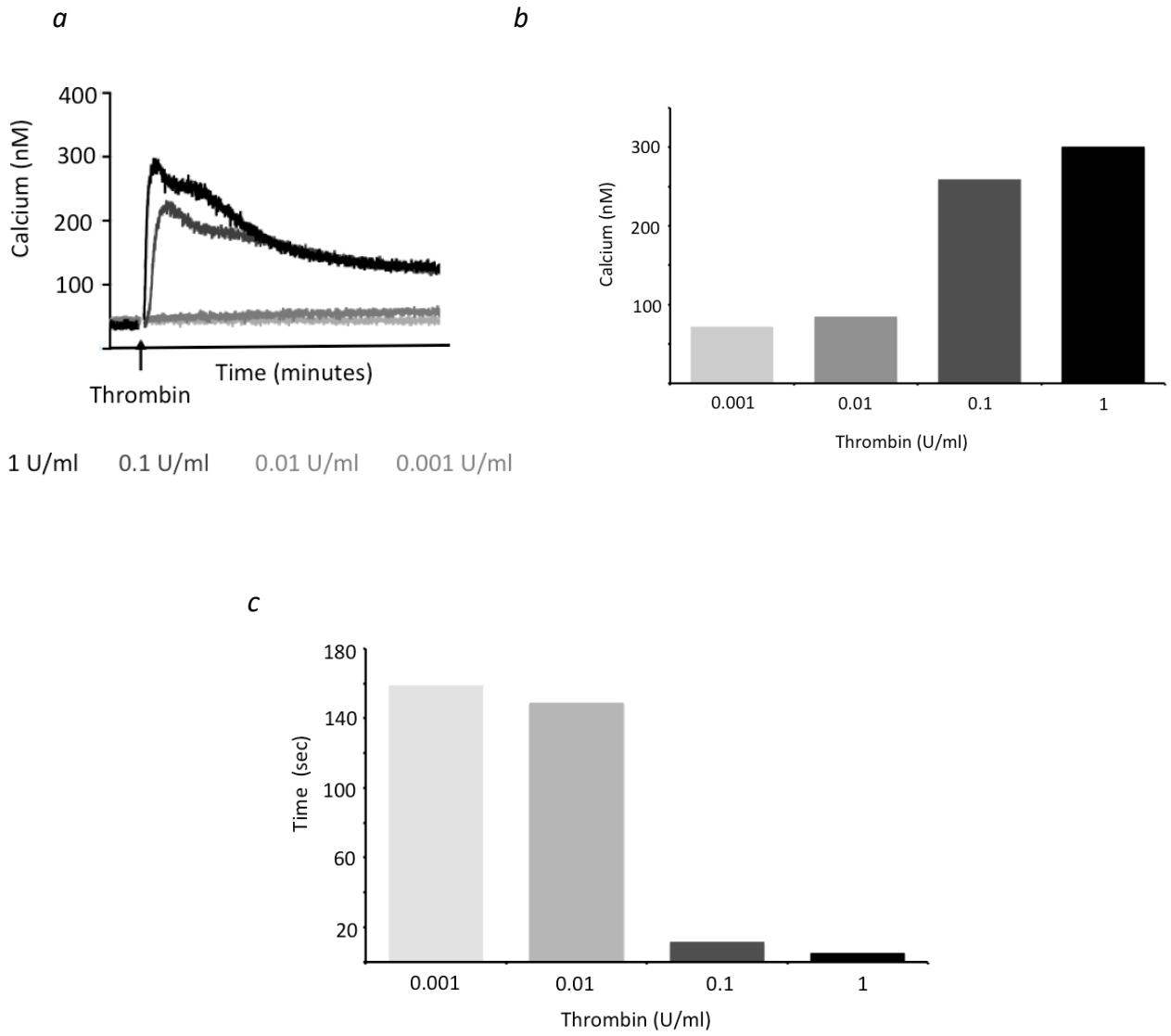

***Figure 4.1.* – Thrombin-induced intracellular Ca^{2+} mobilisation**

(a) Calcium release was measured in Fura-2 loaded washed platelets ($2.5x10^8$cells/ml). Labelled platelet suspension was pre-treated with PGI_2 (1-1000nM) for 1 minute at 37^oC, prior to stimulation with Thrombin (0.1U/ml). The calcium release was measured in dark using Carin Spectrophotometer. The signals were recorded using Cairn proprietary software. A concentration dependant elevation in thrombin was observed. **(b)** The maximal calcium release post-thrombin treatment was proportional to the increase in thrombin concentration but **(c)** showed an inverse relationship with the time required to release the maximal amount of Ca^{2+} (n=1).

4.2.2. Thrombin-induced intracellular Ca^{2+} mobilisation in the presence of PGI_2

PGI_2 has been suggested to inhibit platelet activation by interfering with intracellular Ca^{2+} mobilisation. Studying the effects of PGI_2 on thrombin-induced intracellular Ca^{2+} mobilisation validated these suggestions.

Ca^{2+} mobilisation was measured in suspended Fura-2-AM labelled platelets. The platelets were treated with increasing concentration of PGI_2 (1-1000nM) for 1 minute at 37^{o}C. At the end of the incubation period, the platelets were treated with thrombin (0.1U/ml) and the Ca^{2+} levels were measured for 3 minutes post-stimulation. PGI_2 inhibited Ca^{2+} mobilisation in a concentration-dependent manner (*Figure 4.2a*). Thrombin (0.1U/ml) stimulation caused a maximal release of 415.8±11.9 nM of Ca^{2+} in 20.9±2.9 seconds (at the rate of (26.7±3.4nM/sec), whereas on pre-treatment with PGI_2 (1000nM) blunted this to 255.7±26.5 nM in 81.84±1.14 seconds (at the rate of 2.0±0.3nM/sec). Treatment with PGI_2 (1nM) caused a maximal release of 386.9±20.3nM Ca^{2+} in 30.2±1.1 seconds. The rate of Ca^{2+} mobilisation in response to treatment with 1nM (23.2±2.3) and 10nM (21.6±2.4nM/sec) of PGI_2 was comparable with stimulation with thrombin (0.1U/ml) (26.8±3.nM/sec). Pre-treatment of suspended platelets with 100nM PGI_2 caused Ca^{2+} mobilisation at the rate of 3.22±0.52nM/sec (*Figure 4.2b-d*). The variability in the maximal Ca^{2+} mobilised can be explained by inter-donor variation. In the light of results from §3.2 and these, 100nM PGI_2 was considered to give optimal inhibition of thrombin-induced Ca^{2+} mobilisation. To conclude, thrombin-induced Ca^{2+} mobilisation was blunted in a concentration-dependant manner by PGI_2.

Figure 4.2

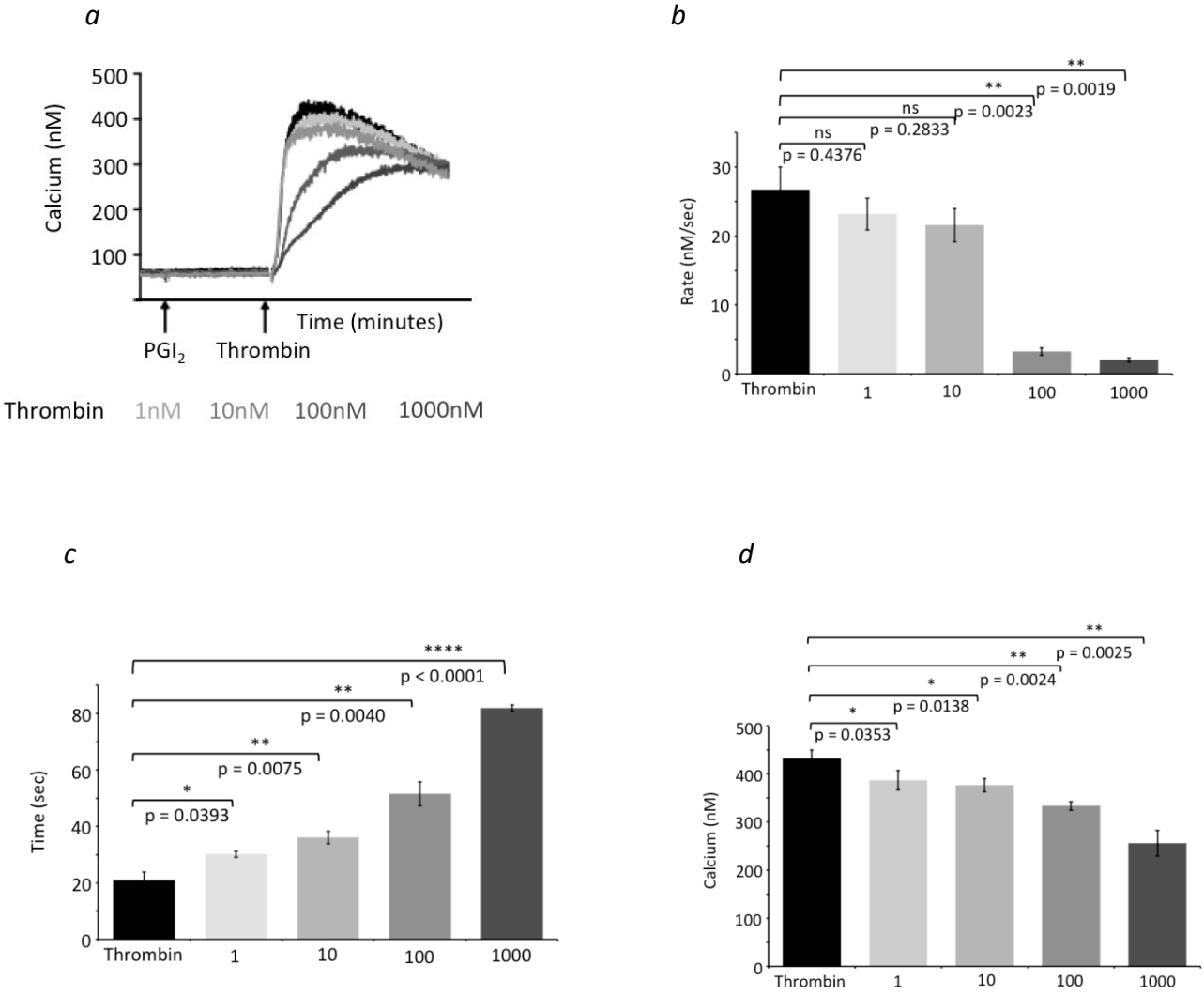

***Figure 4.2.* – Thrombin-induced intracellular Ca^{2+} mobilisation in the presence of PGI_2**

(a) Calcium release was measured in Fura-2 loaded washed platelets ($2.5x10^8$cells/ml). Labelled platelet suspension was pre-treated with PGI_2 (1-1000nM) for 1 minute at 37°C, prior to stimulation with Thrombin (0.1U/ml). The calcium release was measured as described previously. As shown in the representative traces **(b)** the rate of Ca^{2+} release for the first 1 minute post-treatment, **(c)** the time taken to reach the maximal Ca^{2+} and **(d)** the maximal Ca^{2+} concentrations were quantified and plotted as Mean±SEM (n=3). A t-test was performed on the data, the p values of which are shown on the figures. Considering these results, 100nM PGI_2 was considered to give the optimal inhibition of thrombin-induced Ca^{2+} mobilisation (n=3).

4.2.3. Effect of inhibiting IP_3R on intracellular Ca^{2+} mobilisation

IP_3R1 has been reported to be primary source for the mobilisation of intracellular Ca^{2+} in platelets (Varga-Szabo, Braun, & Nieswandt, 2009). 2-Aminoethoxydiphenyl borate (2-APB), a membrane-permeable antagonist was used to block the IP_3-induced Ca^{2+} release (Maruyama et al.,, 1997). Here, we set to investigate the effect of inhibiting IP_3R using 2-APB on intracellular Ca^{2+} mobilisation. To investigate this, intracellular Ca^{2+} levels were measured in a suspended Fura-2-AM labelled platelets that were treated with increasing concentration (10-100µM) of 2-APB, for 3 minutes at 37^{o}C in the dark, followed by treatment with a fixed concentration (0.1U/ml) of thrombin. Calcium mobilisation was measured as described in §2.7.

The rate of Ca^{2+} release induced by thrombin was 25.72 nM/seconds, which was reduced to 0.18 nM/sec in the presence of 100µM 2-APB; (*Figure 4.3a, b*). On further analysis it was also noted that 2-APB pre-treatment increased the time required to cause the maximal Ca^{2+} release in a concentration-dependent manner compared to the control. The rate of Ca^{2+} release in response to 10µM and 100µM of 2-APB treatments was 22.67 seconds and 155.20 seconds compared to 8.62 seconds in control (*Figure 4.3a,c*). Similarly, while the maximal Ca^{2+} release was 281.2nM on stimulation with thrombin, treatment with 2-APB (10µM) reduced it to 198.9nM. Pre-treatment with the highest concentration of 2-APB (100µM) reduced the Ca^{2+} levels to 45.53nM (*Figure 4.3a,d*). Overall, a concentration dependent impediment in the maximal Ca^{2+} release and rate of Ca^{2+} release was observed in the presence of 2-APB, whereas the time required to cause a maximal release of Ca^{2+} was inversely proportional to the concentration of 2-APB used.

Figure 4.3

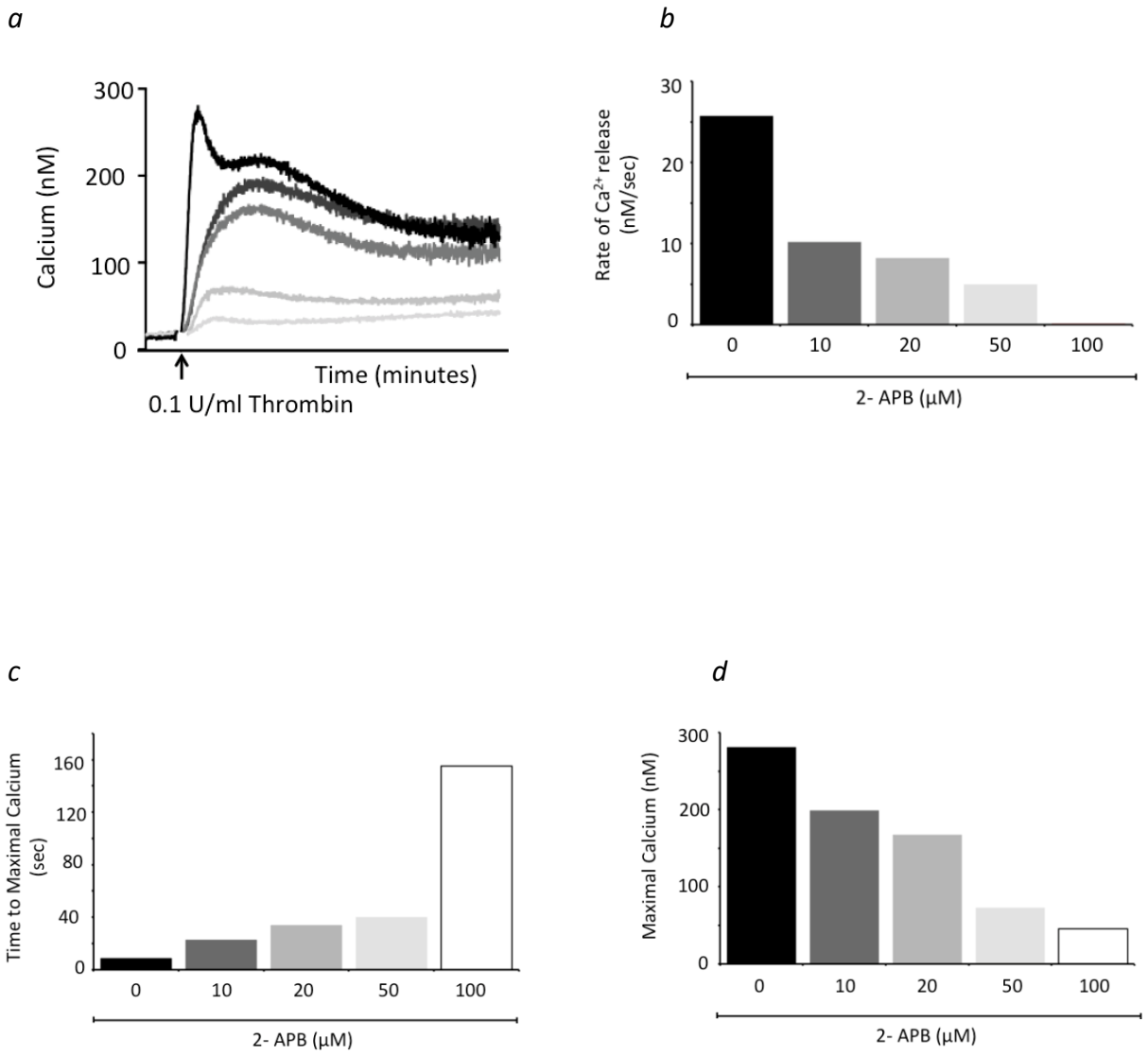

Figure 4.3. **- Calcium mobilisation in response to IP_3R1 inhibition using 2-APB.**

(a) Calcium release was measured in Fura-2 loaded washed platelets ($2.5x10^8$cells/ml). Labelled platelet suspension was pre-treated with 2-APB (10-100µM) for 3 minutes at 37°C, prior to stimulation with Thrombin (0.1U/ml). The calcium release was measured as described previously. **(b)** The rate of Ca^{2+} release for the first 1 minute post-treatment, **(c)** the time required to release the maximal Ca^{2+} and **(d)** the maximal Ca^{2+} released post-treatment was quantified and plotted as Mean. 2-APB pre-treatment blunted the initial rate of Ca^{2+} release and maximal Ca^{2+} released in concentration-dependent manner. The time to release the maximal amount of Ca^{2+} showed an inverse relationship with 2-APB concentration (n=1).

4.2.4. Effect of inhibiting IP_3R on thrombin induced platelet aggregation

The contribution of extracellular Ca^{2+} in platelet aggregation has been well understood (Born, 1962). Although Authi *et al* have shown platelets to aggregate in response to exogenous IP_3 (Authi et al, 1986), the effects antagonising IP_3R-mediated Ca^{2+} mobilisation on platelet aggregation remain to be studied. To investigate this, washed platelets (2.5×10^8 cells/ml) were pre-treated with increasing concentration of 2-APB (10-100µM) for 3 minutes at 37^{o}C in the dark, followed by treatment with a fixed concentration of thrombin (0.1U/ml) (*Figure 4.4a*). Platelet aggregation response was measured for 3 minutes. Treatment with thrombin caused 70±8.2% aggregation, whereas pre-treatment with 10µM 2-APB blunted the aggregation response to 45±5.7%. Treatment with 50µM 2-APB or higher caused a complete inhibition of thrombin-induced platelet aggregation. A concentration-dependent reduction in platelet aggregation on 2-APB treatment (*Figure 4.4*) suggests a function of IP_3R1-mediated Ca^{2+} mobilisation in platelet aggregation, however technical limitations prevented further exploration of the same. It is interesting to note that, even at the highest concentration of 2-APB, a mild platelet shape change is observed. This suggests that perhaps the platelet shape change pathway was independent of IP_3R-mediated Ca^{2+} elevation.

Figure 4.4

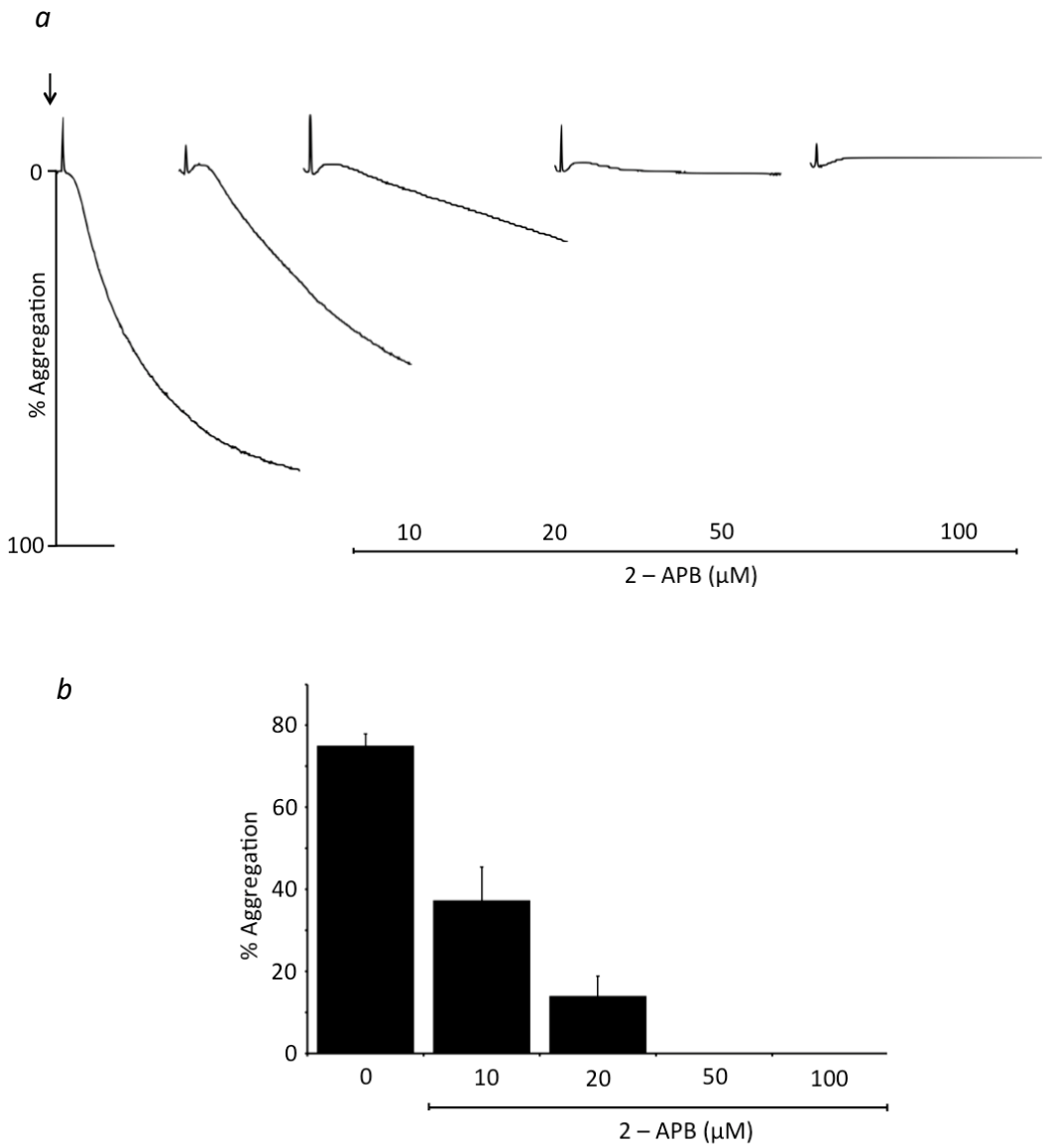

***Figure 4.4* - Platelet aggregation response to increasing dose of 2-APB.**

(a) Washed platelets ($2.5x10^8$cells/ml) were pre-treated with increasing dose of IP_3R1 inhibitor, 2-APB (10-100μM) for 3 minute at 37°C, followed by treatment with thrombin (0.1U/ml). The point of thrombin addition is shown by the arrow. Aggregation was monitored for 3 minutes under constant stirring (1000rpm) at 37°C using Chrono-log dual channel aggregometer. The traces were generated by aggro-link computer software. The representative traces and **(b)** the quantified aggregation data presented as Mean ± SEM suggest that platelets pre-treated with varying concentrations of 2-APB show a concentration-dependant blunting of aggregation but not shape change in response to thrombin (n=3).

4.3. Validating the presence of IP_3R in platelets by immunoblotting

IP_3R has been reported to be the primary intracellular Ca^{2+} release channel. In the light of findings described in *Figure 4.2*, it is vital to appreciate the potential effects of PGI_2 on IP_3R modulation. To begin with, it is essential to test the presence of IP_3R in platelets.

4.3.1. Validating the presence of IP_3R in platelets

Three different subtypes of IP_3R have been reported to be present in platelets (El-Daher et al., 2000) and we set out to validate these findings using immunoblotting. Increasing concentrations of protein from platelet lysate was resolved on Precast 4-20% Mini-PROTEAN TGX Gel followed by immunoblotting using antibodies specific to IP_3R1, IP_3R2 and IP_3R3 respectively. Bands corresponding to the apparent molecular weights of 300, 260 and 250 kDa were observed, suggesting the presence of IP_3R1, IP_3R2 and IP_3R3 respectively. A proportional increase in the band intensity to protein concentration supports the presence of all three IP_3R isoforms in platelets. β-tubulin was used as the loading control to account for discrepancies in protein loading (*Figure 4.5a*).

As a next step, IP_3R were isolated using immunoprecipitation. Unlike western blotting where proteins are detected from a homogenous mixture, immunoprecipitation allows the purification of a single protein from the cell lysates. This makes immunoprecipitation much specific technique of protein detection. IP_3R1 has been reported to be the most abundant of all three IP_3R isoforms in platelets, hence was the focus of this project. The immunoprecipitation conditions for IP_3R1 required optimisation with respect to amount of antibody and solid support. In the first instance increasing concentration of antibody was conjugated with a fixed volume of solid support (either Protein A or Protein G beads). Immunoprecipitation was then performed as described previously (§2.5.4). Data obtained showed that 0.5µg of antibody could precipitate detectable amount of IP_3R1. This was increased until 2µg, but beyond that failed to show any detectable increase in protein precipitation yield. Furthermore, IP_3R1 was undetectable following incubation with protein A beads coated with IgG, suggesting the absence of non-specific binding of IP_3R1 antibody (*Figure 4.5b*).

Figure 4.5

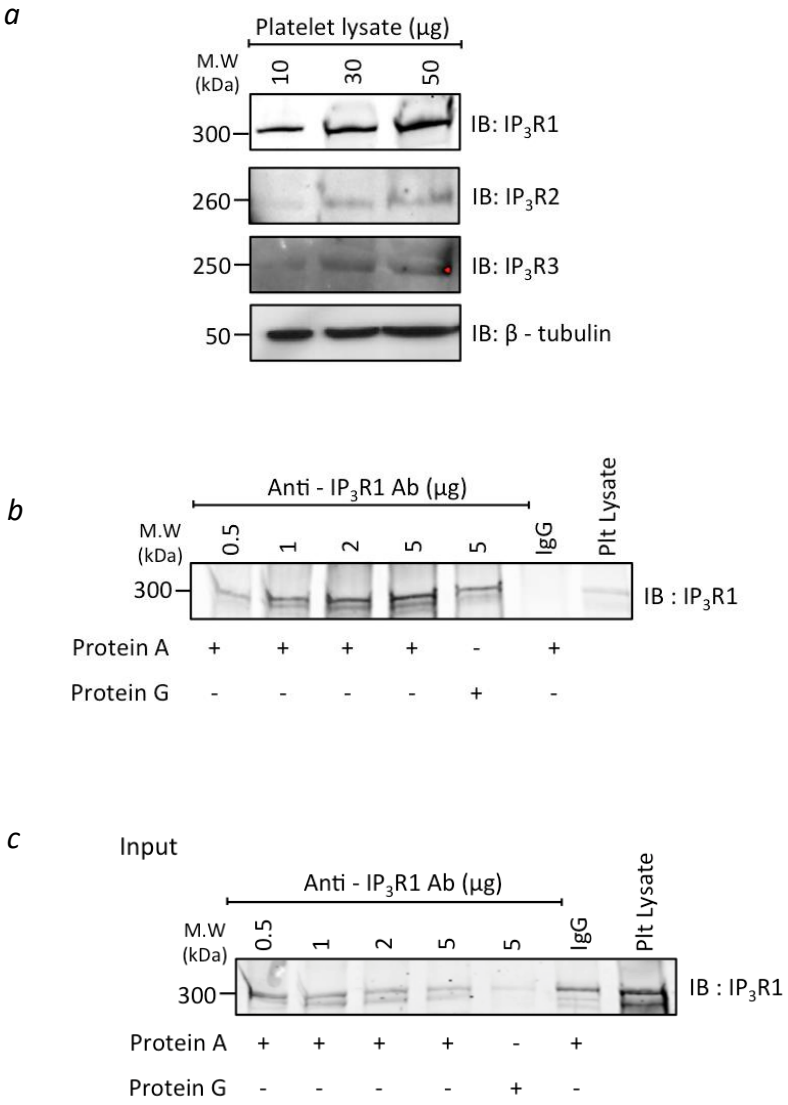

***Figure 4.5* - Validation of the presence of IP_3R in platelets.**

(a) Platelet lysates were loaded in increasing protein concentration and resolved and processed as described previously. The PVDF membranes were probed for anti-IP_3R1, IP_3R2, IP_3R3 and β-tubulin antibodies (1:1000), followed by protein visualisation using ECL (n=3). The appearance of protein bands corresponding to the reported molecular weights suggests the presence of IP_3R isoforms in platelets. **(b)** Platelet lysates (500µg protein) were pre-cleared and IP_3R1 was immunoprecipitated as described previously. The protein was eluted by the addition of Laemelli buffer. The samples were boiled for 10 minutes before being resolved and treated as described previously. **(c)** The immunoprecipitation input was also resolved to assess the efficiency of immunoprecipitation. The optimal protein yield was obtained on using 2µg of antibody with Protein A beads, hence these conditions were used for subsequent experiments.

Input from the immunoprecipitation was also analysed for the presence of residual protein. Although, IP_3R1 could be immunoprecipitated using 0.5µg of antibody, a significant amount of protein still remained in the input. Further analysis of the input did not show any significant difference in the residue remaining from IP performed using 2µg or 5µg antibody (*Figure 4.5c*). For this reason, subsequent immunoprecipitation experiments were performed using 2µg of IP_3R1 antibody. IP_3R1 enrichment was possible using both the types of solid support. However, on comparing the immunoprecipitation yields with the residual protein in the input, we were biased towards Protein A beads being able to precipitate IP_3R1 more efficiently (*Figure 4.5c*). Similarly, immunoprecipitation of IP_3R2 and IP_3R3 was also attempted, however was unsuccessful, perhaps owing to the limitation of the antibodies available.

To summarise, *Figure 4.5* shows the presence of all three IP_3R subtypes in platelets. IP_3R1, being the most abundant (Patterson et al, 2004) was the focus of this project was immunoprecipitated from platelet lysates using 2µg of IP_3R1 antibody and Protein A beads as the solid support. These conditions were deemed optimal for the use in subsequent experiments.

4.4 Characterisation of Serine phosphorylation of IP_3R1

4.4.1. Confirmation of specificity of phospho-IP_3R1 antibody

cAMP signalling pathway is a key pathway that regulates platelet activity. Over 150 PKA substrates, including IP_3R1 have been identified and reported (Beck et al, 2012; El-daher et al., 2000; Margarucci et al., 2011). However, a detailed characterisation of IP_3R1 phosphorylation in response to cAMP signalling is yet to be performed. A specific PKA phosphorylation site on ser1756 has been recognised in other cell types (Joseph, 1996). An antibody specific to this site was acquired. Here, we validate the specificity of phospho-IP_3R1 antibody.

IP_3R1 (2µg) was immunoprecipitated from the lysates of untreated and PGI_2-treated platelet and the phosphorylation status was screened using Anti-p$IP_3R1^{Ser1756}$ antibody. Under these conditions IP_3R1 was found to become phosphorylated on ser1756 after treatment with PGI_2 (100nM) but not under basal conditions. As a means of secondary confirmation, we also probed the immunopreciptate with an antibody that recognised phosphorylated PKA substrates. Again, we observed a strong phosphorylation after treatment with PGI_2, but not under basal conditions (*Figure 4.6*). The data suggests that IP_3R1 is phosphorylated on treatment with PGI_2 but not under untreated conditions. Furthermore, the data establishes that Anti-p$IP_3R1^{Ser1756}$ antibody reliably detects IP_3R1 phosphorylation and was used for subsequent experiments to study IP_3R1 phosphorylation.

Figure 4.6

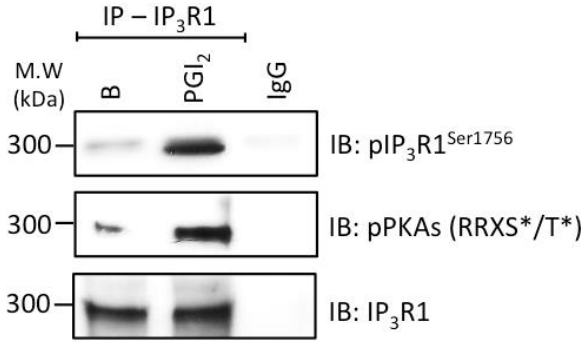

***Figure 4.6* - Confirmation of specificity of phospho-IP_3R1 antibody.**

Untreated and PGI_2-treated (100nM) platelet lysates (500µg protein) were pre-cleared by incubation with 25µl Protein A slurry at 4°C for 2 hours. The immunoprecipitation was performed as described previously. The protein was eluted by the addition of Laemelli buffer. The samples were resolved followed by protein resolution using ECL as described previously (n=3). The results suggest that IP_3R1 is phosphorylated on treatment with PGI_2 and that Anti-$pIP_3R1^{Ser1756}$ antibody reliably detects IP_3R1 phosphorylation. The antibody was therefore used to detect phosphorylation in subsequent experiments.

4.4.2. Phosphorylation of IP_3R1 in response to PGI_2 occurs in a concentration and time-dependant manner

The previous chapter shows that protein substrates are phosphorylated by PKA in a temporal and concentration-dependent manner. Here we characterised PKA-mediated IP_3R1 phosphorylation.

Under basal conditions we found that IP_3R1 was not phosphorylated. However, treatment with increasing concentration of PGI_2 (0.1 – 100nM) led to a concentration-dependent increase in band intensity corresponding to the apparent molecular weight of IP_3R1 suggests that IP_3R1 undergoes concentration-dependent phosphorylation (*Figure 4.7a*). Maximal phosphorylation was observed at 100nM (highest concentration tested) (*Figure 4.7c*). Phosphorylation of VASP (at ser157), an established PKA substrate, was used as a positive control for PKA mediated phosphorylation. Overall, VASP also displayed a concentration-dependent pattern of phosphorylation (*Figure 4.7a*). However, it can be noticed that the phosphorylation bands for IP_3R1 are stronger as compared to VASP, especially at lower concentration of PGI_2. This could perhaps highlight the spatial differences in PKA-mediated substrate phosphorylation, i.e. the possibility of IP_3R1 being more sensitive to PKA-mediated phosphorylation compared to VASP cannot be ignored. Alternatively, these differences could also result from differing sensitive of the antibodies in question.

Temporal pattern of IP_3R1 phosphorylation was also studied by treating platelet lysates with a fixed concentration of PGI_2 (100nM) for increasing time intervals (0.5 – 60 minutes). On immunoblotting with it was revealed that IP_3R1 undergoes a rapid phosphorylation starting at 30 seconds (*Figure 4.7b*). The phosphorylation peaks around 5 minutes, but by 15 minutes it returns back to untreated levels. Unlike IP_3R1 phosphorylation, $pVASP^{Ser157}$ phosphorylation peaked around 2 minutes and was blunted after 15 minutes, however weak phosphorylation could still be detected at 60 minutes (*Figure 4.7b, d*). This suggests a difference in the temporal regulation of PKA-mediated substrate phosphorylation (discussed in §4.8). β-tubulin was used as a control for discrepancies in protein loading (*Figure 4.7b,d*).

Figure 4.7

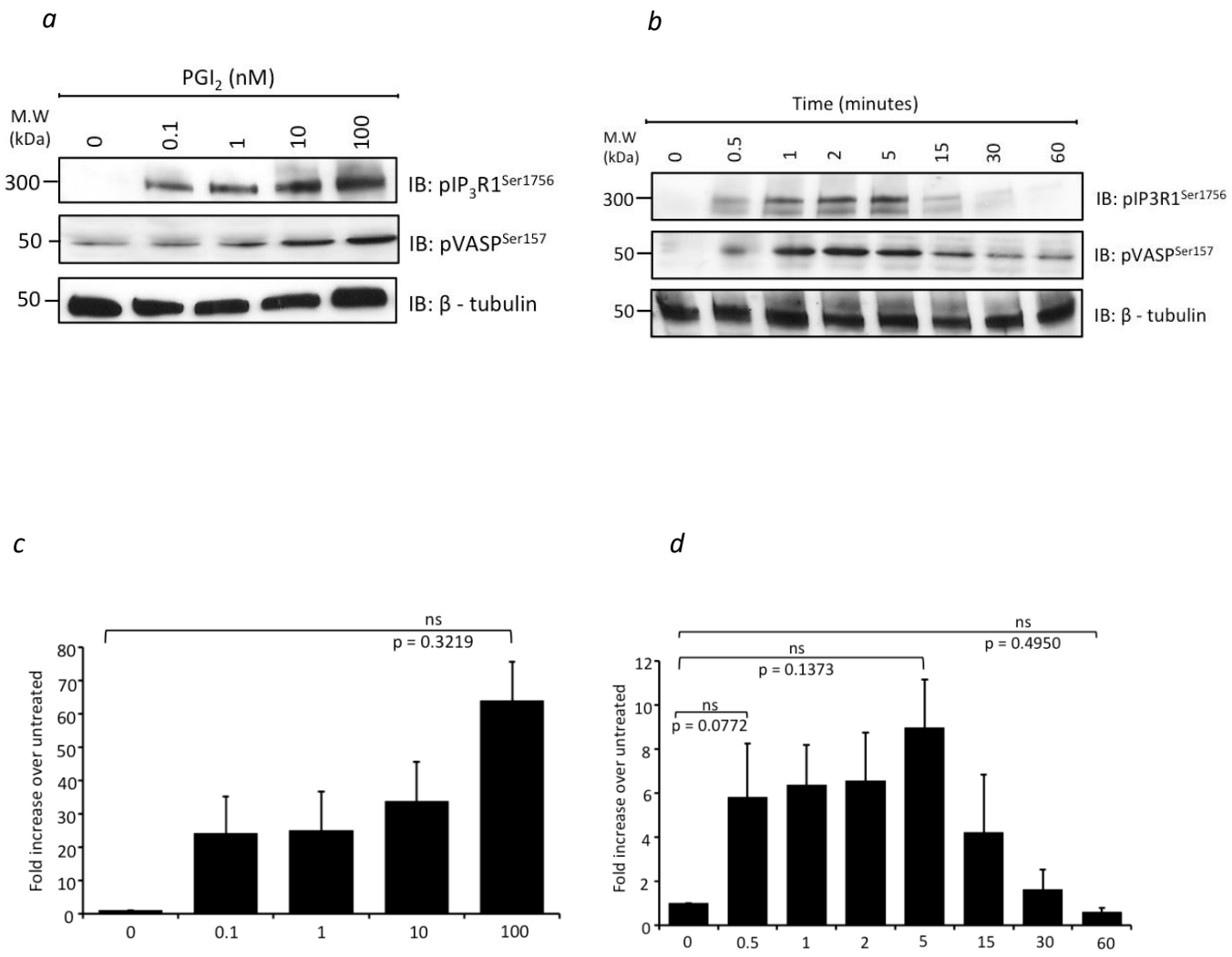

***Figure 4.7* - PGI$_2$-induced IP$_3$R1 phosphorylation.**

(a) Washed Platelets (5x10^8 cells/ml) were treated with increasing concentration of PGI$_2$ (0.1-100nM) for 1 minute at 37^{o}C, with constant stirring for the first 15 seconds. At the end of 1 minute, the signalling was terminated by lysing the platelets with 2x Laemmli buffer (1:1v/v). 30µg of protein was loaded on 4-20% Precast gel and resolved by SDS-PAGE followed by probing with anti-pIP$_3$R1^{Ser1756} antibody (1:1000) and anti-pVASP^{Ser157} antibody. β-tubulin (1:1000) was used as a loading control (n=3). The blots suggest concentration-dependant increase in IP$_3$R1 phosphorylation as quantified in **(b)** using densitometry (n=3)**. (c)** As in (a), except that washed platelets were treated with a constant concentration of PGI$_2$ (100nM) for increasing time periods (0.5-60 minutes). The samples were treated as described previously, and display time-dependant phosphorylation of IP$_3$R1 as quantified in **(d)** (n=3).

4.4.3. IP_3R1 phosphorylation is mediated by PKA

Having established PGI_2-induced phosphorylation of IP_3R1, it was essential to explore phosphorylation events downstream of the Ip receptor. We aimed to achieve this by circumventing the PGI_2 receptor and directly activating AC using forskolin and then activating PKA directly using 8-CPT-6-Phe-cAMP, but also using a number of receptor antagonists and pharmacological inhibitors that targeted various elements of the pathway.

Incubation of washed platelets with forskolin (5µM) and for 5 minutes at 37^{o}C resulted in a significant increase in phosphorylation of IP_3R1 compared to untreated platelets, confirming a role for cAMP. When the experiments were repeated with 8-CPT-6-Phe-cAMP (50µM), we again found significantly elevated phosphorylation of the receptor, suggesting that IP_3R1 is phosphorylated at ser1756 downstream of PKA (*Figure 4.8a,c*). As a control, platelets treated with PGI_2 (100nM) for 1 minute at 37°C were used as a positive control. In contrast no IP_3R1 phosphorylation was observed under untreated conditions. Furthermore, the phosphorylation pattern of VASP at ser157 was also studied in these samples and was found to mirror that of IP_3R1.

We next used a combination of PKA inhibitors (Rp-8-CPT-6-Phe-cAMPS and KT5720) to confirm the role of the kinase. In the presence of these inhibitors we observed a reduction in phosphorylation of IP_3R1 at ser1756 (*Figure 4.8b,d*), while the phosphorylation of VASP at ser157 induced by PGI_2 (100nM) for 1 minute was ablated. Finally we used RO1138452, an Ip receptor antagonist to confirm the contribution of this receptor in the signalling process. Incubation of the platelets with the receptor antagonists prior to PGI_2 abolished the phosphorylation of IP_3R1 at ser1756 and VASP at ser157. Together these data suggest that PGI_2 through Ip receptor induces the phosphorylation of IP_3R1 at ser1756 using a pathway that involves both cAMP and an isoform of PKA (*Figure 4.8*).

Figure 4.8

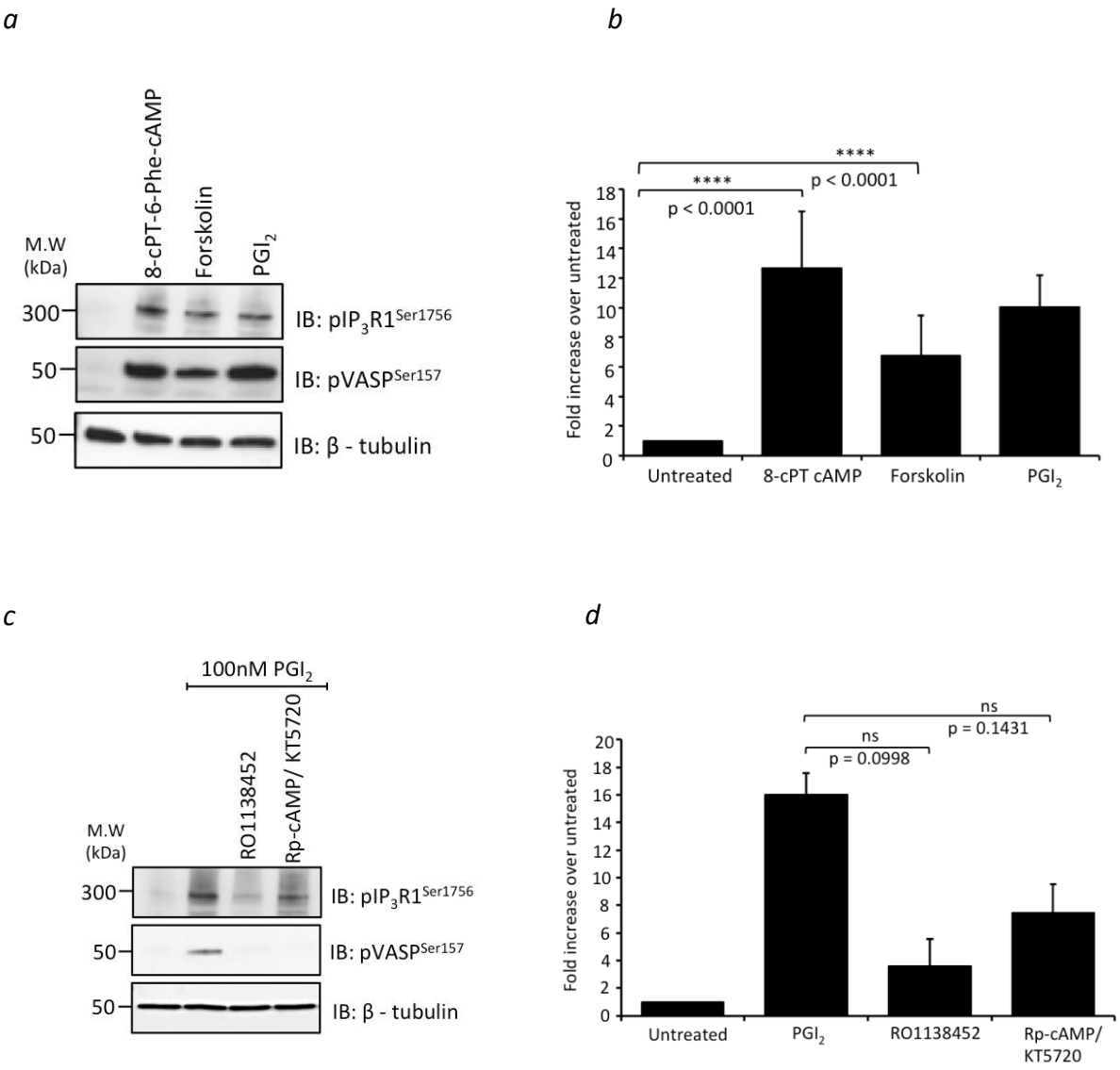

***Figure 4.8* - PKA-mediated IP_3R1 at serine 1756 phosphorylation.**

(a) Washed platelets (5x10^8 cells/ml) were treated with Forskolin (5µM) and 8-CPT-6-Phe-cAMP (50µM) for 5 minutes at 37°C, with constant stirring for the first 15 seconds. At the end of incubation period, signalling was terminated by lysing the platelets with 2x Laemmli buffer (1:1v/v). 30µg of protein was loaded on 10-18% gradient gel and resolved as previously described, followed by immunoblotting using anti-$IP_3R1^{Ser1756}$ antibody (1:1000) and anti-$pVASP^{Ser157}$ antibody. β-tubulin (1:1000) was used as a loading control. **(b)** IP_3R1 phosphorylation was quantified using densitometry (n=3). **(c)** Similarly, washed platelets were treated with RO1138452 and Rp-8-CPT-6-Phe-cAMPS/KT5720 for 20 minutes at 37°C, prior to treatment with PGI_2 (10nM) for 1 minute. The samples were treated as described previously and **(d)** IP_3R1 phosphorylation was quantified using densitometry (n=3). The data suggests that IP_3R1 phosphorylation occurs downstream of PKA.

4.5 Identification of association of IP_3R1 with PKA

4.5.1. Identification of IP_3R1 as a PKA binding protein

Since we established IP_3R1 as a substrate for PKA, we endeavoured to determine its status as a PKA binding protein using the cAMP-linked beads enrichment protocol. Washed platelet lysates were incubated with either 8-AHA-cAMP beads or 8-AHA-cAMP beads saturated with ADP, overnight at 4°C to capture PKA binding proteins. Examination of the proteins in the pull-down demonstrated the presence of bands corresponding to the apparent molecular weight of PKA-RI, PKA-RII and PKA-c (*Figure 4.9a*). Furthermore, quantification of IP_3R1 band intensity suggests a 200-fold increase in band intensity in the cAMP pull-down lane over cAMP saturated control (*Figure 4.9b*). In contrast lysates from beads saturated with ADP failed to enrich the PKA subunits. The inability to detect bands in the cAMP saturated lane points towards the success of the technique and that it can be used to isolate PKA binding proteins. On establishing the success of PKA enrichment, the membranes were probed with antibody against IP_3R1 to assess its status as a PKA-binding protein. The presence of a band corresponding to the apparent molecular weight of IP_3R1 in the pull-down lane and the platelet lysate lane, but not in the cAMP saturated lane. These data suggested that IP_3R1 is associated with PKA binding although it is unclear if this is a direct or indirect association. The association of IP_3R2 and IP_3R3 with PKA was not investigated.

Figure 4.9

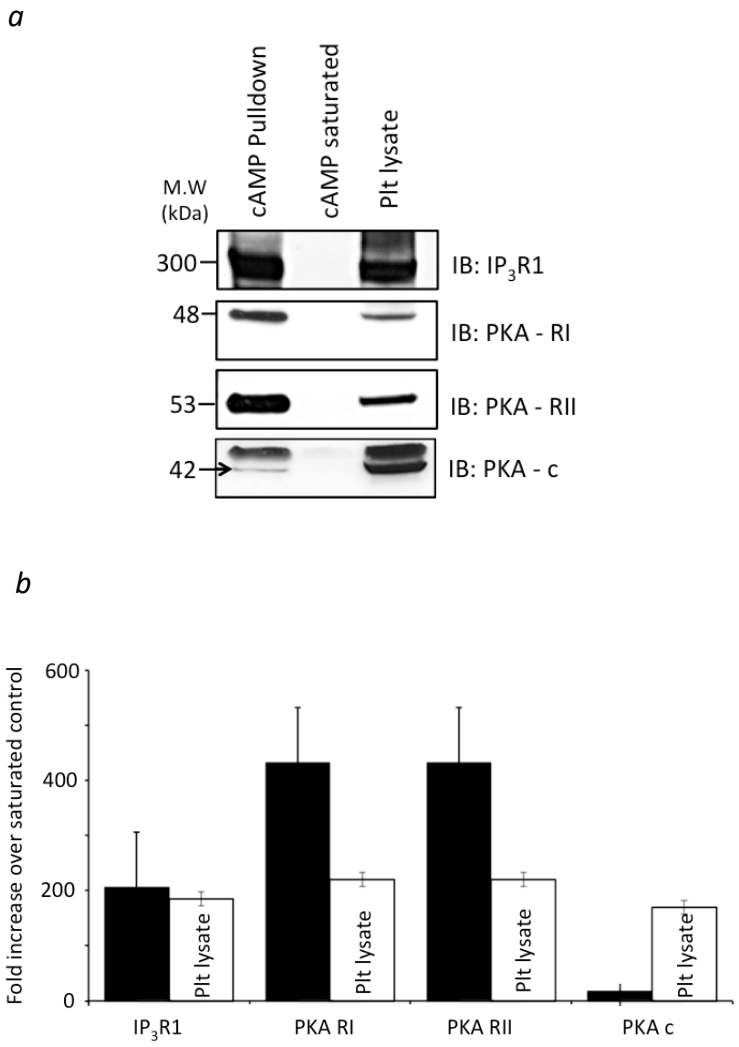

***Figure 4.9* – Status of IP_3R1 as a PKA-binding protein**

(a) Platelet lysates (500µg protein) were pre-cleared by incubation with 25µl EtO-NH beads slurry at 4°C for 2 hours. The samples were centrifuged at 10000rpm for 1 minute and the supernatant was collected and incubated overnight at 4°C with either 8-AHA-cAMP beads slurry or 8-AHA-cAMP beads saturated with ATP. At the end of the incubation period, the beads were pelleted by centrifugation at 10000rpm for 1 minute and washed sequentially with lysis buffer and TBS-T. The protein was eluted by the addition of Laemelli buffer. The samples were boiled for 10 minutes before being resolved and treated as described previously. The presence of a band corresponding to the apparent molecular weight of IP_3R1 in the pull-down lane and the platelet lysate lane, but not in the cAMP saturated lane (n=3) **(b)** as is further supported by the densitometry data showing increased IP_3R1 band intensity in the cAMP pull-down lane over cAMP saturated control.

4.5.2. IP_3R1 associates with PKA type I and II

The suggestion from cAMP pull-down experiments was that IP_3R1 is a PKA-binding protein (*Figure 4.9*). This was further tested using co-immunoprecipitation approach. The IP_3R1 was immunopreciptated using standard conditions described previously and subjected to immunoblotting. Probing of the IP_3R1 immunoprecipates for PKA RI-subunit found that this was associated with receptor under basal conditions and that this was not affected by treated of the platelets with PGI_2 (100nM for 1 minute). Similarly, the association of PKA RII-subunit and c-subunit with IP_3R1 remained unaltered by PGI_2 treatment (*Figure 4.10a*). The quantification data shows no difference in the band intensity, suggesting that the association between IP_3R1 and RI/RII-subunits is unaltered by PGI_2 treatment (*Figure 4.10b*). In all cases the IgG controls showed little or no protein precipitation (*Figure 4.10a-b*). These findings propose an association between IP_3R1 and PKA.

To further strengthen the findings, reverse co-immunoprecpitation experiments were performed. Here PKA RI-subunits (*Figure 4.10d* and PKA RII-subunits (*Figure 4.10c*) were immunoprecipitated from untreated and PGI_2-treated lysates and the membranes were probed with the respective immunoprecipitation controls and IP_3R1. Protein bands corresponding to IP_3R1 were found, albeit weak in both the immunoprecipitation experiments. Nevertheless, it suggests an association with both PKA RI- and RII-subunits. Owing to the presence of multiple PKA substrates, it is possible that only a small percentage of PKA binds to IP_3R1, which could perhaps explain the presence of weak bands in the reverse co-immunoprecipitation experiments.

Figure 4.10

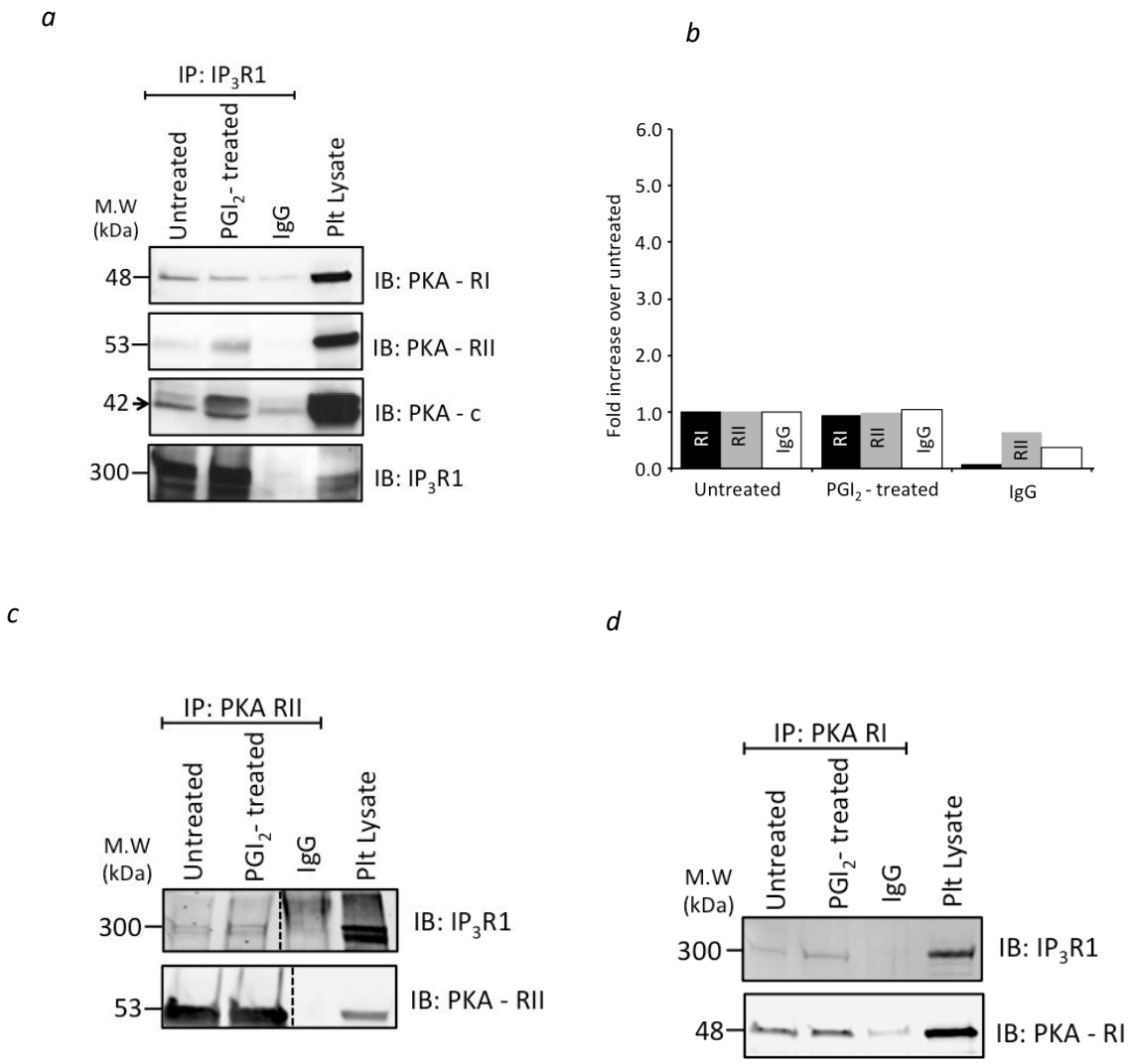

***Figure 4.10* – Association of IP_3R1 with PKA in platelets**

(a) IP_3R1 was immunoprecipitated from platelet lysates as described previously, followed by immunoblotting using anti-PKA RI, anti-PKA RII and anti-PKA c-subunit antibodies to explore if association of IP_3R1 with either PKA-I or PKA-II is altered on PGI_2 treatment. **(b)** The protein bands were quantified using densitometry. The densitometry data shows no difference in the band intensity suggesting association between IP_3R1 and RI/RII-subunits is unaltered by PGI_2 treatment **(c)** PKA RII-subunits (n=3) and **(d)** PKA RI-subunits (n=2) were immunoprecipitated from lysates as described previously. The membranes were subsequently probed with anti-IP_3R1 (1:1000) and the respective immunoprecipitation controls to support the findings using reverse co-immunoprecipitation approach.

4.6. Activity of PKA associated with IP_3R1

Having established the possible association between PKA and IP_3R1, it was essential to investigate if the PKA associated with IP_3R1 had any kinase activity. This was done using non-radioactive PepTag PKA assay (§2.6), which works on the principle that upon phosphorylation, PKA substrate peptide tag (Leu-Arg-Arg-Ala-Ser-Leu-Gly) acquires an overall negative charge and migrates towards the positive electrode on agarose gel therefore providing a visual representation of PKA activity. Alongside the samples, a positive control (of recombinant PKA catalytic subunit; 2µg/ml) and a negative control (no PKA/ sample added) were resolved.

To achieve this, IP_3R1 was immunoprecipitated from treated and untreated lysates with the notion that PKA associated with IP_3R1. On being subjected to the kinase activity assay, IP_3R1 immunoprecipitated from untreated lysate displayed an average of 1.5-fold increase over IgG control, whereas PGI_2-treated lysate displayed a kinase activity similar to IgG control (*Figure 4.11*). Although, untreated lysate displayed a higher kinase activity compared to PGI_2-treated samples, on quantification of the same, the difference between the two failed to reach significance. There was also no significant difference between the associated PKA activity in untreated and IgG control samples (*Figure 4.11a,b*). Apart from the samples, the positive and negative controls migrated towards negative and positive electrodes respectively.

Post PKA activation for the PepTag Assay, the immunoprecipitated protein was eluted from the solid support using 2x Laemmeli buffer and resolved to assess the success of immunoprecipitation. The presence of a band corresponding to the supposed molecular weight of IP_3R1 in the immunoprecipitate lane but its absence in the IgG lane confirms the success of the protein immunoprecipitation (*Figure 4.11c*).

Figure 4.11

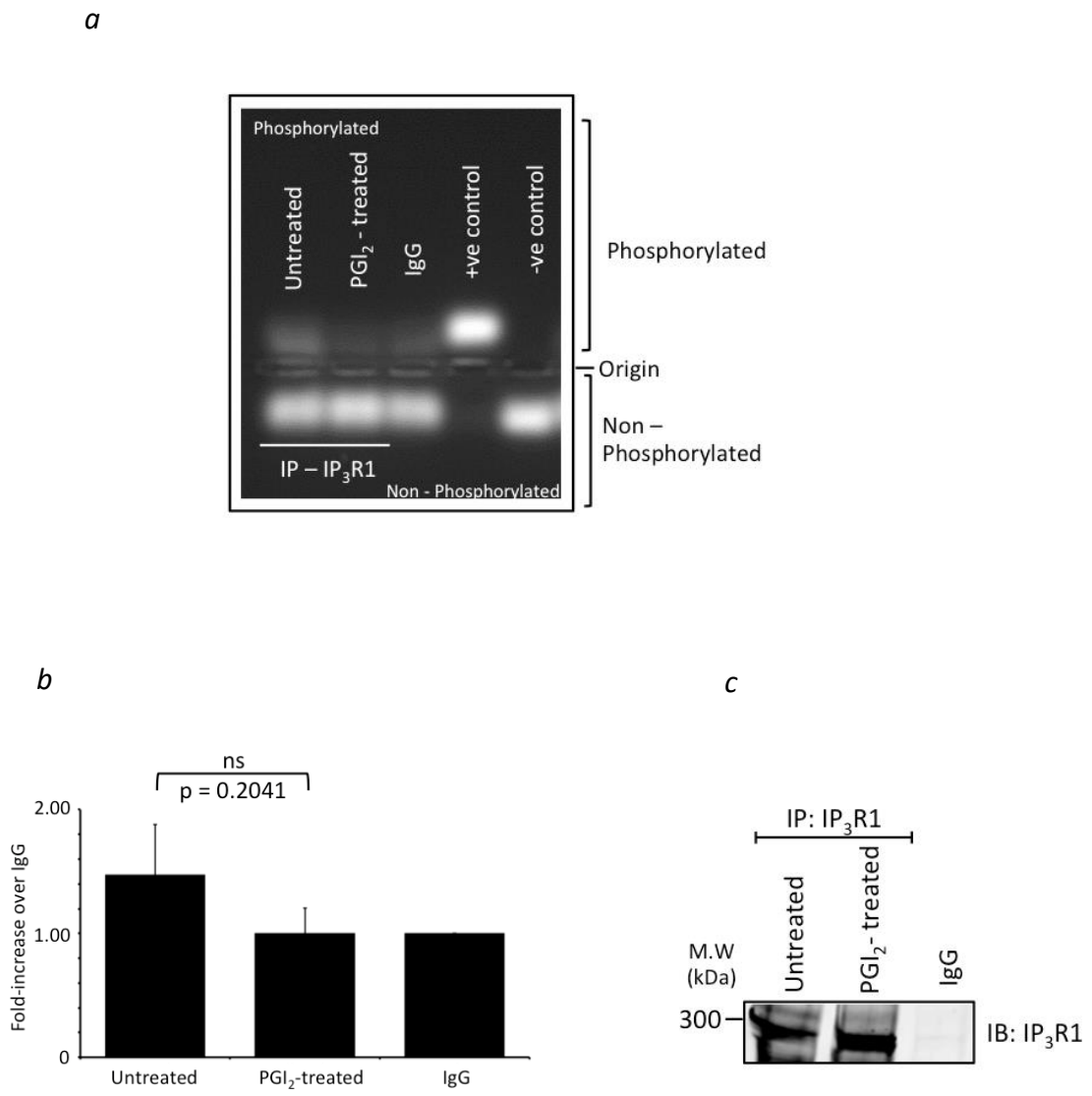

***Figure 4.11* - Associated PKA catalytic activity with the regulatory subunits.**

(a) IP_3R1 was immunoprecipitated as described previously, except that the associated PKA c was released and activated. The net PKA activity was assayed using a highly specific coloured PKA substrate peptide tag and resolved on 0.4% Agarose gel and imaged using Syngene Bio Imagining system **(b)** The coloured bands were melted and quantified using TeCan Spectrophotometer and represented as fold-increase over IgG±SEM (n=3). There was no significant difference between the associated PKA activity in untreated and IgG control samples **(c)** The remaining IP_3R1 was eluted from Protein A beads using 2x Laemmelli buffer. The samples were resolved and treated as described previously, followed by Immunoblotting with anti-IP_3R1 antibody. The presence of a band corresponding to the supposed molecular weight of IP_3R1 in the immunoprecipitate lane but its absence in the IgG lane confirms the success of the protein immunoprecipitation.

4.7. Discussion

Ca^{2+} is a universal second messenger, therefore Ca^{2+} signalling is at the core of various processes such as muscle contraction, fertilisation (Takahashi, et al., 1999) to platelet activation (Hovig, 1964). Elevation of intracellular Ca^{2+} contributes to various platelet activatory mechanisms such as cytoskeletal reorganisation to enable platelet shape change (Hathaway & Adelstein, 1979), platelet aggregation and dense granule secretion (Shattil & Brass, 1987). A significant proportion of the increase in intracellular Ca^{2+} occurs through the release of Ca^{2+} from DTS primarily via the IP_3Rs (Varga-Szabo et al., 2009). In that sense, the dynamics of intracellular Ca^{2+} release would ideally be studied by the addition of IP_3 and therefore isolating this aspect of Ca^{2+} signalling. This would bind to its receptor and cause Ca^{2+} mobilisation. This technique has been applied to study the Ca^{2+} release through the IP_3Rs (Keularts, et al., 2000; van der Meijden et al., 2008; van Gorp, et al., 2002). Our initial aim was to replicate this approach to examine how cAMP signalling targeted IP_3-mediated effects. However, despite numerous attempts we were unable to effectively supplement the platelets with enough IP_3 to cause a measurable Ca^{2+} mobilisation. For this reason, we attempted to employ an alternative approach, whereby Ca^{2+}-mobilisation in platelet suspension was measured using thrombin as the agonist.

Although widely reported, thrombin-induced Ca^{2+} elevation in platelets (Fung et al., 2012; Keularts et al., 2000; van der Meijden et al., 2008; van Gorp et al., 2002) was first validated. Fura-2-AM, a ratiometric Ca^{2+} sensitive indicator was used for these experiments. Fura-2 labelled platelets were treated with thrombin in a concentration-dependant (0.001-1U/ml) manner. Increasing concentration of thrombin mirrored the elevation in Ca^{2+} and elongation of the time required to cause a maximal Ca^{2+} release (*Figure 4.1*). The lower concentrations of thrombin (0.01 and 0.0001U/ml) were unable to induce measurable Ca^{2+} mobilisation; perhaps as a result of being unable to mediate generation of sufficient levels of IP_3 molecules to bind and activate IP_3 receptors; these concentrations were therefore not used for subsequent experiments. Though the highest concentration of thrombin (1U/ml) used caused a significant Ca^{2+} mobilisation, this concentration was deemed toxic for platelets. Reports suggest that potent concentrations of thrombin can have an apoptotic effects on platelets (Leytin, et al., 2007). From the work of others in the laboratory and my own work, a concentration of 0.1U/ml of thrombin was considered optimal for the use in Ca^{2+}

mobilisation studies. It is interesting to note here, that although the maximal Ca^{2+} mobilisation is affected by the concentration of thrombin, once elevated the Ca^{2+} concentration do not return to the basal levels. The reason for this is unclear, although the possibility of Ca^{2+} entry contributing to this cannot be ignored. Further support for this hypothesis comes from the work by Hassock et al, which suggests TRPC6 stimulation in response to thrombin, causes non-SOCE, non-selective cation entry (Hassock et al, 2002).

Having replicated the Ca^{2+} elevations during platelet activation *in-vitro*, Ca^{2+} modulation traces on physiological inhibition of platelets (by PGI_2) were studied. *Figure 4.2* shows a concentration-dependent impediment of Ca^{2+} mobilisation on PGI_2 treatment, but never a complete inhibition. While studies using physiological concentrations of PGI_2 (0.6μg/ml) mirror our findings (Cavallini et al., 1996). It is important to appreciate that although the rate of Ca^{2+} mobilisation and the maximal Ca^{2+} are reduced in response to PGI_2, at the end of the time course the Ca^{2+} concentration was consistent irrespective of the concentration of PGI_2. Thus, it seems that at more physiologically relevant concentrations of PGI_2 used here, PGI_2 acts to blunt but not block Ca^{2+} mobilisation. It is known that PKA activation inhibits non-SOCE medicated Ca^{2+} entry through TRPC6 (Hassock et al, 2002). It is well recognised that STIM1 initiates Ca^{2+} influx by activating SOCE in response to low intracellular Ca^{2+} levels (Authi, 2009). Therefore, the results could perhaps be a consequence of the rate of SOCE being higher than the rate of Ca^{2+} mobilisation at 3 minutes. In the context of cAMP signalling, we speculate moderation but not complete inhibition of Ca^{2+} levels by cAMP due to the physiological involvement of Ca^{2+} in various platelet activatory pathways. This means that cAMP-mediated regulation would moderate the platelet activatory pathways, therefore supporting platelet inhibitory mechanisms. At higher concentrations PGI_2 is reported to cause a complete inhibition of Ca^{2+} mobilisation (Fung et al., 2012). It could be argued that this is perhaps as a result of using a highly potent dose of PGI_2 (60μM) in response to stimulation by 0.03U/ml of thrombin, unlike the case in our experiments (where 0.1U/ml of thrombin was used) (Fung et al., 2012). It is also possible that inter-individual variation and the effect of confounding variables (age, gender, diet) in platelet responses may contribute to the overall response (Jones et al., 2009). The above discussion highlights the difference in the balance of activatory and inhibitory pathways between the two studies.

To further support the findings that in the absence of extracellular Ca^{2+}, thrombin-induced Ca^{2+} mobilisation is primarily IP_3-mediated 2-APB, a membrane-permeable antagonist was used to block the IP_3-induced Ca^{2+} release. 2-APB has displayed coherent blockage of IP_3Rs in platelets (Dobrydneva & Blackmore, 2001; Maruyama et al., 1997). Also, these effects have been reported to be inconsistent across cell types. Since it has also been suggested to display non-specific effects such as interfering with IP_3-generating stimulus in cells or impediment of Ca^{2+} release in striated muscles (Maruyama et al., 1997) making its an non-specific IP_3R inhibitor. Dose-dependent reduction in platelet Ca^{2+} levels (*Figure 4.3*) and platelet aggregation (*Figure 4.4*) in response to a concentration range (10-100μM) of 2-APB was seen. A concentration-dependent reduction in intracellular Ca^{2+} release and platelet aggregation on pre-treatment with 2-APB, was supported by research from other groups (Maruyama et al., 1997, Dobrydneva & Blackmore, 2001, Ma et al., 2001). Furthermore, the concentrations of 2-APB tested here have been used and confirmed by other researchers to show Ca^{2+} release through IP_3Rs (Bootman & Lipp, 1999). Kukknoen et al suggest an isoform-specific selectivity of 2-APB (Kukkonen et al., 2001). In line with these findings, 2-APB has been most effective in cells highly expressing IP_3R1 and IP_3R3. In platelets, IP_3R1 is the most highly expressed of all the three isoforms (Patterson et al., 2004), suggesting that IP_3R1 may play a major role in the mobilisation of Ca^{2+} in response to thrombin. Given that we found that PGI_2 modulates Ca^{2+}, it could suggest that cAMP has a major effect on the signalling by IP_3. While we were unable to show directly that cAMP blocks IP_3-mediated release, this could be inferred from the experimental data with PGI_2 and 2-APB. Work by Watson et al suggests that cAMP and PGI_2 influence the factors that generate IP_3 including PLC isoforms. A possible indirect mechanism of PGI_2-mediated regulation of IP_3 production could be depletion of PIP_2 in the membrane by either down regulating the kinase responsible for its synthesis or up regulating the membrane-bound PDEs to initiate hydrolysis (Irvine, 1982; Watson, et al., 1984). Therefore, perhaps using D-myo-IP_3 or caged IP_3 to study this would be ideal. Furthermore, it can also be inferred from *Figure 4.4* that although there is a 2-APB-dependent reduction in Ca^{2+} mobilisation, the platelet shape change remained unaltered. It can be speculated that the shape-change could be induced by Rho-kinase pathway, which is not known to be regulated by elevation in cytosolic Ca^{2+} or via the Ca^{2+}-dependent activation of MLC kinase (Bauer et al, 1999). To summarise, we show a concentration-

dependent reduction in intracellular Ca^{2+} release and platelet aggregation on pre-treatment with 2-APB, but no significant effects on platelet shape change.

One possible mechanism by which cAMP signalling could modulate IP_3 signalling is through targeting of its receptor. IP_3Rs are known to exist as three different isoforms – IP_3R1, IP_3R2 and IP_3R3. Though these subtypes share a significant sequence similarity, their affinity towards IP_3, the ligand differs. These findings direct towards the possibility that these subtypes perhaps play independent roles in Ca^{2+} regulation. Using western blotting, we showed the presence of all three subtypes of IP_3R in platelets (*Figure 4.5*). These findings are supported by the studies in platelet transcriptome (Margarucci et al., 2011) and in highly purified platelet membranes (El-daher et al., 2000). IP_3R1 was also immunoprecipitated using 2µg of antibody and Protein A-sepharose beads as the solid support. Although, all three subtypes of IP_3R were found in platelets, the research discussed in this thesis focuses primarily on IP_3R1 – the predominant form of IP_3Rs (Patterson et al., 2004) in platelets. Immunoreprecipitation of IP_3R2 and IP_3R3 was attempted but its success was hindered by the tools available. This could perhaps be a limitation of the respective antibodies used. Alternatively, protein concentration of the lysate could be the limiting factor, therefore restricting the immunoprecipitation of IP_3R2 and IP_3R3.

IP_3Rs have been identified as a substrate for PKA (Ferris, et al., 1991). However, a systematic characterisation of PKA-mediated IP_3R1 phosphorylation in platelets has not been performed. In the context to platelet function, it is vital to study PKA-mediated IP_3R phosphorylation as it is reported to alter the sensitivity to IP_3 and subsequent Ca^{2+} mobilisation (DeSouza et al., 2002; Haug, et al., 1999). To address this, concentration and time-dependent phosphorylation patterns of IP_3R1 were studied in response to PGI_2-induced PKA activation. VASP, a well-established PKA substrate (Walter et al., 1993) was used as a positive control and a marker of PKA phosphorylation. PGI_2-induced phosphorylation occurred in a concentration and time-dependent manner (*Figure 4.7*). However, it should be recognized that even though the concentration-dependent phosphorylation pattern of IP_3R1 mirrored that of pVASP (*Figure 4.7a*), the temporal phosphorylation patterns of IP_3R1 at ser1756 and that of VASP at ser157 differed (*Figure 4.7b*). It is worth noting here that, neither of the two phosphorylation sites on IP_3R1 have been reported in platelets. VASP phosphorylation was sustained for longer than IP_3R1

(*Figure 4.7*). A possible explanation for this could perhaps be the two substrates being phosphorylated by different isoforms of PKA. This can perhaps be due to the varied functions and localisations of the two proteins in question. IP_3R1 is localised on the DTS, whereas VASP is membrane-bound. In addition to this, there is also a possibility that different subtypes and perhaps splice variants of PDEs regulate the localised cAMP levels around the two substrates, which could lead to discrepancies in the time cAMP levels sustain for. Further support for this hypothesis comes from the data suggesting that PDEs display differential localisation in myocytes (Omori & Kotera, 2007).

Nevertheless, to fully dissect the cAMP signalling pathway, it was essential to by-pass various signalling components and study PKA phosphorylation. Forskolin-induced elevation in cAMP levels circumvented the PGI_2 receptor (Metzger & Lindner, 1981), by directly activating AC. Similarly, 8-CPT-6-Phe-cAMP, a synthetic analogue of cAMP, which is resistant to PDE-mediated hydrolysis (Miller et al., 1980), was also used. Both the stimulants caused phosphorylation of IP_3R1, which was mirrored by VASP (*Figure 4.8a*). Similarly, RO1138452, an Ip receptor antagonist (Bley et al., 2006) was used to study the consequence blocking PGI_2 signalling on IP_3R1 phosphorylation. PKA inhibitors Rp-8-CPT-6-Phe-cAMPS and KT5720 were used in combination owing to their weak individual effects. ATP binding to PKA catalytic subunit is crucial to cause substrate phosphorylation; KT5720 is a completive inhibitor for the ATP-binding site on PKA catalytic subunit. Rp-8-CPT-6-Phe-cAMPS on the other hand is a competitive inhibitor of the cAMP-binding site (Murray, 2008) on the regulatory subunit. Treatment with both the antagonists blunted the IP_3R1 phosphorylation response, which was mirrored by VASP (*Figure 4.8)*. The findings described above suggest that IP_3R1 is phosphorylated in response to PGI_2 through a pathway that increases cAMP and activates an isoform of PKA.

Having established the status of IP_3R1 as a PKA substrate, we next investigated the association dynamics of the two proteins and in particular testing the possibility that the consistent with other cells that PKA exists complexed to its substrates. A protein enrichment approach used by Scholten et al was adapted and used to precipitate cAMP-binding proteins (Scholten et al., 2006). Using this approach we showed that IP_3R1 could be enriched suggesting that it was associated with a cAMP binding protein. In this case it was most likely that this occurred through its association with a PKA isoform (*Figure 4.9*). This interaction

was further cross-validated using the co-immunoprecipitation approach (*Figure 4.10*). Interestingly these data suggest that presence of IP_3R1 in a complex with PKA-I and IP_3R1-PKA-II, although it is unclear if this is the same complex or two separate complexes. We for the first time report an association between IP_3R1 and PKA RI, however data suggesting IP_3R1-PKA RII association is in parallel with the reported findings (Collado-Hilly & Coquil, 2009; Tu et al., 2004; Zaccolo & Pozzan, 2003). The preference for the formation of PKA-II over PKA-I (Otten & McKnight, 1989) might perhaps reason the presence of a weaker IP_3R1 band in the RI and RII immunoprecipitates. However, the inefficiency of the RI antibody to precipitate the protein could also provide a possible explanation for the weak bands. Nevertheless, the association of IP_3R1 with both PKA-I and PKA-II suggests its importance in regulation of signalling events. Although these findings suggest the presence of a macromolecular complex between PKA-IP_3R1, the strength of the association needs to be quantified.

In an ideal world, the presence of such a macromolecular complex can be investigated using immunoprecipitation to isolate the complex, followed by resolving the eluates using 2-D gel electrophoresis. The relevant bands from the gel should be excised and subjected to LC/MS/MS analysis. Similarly, the eluates from reverse immunoprecipitation experiments should also be treated as described previously. This should reveal the precise identity of the associated proteins. The data may be further supported by PLA assay, which would shed light on the proximity of the proteins in the macromolecular complex.

The activity of the associated PKA also needs to be investigated. To do this, Non-radioactive PepTag® Assay was used. This assay measures the catalytic activity of PKA. The results show that a higher catalytic activity in IP_3R1 immunoprecipitates from untreated lysates compared to PGI_2-treated lysates (*Figure 4.11*). A possible explanation for the results could be that on PGI_2-induced PKA activation, the catalytic subunit is unleashed (Kopperud et al., 2002), which could cause the kinase activity of the sample to diminish. It is also valuable to appreciate that the sample processing times are crucial when dealing with a colorimetric assay such as this. The assay protocol suggests the quantification of kinase activity be performed within less than 10 minutes of the completion of gel electrophoresis to avoid the PepTag® dye to diffuse into surrounding agarose. Therefore, possibly owing to the slightly

prolonged sample processing times between the samples, the diffusion of PepTag® dye could affect the output readings.

Nevertheless, to summarise, the results described in this chapter establish the presence of IP_3R1 in platelets and characterise the PKA-mediated phosphorylation of IP_3R1. The presence of PKA-IP_3R1 complex in platelets was also investigated, however the other components of the PKA-IP_3R1 complex and the scaffolds holding the complex together remains to be explored.

CHAPTER V: EXAMINATION OF THE POTENTIAL ASSOCIATION OF AKAP9 WITH IP$_3$R1-PKA COMPLEX

5.1. Introduction

PKA-mediated substrate phosphorylation is regulated in a spatial and temporal manner. The temporal regulation of the pathway is provided by the action of PDEs, which degrade cAMP. This ensures the maintenance of cAMP levels (Baillie et al. 2005). The spatial regulation of cAMP-signalling pathway is however provided by a group of functionally similar proteins called the A-kinase Anchoring Proteins (AKAPs). A structural hallmark of AKAPs is the presence of an amphiphatic helix which can bind to the D/D' domain of PKA (Carr et al. 1991; Kinderman et al. 2006). There are over 50 individuals AKAPs identified in a variety of different cells types (Pidoux & Tasken 2010). Of these AKAPs, AKAP9 was of particular interest to this project due to its reported association with IP$_3$R1 (Tu et al. 2004; Collado-Hilly & Coquil 2009) in other cell types. AKAP9 was initially believed to be concentrated in the neuromuscular junction and identified as a protein associated with the glutamate receptor (Lin et al., 1998). More recent proteomics and transcriptomics studies have reported its presence in platelets (Pidoux & Tasken, 2010, Margarucci et al., 2011, Rowley et al., 2011). The biology of AKAP9 is complicated by the existence of three splice variants – AKAP250, AKAP350 and AKAP450. The precise reasons for such a large difference in the molecular weights of the splice variants are not known. These variants can be differentially localised depending on the cell type (Lin et al. 1998; Schmidt et al. 1999; Witczak 1999). AKAP250, also known as Yotiao, is localised in the cellular membranes, whereas the other two are predominant in the cytosol (Lin et al. 1998).

Attempts have been made to dissect the functional importance of PKA-AKP interaction using several approaches such as siRNA-mediated knockdown, expression of mutant AKAPs and the generation of AKAP knock-out mice (Pidoux & Tasken 2010). However, these techniques are far from being extrapolated to platelets. As an alternative approach, inhibitory peptides that mimic the amphiphatic helix of AKAPs and compete for binding to the D/D' domain of PKA have been developed to study the functional importance of PKA-AKAP interaction (Carr et al. 1991; Carr et al. 1992). To date, there are three main types of disruptor peptides

available – Ht31, RI anchoring disruptor (RIAD) and SuperAKAP. Ht31 can potentially delineate the interaction of AKAP with both PKA I and PKA II (Herberg et al. 2000). RIAD and SuperAKAP are specific to interactions with PKA I and PKA II respectively (Gold et al. 2006; Carlson et al. 2006).

In this chapter, we endeavour to firstly validate the presence of AKAP9 in platelets. We then explore the association of AKAP9 with IP_3R1-PKA complex using immunoprecipitation. Lastly, the effect of disruption of PKA-AKAP complex using St-Ht31 (and St-Ht31P, the control peptide) on IP_3R1 phosphorylation and Ca^{2+} mobilisation was studied.

5.1.1. Hypothesis

This chapter tests the hypothesis that AKAP9 complexes with IP_3R1 and PKA in platelets to facilitate the spatial regulation of IP_3R1 phosphorylation.

5.1.2. Aims and Objectives

This chapter aims to establish the presence of AKAP with the IP_3R1-PKA complex. Furthermore, disruption of the complex using synthetic cell-permeable peptides was attempted and the phosphorylation-specific and functional effects of the same were studied. The objectives of this chapter were -

1. Validate the presence of AKAP9 in platelets
2. Investigate the association of AKAP9 with IP_3R1-PKA complex
3. Investigate the functional effect of disrupting the AKAP-PKA complex on IP_3R1 phosphorylation and Ca^{2+} mobilisation

5.2 Detection of AKAP9 proteins in human platelets

5.2.1. Validation of presence of AKAP9 in platelets using Immunoblotting

The presence of AKAP9 has been reported in platelets (Margarucci et al. 2011; Rowley et al. 2011) through proteomics studies. Although detection of the protein by other methods is yet to emerge, we used antibodies that were both commercially available and donated by collaborators combined with immunoblotting to examine the presence of AKAP9. Increasing concentrations of protein from platelet lysate was resolved on Precast 4-20% Mini-PROTEAN TGX Gel followed by immunoblotting using a custom-made antibody specific to AKAP9 (a gift from Prof. Dessauer). This antibody was designed to recognise all three-splice variants of AKAP9 at 250kDa, 350kDa and 450kDa (Oral communication with Prof. Dessauer). Protein bands corresponding to the apparent molecular weight of 250kDa and 350kDa appeared at both protein concentrations (*Figure 5.1*). In contrast band corresponding to 450kDa only appeared at higher protein concentrations. This could perhaps be due to the lower abundance of the AKAP450 splice variant. Nevertheless, the band intensity displayed an increase proportional to the protein concentration, indicating the presence of all three isoforms of AKAP9 in platelets (*top panel, Figure 5.1*).

Although the next step to validate these findings would be to isolate the protein using immunoprecipitation, the limited quantity of the AKAP9 antibody gifted from Dessauer laboratory restricted the progress in this direction. For this reason, it was essential to explore an alternative option. A commercially available AKAP9 antibody (*Santa Cruz Biotechnologies*) that recognised Yotiao (250kDa) isoform was first tested on platelet lysates as described previously. A band corresponding to the apparent molecular weight of the protein appeared and showed an increase in intensity proportional to the protein concentration. This suggests the presence of Yotiao isoform in platelets (*second panel, Figure 5.1*) and further validates the blotting results from the custom-made AKAP9 antibody. β-tubulin was used as a loading control to account for discrepancies in protein loading. These results suggested that platelets potentially express all three isoforms of AKAP9.

Figure 5.1

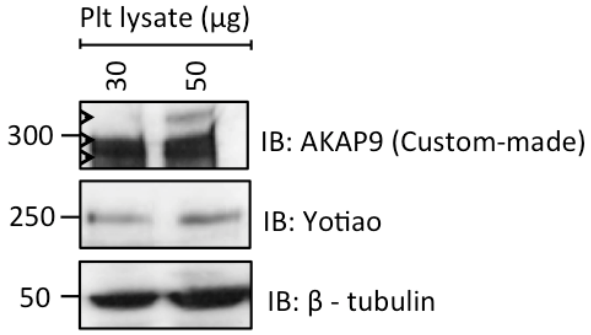

***Figure 5.1* – Confirmation of the presence of AKAP9 in platelets using immunoblotting.**

Washed platelets ($5x10^8$ cells/ml), lysed with with 2x Laemmli buffer (1:1v/v) were resolved as described previously. Membranes were blocked with 10% BSA and immunoblotted using a custom made anti-AKAP9 antibody (1:2000) (a gift from Prof. Carmen Dessauer). The membranes were also probed with commercially available anti-Yotiao antibody (1:1000). Anti-β-tubulin (1:1000) was used as a loading control (n=3). The presence of a band corresponding to the apparent molecular weight of the protein suggests the presence of Yotiao isoform in platelets. Immunoblotting using commercially available anti-AKAP9 antibody further supports these results.

5.2.2. Validation of presence of AKAP9 in platelets using Immunoprecipitation

To further validate the presence of AKAP9 in platelets, attempts were made to immunoprecipitate AKAP9 from untreated platelet lysates. Owing to the limited quantity of custom-made antibody supplied, AKAP9 immunoprecipitation experiments were performed exclusively using the commercial antibody, while the custom-made antibody was used for immunoblotting (*Table 5.1*).

Pre-cleared platelet lysates (500µg) were incubated with commercial anti-Yotiao antibody (5µg), overnight at 4^{o}C with agitation to allow for Protein-antibody binding. The protein-antibody complex was then precipitated out using Protein A-sepharose beads as described in §2.5.4. To assess the success of protein enrichment, the eluted protein was resolved on 4-20% precast gel, followed by immunoblotting using commercially available anti-Yotiao (Santa Cruz). Bands corresponding to the apparent molecular weight of the protein failed to appear in the immunoprecipitate lane. This remained unchanged despite multiple exposures of increasing time intervals. However, a faint band corresponding to the reported molecular weight of Yotiao appeared in the platelet lysate lane. This suggests that though the antibody detected Yotiao in platelet lysates, it was unable to detect immunoprecipitated protein (*Figure 5.2*).

The same experiment was repeated, however in this instance the immunoblotting was performed using the custom-made AKAP9 antibody (*Table 5.1*). A band corresponding to the correct molecular weight of AKAP9 appeared in the immunoprecipitate and platelet lysate lane. The same band also appeared in the IgG control lane, therefore indicating that the antibody possibly interacts non-specifically with Protein A beads (*Figure 5.2*).

Owing to the limitation of the antibodies available, AKAP9 could not successfully be immunoprecipitated from platelet lysates. Custom-made AKAP9 was considered more reliable than anti-Yotiao antibody for immunoblotting, therefore used in further experiments.

Table 5.1

	Immunoprecipitation	Immunoblotting
Panel I	Yotiao (Santa Cruz Biotech)	Yotiao (Santa Cruz Biotech)
Panel II	Yotiao (Santa Cruz Biotech)	AKAP9 (Custom-made)

***Table 5.1* – Antibody combinations used for detection of AKAP9 using immunoprecipitation**

Figure 5.2

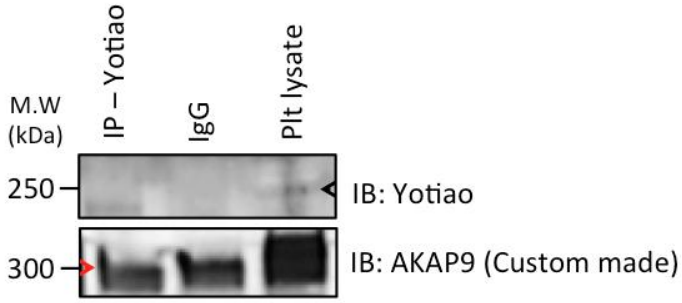

***Figure 5.2* - Immunoprecipitation of AKAP9 from platelet lysates.**

Lysates prepared from untreated and PGI_2-treated were pre-cleared with 25µl of Protein A sepharose bead slurry (50% v/w) for 60 minutes at 4^{o}C with agitation. The pre-cleared lysates (500µg protein) were then incubated overnight, with agitation at 4^{o}C with anti-AKPA9 antibody (5µg) and handled as described previously. The membranes were probed for anti-AKAP9 from Santa Cruz (1:1000) and custom-made antibody (AKAP9 (USA)) (1:2000). The membranes were incubated with HRP-conjugated secondary antibody for 60 minutes at room temperature, followed by protein resolution using ECL (n=3). The anti-AKAP9 antibody from Santa Cruz provided with limited Immunoblotting success. The custom-made anti-AKAP9 antibody was considered more reliable than the commercial anti-AKAP9 antibody and used for subsequent experiments.

5.3 Presence of AKAP9 in IP$_3$R1-PKA complex

5.3.1. AKAP9 as a PKA-binding protein

AKAPs are known to interact with PKA through the D/D' domain of the kinase (Carr et al. 1991; Kinderman et al. 2006). Here, we examined the potential of AKAP9 as a PKA-binding protein using cAMP pull-down approach, which has been shown previously to enrich PKA-binding proteins for proteomic analysis (Scholten et al. 2006). Washed platelet lysates were incubated with either 8-AHA-cAMP beads or 8-AHA-cAMP beads saturated with ADP, overnight at 4°C to capture PKA binding proteins. The beads were sequentially washed with TBS-T and lysis buffer, before eluting the protein (§2.5.5). The proteins were resolved on SDS-PAGE and the membranes were treated as described previously (§2.5.2-3) (*Figure 5.3*).

To test for PKA enrichment and the success of the technique, the membranes were probed with antibodies against individual PKA subunits. Immunoblotting of the bead eluates revealed the presence and bands with apparent molecular weights of the three PKA subunits including PKA RI, PKARII and PKA-catalytic. On Immunoblotting with PKA-catalytic antibody a doublet appeared for unknown reason. Nevertheless, on resolving and probing for PKA-catalytic subunit alongside recombinant PKA-catalytic subunit in a separate experiment (data not shown), it was revealed that the bottom band corresponds to the PKA-catalytic subunit. The identity of the top band remains unknown. The eluates taken from beads that had been saturated with ADP showed none of the cAMP binding proteins when tested by immunoblotting. The inability to detect bands in the cAMP saturated lane points towards the success of the technique to isolate cAMP binding proteins.

Having confirmed the specificity of the pull-down approach we began to determine whether key proteins in our proposed complex could be isolated in this manner. This assay is based on the premise that cAMP-immobilised beads bind and precipitate cAMP-binding proteins such as PKA. For this reason, in theory, proteins associated with PKA should also be to be enriched using this approach. As described in the previous chapter, bands corresponding to the apparent molecular weight of IP$_3$R1 appeared in the pull down, indicating that IP$_3$R1 is a PKA-binding protein. Next, the membrane was probed with the custom-made AKAP9 antibody, which recognises all three splice variants of AKAP9. Bands corresponding to the reported molecular weight of 250kDa and 350kDa were observed in the pull-down and

platelet lysate lane, but not in the negative control lane. This suggests that Yotiao and AKAP350, could both be potential PKA-binding proteins (*Figure 5.3*), however we cannot conclude if the precise nature of association. These results support the finding that AKAPs possess PKA-binding domains that helps anchor them to PKA. Alternatively, the speculation that AKAPs possess direct cAMP-binding sites should also not be ignored.

Figure 5.3

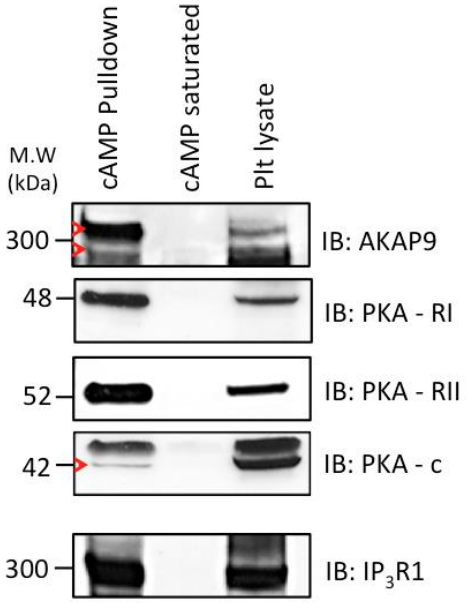

***Figure 5.3* –AKAP9 may form for a of multi-protein complex with IP$_3$R1 and PKA**

Platelet lysates (500µg protein) were pre-cleared by incubation with 25µl EtO-NH beads slurry at 4°C for 2 hours. The samples were centrifuged at 10000rpm for 1 minute and the supernatant was collected and incubated overnight at 4°C with either 8-AHA-cAMP beads slurry or 8-AHA-cAMP beads saturated with ATP. At the end of the incubation period, the beads were pelleted by centrifugation at 10000rpm for 1 minute and washed sequentially with lysis buffer and TBS-T. The protein was eluted by the addition of Laemelli buffer. The samples were boiled for 10 minutes before being resolved on PreCast 4-20% gel as described previously and probed for anti-IP$_3$R1, PKA RI, PKA RII,PKA c (1:1000) and custom-made anti-AKAP9 (1:2000) antibody as discussed previously. The data suggests the existence of a possible multi-protein complex with IP$_3$R1 and PKA.

5.3.2. Establishing AKAP9 as an IP_3R1-binding protein

Having established the status of AKAP9 as a potential PKA-binding protein, we endeavoured to test the possibility of an association between AKAP9 and IP_3R1. To investigate this further, IP_3R1, was precipitated from pre-cleared lysate (500µg) using anti-IP_3R1 antibody (2µg) as described in §2.5.4. The appearance of protein bands corresponding to the expected molecular weight of IP_3R1 in the immunoprecipitate and platelet lysate lane show the success of the protein precipitation protocol. The absence of the bands in the IgG control lane suggests that the antibody does not bind non-specifically to the Protein A beads (*Figure 5.4a*).

We next probed the membranes using the custom-made AKAP9 antibody. The absence of a band corresponding to the molecular weight of AKAP9 in the IgG lane suggests a lack of non-specific interaction with Protein A beads. Although this antibody detects all three splice variants of AKAP9, only a single band corresponding to the approximate molecular weight of 250kDa seems to appear. This suggests that out of all the three AKAP9 isoforms, perhaps only Yotiao interacts with IP_3R1 in platelets. However, owing to poor reagent quality we were unable to explore this further. The bands corresponding to the apparent molecular weight of Yotiao seems to appear in immunoprecipitation samples from untreated and PGI_2-treated lysates with the same intensity (*Figure 5.4b*). This suggests that PGI_2-treatment may not alter the IP_3R1-Yotiao interaction, however we cannot confirm this due to poor reagent quality. Also, we cannot yet speculate if the association with both IP_3R1 (*Figure 4.10*) and AKAP9 (*Figure 5.3*) is direct or via PKA.

Figure 5.4

a

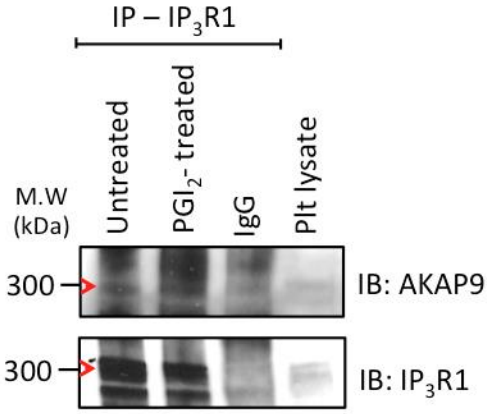

b

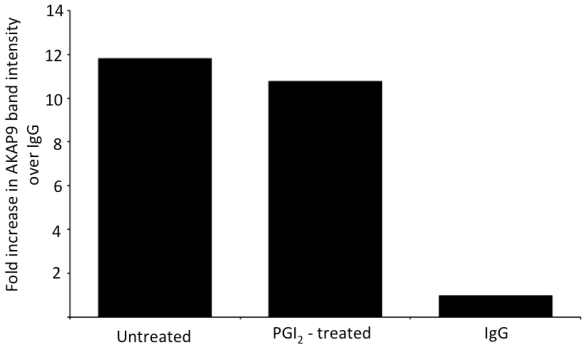

***Figure 5.4* - Co-immunoprecipitation of AKAP9 with IP$_3$R1.**

(a) Lysates prepared from untreated and PGI$_2$-treated platelets were treated and IP$_3$R1 was immunoprecipitated as detailed previously. The membranes were immunoblotted with anti-IP$_3$R1 (1:1000) and custom-made anti-AKAP9 antibody (1:2000). The bands corresponding to the apparent molecular weight of Yotiao seems to appear in immunoprecipitation samples from untreated and PGI$_2$-treated lysates, as quantified using densitometry in **(b)** (n=2), suggesting that PGI$_2$-treatment may not alter the IP$_3$R1-Yotiao interaction, however we cannot confirm this due to poor reagent quality.

5.4. Effect of disruption of AKAP-PKA interactions on IP$_3$R1 phosphorylation

The previous sections have suggested the presence of AKAP9 as a potential PKA-binding protein. However it was also essential to investigate the functional role of AKAPs. Specific AKAP knock-out mice are unavailable, however peptides that mimic the amphipathic helixes have been developed. These display an affinity towards PKA, therefore disrupting the association between PKA-AKAPs (Carr et al. 1992; Carr et al. 1991). Ht31, based on AKAP-Lbc, contains an 18-amino acid amphiphatic helix that can bind to PKA, therefore interfering with PKA-AKAP interaction. Ht31 can delineate the AKAP interaction with both PKA I and PKA II (Carr et al. 1992; Carr et al. 1991; Herberg et al. 2000). However, the negative control peptide, Ht31P, contains two isoleucine to proline substitutions in the helix, therefore it is unable to interfere with the PKA-AKAP binding (Carr et al. 1991; Colledge et al. 1999, Leray 2012; Goueli & Hsaio, 2000). Additionally, peptides such as RIAD and SuperAKAP are specific to interactions with PKA I and PKA II respectively (Gold et al. 2006; Carlson et al. 2006).

5.4.1. Optimisation of St-Ht31 concentration to study the effect of disruption of AKAP-PKA interactions on IP$_3$R1 phosphorylation

St-Ht31, a stearated peptide derived from Human Thyroid Hormone, and based on AKAP-Lbc, was used to disrupt the association of AKAPs with both PKA I and PKAII. Treatment with St-Ht31 should potentially disrupt the interaction between PKA and AKAP, and therefore interfere with the PKA-mediated phosphorylation of IP$_3$R1. Here, we study the consequence of St-Ht31 treatment on IP$_3$R1 phosphorylation in platelets. As a negative control, St-Ht31P peptide has been used. In both the peptides, the stearated hydrophobic moiety allows the uptake of the compound through the plasma membrane (Leray 2012; Goueli & Hsaio, 2000). Washed platelet were incubated with either increasing concentration of St-Ht31 (1-5μM) or St-Ht31P (1-5μM) for 30 minutes at 37°C to allow for the penetration of stearated peptide. At the end of the incubation period, the platelets were treated with a fixed concentration of PGI_2 (100nM) for 1 minute at 37°C, and subsequently lysed using Laemelli buffer. The proteins were resolved on SDS-PAGE and the membranes were treated as described previously (§2.5.2-3). Immunoblotting was performed using Anti-pPKAs antibody to study the effect of PKA-AKAP complex disruption on phosphorylation of all the PKA substrates.

Figure 5.5

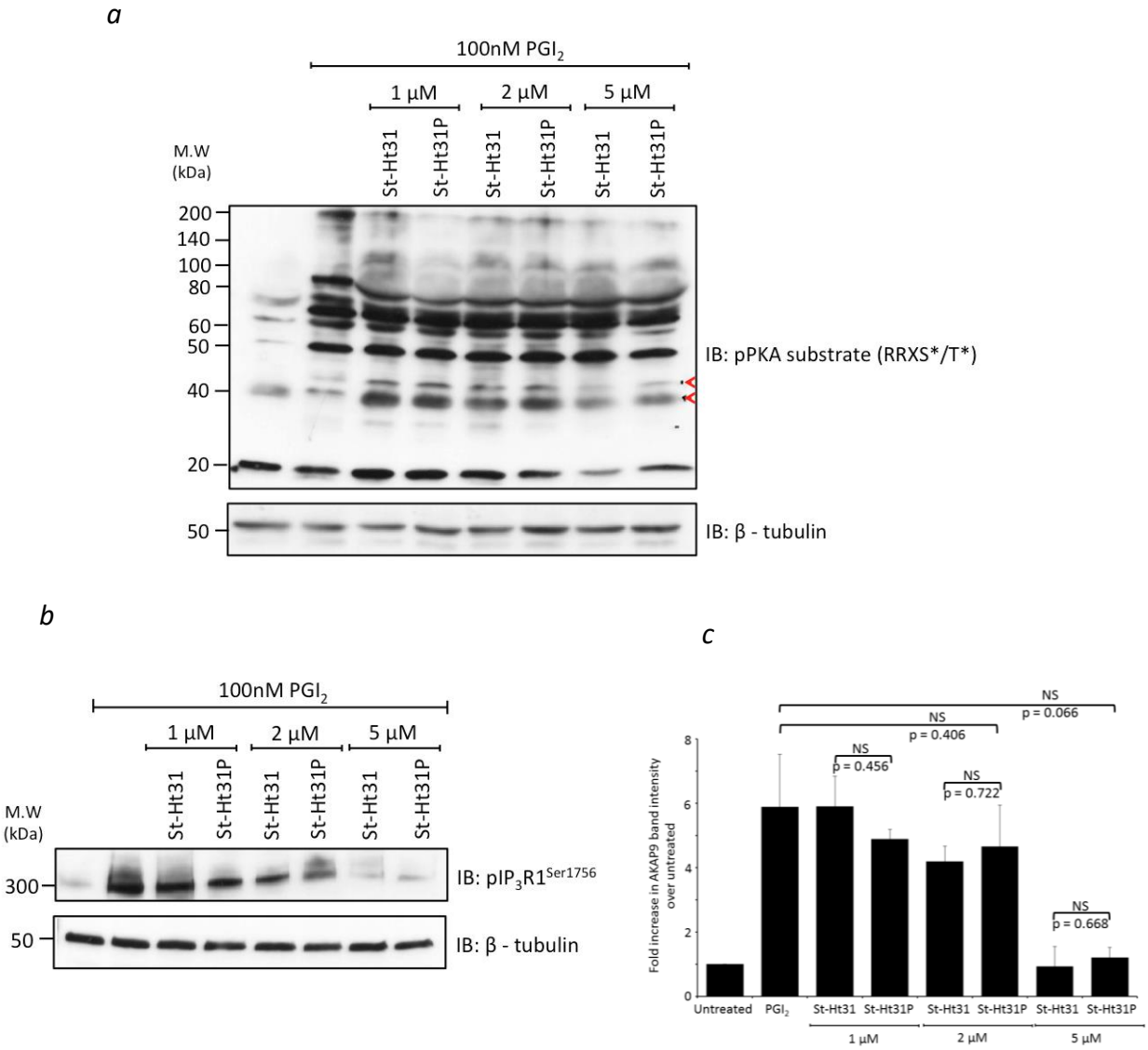

***Figure 5.5* – Effect of disruption of AKAP interaction on substrate phosphorylation in platelets**

(a) Washed platelets ($5x10^8$ cells/ml) were pre-treated with increasing concentration of St-Ht31/St-Ht31P (1-5µM) for 30 minutes at 37°C, followed by treatment with PGI_2 (100nM) for 1 minute at 37°C to initiate PGI_2-induced PKA signalling. The reaction was terminated by lysing the samples with 2x Laemmli buffer (1:1v/v). The lysates were resolved as described previously and immunoblotted with pPKA substrate (1:1000) **(b)** and $pIP_3R1^{Ser1756}$ (1:1000). Anti - β-tubulin (1:1000) was used as a loading control. The protein bands displaying altered phosphorylation pattern compared to PGI_2 control are shown by arrows. **(c)** The band intensity was quantified using densitometry. We failed to detect a significant difference in the band intensities for pIP_3R1 post treatment with St-Ht31 and St-Ht31P (n=3).

Under untreated conditions, only proteins at molecular weights corresponding to 40kDa, 50kDa and 65kDa showed phosphorylation. However upon treatment with PGI_2 (100nM), the phosphorylation bands corresponding to approximate molecular weights of 200kda, 80kDa, 42kDa appeared, in addition to the proteins that displayed protein phosphorylation under untreated conditions. On pre-treatment with St-Ht31, some phosphorylation bands weaken (as shown by arrows; *Figure 5.5a*). For example, protein band corresponding to the approximate molecular weight of 40kDa and 42kDa were not phosphorylated under basal conditions, but undergoes phosphorylation on PGI_2 treatment. On pre-treatment with St-Ht31 (5μM) the protein band intensity subsided to basal levels, however this was not the case when treated with St-Ht31P (*Figure 5.5a*). Similarly, the phosphorylation of protein corresponding to 40kDa was also blunted on treatment with St-Ht31 (5μM), but not with the control peptide St-Ht31P. The lower concentration of St-Ht31 (1-2μM) did not affect the phosphorylation patterns (*Figure 5.5a*).

Similarly, the effect of delineation of PKA-AKAP interaction on IP_3R1 phosphorylation was also studied (*Figure 5.5b*). IP_3R1 was not phosphorylated at ser1756 under basal conditions, but undergoes phosphorylation on treatment with PGI_2 (100nM for 1 minute at 37°C). There was no apparent difference in the extent of IP_3R1 phosphorylation on treatment with St-Ht31 (1μM) as compared to treatment with 1μM St-Ht31P (*Figure 5.5b,c*). Treatment with St-Ht31 (2μM) also did not cause blunting of IP_3R1 phosphorylation at ser1756. Treatment with 5μM St-Ht31/St-Ht31P caused a blunting of IP_3R1 phosphorylation. However, there was no significant difference in effect of St-Ht31 as compared to the control peptide suggesting non-specific effects of St-Ht31/St-Ht31P at the concentrations used (*Figure 5.5b,c*).

The weak effect of St-Ht31 on the phosphorylation of PKA substrates (*Figure 5.5a*) including IP_3R1 (*Figure 5.5b,c*) suggests that this could perhaps be a result of St-Ht31 not being able to permeate the cells. Alternatively, the lack of effect could also be a consequence of imbalance between the concentrations of PGI_2 used as compared to the concentration of St-Ht31 used. To summarise, St-Ht31 treatment was both ineffective and lacked reproducibility in significantly altering PKA substrate phosphorylation including IP_3R1. However, this could be corrected by achieving the correct balance between the St-Ht31-PGI_2 concentrations in platelets.

5.4.2. Optimisation of PGI_2 concentration to study the effect of disruption of AKAP-PKA interactions on IP_3R1 phosphorylation

The effect of St-Ht31 maybe subtle and masked if the concentration of PGI_2 is too high. In order to achieve a balance between the concentrations of St-Ht31 and PGI_2, washed platelets were incubated with St-Ht31 (5μM) or St-Ht31P (5μM) at 37°C to allow for the penetration of the peptide through the plasma membrane. Previous work from colleagues has suggested 30 minutes to be an appropriate time to allow for peptide penetration. At the end of the incubation period, the platelets were treated with PGI_2 (either 1nM or 10nM) for 1 minute at 37°C, and subsequently lysed using Laemelli buffer. The proteins were resolved on SDS-PAGE and the membranes were treated as described previously (§2.5.2-3). Immunoblotting was performed using pPKAs antibody to study the effect of PKA-AKAP complex disruption on phosphorylation of all the PKA substrates.

Under untreated conditions, several proteins including those corresponding to approximate molecular weights of 60 and 140kDa showed phosphorylation. Treatment with PGI_2 (10nM) increased the phosphorylation of bands corresponding to approximate molecular weights of 40, 50 and 80kDa, in addition to the proteins that displayed protein phosphorylation under untreated conditions. On pre-treatment with St-Ht31, the phosphorylation of some bands is reduced (as shown by arrows). For example, protein bands corresponding to the approximate molecular weight of 40 and 50kDa were not phosphorylated under basal conditions, but underwent phosphorylation on treatment with PGI_2 (10nM). The phosphorylation of these proteins was comprised on pre-treatment with St-Ht31 but was recovered on treatment with St-Ht31P (*Figure 5.6a*). Treatment with 1nM PGI_2 did not induce an intense phosphorylation, which means the pre-treatment with St-Ht31 only induced subtle differences in phosphorylation patterns. Phosphorylation of VASP, an established PKA substrate, in response to St-Ht31 pre-treatment was also studied. As can be seen from *Figure 5.6a*, VASP displayed minor basal phosphorylation, which intensified on treatment with 1nM and 10nM PGI_2 in a concentration-dependent manner. Pre-treatment with St-Ht31 (5μM), blunted the phosphorylation of VASP in response to treatment with 10nM PGI_2. In contrast, treatment with 1nM PGI_2 did not seem to alter the extent of VASP phosphorylation (*Figure 5.6a*).

Figure 5.6

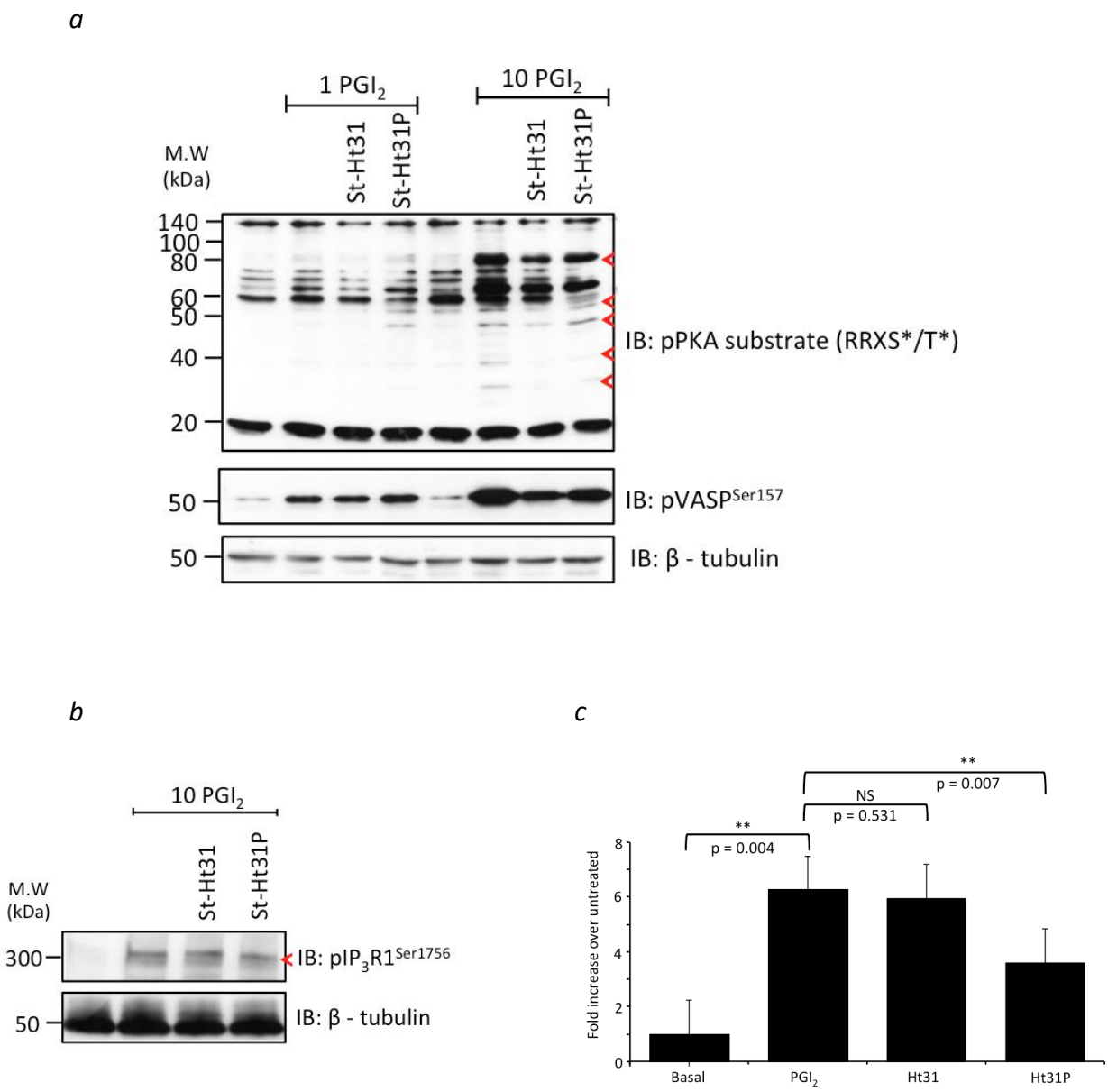

***Figure 5.6* – Effect of disruption of AKAP interaction on substrate phosphorylation in platelets**

(a) Washed platelets (5x10^8 cells/ml) were pre-treated with a fixed concentration of St-Ht31/St-Ht31P (5µM) for 30 minutes at 37°C, followed by treatment with PGI_2 (1nM or 10nM) for 1 minute at 37°C to initiate PGI_2-induced PKA signalling. The reaction was terminated by lysing the samples with 2x Laemmli buffer (1:1v/v). The lysates were resolved and immunoblotted with pPKA substrate (1:1000) and pVASP^{Ser157} (1:1000) **(b)** and pIP$_3$R1^{Ser1756} (1:1000). Anti - β-tubulin (1:1000) was used as a loading control. The protein bands displaying altered phosphorylation pattern compared to PGI_2 control are shown by arrows and **(c)** quantified using densitometry (n=3). The data suggests that treatment of platelets with 5µM St-Ht31/St-Ht31P at 37°C for 30 minutes followed by treatment with 10nM PGI_2 for 1 minute was considered appropriate to be used to study IP$_3$R1 phosphorylation.

To summarise, treatment of platelets with 5µM St-Ht31/St-Ht31P at 37°C for 30 minutes followed by treatment with 10nM PGI_2 for 1 minute was considered appropriate to be used to study IP_3R1 phosphorylation.

Next, platelets were pre-treated with St-Ht31/St-Ht31P (5µM) for 30 minutes at 37°C, followed by treatment with PGI_2 (10nM) for 1 minute at 37°C to study the effect of AKAP-PKA complex disruption on the phosphorylation of IP_3R1. *Figure 5.6b,c* shows that on treatment with 10nM PGI_2, the IP_3R1 undergoes phosphorylation. Although the supposed disruption of PKA-AKAP complex with St-Ht31 alters the phosphorylation of certain substrates (*Figure 5.6a)*, IP_3R1 phosphorylation pattern remained unaltered on St-Ht31 treatment as shown by the quantification data (*Figure 5.6c*). This could suggest that perhaps IP_3R1-PKA-AKAP macromolecular complex is inaccessible to the competitive peptide. To aid the entry of peptide, cell permeabilisation was considered.

5.4.3. Optimisation of permeabilisation conditions to study the effect of disruption of AKAP-PKA interactions on IP_3R1 phosphorylation

The addition of stearic acid residues to compounds allows passage through the plasma membrane (Leray 2012). However a complete access to the site of action may still perhaps be limited due to the subcellular localisation of the PKA-AKAP-IP_3R1 complex. Recognising the potential inability of St-Ht31 to access the protein complex of interest, platelets were permeabilised with mild non-ionic detergent, digitonin. We speculate St-Ht31 to have a greater accessibility to the macromolecular complex of interest in digitonin-permeabilised platelets. Digitonin permeabilises the cells by complexing with the membrane cholesterol (Ahnert-Hilger & Gratzl 1988). Therefore, the platelet permeabilisation protocol was first characterised, before investigating the effect of St-Ht31 on IP_3R1 phosphorylation.

5.4.3.1. Alkaline phosphatase assay

Alkaline phosphatase is found in platelet cytosol. Under alkaline conditions it can catalyse the hydrolysis of phosphate esters to form organic radical and inorganic phosphate. A phosphatase substrate, p-Nitrophenyl phosphate (pNPP) when dephosphorylated by alkaline phosphatase turns yellow and the absorbance can be detected at 405nm. In non-permeabilised platelets, alkaline phosphatase is contained within the cell and therefore unable to catalyse the hydrolysis of phosphate esters. However, on platelet permeabilisation, this enzyme is released to bring about the hydrolysis of esters. Therefore, this property of the cell is exploited to confirm platelet permeabilisation.

Washed platelets (2.5 x 10^8 cells/ml) were treated with an increasing concentration of digitonin (1-20µM) at 37°C for a fixed interval of time (10 minutes). Non-permeabilised platelets were used as a negative control. The colour change of pNPP was measured at an absorbance wavelength of 405nm. The absorbance values per sample were measured in triplicate. All samples displayed an absorbance value over non-permeabilised indicating that digitonin caused platelet permeabilisation. At a concentration of 1µM, the absorbance values showed a 4-fold increase over basal, whereas a concentration of 2µM caused 15-fold increase. However, the absorbance values did not alter on increasing the concentration of digitonin in excess of 2µM (*Figure 5.7a*).

Figure 5.7

a

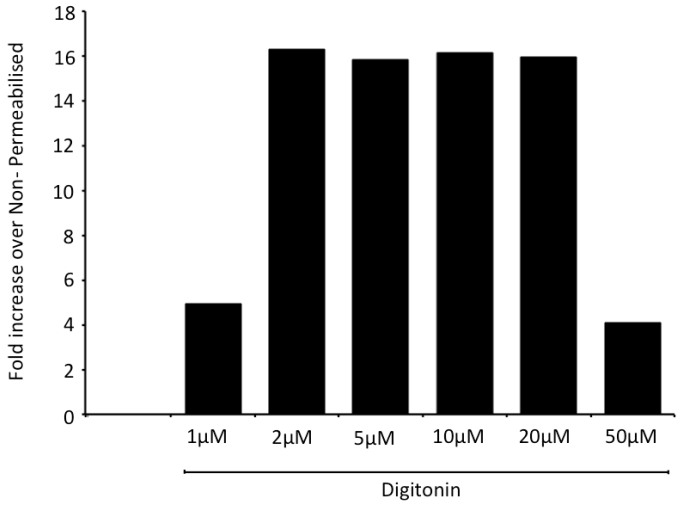

b

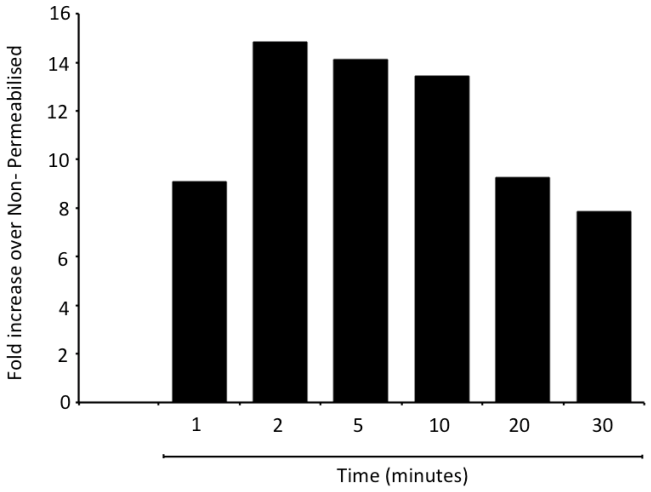

***Figure 5.7* – Testing for Digitonin-induced permeabilisation of platelets using Alkaline phosphatase assay**

(a) Washed platelets (2.5x10^{8}cells/ml) treated with increasing concentration of Digitonin (1 - 50μM) at 37°C for 10 minutes in a 96-well plate. At the end of the incubation period, p-Nitrophenyl phosphate (pNPP) was added to initiate the de-phosphorylation reaction. The reaction was terminated by the addition of stop solution (NaOH, 2M). The absorbance was measured 405nm in TeCan PlateReader (n=1). The absorbance values did not alter on increasing the concentration of digitonin in excess of 2μM **(b)** Washed platelets (2.5x10^{8}cells/ml) treated with a fixed concentration of digitonin (2μM) for increasing time interval (1 – 30 minutes) at 37°C for 10 minutes in a 96-well plate. At the end of the incubation period, the samples were processed as described in (a) (n=1). Although the digitonin permeabilised the platelets, the optimal concentration at which their functional integrity was preserved remained to be explored.

Next, to measure the optimum time required for platelet permeabilisation, washed platelets were treated with a fixed concentration of digitonin (2µM) for increasing interval of time (1-20 minutes) at 37°C. The absorbance values displayed a time-dependant increase until 2 minutes, after which there was a steady decline in the absorbance values. At 1 minute, the absorbance value of 8.10 over basal was seen, which peaked at 2 minutes (14.83), however did not change significantly until 10 minutes (13.44). At 20 minutes, the increase in absorbance over non-permeabilised platelets reduced to 9.25 units (*Figure 5.7b*). These data suggest that digitonin permeabilised the platelets, however it needed to be investigated if the functional response of permeabilised platelets was preserved. From the results described above, platelets were permeabilised with a concentration range of 2-20µM digitonin for 10 minutes to study the functional response.

5.4.3.2. Aggregation response in permeabilised platelets

On confirming digitonin-induced platelet permeabilisation, it was essential to investigate if the platelets retained their functional capacity on permeabilisation as we wanted to perform work on functional platelets. To achieve this, platelets (2.5x 10^8 cells/ml) were first treated an increasing concentration of digitonin (2-20µM) at 37°C for a fixed time (10 minutes) as established in the previous sections. Platelet aggregation response was monitored for 3 minutes in response to Thrombin (0.1U/ml). Non-permeabilised platelets displayed approximately 72% aggregation in response to thrombin. This aggregation response remained unaltered on treatment with digitonin (2-10µM). However, on treatment with 20µM digitonin, platelet aggregation was blunted to 10% (*Figure 5.8a*). Next, the platelets were incubated with a fixed concentration of digitonin (2µM) for increasing time intervals (1-30 minutes) at 37°C. Platelet aggregation response was monitored for 3 minutes in response to thrombin (0.1U/ml). Non-permeabilised platelets displayed approximately 86% aggregation in response to thrombin. On permeabilisation with 2µM digitonin for 1 minute, the aggregation remained unaltered at 86%. At 10, 20 and 30 minutes, the aggregation response was 84%, 83% and 80% respectively, therefore suggesting that platelets remained functional for 30 minutes post-permeabilisation. This

Figure 5.8

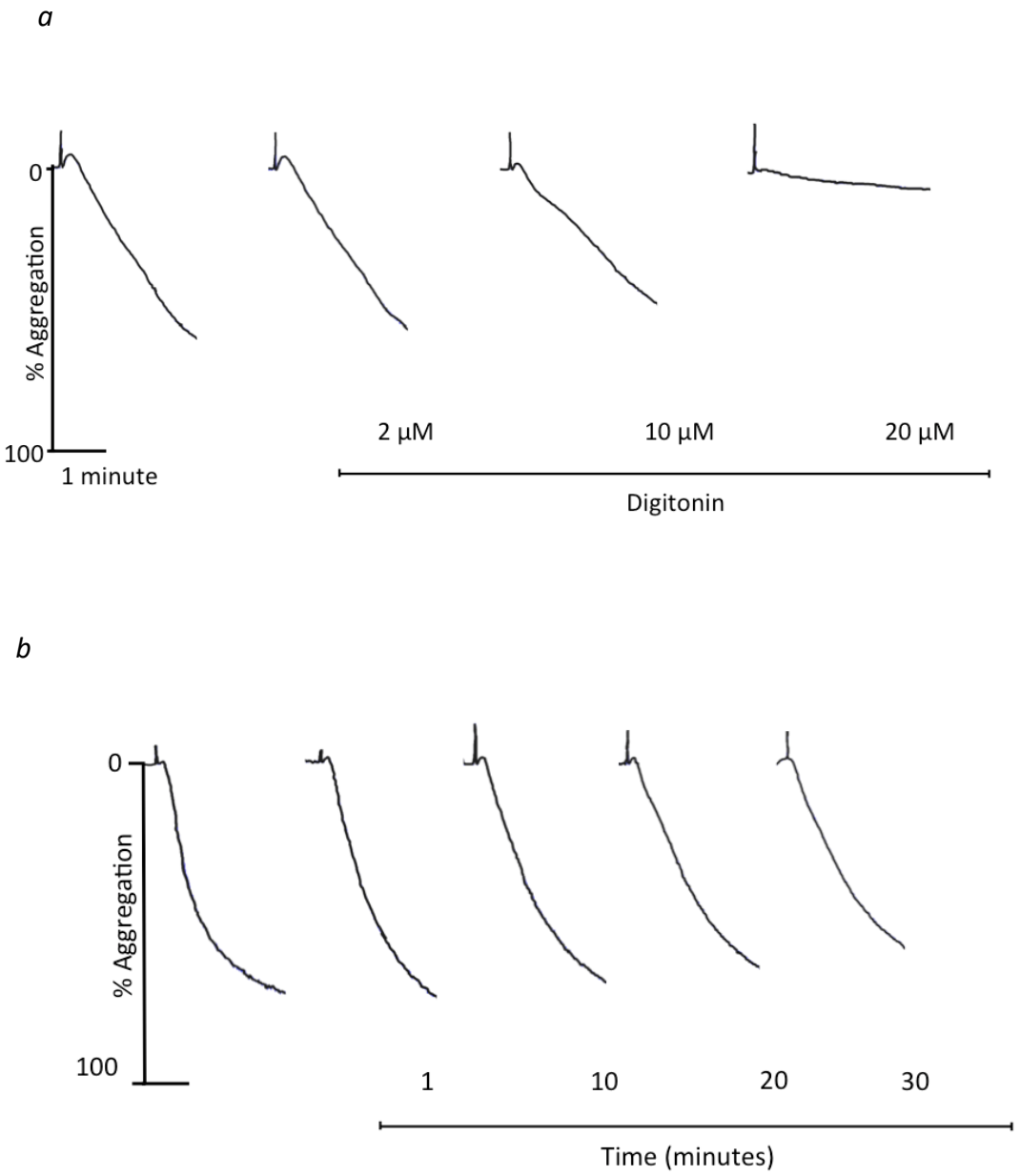

***Figure 5.8* – Aggregation in response to Thrombin in platelets permeabilised with Digitonin**

(a) Washed platelets (2.5x10^{8}cells/ml) treated with increasing concentration of Digitonin (2 - 20µM) at 37°C for 10 minutes. At the end of the incubation period, platelets stimulated with thrombin (0.1U/ml). **(b)** Washed platelets (2.5x10^{8}cells/ml) treated with a fixed concentration of digitonin 2µM at 37°C for increasing time period (1-30 minutes). At the end of the incubation period, platelets stimulated with thrombin (0.1U/ml). The arrow shows the point of addition of thrombin. Aggregation was monitored for 3 minutes under constant stirring (1000rpm) at 37^{o}C using Chrono-log dual channel aggregometer. The traces were generated by aggro-link computer software (n=1). The data suggests that digitonin permeabilisation (2µM for 10 mintues) did not interfere with the ability of platelets to aggregate.

indicates that the aggregation response remained relatively unaltered for up to 30 minutes, at (*Figure 5.8b*). To summarise, *Figure 5.8* shows that platelet permeabilisation with digitonin (2µM) for 10 minutes does not interfere with the platelets ability to aggregate in response to thrombin (0.1U/ml).

5.4.3.3. cAMP Signalling in permeabilised platelets

Digitonin exclusively permeabilises cholesterol-rich membranes such as the plasma membrane, but not endoplasmic reticulum. However, at saturating concentrations of digitonin, the integrity of ER may also be affected (Ahnert-Hilger & Gratzl 1988). Reports have also suggested the loss of cell proteins (Thines-Sempoux et al. 1969). Having established that permeabilising platelets with digitonin (2µM) for 10 minutes, retains its ability to aggregate, we then wished to study if permeabilisation compromised the biochemical pathways in platelets.

To achieve this, platelets were permeabilised with digitonin (2µM) for 10 minutes at 37°C. At the end of the permeabilisation period, the platelets were treated with PGI_2 (10nM) for 1 minute at 37°C, before being lysed using Laemmelli buffer. The platelet lysates centrifuged at 1000rpm and the supernatant were resolved as described previously (§2.5.2-3). The possibility of PKA subunits leaking out of the permeabilised platelets was explored using immunoblotting. *Figure 5.9a* shows that all three PKA subunits were present in both untreated and PGI_2-treated permeabilised platelets. The ability of PKA to phosphorylate IP_3R1 was also tested in permeabilised platelets, using anti-p$IP_3R1^{Ser1756}$ antibody (*Figure 5.9a)*. Like that in non-permeabilised platelets, IP_3R1 was not phosphorylated under untreated conditions however on PGI_2-treatment, IP_3R1 underwent significant PGI_2-induced phosphorylation (*Figure 5.9a,b*). Considering the results from §5.4.3.1., which suggest the leakage of alkaline phosphate in permeabilised platelets, it is interesting to note that the IP_3R1 still undergoes phosphorylation in permeabilised cells. Given that alkaline phosphotase activity was detected outside the cell under these conditions it possible that ATP could also leak. We did not measure this, but our data suggest that sufficient ATP was present to facilitate phosphorylation. To summarise, the data suggests that PKA levels and potential to phosphorylate IP_3R1 remained unaltered on platelet permeabilisation with

Figure 5.9

a

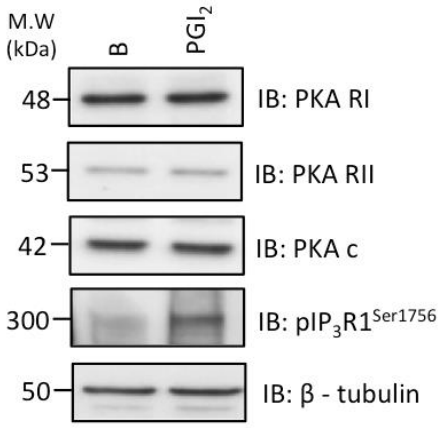

b

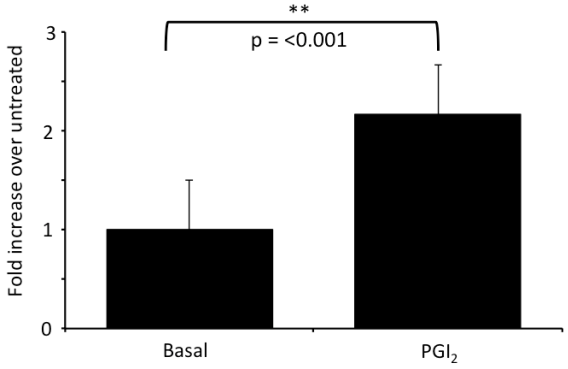

***Figure 5.9* – PGI$_2$-induced IP$_3$R1 phosphorylation in platelets permeabilised with Digitonin**

(a) Washed platelets (5x10^8 cells/ml) were permeabilised with Digitonin (2µM) for 10 minutes at 37°C. At the end of the incubation period, platelets were treated with PGI$_2$ (10nM) for 1 minute at 37°C to initiate PGI$_2$-induced PKA signalling. The signalling was terminated by lysing the samples with 2x Laemmli buffer (1:1v/v) and the lysates were centrifuged and processed as described previously. Immunoblotting was performed using anti-PKA RI, Anti-PKA RII and anti-PKA c antibodies (1:1000). Anti - β-tubulin (1:1000) was used as a loading control. Additionally, the membranes were also probed with pIP$_3$R1^{Ser1756} to assess PGI$_2$-induced IP$_3$R1 phosphorylation in permeabilised platelets (n=3) **(b)** Densitometry showing PGI$_2$-induced IP$_3$R1 phosphorylation in permeabilised platelets (n=3). The data suggests that PKA levels and potential to phosphorylated IP$_3$R1 remained unaltered on platelet permeabilisation, meaning that platelet permeabilisation does not compromise cAMP-signalling machinery.

(2μM) for 10 minutes, meaning that platelet permeabilisation does not compromise cAMP-signalling machinery.

5.4.3.4. Effect of disruption of AKAP interaction in permeabilised platelets

On characterising the permeabilisation conditions, washed platelets were once again treated with St-Ht31 to study the effect of disruption of AKAP-PKA interaction on IP_3R1 phosphorylation. To achieve this, platelets were permeabilised using digitonin (2μM) for 10 minutes at 37°C, treated with St-Ht31/St-Ht31P (5μM) for 30 minutes, followed by treatment with PGI_2 (10nM) for 1 minute at 37°C. Platelet lysates were prepared as previously described and subjected to immmunoblotting with anti-$pIP_3R1^{Ser1756}$ to assess the effect of St-Ht31-mediated disruption of PKA-AKAP complex on IP_3R1 phosphorylation. It can be seen from *Figure 5.10*, that in IP_3R1 is not phosphorylated under non-treated conditions, whereas undergoes phosphorylation on PGI_2 treatment. These results are consistent with our previous findings. On treatment with St-Ht31, the IP_3R1 phosphorylation did not undergo blunting, instead was midly potentiated as compared to PGI_2 treatment/St-Ht31P treatment (*Figure 5.10b*). VASP, a well-established PKA substrate was used as a positive control to assess the success of St-Ht31 treatment. Data shows that VASP is not phosphorylated under basal conditions, however undergoes phosphorylation on treatment with PGI_2. Treatment with St-Ht31 blunted the PGI_2-induced VASP phosphorylation as compared to the control peptide, St-Ht31P and PGI_2-treatment (*Figure 5.10a*).

To summarise, although St-Ht31 treatment is effective at compromising VASP phosphorylation, the same is not true for IP_3R1 phosphorylation. This suggests that perhaps St-Ht31 treatment conditions are substrate-specific and are dependent on the cellular localisation of the substrate. Here, in spite of trying various approaches, we were unable to show any significant effect of PKA-AKAP complex disruption on IP_3R1 phosphorylation.

Figure 5.10

a

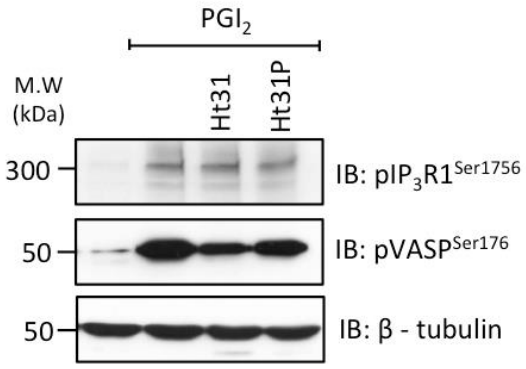

b

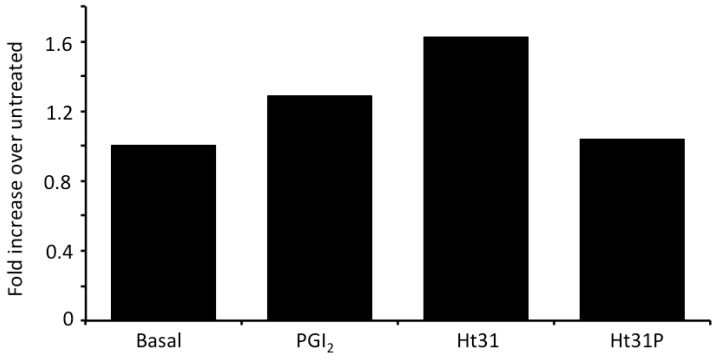

***Figure 5.10* – Effect of disruption of AKAP interaction on IP$_3$R1 phosphorylation in platelets permeabilised with Digitonin**

(a) Washed platelets (5x10^8 cells/ml) were permeabilised with Digitonin (2µM) for 10 minutes, followed by treatment with St-Ht31/St-Ht31P (5µM) for 30 minutes at 37°C. At the end of the incubation period, platelets were treated with PGI_2 (10nM) for 1 minute at 37°C to initiate PGI_2-induced PKA signalling, which was terminated by lysing the samples with 2x Laemmli buffer (1:1v/v) and handled as previously described, until immunoblotting with anti-pIP$_3$R1^{Ser1756} (1:1000). Similarly, the membranes were also probed with anti-pVASP^{Ser157}(1:1000). Anti - β-tubulin (1:1000) was used as a loading control. The data shows that St-Ht31 treatment is effective at compromising VASP phosphorylation, the same is not true for IP$_3$R1 phosphorylation **(b)** as shown by densitometry data for IP$_3$R1 phosphorylation (n=2).

5.5. Effect of disruption of AKAP-PKA interaction on Ca^{2+} mobilisation

Previous research has shown the presence of PKA-AKAP9-IP_3R1 macromolecular complex (Tu et al. 2004; Collado-Hilly & Coquil 2009). These findings were further supported by our results (*Figure 5.3-5.4*). Here, we once again attempt to disrupt this potential macromolecular complex using St-Ht31 and study its consequence on Ca^{2+} mobilisation in platelet suspension.

To achieve this, intracellular Ca^{2+} levels were measured in a suspended Fura-2-AM labelled platelets that were pre-treated with St-Ht31 (5µM) or the control peptide St-Ht31P (5µM) at 37^{o}C for 30 minutes. The platelet suspension was treated with PGI_2 (100nM) for 1 minute. At the end of the incubation period, thrombin (0.1 U/ml) was used to stimulate Ca^{2+} mobilisation. The Ca^{2+} response was measured for 3 minutes post-stimulation. From the Ca^{2+} mobilisation trace (*Figure 5.11a*) and the quantified data, it can be seen that on treatment with thrombin platelets mobilised a maximal of 450.14±89.03nM of Ca^{2+} at the rate of 35.3±9.0nM/sec, whereas on treatment with PGI_2, this reduced to 356.5±82.5nM at the rate of 4.3±2.4nM/sec. The time taken to bring about Ca^{2+} mobilisation was also prolonged on PGI_2 treatment, from 16.0±3.1sec to 103.2±20.1sec. It can be speculated this to be a consequence of PKA-mediated IP_3R1 phosphorylation, which is inhibitory (Cavallini et al. 1996). A similar pattern of compromised Ca^{2+} mobilisation was observed on treatment with IP_3R1 antagonist such as 2-APB (as described in §4.2.3) further suggesting that indeed PGI_2-induced phosphorylation of IP_3R1 is inhibitory.

Platelets were pre-treated with St-Ht31 on the assumption that this would delineate the interaction between PKA-AKAP and therefore prevent PKA from phosphorylating IP_3R1. This means that the potential inhibitory effects of PGI_2 on Ca^{2+} mobilisation could be compromised by the presence of the peptide. On treatment with St-Ht31, the rate or maximal Ca^{2+} mobilisation did not differ significantly compared to treatment with PGI_2 (rate, p=0.1731 and Peak Ca^{2+}, p = 0.7677). However, treatment with St-Ht31 caused a quicker Ca^{2+} mobilisation (69.35±15.45sec) as compared to PGI_2-treatment (103.20±20.14sec) (p=0.0266). However, no significant difference in any of the parameters was observed between the St-Ht31 and control St-Ht31P questioning the specificity of the peptide and making interpretation of the data challenging.

Figure 5.11

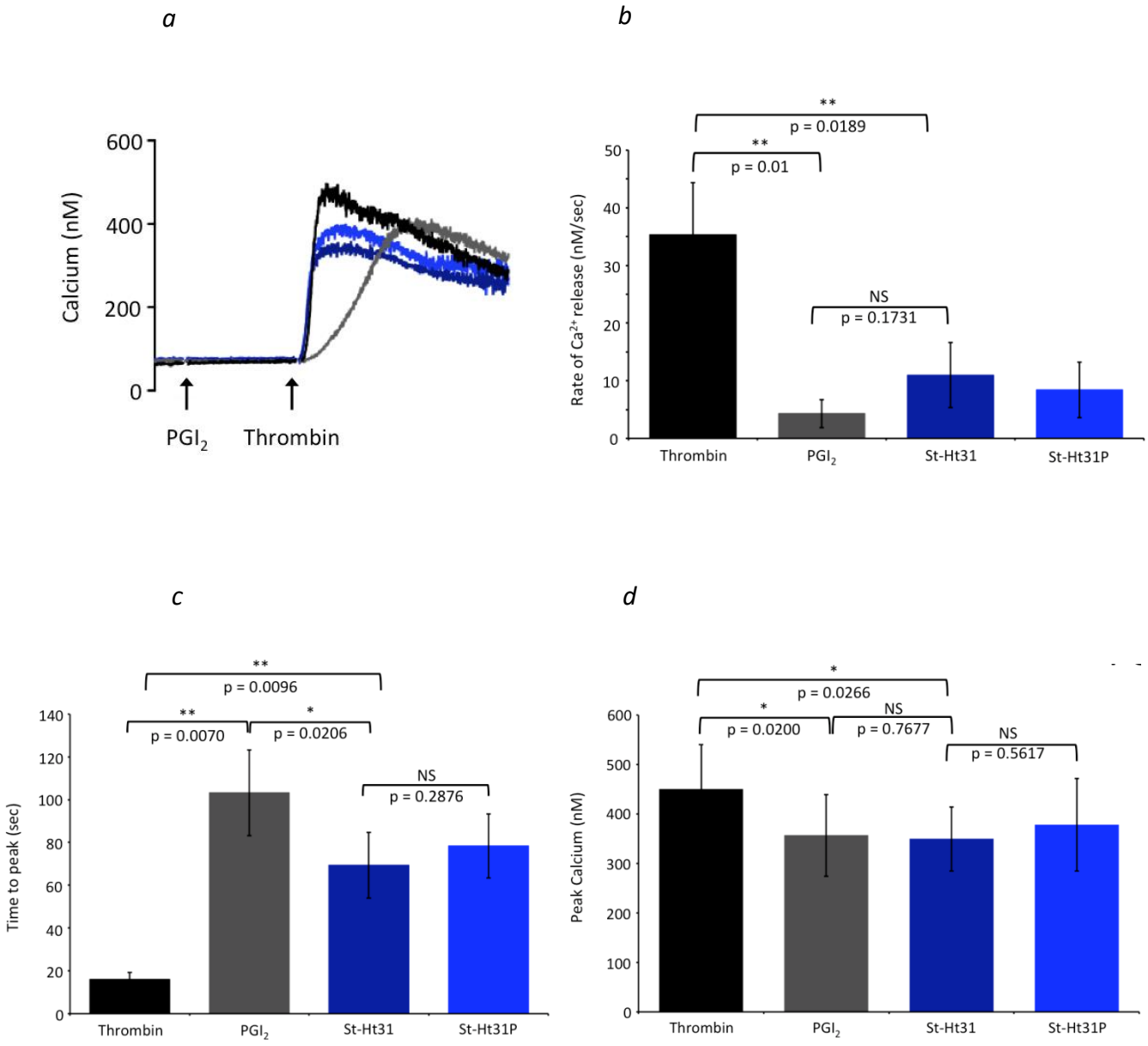

***Figure 5.11.* – Effect of disruption of PKA-AKAP complex on thrombin-induced intracellular Ca^{2+} mobilisation**

(a) Calcium release was measured in Fura-2 loaded washed platelets ($2.5x10^8$cells/ml) pre-treated with St-Ht31/ St-Ht31P (5µM). Labelled platelet suspension was then treated with PGI_2 (100nM) for 1 minute at 37°C, prior to stimulation with Thrombin (0.1U/ml). The calcium release was measured in dark using Carin Spectrophotometer. The signals were recorded using Cairn proprietary software. The traces for thrombin and PGI_2 treatment are shown in black and grey respectively. The traces corresponding to St-Ht31 and St-Ht31P treatment are shown in dark blue and light blue respectively. **(b)** The rate of Ca^{2+} release for the first 1 minute post-treatment was quantified and plotted as Mean. St-Ht31-treatment did not significantly blunt the initial rate of Ca^{2+} release but **(c)** impeded the time required to release the maximal amount of Ca^{2+} as compared to PGI_2 treatment **(d)** The maximal calcium release post-St-Ht31 treatment was not significantly escalated compared to PGI_2 treatment (n=3).

Ideally, we would expect to see a complete recovery of Ca^{2+} mobilisation on St-Ht31 treatment, therefore making the response comparable to thrombin stimulation. However, it can be seen that there is a significant difference between the two conditions (*Figure 5.11*), thus suggesting that the effect of St-Ht31 have been compromised. This could perhaps be due to a limited concentration of the peptide used. Alternatively the limited accessibility of the peptide to the macromolecular complex of interest could also explain these results. Also, the questions on specificity of St-Ht31 and St-Ht31P cannot be ignored.

5.6 Discussion

AKAPs are responsible for the coordination of signals by various macromolecular complexes that form the cAMP signalling pathway (Pidoux & Tasken 2010). All AKAPs bind to PKA via a PKA-binding domain and a unique targeting domain is responsible for the spatial regulation of PKA signals. Additionally, AKAPs are also known to bind to other members of signalling complexes such as PDE and phosphatases. The macromolecular complex is then localised at specific subcellular sites via lipid-protein interactions at the tethering domains (Feliciello et al. 2001; Coghlan et al. 1995; Pidoux & Tasken 2010). Conversely, protein-protein interactions are responsible to ensuring that the kinase is orientated towards the substrate (Carnegie & Scott 2003).

There are over 50 AKAPs that have been identified so far, however this chapter is primarily focused on AKAP9 due to its reported association with IP$_3$R1 (Tu et al. 2004; Collado-Hilly & Coquil 2009). AKAP9 exists as three splice variants Yotiao (250kDa), AKAP350 (350kDa) and AKAP450 (450kDa). The precise reasons for such a large difference in the molecular weights of the splice variants are not known. AKAP9 has been reported to be present in platelets (Margarucci et al. 2011; Rowley et al. 2011), however we validated these findings using western blotting. A commercial antibody that recognised all the splice variants of AKAP9 was not available hence the antibody was requested from Prof. Carmen Dessuaer. This antibody was synthesised by Sigma Genosys against a purified H6-tagged portion of Yotiao (amino acid 808–957) (Piggott et al, 2008). The antibody was kindly gifted by Prof. Dessuaer, however the quantity of the antibody supplied was restrictive. Also, the concentration of the antibody was not supplied, which meant we were unable to perform immunoprecipitation experiments using this antibody. Nevertheless, this antibody was used exclusively for Immunoblotting. Using this we suggest the presence of all three splice variants of AKAP9 in platelets (*Figure 5.1*). In addition to our data, transcriptomics data from Rowley et al (Rowley et al. 2011), also shows the presence of AKAP9 in platelets. An alternative antibody recognising the Yotiao (250kDa) isoform of AKAP9 was first tested on platelet lysates (*Figure 5.1*) and subsequently used for immunoprecipitation. Owing to the issues with specificity, the use of peptide used for immunisation as a competitive peptide for antibody recognition site was considered. However, we were unable to access the peptide, therefore this option was not explored further.

In order to study the presence and behaviour of AKAP9 protein in isolation, attempts were made to immunoprecipitate AKAP9 from untreated platelets lysates using the Yotiao antibody. However AKAP9 could not be successfully immunoprecipitated owing to the presence of non-specific band in IgG control lane (*Figure 5.2*). This issue was addressed by altering the combination of immunoprecipitation/immmunoblotting antibodies, whereby the protein was immunoprecipitated using the commercially available Yotiao antibody, whereas immunoblotting was performed using the custom-made AKAP9 antibody. A non-specific protein band was observed in the IgG control lane, suggesting IgG cross-reactivity (*Figure 5.2*). This could be because both these antibodies were raised in rabbit, which would theoretically be the reason for cross-reactivity between antibodies. Although we wanted to isolate the protein by immunoprecipitation and study its interaction with the IP$_3$R1-PKA macromolecular complex, the tools available proved to be a limiting factor in pursuing this any further; hence we could not isolate AKAP9 by immunoprecipitation. However, antibodies raised against different species could be used in the future to answer these questions.

The PKA-binding capacities of AKAP are well known (Gold et al. 2006), however the presence of a potential PKA-AKAP complex was investigated using protein enrichment approach adapted from Scholten *et al* (Scholten et al. 2006). This approach was based on the principle that cAMP immobilished on agarose beads would bind to PKA and precipitate any other PKA-associating proteins. Here, we show that using this approach two of the three AKAP9 isoforms (Yotiao and AKAP350) are PKA binding proteins (*Figure 5.3*). On the other hand, co-immunoprecipitation data suggest IP3R1-Yotiao interaction (*Figure 5.4*). Although the comparative levels of the three AKAP9 isoforms have not been quantified thus far, it could be speculated that the relatively lower abundance of AKAP450 could explain the absence of band corresponding to its molecular weight in *Figure 5.4*. Also, the poor reagent quality limits further experimental analysis. Nevertheless, the results from *Figure 5.3* show the association between PKA-AKAP9. This is in parallel with findings showing the presence of PKA-binding domain on AKAPs (Gold et al. 2006; Carr et al. 1991; Herberg et al. 2000).

In addition to these findings, we have already shown an association between PKA and IP$_3$R1 (*Figure 4.9*). Considering both these results, the existence of IP$_3$R1-PKA-AKAP9 macromolecuar signalling complex in platelets can be suggested, as is shown in other cell

types (Tu et al. 2004; Collado-Hilly & Coquil 2009). Furthermore, AKAP9 has been shown to be associated with IP$_3$R1 in platelets (*Figure 5.4*) and brain cells. IP$_3$R1 interacts with AKAP9 via leucine/isoleucine zipper (*LIZ*) motifs present in the IP$_3$R1 coupling domain and the *LIZ* motifs on AKAP9. Moreover, of the three subtypes of IP$_3$R, AKAP9 interacts with IP$_3$R1 only (Tu et al. 2004).

Having suggested the presence of IP$_3$R1-PKA-AKAP9 complex in platelets, it was essential to understand its functional importance in platelets. To achieve this, cell permeable synthetic peptide, St-Ht31 was used. Computer-aided analysis of the secondary structure of RII-binding human thyroid protein recognised a 14 amino acid region which could potentially form the amphiphatic helix (Carr et al. 1992; Carr et al. 1991; Herberg et al. 2000). Peptides corresponding to this region of Ht31 can compete for the binding site to PKA regulatory subunit and disrupt PKA-anchoring to cells, therefore compromising substrate phosphorylation (Carr et al. 1991; Colledge et al. 1999). The control peptide, St-Ht31P on the other hand contains two isoleucine to proline substitutions (I502P, I507P) which alters the helical structure of the peptide and abolishes binding to the regulatory subunits of PKA, therefore it does not interfere with PKA–AKAP binding (Carr et al. 1991; Colledge et al. 1999, Leray 2012; Goueli & Hsaio, 2000). Since St-Ht31 competes with the AKAP in binding to PKA, it is important to get the correct balance between the peptide and PGI$_2$ in order to notice the effects of St-Ht31 treatment. In addition to this, the challenges of working with St-Ht31/St-Ht31P are well recognised. For these reasons the concentration of St-Ht31 and PGI$_2$ were optimised using established markers of phosphorylation, pPKAs and pVASP antibodies (*Figure 5.5 - 5.6a*). However, on extrapolating these conditions to IP$_3$R1, no effect of St-Ht31 on IP$_3$R1 phosphorylation response was observed (*Figure 5.6b*). It is essential to appreciate that, although the concentration of the peptide remains the same, different substrates may react differently to St-Ht31 treatment. This suggests that the affinity of PKA-AKAP interaction is perhaps determined by the functional role of the substrate. We speculate that substrates such as IP$_3$R1 that are central to the calcium signalling pathways and therefore platelet function, could possibly be more tightly associated with the PKA-AKAP complex. This could perhaps be the reason why St-Ht31 at the concentration used was unable to disrupt the spatial regulation of PKA-mediated IP$_3$R1 phosphorylation enough to notice a significant effect. On the other hand, an effect was noticed on the PKA-mediated

phosphorylation of VASP. Again, this leads us to hypothesise that PKA-AKAP-VASP interaction may be weaker as compared to that of PKA-AKAP-IP_3R1. Alternatively, the accessibility of the disruptor peptide also determines the extent to which it would compete for the AKAP-binding site on PKA. Considering the subcellular location of IP_3R1 on the ER, it was hypothesised that perhaps St-Ht31 was not being able to access the PKA-AKAP associated with it. Also, St-Ht31 could possibly be confined to inclusion bodies in the cell on being uptaken and not be localised at its site of action (Ma et al, 2010).

To try and circumvent this issue, the platelets were permeabilised using ionic detergent, digitonin. Digitonin complexes with the membrane cholesterol to permeabilise the membranes, however the challenges involved with detergent-induced cell permeabilisation are well recognised. For example, it has been suggested that at higher concentration or if the contact is prolonged, the non-ionic detergent can permeablise the intracellular membranes along with the plasma membrane (Ahnert-Hilger & Gratzl 1988). This could compromise the cell function. Therefore, a complete characterisation of permeabilisation protocol was performed. Firstly, the ability of digitonin to permeabilise the platelets in a concentration and temporal manner was tested using alkaline phosphotase assay (*Figure 5.7*). The assay was based on the premise that the cytosolic alkaline phosphate would leak out upon permeabilisation, which could be detected as a colour change on the addition of phosphatase substrate. Data showed the digitonin permeabilised the platelets, and a concentration of 2μM digitonin for 10 minutes was sufficient to permeabilise the platelets optimally since (*Figure 5.7*), functional integrity of platelets was maintained (*Figure 5.8*). Suggestions of protein leakage from permeabilised platelets have also been made (Ahnert-Hilger & Gratzl 1988), this too was tested using western blotting. It was found that at the concentration of digitonin used for these experiments did not compromise the integrity of cAMP signalling components. Furthermore, the ability of PKA to phosphorylate IP_3R1 at ser1756 in permeabilised platelets was also tested. This was essential since one would assume that like alkaline phosphatase leakage from permeabilised cells, ATP, which is a key to phosphorylation, would also leak out from permeabilised platelets therefore compromising the phosphorylation of substrates. Nevertheless, the data (*Figure 5.9*) indicate that the cAMP signalling machinery is intact even in permeabilised platelets.

Measuring the ATP levels in before studying signalling pathways in permeabilised platelets would shed more light on the substrate phosphorylation dynamics in permeabilised cells.

Next, IP_3R1 phosphorylation in permeabilised platelets pre-treated with St-Ht31 was studied, however even in permeabilised platelets St-Ht31 treatment failed to alter IP_3R1 phosphorylation (*Figure 5.10*). Having said that, a noticeable difference in VASP phosphorylation at ser157 was observed on St-Ht31 treatment. This suggests that perhaps our previous hypothesis of St-Ht31 being unable to access IP_3R1 still holds true. Due to the inconsistencies and the well-known challenges associated with using PKA-AKAP disruptor peptides, we chose not to pursue this any further.

Consequently, instead of focusing the effect of St-Ht31 treatment on substrate phosphorylation, the effect of disruption of PKA-AKAP interaction on Ca^{2+} mobilisation was studied. Ca^{2+} mobilisation was studied in Fura-2 labelled platelets were pre-treated with St-Ht31/St-Ht31P. On stimulation with thrombin, there was a rapid mobilisation of Ca^{2+}, which was blunted on treatment with PGI_2. This shows that in the absence of PGI_2, IP_3R1 is not phosphorylated, therefore can facilitate the mobilisation of Ca^{2+}. However, PGI_2-treatment causes PKA-mediated phosphorylation of IP_3R1. Phosphorylation of IP_3R1 is reported to be inhibitory (Cavallini et al. 1996), therefore blunting the extent of Ca^{2+} mobilisation. It is also essential to value the role of AKAPs in spatial localisation of PKA in the proximity of IP_3R1. Hypothetically, St-Ht31 should competitively delineate the interaction between PKA-AKAP. This means that PKA is now unable to phosphorylate the IP_3R1, therefore the Ca^{2+} mobilisation response should mimic that seen on thrombin treatment (*Figure 5.11*). Although a marginal recovery of Ca^{2+} response was seen on St-Ht31 treatment, it was not significant. The very similar effects of St-Ht31 and the control peptide St-Ht31P, could suggest this to be a consequence of membrane-disruption and not especially as a result of disruption of PKA/AKAP interaction. It is also possible that the concentration of St-Ht31/St-Ht31P used for this assay could be restrictive. Also, it should be appreciated that St-Ht31 is a generic PKA-AKAP disruptor peptide, which means it could compete with the PKA-AKAP complexes that it first interacts with. This could perhaps mean that it is more effective at disrupting membrane-bound PKA-AKAP complexes. The subcellular location of IP_3R1 on the DTS, could perhaps make the complex inaccessible to St-Ht31, therefore limiting its effects. The AKAP field in platelets is still in its infancy, therefore not much research evidence is

available to fully understand these mechanisms. However, in the future the use of alternative PKA-AKAP disruptor peptides such as *SuperAKAP* and RIAD could be attempted. *SuperAKAP* specifically delineates the interaction between AKAP and PKA II, whereas RIAD interferes with AKAP-PKA I interactions (Gold et al. 2011; Carlson et al. 2006). Attempts can also be made to perhaps use these peptides could also perhaps be used in combination. In addition to this, the use of new generation of peptides known to be more specific to PKA I should also be considered (Wang et al. 2015).

To summarise, this chapter validates the presence of AKAP9 in platelets. The presence of IP_3R1-PKA-AKAP9 complex in platelets was also shown. Although attempts were made to delineate the PKA-AKAP interaction, the tools available were restrictive.

CHAPTER VI: GENERAL DISCUSSION

6.1. Discussion

Cellular response and processing of extracellular signals is crucial to cell survival and function. Although there are a wide range of stimuli and cell surface receptors, the multiplicity of signalling molecules is processed by a limited number of signalling pathways. The cAMP signalling pathway is a one such regulatory pathway, which is ubiquitous in mammalian cells. This pathway involves enzymes that synthesise, propagate and terminate cAMP signalling, with the specificity of cellular effects coordinated through a group of scaffolding proteins called AKAPs. Significantly aberrant cAMP signalling is implicated in cancers (Radivojac et al. 2008; Almeida & Stratakis 2011), genetic diseases (Cohen 2001) such as autosomal recessive cytosolic phospholipase A_2 deficiency, P_2Y_{12} deficiency (Freson et al. 2014), and other age-related diseases (Mattson, 2004). Furthermore, platelets from patients with schizophrenia (Tardito et al. 2000) and panic disorders (Tardito et al. 2002) also display dysfunctional PKA signalling. In the context of the work presented in this thesis, dysfunctional cAMP signalling causes cardiovascular disease-associated platelet hyperactivity (Mueller et al. 1986).

It is well recognised that agonist-induced elevations in intracellular Ca^{2+} is a hallmark of platelet activation. This occurs primarily through the mobilisation of Ca^{2+} from intracellular stores (such as DTS) via IP_3R, a Ca^{2+}-release channel (Varga-Szabo et al. 2009). The cAMP signalling pathway is thought to downregulate the bioavailability of platelet intracellular Ca^{2+} by phosphorylating IP_3R and blunting its activity (Quinton & Dean 1992) and thereby contributing to the inhibition of platelet activation (Cavallini et al. 1996). The work described in this thesis examined the spatiotemporal regulation of cAMP pathway in platelets, with a particular focus on IP_3R1 as a substrate for cAMP signalling.

In other cell types, cAMP-signalling is mediated through both Epac (de Rooij et al. 1998) and PKA (Hayes & Mayer 1981). In contrast in platelets, PKA isoforms are the sole effectors of this pathway (Schwarz et al. 2001). This means that in platelets, PKA-mediated substrate phosphorylation can be recognised as the definitive end-point of cAMP pathway activation. The work described in this thesis was performed exclusively using human platelets. While PKA knock-out mice as a tool to study cAMP signalling was initially considered, however

platelet-specific PKA knock out mice are not available. Furthermore, the peri-natal viability of mice lacking the gene for PKA catalytic or regulatory subunits is compromised making them unsuitable for use in platelet studies (Kirschner et al. 2009), thus limiting us to the use of human platelets. Employing Western blotting and using physiological activator of cAMP pathway, PGI_2, we showed a time and concentration-dependent phosphorylation of several PKA substrates in human platelets (*Figure 3.2*). In retrospect, measurement of cAMP levels in response to PGI_2 treatment would aid the understanding of how cAMP levels alter in response activation of platelet inhibitor pathways. Furthermore, these can be correlated to substrate phosphorylation and platelet aggregation under similar treatment conditions. These data would have further strengthened the above described findings. Nevertheless, PGI_2-mediated activation of PKA correlated with inhibition of platelet function (*Figure 3.1*), therefore confirming that activation of cAMP pathway has inhibitory effects on platelet function. These findings are in parallel with the previous reports (Ehrman & Jaffe 1980; Higgs et al. 1997).

One of the key mechanisms by which cAMP pathway blunts platelet activation is thought to be the PKA-mediated phosphorylation of intracellular Ca^{2+} release channel, IP_3R1 (Quinton & Dean 1992; Cavallini et al. 1996; El-daher et al. 2000). The importance of Ca^{2+} mobilisation through IP_3R function was further explored by pharmacological inhibition of IP_3R. Heparin is a commonly used IP_3R blocker, but it is also known to uncouple G-protein signalling (Jonas et al. 1997). For this reason heparin was eliminated as the IP_3R antagonist of choice. Another compound, Xestospongin is a potent IP_3R antagonist, however, its slow mode of action and inconsistent results (Gafni et al. 1997) made interpretation of its effects difficult. Therefore, a low-cost membrane permeable compound, 2-APB was our antagonist of choice. 2-APB is a non-specific IP_3R antagonist, and is known to interfere with SOCE and antagonise TRP channels. Some reports have suggested 2-APB to be inconsistent at blocking IP_3-induced Ca^{2+} release, but its pharmacological effects are known to be specific to each cell type. Studies have shown 2-ABP to be consistent in antagonising IP_3-induced Ca^{2+} release in platelets (Maruyama et al. 1997; Dobrydneva & Blackmore 2001) in the concentration range of 1-100μM (Bootman et al. 2002). In the present study, we show that pharmacological blockade of IP_3R using 2-ABP blunts Ca^{2+} mobilisation (*Figure 4.3*) and platelet aggregation response (*Figure 4.4*). These data reflect the importance of IP_3-

mediated Ca^{2+} mobilisation on platelet function. A limitation of this approach, however is that the antagonists are not specific to the IP_3R sub-type. A number of options were considered to try and focus on a single subtype. As detailed in Authi *et al*'s work, an alternative approach where exogenous IP_3 is used to study aggregation (Authi et al. 1986) and TxB_2 formation (Authi et al. 1987) could have been adopted. Alternatively, the use of IP_3R knock-out mice was also considered. However, due to the abundance of IP_3R1 in the brain, elimination of this gene is embryonically lethal, making these unsuitable for use with regards to this project. However IP_3R2 and IP_3R3 knock-out mice survive (Patterson et al. 2004). Nevertheless, here using a holistic approach, we showed the importance of IP_3R receptor activity in platelet function.

Transcriptomics studies show the presence of all three IP_3R isoforms in platelets (Rowley et al. 2011). Furthermore, using highly purified platelet membranes, El-daher *et al* not only show the presence of all three IP_3R subtypes in platelets, but also suggest these subtypes to undergo differential phosphorylation in response to PKA activation (El-daher et al. 2000). We successfully validated the presence of all three IP_3R subtypes in platelets (*Figure 4.5*), but we specifically focused on the characterisation of PKA-mediated IP_3R1 phosphorylation at ser1756 using site-specific antibody ($pIP_3R1^{Ser1756}$). This is primarily because IP_3R1 is reported to be the predominant subtype present in platelets (Varga-Szabo et al. 2009). There are two serine sites on IP_3R1, ser1589 and ser1756, that can undergo PKA phosphorylation in brain, however ser1756 was the predominant site for PKA-mediated phosphorylation (Danoff et al. 1991; Krizanova & Ondrias 2003). This makes phosphorylation at ser1756 a crucial regulator of channel activity. It is for this reason; we focused our attention to characterisation of PKA-mediated phosphorylation at IP_3R1 ser1756. Using PGI_2 (*Figure 4.6-4.7*) and isolating various components of cAMP pathway using pharmacological compounds (*Figure 4.8*), we show for that IP_3R1 is direct a substrate for cAMP signalling and is targeted by a PKA isoform. Although IP_3R1 has been previously reported as a substrate for PKA (Ferris et al. 1991), we for the first time perform a full characterisation of phosphorylation at ser1756 in platelets.

We next wished to determine the physiological importance of the phosphorylation event. Using exogenous IP_3 in permeabilised platelets, Cavallini *et al* show PGI_2 counteracts the IP_3-induced elevation in Ca^{2+} mobilisation, therefore suggesting that IP_3R phosphorylation

modulates the channel opening, and limits the release of Ca^{2+} from DTS (Cavallini et al. 1996). This is an elegant approach whereby thapsigargin was used to inhibit SERCA, which means that Ca^{2+} measurements were exclusively due to IP_3R channel opening. We attempted to replicate this experimental approach under the guidance of Prof. Martyn Mahaut-Smith (University of Leicester, UK). However, we were unable to reproduce previous studies. Cavallini *et al* performed experiments using Indo-1-labelled platelets, whereas we attempted to label platelets using Fura-2 dyes; albeit both belong to the group of ratiometric Ca^{2+} indicators. Both the approaches differed in the choice of detergent for platelet permeabilisation too. We used digitonin which complexes with membrane cholesterol to permeabilise the platelets, as opposed to saponin which complexes with saccharides (Ahnert-Hilger & Gratzl 1988). In both the studies D-myo-IP_3 was used to trigger IP_3R activation. However, even after repeated attempts we were unable to detect any alternations in Ca^{2+} levels. To make progress in this direction, an alternative holistic approach was adopted whereby Ca^{2+} mobilisation was measured in Fura-2-labelled washed platelet suspension. This approach was based on the premise that DTS is the largest store of intracellular Ca^{2+} and IP_3R is the primary Ca^{2+} release channel on DTS (Varga-Szabo et al. 2009), which means that IP_3 produced as a result of thrombin-induced platelet activation would bind IP_3R. Ligand binding should activate IP_3R and cause channel opening, through which Ca^{2+} from DTS would be released. Using this approach, we showed that PGI_2-treatment caused a reduction in Ca^{2+} mobilisation in response to thrombin (*Figure 4.1-4.2*). These findings are in parallel with the previously published work in cerebellar cells (Supattapone et al. 1988) and platelets (Quinton & Dean 1992; Cavallini et al. 1996). It is interesting to note that physiological concentrations, PGI_2 modulates Ca^{2+} mobilisation but does not block it. A complete blockade of Ca^{2+}-mobilisation in response to IP_3R phosphorylation could compromise the activity of a multitude of other platelet signalling pathways regulated by Ca^{2+}. Therefore, we speculate that PKA-phosphorylation mediated modulation of Ca^{2+} release through IP_3R to be an evolutionary mechanism to protect the integrity of platelet signalling pathways.

In the next part of the study we begin to examine the molecular mechanism that allows cAMP signalling to target IP_3R1. Using protein enrichment and co-immunoprecipitation approach, we suggest IP_3R1 could be associated with both PKA I and PKA II (*Figure 4.9* –

4.10). These findings are novel with regards to platelets and suggest towards spatial regulation of PKA signalling. It is essential to appreciate that whilst PKA I is concentrated the cytosol, PKA II is membrane-bound (Skalhegg & Tasken 2000). It should also be recognised that there are two PKA phosphorylation sites on IP_3R1 – ser1589 and ser1756 (Ferris et al. 1991). It can be speculated that perhaps one isoform of PKA phosphorylates the predominant site of ser1756, whereas the other phosphorylates the ser1589 site. However, this is merely a speculation as phospho-specific antibody towards IP_3R1 Ser1589 was unavailable to test this hypothesis. Alternatively, considering the vital regulatory role of IP_3R1 in Ca^{2+} homeostasis, the idea that both PKA isoforms contribute towards ser1756 phosphorylation should not be ignored. PKA I and PKA II respond differently to localised elevation in cAMP (Skalhegg & Tasken 2000). Association of IP_3R1 with both PKA I and PKA II could therefore be a mechanism to control IP_3R1 phosphorylation in response to activation of both the PKA isoforms. Perhaps, this could therefore be a physiological fine-tuning mechanism to ensure appropriate Ca^{2+} response to localised elevation in cAMP levels. The association between IP_3R1 and PKA II has been previously reported in brain cells (Collado-Hilly & Coquil 2009), but that of IP_3R1-PKA I has not. It is vital to recognise that the strength of these findings is dependent on the specificity of the antibodies in question. Ideally, using LC/MS/MS the precise identity of IP_3R binding proteins can be revealed. To achieve this, the IP_3R1 immunoprecipitates should be subjected to 2-D gel electrophoresis, the bands corresponding to the molecular weights of interest be excised, melted and subsequently analysed using LC/MS/MS. In addition to this, the strength of the IP_3R1-PKA interaction and the proximity of the two proteins also remain to be determined. Ideally, this could be studied using the proximity ligation assay. This assay identifies the cellular localisation and interactions between the proteins of interest.

The compartmentalisation of PKA signalling is regulated by AKAPs. Although over 50 AKAPs have been identified so far, we focused our attention towards AKAP9. This is because previous research has shown an association between IP_3R1 and AKAP9 (Tu et al. 2004; Collado-Hilly & Coquil 2009). However, due to the limitation of the antibodies available, we were unable to conclusively show the presence of AKAP9 in platelets (*Figure 5.1 – 5.2*). Although it is noteworthy that AKAP9 had been identified in platelet transcriptomics study and gave us the confidence in pursuing it further. Furthermore, AKAP9 was also detected by

LC/MS/MS in a study investigating all the PKA-binding proteins in platelets (Rowley et al. 2011; Margarucci et al. 2011). Using co-immunoprecipitation (*Figure 5.4*) and PKA-binding protein enrichment (*Figure 5.3*), we speculate the presence of IP_3R1-PKA-AKAP9 complex in platelets, although we cannot conclusively determine its presence owing to the challenges with detecting AKAP9 in platelets. Next, we tested the hypothesis that, PKA-AKAP disruptor peptides should disrupt the PKA-AKAP association and consequently lead to a loss of spatial regulation of PKA activity. Firstly, the effect lack of compartmentalisation of PKA signalling on IP_3R1 phosphorylation was tested, using St-Ht31. Whilst the effect of PGI_2 on IP_3R1 phosphorylation were not compromised, that on PGI_2-induced VASP phosphorylation was (§5.4). This suggests that the affinity of PKA-AKAP interaction could perhaps be determined by the functional role of the substrate. Also, the suggestion that two PKA isoforms target the phosphorylation of IP_3R1 (*Figure 4.9 – 4.10*) further supports this theory. We speculate that perhaps due to the functional importance of IP_3R, the affinity of PKA-AKAP interaction associated with IP_3R1 is perhaps stronger than that in PKA-AKAP-VASP macromolecular complex.

The effect of St-Ht31 treatment on Ca^{2+} mobilisation in suspension was also studied using Fura-2 labelled platelets. We tested the hypothesis that St-Ht31-induced loss of spatial regulation of PKA should revert the inhibitory effect of PGI_2 on Ca^{2+} mobilisation through IP_3R. Here, we show that pre-treatment with St-Ht31 compromises the effect of PGI_2 on Ca^{2+} mobilisation; albeit only partially (*Figure 5.11*). Although St-Ht31 is widely marketed as a generic PKA-AKAP disruptor, it has an affinity towards delineation of AKAP interaction with RII (Gold et al. 2006). In hindsight, the use of an alternative PKA-AKAP disruptor peptide, RIAD could not have gone amiss. RIAD interferes with the RI-AKAP interaction (Gold et al. 2006). Furthermore, owing to the challenges associated with disruption of PKA-AKAP complex, the use of these peptides in combination could also have been explored.

6.2. Future Work

The key findings from this work provide an insight into spatiotemporal regulation of cAMP pathway, further work is required to gain an in-depth understanding of the same and answer the unanswered questions as outlined below –

- *Use of exogenous IP_3 to study platelet shape change and aggregation*
  Previous research has shown saponin-permeabilised platelets to undergo aggregation (Authi et al. 1986; Watson et al. 1986) and formation of platelet eicosanoids such as TxB_2 (Authi et al. 1987) in response to exogenous IP_3. In the context of this work, platelet aggregation and shape change should be measured in response to exogenous IP_3 in digitonin permeabilised platelets. The findings described in this thesis suggest that the pharmacological blockade of IP_3R using 2-ABP compromises platelet aggregation and Ca^{2+} mobilisation. Not only should these findings be tested using exogenous IP_3, but also physiological and pharmacological activators of cAMP pathway should be employed to understand the functional consequence of IP_3R1 phosphorylation.

- *Successful identification of the presence of IP_3R1-PKA-AKAP complex in platelets*
  The results discussed in this thesis suggest towards the presence of IP_3R1-PKA-AKAP complex in platelets. However, due to limitations of the antibodies in question we were unable to pursue it further. Nevertheless, to conclusively identify this macromolecular complex in platelets, data from the steps discussed below should be analysed in combination -

  - Using PKA enrichment approach, the PKA binding proteins can be precipitated and analysed using Mass Spectrometry as described by Burkart *et al* (Burkhart et al. 2014). This would suggest if proteins corresponding to the *m/z* ratio of IP_3R1 and AKAP9 are associated with PKA. Additionally, other potential PKA-binding proteins such as PDEs and phosphatases can also be identified.
  - To identify the association between IP_3R1 and PKA, the two proteins be isolated using immunoprecipitation. These can then be subjected to 2D gel electrophoresis. The bands corresponding to the protein of interest can be excised and subjected

to LC/MS/MS analysis. LC/MS/MS analysis identifies a particular *m/z* ratio, which means that the protein of interest can be conclusively identified.

- To identify the AKAP of interest, the eluates from IP_3R1 and PKA immunoprecipitation can be subjected to RII overlay assay. This is a well-established protocol to identify AKAPs (Carr & Scott 1992). Using this approach all the potential AKAPs binding to IP_3R1 and PKA can be identified.
- Finally, using PLA assay and confocal microscopy, the localisation of proteins of interest should be performed.

- *Use alternative AKAP-PKA disruptor peptides to understand the consequence of PKA-AKAP complex disruption on the function of IP_3R*

  The work described in this thesis was limited to the use of St-Ht31 to delineate the PKA-AKAP interaction, however the use of alternative traditional disruptor peptides such as RIAD and SuperAKAP should also be explored. Furthermore, the use of these peptides in combination with each other should also be attempted. What's more, the use of new generation high affinity AKAP-PKA disruptor peptides such as RI-STapled Anchoring disruptors (RI-STADs) should also be considered. These peptides are cell-permeable and are reported to specifically interfere with PKA I-mediated phosphorylation (Wang et al. 2015). The use of these peptides will not only enable understand the functional consequence of PKA-AKAP complex disruption, but also help recognise the importance specific PKA isoforms in protein macromolecular complexes.

6.3 Conclusion

To summarise, here we show the activity of PKA signalling pathway in platelets, and provide robust evidence to the PKA-mediated phosphorylation of IP_3R1. The possible association of IP_3R1 with PKA I and PKA II was also explored. PKA-mediated phosphorylation was suggested to compromise Ca^{2+}-mobilisation through IP_3R. We speculate this to be a consequence of spatial regulation of PKA signalling, mediated by the possible presence of IP_3R1-PKA-AKAP complex in platelets. On disruption of this complex using peptides, the restraining effect of PGI_2 on Ca^{2+}-release through IP_3R1 was partially reverted (*Figure 6.1*). However, more work is needed to conclusively identify this complex and understand its functional significance.

Figure 6.1

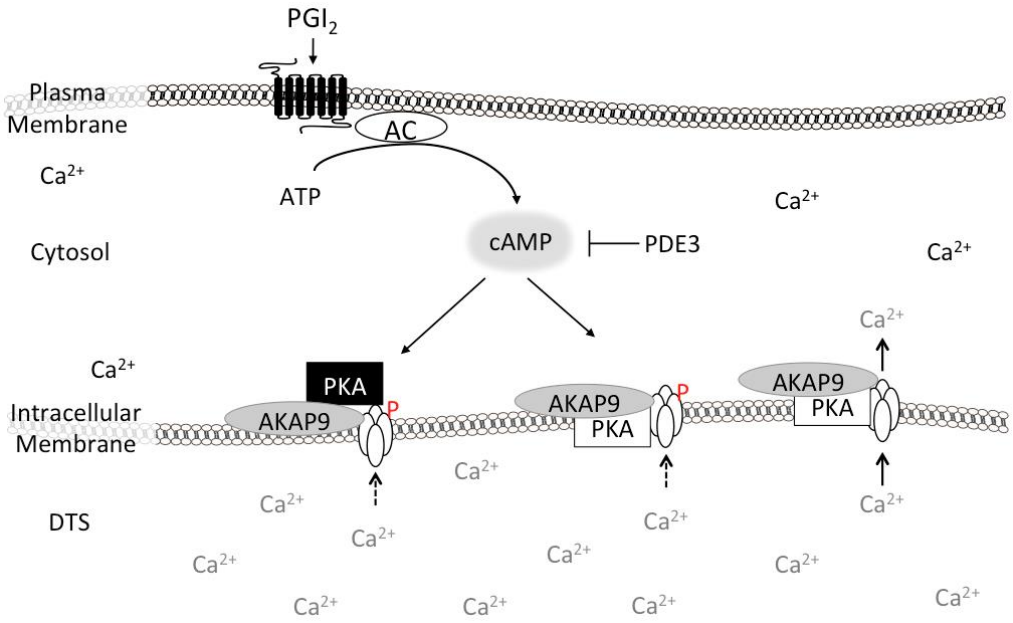

***Figure 6.1* – A hypothetical model of Ca^{2+} mobilisation in platelets based on the findings described in this thesis**

PGI_2 binds IP receptor and activates AC. Activated AC can hydrolyse ATP to form of cAMP. cAMP can in turn bind and activate the cytosolic PKA I (shown as black rectangle) and membrane bound PKA II (shown as white rectangle). Activated PKA can phosphorylate substrates such as IP_3R1, located on the intracellular membrane of DTS, a store of intracellular Ca^{2+}. IP_3R1 and PKA are suggested to be in a complex, with AKAP9, which is suggested to regulate PKA in a spatial manner. PKA-mediated phosphorylation blunts the Ca^{2+} mobilising ability of IP_3R1. However, more work is required to conclusively identify this macromolecular complex and understand its functional importance.

CHAPTER VII: REFERENCES

Aburima, A, Wraith, K. S., Raslan, Z., Law, R., Magwenzi, S. & Naseem, K. M. 2013. cAMP signaling regulates platelet myosin light chain (MLC) phosphorylation and shape change through targeting the RhoA-Rho kinase-MLC phosphatase signalling pathway. Blood, 122, 3533-45.

Ahnert-Hilger, G. & Gratzl, M., 1988. Controlled manipulation of the cell interior by pore-forming proteins. Trends in pharmacological sciences, 9(6), pp.195–7.

Akopov, S., Darbinian, V., Grigorian, G., Kosyan, A., Gabrielian, E., 1993. Elevated velocity of prostacyclin degradation in blood as a possible risk factor in patients with cerebrovascular disorders. European neurology, 33(3), pp.252–5.

Almeida, M.Q. & Stratakis, C.A., 2011. How does cAMP/protein kinase A signaling lead to tumors in the adrenal cortex and other tissues? Molecular and cellular endocrinology, 336(1-2), pp.162–8.

Altschuler, D. & Lapetina, E.G., 1993. Mutational analysis of the cAMP-dependent protein kinase-mediated phosphorylation site of Rap1b. The Journal of biological chemistry, 268(10), pp.7527–31.

Anon, Protein Phosphorylation in Aging and Age-Related Disease | 978-0-444-51583-4 | Elsevier.

Armstrong, R.A., 1996. Platelet prostanoid receptors. Pharmacology & therapeutics, 72(3), pp.171–91.

Artymiuk, P.J., Poirrette, A. R., Rice, D. W., and Willett, P., 1997. A polymerase I palm in adenylyl cyclase? Nature, 388(6637), pp.33–4.

Aszódi, A., Pfeifer, A., Ahmad, M., Glauner, M., Zhou, X. H., Ny, L., Andersson, K. E., Kehrel, B., Offermanns, S., Fässler, R., 1999. The vasodilator-stimulated phospho-protein (VASP) is involved in cGMP- and cAMP-mediated inhibition of agonist-induced platelet

aggregation, but is dispensable for smooth muscle function. The EMBO journal, 18(1), pp.37–48.

Authi, K. S., Hornby, E. J., Evenden, B. J., Crawford, N., 1987. Inositol 1,4,5-trisphosphate (IP3) induced rapid formation of thromboxane B2 in saponin-permeabilised human platelets: mechanism of IP3 action. FEBS letters, 213(1), pp.95–101.

Authi, K. S., Bokkala, S ., Patel, Y., Kakkar, V. V., Munkonge, F., 1993. Ca2+ release from platelet intracellular stores by thapsigargin and 2,5-di-(t-butyl)-1,4-benzohydroquinone: relationship to Ca2+ pools and relevance in platelet activation. The Biochemical journal, 294(1), pp.119–26.

Authi, K.S., 2007. TRP channels in platelet function. Handbook of experimental pharmacology, (179), pp.425–43.

Authi, K.S., 2009. Orai1: a channel to safer antithrombotic therapy. Blood, 113(9), pp.1872–3.

Authi, K.S., Evenden, B.J. & Crawford, N., 1986. Metabolic and functional consequences of introducing inositol 1,4,5-trisphosphate into saponin-permeabilized human platelets. The Biochemical journal, 233(3), pp.707–18.

Aye,T. T., Mohammed, S., van den Toorn, W. P. H., van Veen, T. A. B., van der Heyden, M. A. G., Scholten, A., Heck, A. J. R., 2009. Selectivity in Enrichment of cAMP-dependent Protein Kinase Regulatory Subunits Type I and Type II and Their Interactors Using Modified cAMP Affinity Resins, Mol Cell Proteomics. 8(5): 1016–1028.

Baillie, G.S., Scott, J.D. & Houslay, M.D., 2005. Compartmentalisation of phosphodiesterases and protein kinase A: opposites attract. FEBS letters, 579(15), pp.3264–70.

Banky, P., Huang, L.J. & Taylor, S.S., 1998. Dimerization/docking domain of the type I alpha regulatory subunit of cAMP-dependent protein kinase. Requirements for dimerization and docking are distinct but overlapping. The Journal of biological chemistry, 273(52), pp.35048–55.

Bauer. M., Retzer, M., Wilde, J.I., Maschberger, P., Essler, M., Aepfelbacher, M., Watson, S.P., Siess, W. 1999, Dichotomous regulation of myosin phosphorylation and shape change by Rho-kinase and calcium in intact human platelets. Blood. 94:1665–72.

Beck, F., Burkhart, J., Geiger, J. M., Zahedi, R. P., Sickmann, A., 2012. Robust workflow for iTRAQ-based peptide and protein quantification. Methods in molecular biology (Clifton, N.J.), 893, pp.101–13.

Bender, A.T. & Beavo, J.A., 2006. Cyclic nucleotide phosphodiesterases: molecular regulation to clinical use. Pharmacological reviews, 58(3), pp.488–520.

Bennett, J. S., Zigmond, S., Vilaire, G., Cunningham, M. E., Bednar, B., 1999. The platelet cytoskeleton regulates the affinity of the integrin alpha(IIb)beta(3) for fibrinogen. The Journal of biological chemistry, 274(36), pp.25301–7.

Berg, L. P., Shamsher, M. K., El-Daher, S. S., Kakkar, V. V., Authi, K S., 1997. Expression of human TRPC genes in the megakaryocytic cell lines MEG01, DAMI and HEL. FEBS letters, 403(1), pp.83–6.

Berridge, M.J., Bootman, M.D. & Roderick, H.L., 2003b. Calcium signalling: dynamics, homeostasis and remodelling. Nature reviews. Molecular cell biology, 4(7), pp.517–29.

Bird, G.S., Aziz, O., Lievremont, J. P., Wedel, B., Trebak, M., Vazquez, G., Putney, J. W., 2004. Mechanisms of phospholipase C-regulated calcium entry. Current molecular medicine, 4(3), pp.291–301.

Blake, R. A., Schieven, G. L. & Watson, S. P. 1994. Collagen stimulates tyrosine phosphorylation of phospholipase C-gamma 2 but not phospholipase C- gamma 1 in human platelets. FEBS Lett, 353, 212-6.

Bley, K.R., Bhattacharya, A., Daniels, D. V., Gever, J., Jahangir, A., O'Yang, C., Smith, S., Srinivasan, D., Ford, A. P. D. W., Jett, M.F., 2006. RO1138452 and RO3244794: characterization of structurally distinct, potent and selective IP (prostacyclin) receptor antagonists. British journal of pharmacology, 147(3), pp.335–45.

Boehning, D. & Joseph, S.K., 2000. Functional properties of recombinant type I and type III inositol 1, 4,5-trisphosphate receptor isoforms expressed in COS-7 cells. The Journal of biological chemistry, 275(28), pp.21492–9.

Boehning, D., Mak, D. O., Foskett, J. K., Joseph, S. K., 2001. Molecular determinants of ion permeation and selectivity in inositol 1,4,5-trisphosphate receptor Ca2+ channels. The Journal of biological chemistry, 276(17), pp.13509–12.

Bootman, M.D. & Lipp, P., 1999. Calcium signalling : Ringing changes to the " bell-shaped curve ." , pp.876–878.

Bootman, M. D ., Collins, T. J., Mackenzie, L., Roderick, H. L., Berridge, M. J., Peppiatt, C. M., 2002. 2-aminoethoxydiphenyl borate (2-APB) is a reliable blocker of store-operated Ca2+ entry but an inconsistent inhibitor of InsP3-induced Ca^{2+} release. FASEB journal : official publication of the Federation of American Societies for Experimental Biology, 16(10), pp.1145–50.

Booyse, F. M., Marr, J., Yang, D. C., Guiliani, D. & Rafelson, M. E., jr. (1976). Adenosine cyclic 3',5'-monophosphate-dependent protein kinase from human platelets. Biochim Biophys Acta, 422, 60-72.

Born, G. V. 1962. Aggregation of blood platelets by adenosine diphosphate and its reversal. Nature, 194, 927-9.

Born, G. V., Dearnley, R., Foulks, J. G. & Sharp, D. E. 1978. Quantification of the morphological reaction of platelets to aggregating agents and of its reversal by aggregation inhibitors. J Physiol, 280, 193-212.

Brass, L.F., Zhu, L. & Stalker, T.J., 2008. Novel therapeutic targets at the platelet vascular interface. Arteriosclerosis, thrombosis, and vascular biology, 28(3), pp.s43–50.

Braun, A., Varga-Szabo, D., Kleinschnitz, C., Pleines, I., Bender, M., Austinat, M., Bösl, M., Stoll, G., Nieswandt, B., 2009. Orai1 (CRACM1) is the platelet SOC channel and essential for pathological thrombus formation. Blood, 113(9), pp.2056–63.

Briggs, C., Harrison, P. & Machin, S. J. 2007. Continuing developments with the automated platelet count. Int J Lab Hematol, 29, 77-91.

Brownlow, S.L. & Sage, S.O., 2005. TRPC subunit assembly and membrane distribution in human platelets. Thrombosis and Haemostasis, 94(4), pp.839–45.

Bult, H., Fret, H. R., Van den Bossche, R. M., Herman, A. G., 1988. Platelet inhibition by endothelium-derived relaxing factor from the rabbit perfused aorta. British journal of pharmacology, 95(4), pp.1308–14.

Burgess, G. M., Bird, G. S., Obie, J. F., Putney, J. W., 1991. The mechanism for synergism between phospholipase C- and adenylyl cyclase-linked hormones in liver. Cyclic AMP-dependent kinase augments inositol trisphosphate-mediated Ca2+ mobilization without increasing the cellular levels of inositol polyphosphates. The Journal of biological chemistry, 266(8), pp.4772–81.

Burkhart, J. M., Gambaryan, S., Watson, S. P., Jurk, K., Walter, U., Sickmann, A., Heemskerk, J. W. M., Zahedi, R. P., 2014. What can proteomics tell us about platelets? Circulation research, 114(7), pp.1204–19.

Butt, E., Immler, D., Meyer, H. E., Kotlyarov, A., Laass, K., Gaestel, M., 2001. Heat shock protein 27 is a substrate of cGMP-dependent protein kinase in intact human platelets: phosphorylation-induced actin polymerization caused by HSP27 mutants. The Journal of biological chemistry, 276(10), pp.7108–13.

Calderwood, D.A., Shattil, S.J. & Ginsberg, M.H., 2000. Integrins and actin filaments: reciprocal regulation of cell adhesion and signalling. The Journal of biological chemistry, 275(30), pp.22607–10.

Canaves, J.M. & Taylor, S.S., 2002. Classification and phylogenetic analysis of the cAMP-dependent protein kinase regulatory subunit family. Journal of molecular evolution, 54(1), pp.17–29.

Carlson, C. R., Lygren, B., Berge, T., Hoshi, N., Wong, W., Taskén, K., Scott, J. D., 2006. Delineation of type I protein kinase A-selective signalling events using an RI anchoring disruptor. The Journal of biological chemistry, 281(30), pp.21535–45.

Cancela, J. M., Van Coppenolle, F., Galione, A., Tepikin, A. V., Petersen, O. H., 2002. Transformation of local Ca2+ spikes to global Ca2+ transients: the combinatorial roles of multiple Ca2+ releasing messengers. *The EMBO journal*, 21(5), pp.909–19.

Carnegie, G.K. & Scott, J.D., 2003. A-kinase anchoring proteins and neuronal signalling mechanisms. Genes & development, 17(13), pp.1557–68.

Carr, D.W. & Scott, J.D., 1992. Blotting and band-shifting: techniques for studying protein-protein interactions. Trends in biochemical sciences, 17(7), pp.246–9.

Carr, D. W., Stofko-Hahn, R. E., Fraser, I. D. C., Bishop, S. M., Acott, T. S., Brennan, R. G. Scott, J. D., 1991. Interaction of the regulatory subunit (RII) of cAMP-dependent protein kinase with RII-anchoring proteins occurs through an amphipathic helix binding motif. Journal of Biological Chemistry, 266(22), pp.14188–14192.

Carr, D. W., Hausken, Z. E., Fraser, D. C., Stofko-hahn, R. E., 1992. Association of the type II cAMP-dependent protein kinase with a human thyroid RII-anchoring protein. Cloning and characterization of the RII-binding domain. The Journal of biological chemistry, 267(19), pp.13376–82.

Carter, R. N., Tolhurst, G., Walmsley, G., Vizuete-Forster, M., Miller, N., Mahaut-Smith, M. P., 2006. Molecular and electrophysiological characterization of transient receptor potential ion channels in the primary murine megakaryocyte. The Journal of physiology, 576(Pt 1), pp.151–62.

Cavallini, L., Coassin, M., Borean, A., Alexandre, A., 1996. Prostacyclin and sodium nitroprusside inhibit the activity of the platelet inositol 1,4,5-trisphosphate receptor and promote its phosphorylation. Journal of Biological Chemistry, 271(10), pp.5545–5551.

Chen, L. & Kass, R.S., 2006. Dual roles of the A kinase-anchoring protein Yotiao in the modulation of a cardiac potassium channel: a passive adaptor versus an active regulator. European journal of cell biology, 85(7), pp.623–6.

Chen, M. & Stracher, A., 1989. In situ phosphorylation of platelet actin-binding protein by cAMP-dependent protein kinase stabilizes it against proteolysis by calpain. The Journal of biological chemistry, 264(24), pp.14282–9.

Chijiwa, T., Mishima, A., Hagiwara, M., Sano, M., Hayashi, K., Inoue, T., Naito, K., Toshioka, T., Hidaka, H., 1990. Inhibition of forskolin-induced neurite outgrowth and protein phosphorylation by a newly synthesized selective inhibitor of cyclic AMP-dependent protein kinase, N-[2-(p-bromocinnamylamino)ethyl]-5-isoquinolinesulfonamide (H-89), of PC12D pheochromocytoma . The Journal of biological chemistry, 265(9), pp.5267–72.

Christensen, A.E., 2003. cAMP Analog Mapping of Epac1 and cAMP Kinase: Discriminating analogs demonstrate that Epac and cAMP kinase act synergistically to promote PC-12 cell neurite extension. Journal of Biological Chemistry, 278(37), pp.35394–35402.

Clapham, D.E., Runnels, L.W. & Strübing, C., 2001. The TRP ion channel family. Nature reviews. Neuroscience, 2(6), pp.387–96.

Clegg, C.H., Cadd, G.G. & McKnight, G.S., 1988. Genetic characterization of a brain-specific form of the type I regulatory subunit of cAMP-dependent protein kinase. Proceedings of the National Academy of Sciences of the United States of America, 85(11), pp.3703–7.

Clemetson, K.J., 1999. Primary haemostasis: Sticky fingers cement the relationship. Current Biology, 9(3), pp.R110–R112.

Coghlan, V. M., Perrino, B. A., Howard, M., Langeberg, L. K., Hicks, J. B., Gallatin, W. M., Scott, J. D., 1995. Association of protein kinase A and protein phosphatase 2B with a common anchoring protein. Science (New York, N.Y.), 267(5194), pp.108–11.

Cohen, P., 2001. The role of protein phosphorylation in human health and disease. The Sir Hans Krebs Medal Lecture. European journal of biochemistry / FEBS, 268(19), pp.5001–10.

Collado-Hilly, M. & Coquil, J.-F., 2009. Ins(1,4,5)P3 receptor type 1 associates with AKAP9 (AKAP450 variant) and protein kinase A type IIbeta in the Golgi apparatus in cerebellar granule cells. *Biology of the cell / under the auspices of the European Cell Biology Organization*, 101(8), pp.469–80.

Colledge, M. & Scott, J. D. 1999. AKAPS: from structure to function. Trends Cell Biol 9: 216–221.

Corbin, J.D., Keely, S.L. & Park, C.R., 1975. The distribution and dissociation of cyclic adenosine 3':5'-monophosphate-dependent protein kinases in adipose, cardiac, and other tissues. The Journal of biological chemistry, 250(1), pp.218–25.

Daleke, D.L., 2003. Regulation of transbilayer plasma membrane phospholipid asymmetry. Journal of lipid research, 44(2), pp.233–242.

Daniel, J. L., Dangelmaier, C., Jin, J., Ashby, B., Smith, J. B., Kunapuli, S. P., 1998. Molecular basis for ADP-induced platelet activation. I. Evidence for three distinct ADP receptors on human platelets. The Journal of biological chemistry, 273(4), pp.2024–9.

Danoff, S. K., Ferris, C. D., Donatht, C., Fischert, G. A., Munemitsut, S., Ullricht, A., Snyder, S. H., Ross, C. A., 1991. Inositol 1 , 4 , 5-trisphosphate receptors : Distinct neuronal and non-neuronal forms derived by alternative splicing differ in phosphorylation. , 88(April), pp.2951–2955.

de Rooij, J., Zwartkruis, F. J., Verheijen, M. H., Cool, R. H., Nijman, S. M., Wittinghofer, A., Bos, J. L. 1998. Epac is a Rap1 guanine-nucleotide-exchange factor directly activated by cyclic AMP. Nature, 396(6710), pp.474–7.

de Wit, R. J., Hekstra, D., Jastorff, B., Stec, W. J., Baraniak, J., Van Driel, R., Van Haastert, P. J., 1984. Inhibitory action of certain cyclophosphate derivatives of cAMP on cAMP-dependent protein kinases. European journal of biochemistry / FEBS, 142(2), pp.255–60.

den Dekker, E., Molin, D. G., Breikers, G., van Oerle, R., Akkerman, J. W., van Eys, G. J., Heemskerk, J. W., 2001. Expression of transient receptor potential mRNA isoforms and Ca(2+) influx in differentiating human stem cells and platelets. Biochimica et biophysica acta, 1539(3), pp.243–55.

den Dekker, E.,Gorter, G, Heemskerk, J. W. M., Akkerman, J. N., 2002a. Development of platelet inhibition by cAMP during megakaryocytopoiesis. Journal of biological chemistry, 277(32):29321-9

den Dekker, E., Heemskerk, J. W., Gorter, G., van der Vuurst, H., Donath, J., Kroner, C., Mikoshiba, K., Akkerman, J. W., 2002b. Cyclic AMP raises intracellular Ca(2+) in human

megakaryocytes independent of protein kinase A.. Arterioscler Thromb Vasc Biol, 22(1):179-86.

DeSouza, N., Reiken, S., Ondrias, K., Yang, Y., Matkovich, S., Marks, A. R., 2002. Protein kinase A and two phosphatases are components of the inositol 1,4,5-trisphosphate receptor macromolecular signaling complex. The Journal of biological chemistry, 277(42), pp.39397–400.

Di Buduo, C. A., Moccia, F., Battiston, M., De Marco, L., Mazzucato, M., Moratti, R., Tanzi, F., Balduini, A., 2014. The importance of calcium in the regulation of megakaryocyte function. Haematologica, 99(4), pp.769–778.

Dickinson, N.T., Jang, E.K. & Haslam, R.J., 1997. Activation of cGMP-stimulated phosphodiesterase by nitroprusside limits cAMP accumulation in human platelets: effects on platelet aggregation. The Biochemical journal, 323 (Pt 2, pp.371–7.

Dobrydneva, Y. & Blackmore, P., 2001. 2-Aminoethoxydiphenyl borate directly inhibits store-operated calcium entry channels in human platelets. Molecular pharmacology, 60(3), pp.541–52.

Dong, F., Feldmesser, M., Casadevall, A., Rubin, C. S., 1998. Molecular characterization of a cDNA that encodes six isoforms of a novel murine A kinase anchor protein. The Journal of biological chemistry, 273(11), pp.6533–41.

Dufour, J.F., Arias, I.M. & Turner, T.J., 1997. Inositol 1,4,5-trisphosphate and calcium regulate the calcium channel function of the hepatic inositol 1,4,5-trisphosphate receptor. The Journal of biological chemistry, 272(5), pp.2675–81.

Dunkern, T.R. & Hatzelmann, A., 2005. The effect of Sildenafil on human platelet secretory function is controlled by a complex interplay between phosphodiesterases 2, 3 and 5. Cellular signalling, 17(3), pp.331–9.

Ehrman, M.L. & Jaffe, E.A., 1980. Prostacyclin (PGI2) inhibits the development in human platelets of ADP and arachidonic acid-induced shape change and procoagulant activity. Prostaglandins, 20(6), pp.1103–16.

El-daher, S. S., Patel, Y., Siddiqua, A., Hassock, S., Edmunds, S., Maddison, B., Patel, G., Goulding, D., Lupu, F., Wojcikiewicz, R. J. H., Authi, K. S. 2000. Distinct localization and function of 1,4,5IP3 receptor subtypes and the 1,3,4,5IP4 receptor GAP1 IP4BP in highly purified human platelet membranes. , 95(11), pp.3412–3422.

Elzagallaai, A., Rosé, S.D. & Trifaró, J.M., 2000. Platelet secretion induced by phorbol esters stimulation is mediated through phosphorylation of MARCKS: a MARCKS-derived peptide blocks MARCKS phosphorylation and serotonin release without affecting pleckstrin phosphorylation. Blood, 95(3), pp.894–902.

Feliciello, A., Gottesman, M.E. & Avvedimento, E. V, 2001. The biological functions of A-kinase anchor proteins. Journal of molecular biology, 308(2), pp.99–114.

Ferris, C. D., Cameron, A. M., Bredt, D. S., Huganir, R. L. & Snyder, S. H. (1991). Inositol 1,4,5-trisphosphate receptor is phosphorylated by cyclic amp-dependent protein kinase at serines 1755 and 1589. Biochem biophys res commun, 175, 192-8.

Ferris, C. D., Huganir, R. L., Supattapone, S., Snyder, S. H., 1989. Purified inositol 1,4,5-trisphosphate receptor mediates calcium flux in reconstituted lipid vesicles. Nature, 342(6245), pp.87–9.

Ferris, C. D., Cameron, A. M., Bredt, D. S., Huganir, R. L., Snyder, S. H., 1991. Inositol 1,4,5-trisphosphate receptor is phosphorylated by cyclic AMP-dependent protein kinase at serines 1755 and 1589. Biochemical and biophysical research communications, 175(1), pp.192–8.

Fitscha, P., Kaliman, J. & Sinzinger, H., 1985. Platelet sensitivity to antiaggregatory prostaglandins (PGE1,D2,I2) in patients with peripheral vascular disease. American journal of hematology, 19(1), pp.13–9.

FitzGerald, G. A., Smith, B., Pedersen, A. K., Brash, A. R., 1984. Increased prostacyclin biosynthesis in patients with severe atherosclerosis and platelet activation. The New England journal of medicine, 310(17), pp.1065–8.

Foskett, J. K., White, C., Cheung, K., Mak, D. D. 2007. Inositol trisphosphate receptor Ca^{2+} release channels. Physiological reviews, 87(2), pp.593–658.

Fox, J. E., & Phillips, D. R. (1982). Role of phosphorylation in mediating the association of myosin with the cytoskeletal structures of human platelets. The Journal Of Biological Chemistry, 257(8), 4120–6.

Fox, J.E. & Berndt, M.C., 1989. Cyclic AMP-dependent phosphorylation of glycoprotein Ib inhibits collagen-induced polymerization of actin in platelets. *The Journal of biological chemistry*, 264(16), pp.9520–6.

Fraser, I. D., Tavalin, S. J., Lester, L. B., Langeberg, L. K., Westphal, A. M., Dean, R. A., 1998. A novel lipid-anchored A-kinase Anchoring Protein facilitates cAMP-responsive membrane events. The EMBO journal, 17(8), pp.2261–72.

Freson, K., Wijgaerts, A. & van Geet, C., 2014. Update on the causes of platelet disorders and functional consequences. International Journal of Laboratory Hematology, 36(3), pp.313–325.

Frojmovic, M.M. & Milton, J.G., 1982. Human platelet size, shape, and related functions in health and disease. Physiological reviews, 62(1), pp.185–261.

Fung, C. Y. E., Jones, S., Ntrakwah, A., Naseem, K. M., Farndale, R. W., Mahaut-smith, M. P., 2012. Platelet Ca^{2+} responses coupled to glycoprotein VI and Toll-like receptors persist in the presence of endothelial-derived inhibitors : roles for secondary activation of P_2X1 receptors and release from intracellular Ca^{2+} stores., 119(15), pp.3613–3621.

Furchgott, R.F. & Zawadzki, J. V, 1980. The obligatory role of endothelial cells in the relaxation of arterial smooth muscle by acetylcholine. Nature, 288(5789), pp.373–6.

Furuichi, T., Yoshikawa, S., Miyawaki, A., Wada, K., Maeda, N., Mikoshiba, K.,1989. Primary structure and functional expression of the inositol 1,4,5-trisphosphate-binding protein P400. Nature, 342(6245), pp.32–8.

Gafni, J., Munsch, J. A., Lam, T. H., Catlin, M. C., Costa, L. G., Molinski, T. F., Pessah, I. N., 1997. Xestospongins: potent membrane permeable blockers of the inositol 1,4,5-trisphosphate receptor. Neuron, 19(3), pp.723–33.

Gawaz, M., 2004. Role of platelets in coronary thrombosis and reperfusion of ischemic myocardium. Cardiovascular research, 61(3), pp.498–511.

Geiger, J., Nolte, C. & Walter, U., 1994. Regulation of calcium mobilization and entry in human platelets by endothelium-derived factors. Am J Physiol Cell Physiol, 267(1), pp.C236–244.

George, J.N., 2000. Platelets. Lancet (London, England), 355(9214), pp.1531–9.

Gold, M. G., Lygren, B., Dokurno, P., Hoshi, N., McConnachie, G., Taskén, K., Carlson, C. R., Scott, J. D. Barford, D., 2006. Molecular Basis of AKAP Specificity for PKA Regulatory Subunits. Molecular Cell, 24(3), pp.383–395.

Grosse, J., Braun, A., Varga-Szabo, D., Beyersdorf, N., Schneider, B., Zeitlmann, L., Hanke, P., Schropp, P., Mühlstedt, S., Zorn, C., Huber, M., Schmittwolf, C., Jagla, W., Yu, P., Kerkau, T., Schulze, H., Nehls, M., Nieswandt, B., 2007. An EF hand mutation in STIM1 causes premature platelet activation and bleeding in mice. The Journal of clinical investigation, 117(11), pp.3540–50.

Grynkiewicz, G., Poenie, M. & Tsien, R.Y., 1985. A new generation of Ca^{2+} indicators with greatly improved fluorescence properties. The Journal of biological chemistry, 260(6), pp.3440–50.

Hajnóczky, G. Gao, E., Nomura, T., Hoek, J. B., Thomas, A. P. 1993. Multiple mechanisms by which protein kinase A potentiates inositol 1,4,5-trisphosphate-induced Ca2+ mobilization in permeabilized hepatocytes. The Biochemical journal, 293, pp.413–22.

Hanafy, K. A, Krumenacker, J.S. & Murad, F., 2001. NO, nitrotyrosine, and cyclic GMP in signal transduction. Medical science monitor : international medical journal of experimental and clinical research, 7(4), pp.801–19.

Hanoune, J. & Defer, N., 2001. Regulation and role of adenylyl cyclase isoforms. Annual review of pharmacology and toxicology, 41, pp.145–74.

Harbeck, B., Hüttelmaier, S., Schluter, K., Jockusch, B. M., Illenberger, S., 2000. Phosphorylation of the vasodilator-stimulated phosphoprotein regulates its interaction with actin. The Journal of biological chemistry, 275(40), pp.30817–25.

Harnick, D. J., Jayaraman, T., Ma, Y., Mulieri, P., Go, L.O., Marks, A.R. 1995. The human type 1 inositol 1,4,5- trisphosphate receptor from T lymphocytes: Structure, localization, and tyrosine phosphorylation. Journal of biological chemistry, 270:2833–2840.

Hartwig, J. & Italiano, J., 2003. The birth of the platelet. Journal of thrombosis and haemostasis : JTH, 1(7), pp.1580–6.

Hartwig, J.H. & Italiano, J.E., Cytoskeletal mechanisms for platelet production. Blood cells, molecules & diseases, 36(2), pp.99–103.

Hartwig, J. H., Thelen, M., Rosen, A., Janmey, P. A., Nairn, A. C., Aderem, A., 1992. MARCKS is an actin filament crosslinking protein regulated by protein kinase C and calcium-calmodulin. Nature, 356(6370), pp.618–22.

Haslam, R. J., Davidson, M. M., Fox, J. E. & Lynham, J. A. 1999. Cyclic nucleotides in platelet function. Thromb Haemost, 40, 232-40.

Hassock, S. R., Zhu, M. X., Trost, C., Flockerzi, V., Authi, K. S., 2002. Expression and role of TRPC proteins in human platelets: evidence that TRPC6 forms the store-independent calcium entry channel. Blood, 100(8), pp.2801–2811.

Hathaway, D.R. & Adelstein, R.S., 1979. Human platelet myosin light chain kinase requires the calcium-binding protein calmodulin for activity. Proceedings of the National Academy of Sciences of the United States of America, 76(4), pp.1653–7.

Haug, L. S., Jensen, V., Hvalby, O., Walaas, S. I., Ostvold, A. C., 1999. Phosphorylation of the inositol 1,4,5-trisphosphate receptor by cyclic nucleotide-dependent kinases in vitro and in rat cerebellar slices in situ. The Journal of biological chemistry, 274(11), pp.7467–73.

Hayes, J. S., Lawler, O. A., Walsh, M. T., Kinsella, B. T., 1999. The prostacyclin receptor is isoprenylated. Isoprenylation is required for efficient receptor-effector coupling. *The Journal of biological chemistry*, 274(34), pp.23707–18.

Hayes, J.S. & Mayer, S.E., 1981. Regulation of guinea pig heart phosphorylase kinase by cAMP, protein kinase, and calcium. Am J Physiol Endocrinol Metab, 240(3), pp.E340–349.

Hechler, B., Lenain, N., Marchese, P., Vial, C., Heim, V., Freund, M., Cazenave, J., Cattaneo, M., Ruggeri, Z. M., Evans, R., Gachet, C., 2003. A role of the fast ATP-gated P2X1 cation channel in thrombosis of small arteries in vivo. The Journal of experimental medicine, 198(4), pp.661–7.

Heemskerk, J. W., Bevers, E. M., Lindhout, T. 2002. Platelet activation and blood coagulation. Thromb Haemost, 88, 186-93.

Heller, W. T., Vigil, D., Brown, S., Blumenthal, D. K., Taylor, S. S., Trewhella, J., 2004. C subunits binding to the protein kinase A RI alpha dimer induce a large conformational change. The Journal of biological chemistry, 279(18), pp.19084–90.

Hemric, M.E., Tracy, P.B. & Haeberle, J.R., 1994. Caldesmon enhances the binding of myosin to the cytoskeleton during platelet activation. The Journal of biological chemistry, 269(6), pp.4125–8.

Herberg, F. W., Maleszka, A., Eide, T., Vossebein, L., Tasken, K., 2000. Analysis of A-kinase anchoring protein (AKAP) interaction with protein kinase A (PKA) regulatory subunits: PKA isoform specificity in AKAP binding. Journal of molecular biology, 298(2), pp.329–39.

Hettasch, J.M. & Sellers, J.R., 1991. Caldesmon phosphorylation in intact human platelets by cAMP-dependent protein kinase and protein kinase C. The Journal of biological chemistry, 266(18), pp.11876–81.

Higgs, E. A., Higgs, G. A., Moncada, S., Vane, J. R., 1997. Prostacyclin (PGI_2) inhibits the formation of platelet thrombi in arterioles and venules of the hamster cheek pouch. 1977. British journal of pharmacology, 120(4 Suppl), pp.439–43

Hirata, M., Suematsu, E., Hashimoto, T., Hamachi, T., Koga, T., 1984. Release of Ca^{2+} from a non-mitochondrial store site in peritoneal macrophages treated with saponin by inositol 1,4,5-trisphosphate. The Biochemical Journal, 223(1), pp.229–36.

Hofmann, F., 2005. The biology of cyclic GMP-dependent protein kinases. Journal of

biological chemistry, 280(1), pp.1–4.

Holt, M.R., Critchley, D.R. & Brindle, N.P., 1998. The focal adhesion phosphoprotein, VASP. *The international journal of biochemistry & cell biology*, 30(3), pp.307–11.

Horstrup, K. et al., 1994. Phosphorylation of focal adhesion vasodilator-stimulated phosphoprotein at Ser157 in intact human platelets correlates with fibrinogen receptor inhibition. European journal of biochemistry / FEBS, 225(1), pp.21–7.

Hovig, T., 1964. The effect of calcium and magnesium on rabbit blood platelet aggregation in vitro. Thrombosis et diathesis haemorrhagica, 12, pp.179–200.

Hur, E.-M. et al., 2005. Junctional membrane inositol 1,4,5-trisphosphate receptor complex coordinates sensitization of the silent EGF-induced Ca2+ signaling. The Journal of cell biology, 169(4), pp.657–67.

Hurley, J.H., 1999. Structure, Mechanism, and Regulation of Mammalian Adenylyl Cyclase, The journal of biological chemistry, 274 (12), pp. 7599–7602, 1999

Iino, M., 1990. Biphasic Ca2+ dependence of inositol 1,4,5-trisphosphate-induced Ca release in smooth muscle cells of the guinea pig taenia caeci. The Journal of general physiology, 95(6), pp.1103–22.

Irvine, R.F., 1982. How is the level of free arachidonic acid controlled in mammalian cells? The Biochemical journal, 204(1), pp.3–16.

Ito, M., Nishikawa, M., Fujioka, M., Miyahara, M., Isaka, N., Shiku, H., Nakano, T., 1996. Characterization of the isoenzymes of cyclic nucleotide phosphodiesterase in human platelets and the effects of E4021. Cellular signalling, 8(8), pp.575–81.

Jardín, I., Redondo, P. C., Salido, G. M., Rosado, J. A., 2008. Phosphatidylinositol 4,5-bisphosphate enhances store-operated calcium entry through hTRPC6 channel in human platelets. Biochimica et biophysica acta, 1783(1), pp.84–97.

Jean, T. & Klee, C.B., 1986. Calcium modulation of inositol 1,4,5-trisphosphate-induced calcium release from neuroblastoma x glioma hybrid (NG108-15) microsomes. The Journal of biological chemistry, 261(35), pp.16414–20.

Jiang, Q., Thrower, E. C., Chester, D. W., Ehrlich, B. E., Sigworth, F. J., 2002. Three-dimensional structure of the type 1 inositol 1,4,5-trisphosphate receptor at 24 A resolution. The EMBO journal, 21(14), pp.3575–81.

Jin, J. & Kunapuli, S.P., 1998. Coactivation of two different G protein-coupled receptors is essential for ADP-induced platelet aggregation. Proceedings of the National Academy of Sciences of the United States of America, 95(14), pp.8070–4.

Jin, J., Daniel, J.L. & Kunapuli, S.P., 1998. Molecular basis for ADP-induced platelet activation. II. The P2Y1 receptor mediates ADP-induced intracellular calcium mobilization and shape change in platelets. The Journal of biological chemistry, 273(4), pp.2030–4.

Jonas, S., Sugimori, M. & Llinás, R., 1997. Is low molecular weight heparin a neuroprotectant? Annals of the New York Academy of Sciences, 825, pp.389–93.

Jones, C. I., Bray, S., Garner, S. F., Stephens, J., de Bono, B., Angenent, W. G. J., Bentley, D., Burns, P., Coffey, A., Deloukas, P., Earthrowl, M., Farndale, R. W., Hoylaerts, M. F., Koch, K., Rankin, A., Rice, C. M., Rogers, J., Samani, N. J., Steward, M. W., Adam W., Nicholas A., Akkerman, J., Dudbridge, F., Goodall, A. H., Ouwehand, W. H., 2009. A functional genomics approach reveals novel quantitative trait loci associated with platelet signaling pathways. Blood, 114(7), pp.1405–16.

Jones, R. L., Wise, H., Clark, R., Whiting, R. L., Bley, K. R., 2006. Investigation of the prostacyclin (IP) receptor antagonist RO1138452 on isolated blood vessel and platelet preparations. British journal of pharmacology, 149(1), pp.110–20.

Joseph, S.K., 1996. The Inositol Triphosphate Receptor Family. , 8(1), pp.1–7.

Kahn, N.N., Bauman, W.A. & Sinha, A.K., 1996. Loss of high-affinity prostacyclin receptors in platelets and the lack of prostaglandin-induced inhibition of platelet-stimulated thrombin generation in subjects with spinal cord injury. Proceedings of the National Academy of Sciences of the United States of America, 93(1), pp.245–9.

Kang, S., Kwon, H., Wen, H., Song, Y., Frueh, D., Ahn, H., Yoo, S. H., Wagner, G., Park, S.,2011. Global dynamic conformational changes in the suppressor domain of IP3 receptor by stepwise binding of the two lobes of calmodulin. FASEB, 25(3), pp.840–50.

Kase, H., Iwahashi, K., Nakanishi, S., Matsuda, Y., Yamada, K., Takahashi, M., Murakata, C., Sato, A., Kaneko, M., 1987. K-252 compounds, novel and potent inhibitors of protein kinase C and cyclic nucleotide-dependent protein kinases. Biochemical and biophysical research communications, 142(2), pp.436–40.

Kashiwagi, H., Schwartz, M. A., Eigenthaler, M., Davis, K. A., Ginsberg, M. H., Shattil, S. J., 1997. Affinity modulation of platelet integrin alphaIIbbeta3 by beta3-endonexin, a selective binding partner of the beta3 integrin cytoplasmic tail. The Journal of cell biology, 137(6), pp.1433–43.

Kaulen, H. D. & Gross, R. (1974). Purification and properties of a soluble cyclic amp-dependent protein kinase from human platelets. Hoppe Seylers Z Physiol Chem, 355, 471-80.

Keularts, I. M., van Gorp, R. M., Feijge, M. A., Vuist, W. M., Heemskerk, J. W., 2000. alpha(2A)-adrenergic receptor stimulation potentiates calcium release in platelets by modulating cAMP levels. The Journal of biological chemistry, 275(3), pp.1763–72.

Kim, C., Cheng, C. Y., Saldanha, S. A., Taylor, S S., 2007. PKA-I holoenzyme structure reveals a mechanism for cAMP-dependent activation. Cell, 130(6), pp.1032–43..

Kinderman, F. S., Kim, C., von Daake, S., Ma, Y., Pham, B. Q., Spraggon, G., Xuong, N., Jennings, P. A., Taylor, S. S., 2006. A dynamic mechanism for AKAP binding to RII isoforms of cAMP-dependent protein kinase. Molecular cell, 24(3), pp.397–408.

Kirschner, L. S., Yin, Z., Jones, G. N., Mahoney, E., 2009. Mouse models of altered protein kinase A signaling. Endocrine-related cancer, 16(3), pp.773–93.

Komalavilas, P. & Lincoln, T.M., 1996. Phosphorylation of the inositol 1,4,5-trisphosphate receptor. Cyclic GMP-dependent protein kinase mediates cAMP and cGMP dependent phosphorylation in the intact rat aorta. The Journal of biological chemistry, 271(36), pp.21933–8.

Kopperud, R. et al., 2002. Formation of inactive cAMP-saturated holoenzyme of cAMP-dependent protein kinase under physiological conditions. The Journal of biological chemistry, 277(16), pp.13443–8.

Koyama, H. & Nishizawa, Y., 2005. Platelet in progression of atherosclerosis: a potential target in diabetic patients. Current diabetes reviews, 1(2), pp.159–65.

Krizanova, O. & Ondrias, K., 2003. The inositol 1,4,5-trisphosphate receptor--transcriptional regulation and modulation by phosphorylation. General physiology and biophysics, 22(3), pp.295–311.

Krupinski, J., Coussen, F., Bakalyar, H. A., Tang, W. J., Feinstein, P. G., Orth, K., Slaughter, C., Reed, R. R., Gilman, A. G., 1989. Adenylyl cyclase amino acid sequence: possible channel- or transporter-like structure. Science (New York, N.Y.), 244(4912), pp.1558–64.

Kukkonen, J. P., Lund, P.E., and Åkerman, K. E. O. 2001. 2-aminoethoxydiphenyl borate reveals heterogeneity in receptor-activated Ca^{2+} discharge and store-operated Ca^{2+} influx. Cell Calcium 30, 117–129

Kurokawa, J., Motoike, H. K., Rao, J., Kass, R. S. 2004. Regulatory actions of the A-kinase anchoring protein Yotiao on a heart potassium channel downstream of PKA phosphorylation. Proceedings of the National Academy of Sciences of the United States of America, 101(46), pp.16374–8.

Laemmli, U. K. 1970. Cleavage of structural proteins during the assembly of the head of bacteriophage T4. Nature, 227, 680-5.

Lapetina, E. G., Lacal, J. C., Reep, B. R., Molina, Y., Vedia, L., 1989. A ras-related protein is phosphorylated and translocated by agonists that increase cAMP levels in human platelets. Proceedings of the National Academy of Sciences of the United States of America, 86(9), pp.3131–4.

Lee, D. C., Carmichael, D. F., Krebs, E. G., McKnight, G. S., 1983. Isolation of a cDNA clone for the type I regulatory subunit of bovine cAMP-dependent protein kinase. Proceedings of the National Academy of Sciences of the United States of America, 80(12), pp.3608–12.

Leray, C., 2012. Introduction to Lipidomics: From Bacteria to Man, CRC Press.

Leytin, V. et al., 2007. Higher thrombin concentrations are required to induce platelet apoptosis than to induce platelet activation. British journal of haematology, 136(5), pp.762–4.

Lin, J. W., Wyszynski, M., Madhavan, R., Sealock, R., Kim, J. U., Sheng, M., 1998. Yotiao, a Novel Protein of Neuromuscular Junction and Brain That Interacts with Specific Splice Variants of NMDA Receptor Subunit NR1. J. Neurosci., 18(6), pp.2017–2027.

Liou, J., Kim, Man L. D., Heo, W., Jones, J. T., Myers, J. W., Ferrell, J. E., Meyer, T., 2005. STIM Is a Ca2+ Sensor Essential for Ca2+-Store-Depletion-Triggered Ca2+ Influx. Current Biology, 15(13), pp.1235–1241.

Liu, Y., Ruoho, A. E., Rao, V. D., Hurley, J. H., 1997. Catalytic mechanism of the adenylyl and guanylyl cyclases: modeling and mutational analysis. Proceedings of the National Academy of Sciences of the United States of America, 94(25), pp.13414–9.

Lowry, O. H., Rosebrough, N. J., Farr, A. L. & Randall, R. J. 1951. Protein measurement with the Folin phenol reagent. Journal of biological chemistry, 193, 265-75.

MacKenzie, A.B., Mahaut-Smith, M.P. & Sage, S.O., 1996. Activation of receptor-operated cation channels via P2X1 not P2T purinoceptors in human platelets. The Journal of biological chemistry, 271(6), pp.2879–81.

Macphee, C. H., Reifsnyder, D. H., Moore, T. A., Lerea, K. M., Beavo, J. A., 1988. Phosphorylation results in activation of a cAMP phosphodiesterase in human platelets. The Journal of biological chemistry, 263(21), pp.10353–8.

Maeda, N., Kawasaki, T., Nakade, S., Yokota, N., Taguchi, T., Kasai, M., Mikoshiba, K., 1991. Structural and functional characterization of inositol 1,4,5-trisphosphate receptor channel from mouse cerebellum. The Journal of biological chemistry, 266(2), pp.1109–16.

Mak, D-O. D., McBride, S. M. J., Petrenko, N. B., Foskett, J. K., 2003. Novel regulation of calcium inhibition of the inositol 1,4,5-trisphosphate receptor calcium-release channel. The Journal of general physiology, 122(5), pp.569–81.

Manganello, J. M., Djellas, Y., Borg, C., Antonakis, K., Le Breton, G. C., 1999. Cyclic AMP-dependent phosphorylation of thromboxane A(2) receptor-associated Galpha(13). The Journal of biological chemistry, 274(39), pp.28003–10.

Manns, J. M., Brenna, K. J., Colman, R. W., Sheth, S. B., 2002. Differential regulation of human platelet responses by cGMP inhibited and stimulated cAMP phosphodiesterases. Thrombosis and haemostasis, 87(5), pp.873–9.

Marchant, J.S. & Taylor, C.W., 1997. Cooperative activation of IP3 receptors by sequential binding of IP3 and Ca2+ safeguards against spontaneous activity. Current biology : CB, 7(7), pp.510–8.

Marcus, A.J. & Safier, L.B., 1993. Thromboregulation: multicellular modulation of platelet reactivity in hemostasis and thrombosis. FASEB journal : official publication of the Federation of American Societies for Experimental Biology, 7(6), pp.516–22.

Margarucci, L., Roest, M., Preisinger, C., Bleijerveld, O. B., van Holten, T. C., Heck, A. J. R., Scholten, A., 2011. Collagen stimulation of platelets induces a rapid spatial response of cAMP and cGMP signaling scaffolds. Molecular bioSystems, 7(7), pp.2311–9.

Martin, B. R., Deerinck, T. J., Ellisman, M. H., Taylor, S. S., Tsien, R. Y., 2007. Isoform-specific PKA dynamics revealed by dye-triggered aggregation and DAKAP1 alpha-mediated localization in living cells. Chemistry & biology, 14(9), pp.1031–42.

Maruyama, T., Kanaji, T., Nakade, S., Kanno, T., Mikoshiba, K., 1997. 2-APB, 2-Aminoethoxydiphenyl Borate, a Membrane-Penetrable Modulator of Ins(1,4,5)P3-Induced Ca^{2+} Release. Journal of Biochemistry, 122(3), pp.498–505.

Mattson, P. M., 2004, Protein Phosphorylation in Aging and Age-Related Disease , 978-0-444-51583-4 , Elsevier.

Maurice, D.H. & Haslam, R.J., 1990. Molecular basis of the synergistic inhibition of platelet function by nitrovasodilators and activators of adenylate cyclase: inhibition of cyclic AMP breakdown by cyclic GMP. Molecular pharmacology, 37(5), pp.671–81.

Mehta, J. L., Chen, L. Y., Kone, B. C., Mehta, P., Turner, P. 1995. Identification of constitutive and inducible forms of nitric oxide synthase in human platelets. The Journal of laboratory and clinical medicine, 125(3), pp.370–7.

Metzger, H. & Lindner, E. 1981 The positive inotropic-acting forskolin, a potent adenylate cyclase activator. IRCS Medical Science, 9, 99.

Mignery, G.A. & Südhof, T.C., 1990. The ligand binding site and transduction mechanism in the inositol-1,4,5-triphosphate receptor. The EMBO journal, 9(12), pp.3893–8.

Miller, J. P., Boswell, K. H., Meyer, R. B., Christensen, L. F., Robins R. K., 1980, Synthesis and Enzymatic and Inotropic Activity of Some New 8-Substituted and 6,8-Disubstituted Derivatives of Adenosine Cyclic 3',5- Monophosphate J. Med. Chem., 23, 242 - 251

Modderman, P. W., Admiraal, L. G., Sonnenberg, A., von dem Borne, A. E., 1992. Glycoproteins V and Ib-IX form a noncovalent complex in the platelet membrane. The Journal of biological chemistry, 267(1), pp.364–9.

Moncada, S., Gryglewski, R., Bunting, S., Vane, J. R., 1976. An enzyme isolated from arteries transforms prostaglandin endoperoxides to an unstable substance that inhibits platelet aggregation. Nature, 263(5579), pp.663–5.

Moncada, S., 1982 Prostacyclin and arterial wall biology. Arteriosclerosis, 2(3), pp.193–207.

Mueller, H. S., Rao, P. S., Greenberg, M. A., Buttrick, P. M., Sussman, I. I., Levite, H. A., Grose, R. M., Perez-Davila, V., Strain, J. E., Spaet, T. H., 1986. Platelet hyperactivity in acute myocardial infarction in man--effects of prostacyclin. Herz, 11(2), pp.116–26.

Murata, T., Ushikubi, F., Matsuoka, T., Hirata, M., Yamasaki, A., Sugimoto, Y., Ichikawa, A., Aze, Y., Tanaka, T., Yoshida, N., Ueno, A., Oh-ishi, S., Narumiya, S., 1997. Altered pain perception and inflammatory response in mice lacking prostacyclin receptor. Nature, 388(6643), pp.678–82.

Murphy, J. A., Stein, I. S., Lau, C. G., Peixoto, R. T., Aman, T. K., Kaneko, N., Aromolaran, K., Saulnier, J. L., Popescu, G. K., Sabatini, B. L., Hell, J. W., Zukin, R. S., 2014. Phosphorylation of Ser1166 on GluN2B by PKA is critical to synaptic NMDA receptor function and Ca2+ signaling

in spines. The Journal of neuroscience : the official journal of the Society for Neuroscience, 34(3), pp.869–79.

Murray, A.J., 2008. Pharmacological PKA inhibition: all may not be what it seems. Science signaling, 1(22), p.re4.

Mustard, J. F., Kinlough-Rathbone, R. L. & Packham, M. A. 1989. Isolation of human platelets from plasma by centrifugation and washing. Methods Enzymol, 169, 3-11.

Nakade, S., Maeda, N. & Mikoshiba, K., 1991. Involvement of the C-terminus of the inositol 1,4,5-trisphosphate receptor in Ca^{2+} release analysed using region-specific monoclonal antibodies. The Biochemical journal, 277 (Pt 1, pp.125–31.

Nakagawa, T., Okano, H., Furuichi, T., Aruga, J., Mikoshiba, K., 1991. The subtypes of the mouse inositol 1,4,5-trisphosphate receptor are expressed in a tissue-specific and developmentally specific manner. Proceedings of the National Academy of Sciences of the United States of America, 88(14), pp.6244–8.

Nakamura, T. & Gold, G.H., 1987. A cyclic nucleotide-gated conductance in olfactory receptor cilia. Nature, 325(6103), pp.442–4.

Narumiya, S., Sugimoto, Y. & Ushikubi, F., 1999. Prostanoid receptors: structures, properties, and functions. Physiological reviews, 79(4), pp.1193–226.

Naseem, K. M. & Roberts, W., 2011, Platelets 22(2):148-52

Needleman, P., Moncada, S., Bunting, S., Vane, J. R., Hamberg, M., Samuelsson, B., 1976. Identification of an enzyme in platelet microsomes which generates thromboxane A2 from prostaglandin endoperoxides. Nature, 261(5561), pp.558–60.

Newton, C.L., Migneryo, a & Siidhofn, T.C., 1994. Co-expression in Vertebrate Tissues and Cell Lines of Multiple Inositol 1,4,5 trisphosphate (InsP,) Receptors with Distinct affinities for InsP, The Journal of Biological Chemistry, Vol. 269 (46), pp. 28613-28619, 199

Nishikawa, M., Lanerolle, P., De Lincoln, T. M., Adelstein, R. S., 1984. Phosphorylation of Mammalian Myosin Light Chain Kinases by the Catalytic Subunit of Cyclic AMP-dependent

Protein Kinase and by cyclic GMP-dependent protein kinase, The Journal of Biological Chemistry. 1984 Jul 10;259(13):8429-36.

Nunn, D.L. & Taylor, C.W., 1990. Liver inositol, 1,4,5-trisphosphate-binding sites are the Ca2(+)-mobilizing receptors. The Biochemical journal, 270(1), pp.227–32.

O'brien J, R., 1963 Further observations on platelet aggregation induced by adenosine diphosphate thrombin and tri-ethyl tin. Journal Clinical Pathology, 16, 223-6.

Offermanns, S., Laugwitz, K. L., Spicher, K., Schultz, G., 1994. G proteins of the G12 family are activated via thromboxane A_2 and thrombin receptors in human platelets. Proceedings of the National Academy of Sciences of the United States of America, 91(2), pp.504–8.

Oliveria, S.F., Dell'Acqua, M.L. & Sather, W.A., 2007. AKAP79/150 anchoring of calcineurin controls neuronal L-type Ca2+ channel activity and nuclear signaling. Neuron, 55(2), pp.261–75.

Omori, K. & Kotera, J., 2007. Overview of PDEs and their regulation. Circulation research, 100(3), pp.309–27.

Otten, D. & McKnight, G.S., 1989. Overexpression of the type II regulatory subunit of the cAMP-dependent protein kinase eliminates the type I holoenzyme in mouse cells. The Journal of biological chemistry, 264(34), pp.20255–60.

Parekh, A.B. & Putney, J.W., 2005. Store-operated calcium channels. Physiological reviews, 85(2), pp.757–810.

Parente, L. & Perretti, M., 2003. Advances in the pathophysiology of constitutive and inducible cyclooxygenases: two enzymes in the spotlight. Biochemical pharmacology, 65(2), pp.153–9.

Patterson, R.L., Boehning, D. & Snyder, S.H., 2004. Inositol 1,4,5-trisphosphate receptors as signal integrators. Annual review of biochemistry, 73, pp.437–65.

Pei, G., Powers, D. D. & Lentz, B. R. 1993. Specific contribution of different phospholipid surfaces to the activation of prothrombin by the fully assembled prothrombinase. J Biol Chem, 268, 3226-33

Pidoux, G. & Tasken, K., 2010. Specificity and spatial dynamics of protein kinase A signaling organized by A-kinase-anchoring proteins. Journal of Molecular Endocrinology, 44(5), pp.271–284.

Piggott, L. A., Bauman, A. L., Scott, J. D., Dessauer, C. W., 2008. The A-kinase anchoring protein Yotiao binds and regulates adenylyl cyclase in brain. Proceedings of the National Academy of Sciences of the United States of America, 105(37), pp.13835–40.

Pleines, I., Hagedorn, I., Gupta, S., May, F., Chakarova, L., van Hengel, J., Offermanns, S., Krohne, G., Kleinschnitz, C., Brakebusch, C., Nieswandt, B., 2012. Megakaryocyte-specific RhoA deficiency causes macrothrombocytopenia and defective platelet activation in hemostasis and thrombosis. Blood, 119(4), pp.1054–63.

Poenie, M., 1990. Alteration of intracellular Fura-2 fluorescence by viscosity: a simple correction. Cell calcium, 11(2-3), pp.85–91.

Potter, R.L., Taylor, S.S. & Chem, J.B., 1979. Relationships between structural domains and function in the regulatory subunit of cAMP-dependent protein kinases I and II from porcine skeletal muscle. Relationships between Structural Domains and Function Regulatory Subunit of CAMP-dependent Protein Ki. , 254(7), pp.2413–2418.

Putney, J.W., 2007. Recent breakthroughs in the molecular mechanism of capacitative calcium entry (with thoughts on how we got here). Cell calcium, 42(2), pp.103–10.

Quinton, T.M. & Dean, W.L., 1992. Cyclic AMP-dependent phosphorylation of the inositol-1,4,5-trisphosphate receptor inhibits Ca2+ release from platelet membranes. Biochemical and biophysical research communications, 184(2), pp.893–9.

Radivojac, P., Baenziger, P. H., Kann, M. G., Mort, M. E.; Hahn, M. W., Mooney, S. D., 2008. Gain and loss of phosphorylation sites in human cancer. Bioinformatics (Oxford, England), 24(16), pp.i241–7.

Radomski, M.W., Palmer, R.M. & Moncada, S., 1990. Characterization of the L-arginine:nitric oxide pathway in human platelets. British journal of pharmacology, 101(2), pp.325–8.

Raslan, Z., Aburima, A., Naseem, K. M., 2015a. Targeting of type I protein kinase A to lipid rafts is required for platelet inhibition by the 3',5'-cyclic adenosine monophosphate-signaling pathway. Journal of thrombosis and haemostasis, 13(9), pp.1721–34.

Raslan, Z., Aburima, A. & Naseem, K.M., 2015. The Spatiotemporal Regulation of cAMP Signaling in Blood Platelets—Old Friends and New Players. Frontiers in Pharmacology, 6, p.266.

Reid, H.M. & Kinsella, B.T., 2003. The alpha, but not the beta, isoform of the human thromboxane A2 receptor is a target for nitric oxide-mediated desensitization. Independent modulation of Tp alpha signaling by nitric oxide and prostacyclin. The Journal of biological chemistry, 278(51), pp.51190–202.

Reinhard, M., Jarchau, T. & Walter, U., 2001. Actin-based motility: stop and go with Ena/VASP proteins. Trends in biochemical sciences, 26(4), pp.243–9.

Riba, R., Patel, B., Aburima, A. & Naseem, K. M. 2008. Globular adiponectin increases cGMP formation in blood platelets independently of nitric oxide. J Thromb Haemost, 6, 2121-31.

Rivera, J., Lozano, M. L., Navarro-Núñez, L., Vicente, V., 2009. Platelet receptors and signaling in the dynamics of thrombus formation. Haematologica, 94(5), pp.700–11.

Rosado, J.A. & Sage, S.O., 2000. Coupling between inositol 1,4,5-trisphosphate receptors and human transient receptor potential channel 1 when intracellular Ca2+ stores are depleted. The Biochemical journal, 350 (3), pp.631–5.

Rowley, J. W., Oler, A. J., Tolley, N. D., Hunter, B. N., Low, E. N., Nix, D. A., Yost, C. C., Zimmerman, G. A., Weyrich, A. S., 2011. Genome-wide RNA-seq analysis of human and mouse platelet transcriptomes. Blood, 118(14), pp.e101–e111.

Rubin, L.J., 1995. Pathology and pathophysiology of primary pulmonary hypertension. The American journal of cardiology, 75(3), p.51A–54A.

Said Goueli, and Hsaio, K., 2000. Using InCELLect™ Cell-Permeable, Stearated Peptides to Probe cAMP-Dependent Protein Kinase-Mediated Cellular Signaling Reactions In Vivo. High Throughput Systems for Drug Discovery.

Sandberg, M., Taskén, K., Øyen, O., Hansson, V., Jahnsen, T., 1987. Molecular cloning, cDNA structure and deduced amino acid sequence for a type I regulatory subunit of cAMP-dependent protein kinase from human testis. Biochemical and Biophysical Research Communications, 149(3), pp.939–945.

Saunders, C. M., Larman, M. G., Parrington, J., Cox, L. J., Royse, J., Blayney, L. M., Swann, K., Lai, F. A., 2002. PLC zeta: a sperm-specific trigger of Ca(2+) oscillations in eggs and embryo development. Development (Cambridge, England), 129(15), pp.3533–44.

Savage, B., Saldívar, E. & Ruggeri, Z.M., 1996. Initiation of platelet adhesion by arrest onto fibrinogen or translocation on von Willebrand factor. Cell, 84(2), pp.289–97.

Savage, B., Shattil, S.J. & Ruggeri, Z.M., 1992. Modulation of platelet function through adhesion receptors. A dual role for glycoprotein IIb-IIIa (integrin alpha IIb beta 3) mediated by fibrinogen and glycoprotein Ib-von Willebrand factor. The Journal of biological chemistry, 267(16), pp.11300–6.

Schmidt, M., Dekker, F. J., Maarsingh, H., 2013. Exchange Protein Directly Activated by cAMP (epac): A Multidomain cAMP Mediator in the Regulation of Diverse Biological Functions. Pharmacological Reviews ,65 (2) 670-709

Schmidt, P. H., Dransfield, D. T., Claudio, J. O., Hawley, R. G., Trotter, K. W., Milgram, S. L., Goldenring, J. R., 1999. AKAP350, a multiply spliced protein kinase A-anchoring protein associated with centrosomes. The Journal of biological chemistry, 274(5), pp.3055–66.

Scholten, A., Poh, M. K., Veen, T. A. B., Van Breukelen, B., Van Vos, M. A., Heck, A. J. R., 2006. Analysis of the cGMP / cAMP Interactome Using a Chemical Proteomics Approach in Mammalian Heart Tissue Validates Sphingosine Kinase Type 1-interacting Protein as a Genuine and Highly Abundant AKAP research articles. , pp.1435–1447.

Schwarz, U.R., Walter, U. & Eigenthaler, M., 2001. Taming platelets with cyclic nucleotides. Biochemical pharmacology, 62(9), pp.1153–61.

Schwede, F., Christensen, A.,Liauw, s., Hippe, T., Kopperud, R., Jastorff, b., & Døskeland, S. O., 2000. 8-substituted camp analogues reveal marked differences in adaptability, hydrogen

bonding, and charge accommodation between homologous binding sites (ai/aii and bi/bii) in cAMP kinase i and ii. Biochemistry, 39(30), 8803–12.

Scott, J. D., Glaccum, M. B., Zoller, M. J., Uhler, M. D., Helfman, D. M., McKnight, G. S., Krebs, E. G., 1987. The molecular cloning of a type II regulatory subunit of the cAMP-dependent protein kinase from rat skeletal muscle and mouse brain. Proceedings of the National Academy of Sciences of the United States of America, 84(15), pp.5192–6.

Seamon, K. B., Padgett, W. & Daly, J. W. 1981. Forskolin: unique diterpene activator of adenylate cyclase in membranes and in intact cells. Proc natl acad sci u s a, 78, 3363-7.

Shakur, Y., Holst, L. S., Landstrom, T. R., Movsesian, M., Degerman, E., Manganiello, V., 2001. Regulation and function of the cyclic nucleotide phosphodiesterase (PDE3) gene family. Progress in nucleic acid research and molecular biology, 66, pp.241–77.

Shattil, S.J. & Brass, L.F., 1987. Induction of the fibrinogen receptor on human platelets by intracellular mediators. The Journal of biological chemistry, 262(3), pp.992–1000.

Shattil, S. J., O'Toole, T., Eigenthaler, M., Thon, V., Williams, M., Babior, B. M., Ginsberg, M. H., 1995. Beta 3-endonexin, a novel polypeptide that interacts specifically with the cytoplasmic tail of the integrin beta 3 subunit. The Journal of cell biology, 131(3), pp.807–16.

Shattil, S.J., Kashiwagi, H. & Pampori, N., 1998. Integrin signaling: the platelet paradigm. Blood, 91(8), pp.2645–57.

Siedlecki, C. A., Lestini, B. J., Kottke-Marchant, K. K., Eppell, S. J., Wilson, D. L., Marchant, R. E., 1996. Shear-dependent changes in the three-dimensional structure of human von Willebrand factor. Blood, 88(8), pp.2939–50.

Sims, P. J., Wiedmer, T., Esmon, C. T., Weiss, H. J. & Shattil, S. J. 1989. Assembly of the platelet prothrombinase complex is linked to vesiculation of the platelet plasma membrane. Studies in Scott syndrome: an isolated defect in platelet procoagulant activity. J Biol Chem, 264, 17049-57.

Sinzinger, H., Silberbauer, K., Horsch, A. K., Gall, A., 1981. Decreased sensitivity of human platelets to PGI2 during long-term intraarterial prostacyclin infusion in patients with peripheral vascular disease--a rebound phenomenon? Prostaglandins, 21(1), pp.49–51.

Skalhegg, B.S. & Tasken, K., 2000. Specificity in the cAMP/PKA signaling pathway. Differential expression,regulation, and subcellular localization of subunits of PKA. Frontiers in bioscience : a journal and virtual library, 5, pp.D678–93.

Skeberdis, V. A., Chevaleyre, V., Lau, C. G., Goldberg, J. H., Pettit, D. L., Suadicani, S. O., Lin, Y., Bennett, M. V. L., Yuste, R., Castillo, P. E., Zukin, R S., 2006. Protein kinase A regulates calcium permeability of NMDA receptors. Nature neuroscience, 9(4), pp.501–10.

Smith, F. D., & Scott, J. D. 2006. Anchored cAMP signaling: onward and upward - a short history of compartmentalized camp signal transduction. European Journal Of Cell Biology, 85(7), 585–592.

Smith, S.A., 2009. The cell-based model of coagulation. Journal of veterinary emergency and critical care (San Antonio, Tex. : 2001), 19(1), pp.3–10.

Smolenski, 2012. Novel roles of cAMP/cGMP-dependent signaling in platelets. Journal of thrombosis and haemostasis : JTH, 10(2), pp.167–76.

Smyth, E.M. & FitzGerald, G.A., 2002. Human prostacyclin receptor. Vitamins and hormones, 65, pp.149–65.

Smyth, E.M., Li, W.H. & FitzGerald, G.A., 1998. Phosphorylation of the prostacyclin receptor during homologous desensitization. A critical role for protein kinase c. The Journal of biological chemistry, 273(36), pp.23258–66.

Smyth, E.M., Nestor, P. V & FitzGerald, G.A., 1996. Agonist-dependent phosphorylation of an epitope-tagged human prostacyclin receptor. The Journal of biological chemistry, 271(52), pp.33698–704.

Stalker, T. J., Newman, D. K., Ma, P., Wannemacher, K. M., Brass, L. F., 2012. Platelet signaling. Handbook of experimental pharmacology, (210), pp.59–85.

Stalker, T.J., Welsh, J.D. & Brass, L.F., 2014. Shaping the platelet response to vascular injury. Current opinion in hematology, 21(5), pp.410–7.

Stein, R. W., Papp, A. C., Weiner, W. J., Wu, K. K., 1985, Reduction of serum prostacyclin stability in ischemic stroke. Stroke; a journal of cerebral circulation, 16(1), pp.16–8.

Suematsu, E., Hirata, M., Hashimoto, T., Kuriyama, H., 1984. Inositol 1,4,5-trisphosphate releases Ca2+ from intracellular store sites in skinned single cells of porcine coronary artery. Biochemical and biophysical research communications, 120(2), pp.481–5.

Sugawara, H., Kurosaki, M., Takata, M., Kurosaki, T., 1997. Genetic evidence for involvement of type 1, type 2 and type 3 inositol 1,4,5-trisphosphate receptors in signal transduction through the B-cell antigen receptor. The EMBO journal, 16(11), pp.3078–88.

Supattapone, S., Danoff, S. K., Theibert, A., Joseph, S. K., Steiner, J., Snyder, S. H., 1988. Cyclic AMP-dependent phosphorylation of a brain inositol trisphosphate receptor decreases its release of calcium. Proceedings of the National Academy of Sciences of the United States of America, 85(22), pp.8747–50.

Takahashi, A., Camacho, P., Lechleiter, J. D., Herman, B., 1999. Measurement of intracellular calcium. Physiological reviews, 79(4), pp.1089–125.

Tardito, D., Tura, G. B., Bocchio, L., Bignotti, S., Pioli, R., Racagni, G., Perez, J., 2000. Abnormal levels of cAMP-dependent protein kinase regulatory subunits in platelets from schizophrenic patients. Neuropsychopharmacology : official publication of the American College of Neuropsychopharmacology, 23(2), pp.216–9.

Tardito, D., Zanardi, R., Racagni, G., Manzoni, T., Perez, J., 2002. The protein kinase A in platelets from patients with panic disorder. European neuropsychopharmacology : the journal of the European College of Neuropsychopharmacology, 12(5), pp.483–7.

Taskén, K. & Aandahl, E.M., 2004. Localized effects of cAMP mediated by distinct routes of protein kinase A. Physiological reviews, 84(1), pp.137–67.

Tateson, J. E., Moncada, S. & Vane, J. R. 1977. Effects of prostacyclin (PGx) on cyclic amp concentrations in human platelets. Prostaglandins, 13, 389-97.

Taylor, C. W. & Tovey, S. C. 2010. IP(3) receptors: toward understanding their activation. Cold Spring Harb Perspect Biol, 2, A004010.

Taylor, C.W. & Laude, A.J., IP3 receptors and their regulation by calmodulin and cytosolic Ca2+. Cell calcium, 32(5-6), pp.321–34.

Taylor, C.W. & Tovey, S.C., 2010. IP(3) receptors: toward understanding their activation. Cold Spring Harbor perspectives in biology, 2(12), p.a004010.

Taylor, C.W., Genazzani, A.A. & Morris, S.A., 1999. Expression of inositol trisphosphate receptors. , 26, pp.237–251.

Taylor, S. S. 1989. cAMP-dependent protein kinase. Model for an enzyme family. Journal of biological chemistry, 264, 8443-6.

Taylor, S. S., Kim, C., Cheng, C. Y., Brown, S. H. J., Wu, J., 2008. Diverse Strategies for Drug Design. , 1784(1), pp.16–26.

Tesmer, J. J., Sunahara, R. K., Gilman, A G., & Sprang, S. R. (1997). Crystal structure of the catalytic domains of adenylyl cyclase in a complex with gsalpha.gtpgammas. Science (new york, n.y.), 278(5345), 1907–1916.

Thines-Sempoux, D., Amar-Costesec, A., Beaufay, H., Berthet, J., 1969. The association of cholesterol, 5'-nucleotidase, and alkaline phosphodiesterase I with a distinct group of microsomal particles. The Journal of cell biology, 43(1), pp.189–92.

Thorpe, G. H., Kricka, L. J., Moseley, S. B. & Whitehead, T. P. 1985. Phenols as enhancers of the chemiluminescent horseradish peroxidase-luminol-hydrogen peroxide reaction: application in luminescence-monitored enzyme immunoassays. Clin Chem, 31, 1335-41.

Tournoij, E., Weber, G. J., Akkerman, J. W. N., de Groot, P. G., Zon, L. I., Moll, F. L., Schulte-Merker, S., 2010. MLCK1A is expressed in zebrafish thrombocytes and is an essential component of thrombus formation. Journal of thrombosis and haemostasis : JTH, 8(3), pp.588–95.

Towbin, H., Staehelin, T. & Gordon, J. 1979. Electrophoretic transfer of proteins from polyacrylamide gels to nitrocellulose sheets: procedure and some applications. Proc Natl Acad Sci U S A, 76, 4350-4.

Tu, H., Miyakawa, T., Wang, Z., Glouchankova, L. Iino, M., Bezprozvanny, I., 2002. Functional characterization of the type 1 inositol 1,4,5-trisphosphate receptor coupling domain SII(+/-) splice variants and the Opisthotonos mutant form. Biophysical journal, 82(4), pp.1995–2004.

Tu, H., Tang, T., Wang, Z., Bezprozvanny, I., 2004. Association of type 1 inositol 1,4,5-trisphosphate receptor with AKAP9 (Yotiao) and protein kinase A. The Journal of biological chemistry, 279(18), pp.19375–82.

van der Meijden, P. E. J et al, 2007, Dual P2Y12 receptor signaling in thrombin-stimulated platelets – involvement of phosphoinositide 3-kinase b but not c isoform in Ca2+ mobilization and procoagulant activity. FEBS Journal, 275 (2) 371–385

van Gorp, R. M., Feijge, M. H., Vuist, W. M. J., Rook, M. B., Heemskerk, J. W. M., 2002. Irregular spiking in free calcium concentration in single, human platelets. Regulation by modulation of the inositol trisphosphate receptors. European journal of biochemistry / FEBS, 269(5), pp.1543–52.

Vane, J.R. & Botting, R.M., 1995. Pharmacodynamic profile of prostacyclin. The American journal of cardiology, 75(3), p.3A–10A.

Varga-Szabo, D., Authi, K. S., Braun, A, Bender, M., Ambily, A., Hassock, S. R., Gudermann, T., Dietrich, A., Nieswandt, B., 2008. Store-operated Ca(2+) entry in platelets occurs independently of transient receptor potential (TRP) C1. Pflügers Archiv : European journal of physiology, 457(2), pp.377–87.

Varga-Szabo, D., Braun, A. & Nieswandt, B., 2009. Calcium signaling in platelets. Journal of thrombosis and haemostasis : JTH, 7(7), pp.1057–66.

Varga-Szabo, D., Braun, A., Kleinschnitz, C., Bender, M., Pleines, I., Pham, M., Renné, T., Stoll, G., Nieswandt, B., 2008. The calcium sensor STIM1 is an essential mediator of arterial thrombosis and ischemic brain infarction. The Journal of experimental medicine, 205(7), pp.1583–91.

Vermassen, E., Parys, J.B. & Mauger, J.-P., 2004. Subcellular distribution of the inositol 1,4,5-trisphosphate receptors: functional relevance and molecular determinants. Biology of the cell / under the auspices of the European Cell Biology Organization, 96(1), pp.3–17.

Vig, M., Beck, A., Billingsley, J. M., Lis, A., Parvez, S., Peinelt, C., Koomoa, D. L., Soboloff, J., Gill, D. L., Fleig, A., Kinet, J., Penner, R., 2006. CRACM1 multimers form the ion-selective pore of the CRAC channel. Current biology : CB, 16(20), pp.2073–9.

Vigdahl, R. L., Marquis, N. R. & Tavormina, P. A. 1969. Platelet aggregation. Ii. Adenyl cyclase, prostaglandin e1, and calcium. Biochem Biophys Res Commun, 37, 409-15.

Vigil, D., Blumenthal, D. K., Taylor, S. S., Trewhella, J., 2006. Solution scattering reveals large differences in the global structures of type II protein kinase A isoforms. Journal of molecular biology, 357(3), pp.880–9.

Volpe, P., Alderson-Lang, B.H. & Nickols, G.A., 1990. Regulation of inositol 1,4,5-trisphosphate-induced Ca2+ release. I. Effect of Mg2+. The American journal of physiology, 258(6 Pt 1), pp.C1077–85.

Wagner, L.E., Li, W.-H. & Yule, D.I., 2003. Phosphorylation of type-1 inositol 1,4,5-trisphosphate receptors by cyclic nucleotide-dependent protein kinases: a mutational analysis of the functionally important sites in the S2+ and S2- splice variants. *The Journal of biological chemistry*, 278(46), pp.45811–7.

Walsh, D. A., Brostrom, C. O., Brostrom, M. A., Chen, l., Corbin, J. D., Reimann, E., Krebs, E. G. 1972. Cyclic amp-dependent protein kinases from skeletal muscle and liver. Advances In Cyclic Nucleotide Research, 1, 33–45.

Walter, U., Eigenthaler, M., Geiger, J., Reinhard, M., 1993, Role of cyclic nucleotide-dependent protein kinases and their common substrate VASP in the regulation of human platelets, 344, 237-249

Wang, Y., Ho, T. G., Franz, E., Hermann, J. S., Smith, F. D., Hehnly, H., Esseltine, J. L., Hanold, L. E., Murph, M. M., Bertinetti, D., Scott, J. D., Herberg, F. W., Kennedy, E. J., 2015. PKA-Type i Selective Constrained Peptide Disruptors of AKAP Complexes. ACS Chemical Biology, 10(6), pp.1502–1510.

Watson, S. P., Ruggiero, M., Abrahams, S. L., Lapetina, E. G., 1984. Inositol 1,4,5-trisphosphate induces aggregation and release of 5-hydroxytryptamine from saponin-permeabilized human platelets. The Journal of biological chemistry, 261(12), pp.5368–72.

Weksler, B.B., Marcus, A.J. & Jaffe, E.A., 1977. Synthesis of prostaglandin I2 (prostacyclin) by cultured human and bovine endothelial cells. Proceedings of the National Academy of Sciences of the United States of America, 74(9), pp.3922–6.

Westphal, R. S., Tavalin, S. J., Lin, J. W., Alto, N. M., Fraser, I. D., Langeberg, L. K., Sheng, M., Scott, J. D., 1999. Regulation of NMDA receptors by an associated phosphatase-kinase signaling complex. Science, 285(5424), pp.93–6.

Willcocks, A. L., Cooke, A. M., Potter, B. V., Nahorski, S. R., 1987. Stereospecific recognition sites for [3H]inositol(1,4,5)-triphosphate in particulate preparations of rat cerebellum. Biochemical and biophysical research communications, 146(3), pp.1071–8.

Willoughby, D. & Cooper, D.M.F., 2007. Organization and Ca2+ Regulation of Adenylyl Cyclases in cAMP Microdomains. Physiological reviews, 87(3), pp.965–1010.

Wirtenberger, M., Schmutzhard, J., Hemminki, K., Meindl, A., Sutter, C., Schmutzler, R. K., Wappenschmidt, B., Kiechle, M., Arnold, N., Weber, B. H. F., Niederacher, D., Bartram, C. R., Burwinkel, B., 2007. The functional genetic variant Ile646Val located in the kinase binding domain of the A-kinase anchoring protein 10 is associated with familial breast cancer. Carcinogenesis, 28(2), pp.423–6.

Witczak, O., 1999. Cloning and characterization of a cDNA encoding an A-kinase anchoring protein located in the centrosome, AKAP450. The EMBO Journal, 18(7), pp.1858–1868.

Wojcikiewicz, R.J.H. & Luo, S.G., 1998. Phosphorylation of Inositol 1,4,5-Trisphosphate Receptors by cAMP-dependent Protein Kinase. Journal of biological chemistry, 273(10), pp.5670–5677.

Woulfe, D., Yang, J., Prevost, N., O'Brien, P., Fortna, R., Tognolini, M., Jiang, H., Wu, J., Brass, L. F., 2004. Signaling receptors on platelets and megakaryocytes. *Methods in molecular biology (Clifton, N.J.)*, 273, pp.3–32.

Yang, J., Wu, J., Jiang, H., Mortensen, R., Austin, S., Manning, D. R., Woulfe, D., Brass, L. F., 2002. Signaling through Gi family members in platelets. Redundancy and specificity in the regulation of adenylyl cyclase and other effectors. The Journal of biological chemistry, 277(48), pp.46035–42.

Yokoyama, C., Yabuki, T., Shimonishi, M., Wada, M., Hatae, T., Ohkawara, S., Takeda, J., Kinoshita, T., Okabe, M., Tanabe, T., 2002. Prostacyclin-deficient mice develop ischemic renal disorders, including nephrosclerosis and renal infarction. Circulation, 106(18), pp.2397–403.

Yoshikawa, F., Morita, M., Monkawa, T., Michikawa, T., Furuichi, T., Mikoshiba, K., 1996. Mutational analysis of the ligand binding site of the inositol 1,4,5-trisphosphate receptor. The Journal of biological chemistry, 271(30), pp.18277–84.

Yoshikawa, F., Iwasaki, H., Michikawa, T., Furuichi, T., Mikoshiba, K., 1999. Trypsinized Cerebellar Inositol 1,4,5-Trisphosphate Receptor: structural and functional coupling of cleaved ligand binding and channel domains. Journal of Biological Chemistry, 274(1), pp.316–327.

Yu, X., Carroll, S., Rigaud, J. L., Inesi, G., 1993. H+ countertransport and electrogenicity of the sarcoplasmic reticulum Ca2+ pump in reconstituted proteoliposomes. Biophysical journal, 64(4), pp.1232–42.

Zaccolo, M. & Pozzan, T., 2002. Discrete microdomains with high concentration of cAMP in stimulated rat neonatal cardiac myocytes. Science, 295(5560), pp.1711–5.

Zhang, G., Xiang, B., Dong, A., Skoda, R., C., Daugherty, A., Smyth, S. S., Du, X., Li, Z., 2011. Biphasic roles for soluble guanylyl cyclase (sGC) in platelet activation. Blood, 118(13), pp.3670–9.

Zhang, S. L., Yu, Y., Roos, J., Kozak, J. A., Deerinck, T. J., Ellisman, M. H., Stauderman, K. A., Cahalan, M. D., 2005. STIM1 is a Ca2+ sensor that activates CRAC channels and migrates from the Ca2+ store to the plasma membrane. Nature, 437(7060), pp.902–5.

Zhang, X. & Joseph, S.K., 2001. Effect of mutation of a calmodulin binding site on Ca2+ regulation of inositol trisphosphate receptors. The Biochemical journal, 360(Pt 2), pp.395–400.

Zhang, Z., Austin, S.C. & Smyth, E.M., 2001. Glycosylation of the human prostacyclin receptor: role in ligand binding and signal transduction. Molecular pharmacology, 60(3), pp.480–7.

APPENDIX I : CHEMICALS AND REAGENTS

Chemical	Function	Final Concentration	Supplier
0.2µm polyvinylidene difluoride (PVDF)	Immunoblotting	N/A	Sigma Aldrich (*St. Louis, MO*)
1,4-Dithiothreitol (DTT)	Extraction buffer	As required	Sigma Aldrich (*St. Louis, MO*)
2-Mercaptoethanol	Ingredient in Laemmli buffer	5% v/v	Sigma Aldrich (*St. Louis, MO*)
8-AHA-cAMP beads	cAMP pull-down assay	N/A	BioLog (*Bremen,Germany*)
8-CPT-6-Phe-cAMP	PKA activator	50µM	BioLog (*Bremen, Germany*)
Acrylamide	Gel electrophoresis	As required	BioRad *(Hercules, CA)*
Ammonium Persulphate (APS)	Gel electrophoresis	10% solution	Sigma Aldrich (*St. Louis, MO*)
Anti-biotin	Gel electrophoresis	1:2000	BioRad *(Hercules, CA)*
Bio-Rad *DC* Protein Assay kit	Protein assay	N/A	BioRad *(Hercules, CA)*
Biotinylated Marker	Protein marker	N/A	BioRad *(Hercules, CA)*
Bovine Serum Albumin (BSA)	Blocking agent	As required	Sigma Aldrich (*St. Louis, MO*)
Bromophenol Blue	Ingredient in Laemmli buffer	Trace	Sigma Aldrich (*St. Louis, MO*)
Calcium chloride	Calibrator for CA2+ measurement	2mM	Sigma Aldrich (*St. Louis, MO*)
Citric Acid	Ingredient in ACD	2.9mM	Sigma Aldrich (*St. Louis, MO*)
Coulter® Isoton® II diluent	Platelet counting	1:20,000	Beckam Coulter, (*High Wyecombe, UK*)
D- glucose	Ingredient in various buffers	As required	Sigma Aldrich (*St. Louis, MO*)
Digitonin	Platelet permeabilisation	As required	Sigma Aldrich (*St. Louis, MO*)
Ethylenediaminetetraacetic acid (EDTA)	Ingredient in various buffers	0.1M	Sigma Aldrich (*St. Louis, MO*)
Ethyleneglycoltetraacetic acid (EGTA)	Ingredient in Lysis buffer	1mM	Sigma Aldrich (*St. Louis, MO*)
Et-OH-NH agarose beads	cAMP pull-down assay	As required	BioLog (*Bremen,Germany*)
Forskolin	Adenylyl Cyclase	10µM	Sigma Aldrich

	Activator		(*St. Louis, MO*)
Fura-2 (AM)	Ca^{2+} dye	2µM	Sigma Aldrich (*St. Louis, MO*)
Glacial Acetic Acid	Kemptide assay	As required	Sigma Aldrich (*St. Louis, MO*)
Glycerol	Ingredient in various buffers	As required	Sigma Aldrich (*St. Louis, MO*)
HEPES	Buffering agent	As required	Sigma Aldrich (*St. Louis, MO*)
Human α-thrombin	Platelet agonist	As required	Sigma Aldrich (*St. Louis, MO*)
Hydrogen Peroxide	Ingredient in ECL	65µl	Sigma Aldrich (*St. Louis, MO*)
Hyperfilm ECL	Immunoblotting	N/A	Amersham, GE healthcare
IgePal	Lysis buffer	1% v/v	Sigma Aldrich (*St. Louis, MO*)
InCELLect™ AKAP St-Ht31 Inhibitor Peptide / St-Ht31P Control Peptide	AKAP disruptor peptide	5µM	Promega *(Madison, Wisconsin)*
Kodak® autoradiography GBX developer	Immunoblotting	N/A	Sigma Aldrich (*St. Louis, MO*)
Kodak® autoradiography GBX developer/replenisher	Immunoblotting	1:50	Sigma Aldrich (*St. Louis, MO*)
Kodak® autoradiography GBX fixer	Immunoblotting		Sigma Aldrich (*St. Louis, MO*)
Kodak® autoradiography GBX fixer/replenisher	Immunoblotting	1:50	Sigma Aldrich (*St. Louis, MO*)
Luminol	Ingredient in ECL	0.996% v/v	Sigma Aldrich (*St. Louis, MO*)
Magnesium chloride	Ingredient in Tyrode's buffer	1mM	Sigma Aldrich (*St. Louis, MO*)
Manganese Chloride	Calibrator	10mM	Sigma Aldrich (*St. Louis, MO*)
P-Coumaric Acid	Ingredient in ECL	0.465% v/v	Sigma Aldrich (*St. Louis, MO*)
PepTag® Assay for Non-Radioactive Detection of PKA activity	PKA activity assay	N/A	Promega *(Madison, Wisconsin)*
Phosphatase Inhibitor Cocktail	Sample preparation	1:200	Sigma Aldrich (*St. Louis, MO*)
Potassium Chloride	Ingredient in Wash buffer	0.05M	Sigma Aldrich (*St. Louis, MO*)
Potassium phosphate	Extraction buffer	As required	Sigma Aldrich (*St. Louis, MO*)
Precast 4-20% Mini-	Gel electrophoresis	N/A	BioRad (*Hercules,*

PROTEAN® TGX™ gels			*CA*)
Protease Inhibitor Cocktail	Sample preparation	1:100	Sigma Aldrich (*St. Louis, MO*)
Protein A sepharose beads	Immunoprecipitation	As required	Sigma Aldrich (*St. Louis, MO*)
Protein G sepharose beads	Immunoprecipitation	As required	Sigma Aldrich (*St. Louis, MO*)
RIAD	AKAP-PKA disruptor peptide	As required	Promega *(Madison, Wisconsin)*
Semi skimmed milk powder	Blocking agent	5% w/v	Tesco
Sodium Chloride (NaCl)	Ingredient in various buffers	As required	Sigma Aldrich (*St. Louis, MO*)
Sodium Citrate	Ingredient in various buffers	As required	Sigma Aldrich (*St. Louis, MO*)
Sodium dodecyl sulphate	Ingredient in various buffers	As required	Sigma Aldrich (*St. Louis, MO*)
Sodium Hydrogen Phosphate	Ingredient in Tyrode's buffer	3.3mM	Sigma Aldrich (*St. Louis, MO*)
Tetramethylethylenediamine (TEMED)	Gel electrophoresis	As required	Sigma Aldrich *(St. Louis, MO)*
Trizma Base	Ingredient in various buffers	As required	Sigma Aldrich *(St. Louis, MO)*
Tween-20	Immunoblotting	As required	Sigma Aldrich *(St. Louis, MO)*

APPENDIX II : COMPOSITION OF POLYACRYLAMIDE GELS

Gradient gel compositions for 1.5mm casting plates

Ingredient	**Stacking gel**	**Resolving gel**	
	3%	**10%**	**18%**
dH_2O	4.87 mL	1.418 mL	0.708 mL
Acrylamide (30%)	0.75 mL	1.182 mL	1.961 mL
Buffer I	-----	0.886 mL	0.886 mL
Buffer II	1.87 mL	----	----
APS (10%)	75.00 µL	18.00 µL	18.00 µL
TEMED	10.00 µL	2.00 µL	2.00 µL

10% gel compositions for 1.5mm casting plates

Ingredient	**Stacking gel**	**Resolving gel**
	3%	**10%**
dH_2O	4.87 mL	6.40 mL
Acrylamide (30%)	0.75 mL	5.30 mL
Buffer I	-----	4.00 mL
Buffer II	1.87 mL	----
APS (10%)	75.00 µL	75.00 µL
TEMED	10.00 µL	5.30 µL

7.5% gel compositions for 1.5mm casting plates

Ingredient	**Stacking gel**	**Resolving gel**
	3%	**7.5%**
dH_2O	4.87 mL	9.90 mL
Acrylamide (30%)	0.75 mL	6.25 mL
50% (v/v) Glycerol/Water	-----	1.60 mL
Buffer I	-----	6.00 mL
Buffer II	1.87 mL	----
APS (10%)	75.0 µL	90.00 µL
TEMED	10.0 µL	8.00 µL